

Swansea University E-Theses

Modern perturbative techniques applied to Yang-Mills and gravity theories.

Alston, Sam D

How to cite:

Alston, Sam D (2013) *Modern perturbative techniques applied to Yang-Mills and gravity theories..* thesis, Swansea University.

<http://cronfa.swan.ac.uk/Record/cronfa42943>

Use policy:

This item is brought to you by Swansea University. Any person downloading material is agreeing to abide by the terms of the repository licence: copies of full text items may be used or reproduced in any format or medium, without prior permission for personal research or study, educational or non-commercial purposes only. The copyright for any work remains with the original author unless otherwise specified. The full-text must not be sold in any format or medium without the formal permission of the copyright holder. Permission for multiple reproductions should be obtained from the original author.

Authors are personally responsible for adhering to copyright and publisher restrictions when uploading content to the repository.

Please link to the metadata record in the Swansea University repository, Cronfa (link given in the citation reference above.)

<http://www.swansea.ac.uk/library/researchsupport/ris-support/>



Swansea University
Prifysgol Abertawe

**Modern perturbative techniques
applied to Yang-Mills and gravity theories**

Sam D. Alston

Ph.D.

A thesis submitted to Swansea University
for the degree of Doctor of Philosophy

College of Science

2013

ProQuest Number: 10821333

All rights reserved

INFORMATION TO ALL USERS

The quality of this reproduction is dependent upon the quality of the copy submitted.

In the unlikely event that the author did not send a complete manuscript and there are missing pages, these will be noted. Also, if material had to be removed, a note will indicate the deletion.



ProQuest 10821333

Published by ProQuest LLC (2018). Copyright of the Dissertation is held by the Author.

All rights reserved.

This work is protected against unauthorized copying under Title 17, United States Code
Microform Edition © ProQuest LLC.

ProQuest LLC.
789 East Eisenhower Parkway
P.O. Box 1346
Ann Arbor, MI 48106 – 1346

Declaration

This work has not previously been accepted in substance for any degree and is not being concurrently submitted for any degree.

Signed: (candidate)

Date: 11/09/13

Statement 1

This thesis is the result of my own investigations, except where otherwise stated. Where correction services have been used, the extent and nature of the correction is clearly marked in a footnote(s). Other sources are acknowledged by references using square brackets throughout that direct the reader to an appended bibliography.

Signed: (candidate)

Date: 11/09/13

Statement 2

I hereby give consent for my thesis, if accepted, to be available for photocopying and for inter-library loan, and for the title and summary to be made available to outside organisations.

Signed: (candidate)

Date: 11/09/13

Abstract

In perturbative particle physics, theoretical developments over the past few decades have greatly improved the understanding of the structure inherent in scattering amplitudes. Their structure is much simpler than the traditional sum over Feynman diagrams ever suggested. We make use of many of the developments of the last thirty years to present a new method for dealing with rational one-loop amplitudes of massless theories in a recursive formalism. On-shell recursion in massless gauge theories relies on continuing momenta into the complex plane to induce poles over which amplitudes factorise, introduced by Britto, Cachazo, Feng and Witten (BCFW). We consider the factorisation of rational one-loop amplitudes in massless theories. Double poles arise which require modification from the normal BCFW prescription. We setup a modified factorisation that deals with specialist double poles and their pole-under-the-pole (PUP) counterparts in the pure Yang-Mills n -point one-loop amplitude with single negative helicity. It is separately supplemented by the normal on shell recursion for the rest of the single poles in the amplitude. Our result matches that of Bern et al, but with the PUP terms in a form that allows applications to pure gravity amplitudes. The gauge-gravity relations developed by Kawai-Lewellen-Tai (KLT) allow graviton scattering calculations to be formulated in terms of products of different orderings of partial gauge theory amplitudes. We develop a similar n -point recursion for the pure graviton one-loop amplitudes with single negative helicity, that agrees at $n = 5, 6$ with calculations by Dunbar, Eittle and Perkins. The double pole and PUP are KLT combinations of the simple interchange amplitudes seen in the Yang Mills case.

Acknowledgements

In finally reaching the summit of this mountain, I admire the view and take in a breath before the trek back down towards the viva. While I glance back along the path I have just taken I must acknowledge the people who helped directly and indirectly for their support on the route here.

I would like to start by thanking my supervisor Warren Perkins, for providing the impetus and encouragement when I sometimes felt lacking. I thank Warren Perkins, Dave Dunbar and James Eittle for help over the years on work and discussions on the subject.

The many years that I have spent so happily at Swansea University would not have been so good-humoured and enjoyable without my fellow students. In particular to Wynne Evans, Vladislav Vaganov, David Chung, Martyn Jones and Cassy Jones, thank you for proof-reading parts of this document. Special thanks goes to Ed Bennett who provided computer run time for checking the validity of the recursive algorithms at high numbers of gluons. Also thanks to the rest of the undergraduate students, PhD students and postdoctoral researchers I have encountered throughout my time at Swansea for the constant comic relief and support in various guises.

I also thank the STFC for providing funding for the duration and the Physics department for giving me the opportunity to study at both undergraduate and postgraduate level.

Lastly, to my family who are the ever-constant bedrock on my travels in life, thank you.

Contents

List of Figures	vi
1 Introduction	1
2 Gauge Theory	12
2.1 Yang-Mills theory	12
2.2 Feynman vertices	16
2.3 Scattering amplitudes and their divergences	18
2.4 Passarino-Veltmann reduction	20
2.4.1 The reduction by example	22
2.4.2 The scalar integrals	24
3 Organised amplitudes	26
3.1 Color ordered amplitudes	26
3.1.1 Tree level	26
3.1.2 Loop level	28
3.2 Spinor helicity formalism	29
3.2.1 Complex momenta	33
3.2.2 Polarisation vectors for massless particles	34
3.3 Axial gauge rules	35
3.4 CSW construction from axial gauge	37
3.5 n -point MHV amplitudes as an example	38
4 Utilising supersymmetry in Yang-Mills and Gravity	41
4.1 Supersymmetric field theories	42
4.1.1 $\mathcal{N} = 4$ sYM	43
4.1.2 Twistor space	44
4.1.3 Superamplitudes	45
4.1.4 Supersymmetric ward identities	47
4.1.5 One-loop SUSY decomposition for QCD	47
4.2 Supergravity theories	49
4.2.1 The finiteness of $\mathcal{N} = 8$ supergravity debate	50
4.2.2 KLT Relations for Gravity	51

4.2.3	One-loop SUSY decomposition for graviton amplitudes	54
5	Analytic Properties of Amplitudes	56
5.1	Multi-particle poles, collinear and soft limits	56
5.1.1	Tree level	56
5.1.2	Loop level	59
5.2	Unitarity	62
5.2.1	Optical theorem	62
5.2.2	Cutkosky Rules	64
5.2.3	Unitarity method	66
5.2.3.1	An example of unitarity	67
5.2.4	Generalised Unitarity	69
5.2.5	A Box example	72
5.3	On-shell recursion	75
5.3.1	Tree-level amplitudes by recursion	76
5.3.1.1	Example of tree-level recursion - MHV amplitudes . . .	78
5.3.2	The tree-level \mathcal{S} -matrix of $\mathcal{N} = 4$ sYM theory	80
5.3.3	Recursion for rational terms at one-loop	82
5.3.3.1	One-loop on-shell recursion – an example	85
6	One-loop n-point single-minus Yang-Mills amplitudes	89
6.1	Complex factorisation	90
6.2	Computation setup	92
6.3	The full axial gauge treatment at five-point	95
6.3.1	Axial gauge diagrams	97
6.3.2	Contributions to the final residue diagrammatically	98
6.3.3	The five-point result	102
6.4	n -point calculation	103
6.4.1	Useful off-shell currents	104
6.4.2	Diagrammatic contributions	105
6.4.3	Integration and BCFW evaluation	106
6.4.4	Reinterpreting the PUP contribution	108
7	One-loop n-point single-minus graviton amplitudes	111
7.1	The calculation	112
7.2	Tackling loop integration in pure gravity	116
7.3	Complex factorisation for the 5-point case	120
7.3.1	Off shell contribution to $C_{\text{grav}}^{n-s f} _5$	121
7.3.2	Re-interpreting the sub-leading contribution in $C_{\text{grav}}^{n-s f} _5^a$	125
7.4	Off shell MHV current with wandering a^- leg	132
7.5	τ_n^{YM} with wandering-minus	135
7.6	The n -point complex factorisation: $C_{\text{grav}}^{n-s f}$	142
7.6.1	Employing the KLT relation	142
7.6.2	Terms including a double pole	143

7.6.3	Applying BCFW shift to double pole terms	145
7.6.4	PUP contributions: class a	146
7.6.5	PUP contributions: class b	147
7.6.6	PUP contributions: class c	150
7.6.7	Putting it all together	151
7.7	Ansatz for n -point recursion relation	153
8	Conclusions	156
A	Loop integration	161
A.1	Yang Mills integrals	161
A.2	Gravity Integrals	163
A.2.1	Dealing with higher rank in ℓ	163
A.2.2	More examples	168
B	Reorganisation of the wandering minus current	172
	References	191

List of Figures

2.1	The Feynman rules for pure QCD. Figure 2.1a highlights the flow of color and momentum for the propagator. Figure 2.1b is the three-gluon vertex V_3 , with all indices and momenta labelled. Figure 2.1c indicates the four-gluon vertex V_4 with indices for color and the metric.	16
2.2	The box contributions, including the four-mass, three-mass, two-mass hard and two mass easy, the one-mass and zero-mass integrals.	25
2.3	The three-mass, two-mass and one-mass triangle contributions.	25
2.4	The two mass bubble contribution $I_{2;\tau;i}$	25
3.1	Contributions to the partial amplitude $A_4(1^-, 2^-, 3^+, 4^+)$ include three diagrams of which two vanish by gauge choice and judicious choice of vector q	38
4.1	Firstly, an amplitude in twistor space of degree d , which is a union of MHV amplitudes, or $d = 1$ curves in twistor space. Two lines intersecting in twistor space is an MHV vertex in spacetime. Thus amplitudes can be written as connected lines in twistor space.	45
5.1	The optical theorem: the imaginary part of a forward scattering one-loop amplitude arises as a sum over contributions of products of on-shell tree-level amplitudes from all possible intermediate particles i	64
5.2	The two arrangements of negative helicities on either side of the cut, using MHV tree-level amplitudes. There is one helicity configuration non-vanishing in (a), while (b) allows both cases.	68
5.3	The maximal cuts for a box that isolates the integral's coefficient precisely, as the product of four on-shell tree-level amplitudes.	70
5.4	One of the five arrangements for the quadruple cut integral with massive leg K_{12}	72
5.5	The factorisations that occur for tree-level recursion, summing over all i partitions of momenta on the left, \mathcal{L}_i and right \mathcal{R}_i and internal helicity configurations σ	78

5.6	The factorisations that occur for the rational terms R_n at one-loop on-shell recursion. For a particular shift, the factorisations include those with lower point tree-level amplitudes connected to lower point rational terms, and the swap for the shifted momenta attached to the opposite functions. The one-loop factorisation function \mathcal{F}_n contributes only in amplitudes with multiparticle poles. Sums over i partitions of momenta on the left \mathcal{L}_i and right \mathcal{R}_i , and internal helicity configurations λ are required.	83
5.7	These are the possible connections of tree-level and one-loop amplitudes that contribute to the recursive expression for $A_5^{1\text{-loop}}(a^-, b^+, c^+, d^+, e^+)$, where T are trees and L are loops.	85
6.1	The modified all plus collinear loop splitting amplitude, written at the integrand level as an ℓ -dependent off-shell current, τ_n with a common LHS. The current can contain in principle any helicity configuration provided at least one external leg has negative helicity. Contributions required for on-shell recursion procedures require shifting the ‘hatted’ momenta on the residue after the integral.	92
6.2	The MHV off-shell current $\tau_5(\hat{a}^-, (\hat{b} + \ell)^-, (c - \ell)^+, d^+, e^+)$, that contributes to the non-standard factorisation C^{n-sf} . The sum over the two internal helicity configurations generates an overall factor of two.	95
6.3	The two sets of diagrams that contribute to the integrals in C^{n-sf} . All original standard MHV diagrams are in the first set. Diagrams sub-leading in $O(s_{bc})$ include in this case two boxes and a pentagon.	96
6.4	Five diagrams are included in building the off-shell amplitude τ_5 in figure 6.2, where the capital momenta indicate off-shell momenta, i.e. $B = l + b$ and $-C = c - l$. There is only one helicity configuration that is non-vanishing, that permits one MHV vertex where a^- enters, and two $\overline{\text{MHV}}$ vertices for the other legs.	98
6.5	An organisation of the diagrams within τ_n showing triangle contributions to C^{n-sf} on the left with boxes, pentagons, etc., in the $B^2 = C^2 = 0$ case to the right.	103
7.1	The factorisations that occur for $M_n^{1\text{-loop}}(\hat{a}^-, \hat{b}^+, c^+, d^+, \dots, n^+)$. T represents a tree-level MHV or $\overline{\text{MHV}}$ amplitude, while L represents a lower point rational one-loop graviton amplitude. The diagram containing τ_n^{grav} is the modified non-standard factorisation for the all positive helicity one-loop splitting amplitude. The $\mathcal{P}_D(x \in y)$ are permutations over the diagrams for the choices of assigning legs x through y	113
7.2	The set of diagrams for $\frac{\tau^{\text{MHV}}(a^-, b^+ \dots f^+, P^-, g^+ \dots n^+)}{P^2(Pa)^2}$	133
7.3	The set of diagrams required for the C^{n-sf} where the negative helicity leg a^- is free to wander away from the off shell momenta B and C	135
7.4	The first set of diagrams for $\tau(a^-, b^+ \dots f^+, \beta^-, \gamma^+, g^+ \dots n^+)$	136

LIST OF FIGURES

7.5	The second set of diagrams for $\tau(a^-, b^+ \dots f^+, \beta^-, \gamma^+, g^+ \dots n^+)$.	136
7.6	The third set of diagrams for $\tau(a^-, b^+ \dots f^+, \beta^-, \gamma^+, g^+ \dots n^+)$.	137

Chapter 1

Introduction

The total number of particles in the universe is not a conserved quantity. This is revealed with the help of quantum mechanics, which reveals the ephemeral and fleeting nature of particles. This was pioneered by Dirac who understood how relativity implied the necessity for anti-particles [1]. For example, the vacuum of space is not empty due to particle anti-particle pairs popping into and out of existence from quantum fluctuations in spacetime. It has been experimentally demonstrated to a very high degree of accuracy in many cases that the true nature of a particle is governed by the laws of quantum mechanics. They describe particles as having an infinite tower of discrete energy states that may be occupied.

The particles themselves are the only pieces of nature that can be manipulated experimentally, whether they are mediating force carriers or parts of subatomic nuclei. The study of the behaviour of particles is and always has been to smash them together and observe the properties of the constituent remnants as best as possible. The more energetically the products can be made to collide at, the larger the possibilities of studying new physics. The study of particle physics is always breaking new ground with experiments at the frontier of energy scales, such as the Large Hadron Collider (LHC) in Cern, Switzerland.

In theoretical developments since Dirac's work the discrete energy states of a particle are reinterpreted as excited states of a field. The viewpoint on particles as being fundamental has changed to fields that extend over all spacetime. When the fields are treated with a local framework they give rise to particles, if treated consistently with

a quantum field theory. Studying particle interactions on a fundamental level requires formulating field theories in this local fashion, including particles as quantisation of the fields. Therefore, quantum field theory contains the necessary mathematical framework to describe the fundamental characteristics of the quantum nature of particles, and the dynamics of their interactions. It defines the universe as excitations of fields and provides the basis for modelling the required infinite number of degrees of freedom. During the 20th century, quantum field theory was successfully developed into the best description of nature at the fundamental level so far; the Standard Model of particle physics. The predictions of the Standard Model went hand in hand with the testing and discovery of experimental phenomena, with both leading the way at some point. Many complicated simulations are now possible due to the progression of technology throughout the last century, applied at ever rising energy scales to match experimental requirements. This makes the Standard Model a combined success of many theoretical insights verified by experimental evidence as the encompassing theory of particle physics.

Currently, the Standard Model combines three of the four fundamental forces of nature; the strong, weak and electromagnetic interactions. The theory that deals with the strong force is called Quantum Chromo-Dynamics (QCD), that grew out of work pioneered by Yang and Mills [2]. The strong interaction is confined to an area the size of a large nucleus, while “color-less” particles are oblivious to the strong force at these scales. It binds quarks together inside hadrons, in pairs called mesons, or triplets called baryons, that make up the constituents of sub-atomic nuclei. The binding force is mediated by the gluon, (of which there are eight types) that carry a combination of “color” and “anti-color” charges. The weak interaction deals with radioactive decay, that affects all fermions; particles whose spin is half-integer. It is mediated by the W and Z bosons, which due to their relatively high mass, occurs over very short distance scales. Electromagnetism deals with the forces between electrically charged particles, mediated by photons and responsible for most of the phenomena in everyday life – besides gravity. It is not currently described by local interactions in the Standard Model. Nevertheless, it is as an effective theory that still stands up to almost every experimentally tested observation with aplomb.

The individual forces of the Standard Model can be described by three gauge symmetries; $SU(3)_C \times SU(2)_L \times U(1)_Y$. The weak isospin T_3 is the conserved quantum

number that transforms between the left-handed doublets of fermions only, and hence named a chiral symmetry. This is the $SU(2)_L$ part of the Standard Model, that governs the transformations of the W^+, W^- and W^0 bosons. The weak hypercharge Y is the generator of the symmetry $U(1)_Y$, corresponding to the B^0 boson. These four bosons would be massless, but the weak interaction requires a massive boson to restrict its influence to short distances. To realise the massive particles in nature, a spontaneous breaking of the chiral symmetry is required, provided by the Higgs mechanism [3, 4]. It breaks the $SU(2)_L \times U(1)_Y$ part of the gauge symmetry in a certain regime to form the electroweak interaction with $U(1)_{EM}$ gauge symmetry, combining the weak force with electromagnetism. The Higgs field is an $SU(2)$ doublet with four real components, inducing this chiral symmetry breaking via setting three of the four components to zero. The final degree of freedom describes the massive manifestation of the Higgs boson through the vacuum expectation value of the Higgs field. Below energies of around 100GeV, spontaneous symmetry breaking occurs; and the W^0 and B^0 undergo mixing via the weak mixing angle to result in the observed Z^0 boson and photon (γ) of Quantum Electro-Dynamics (QED). This symmetry breaking, of $SU(2)_L \times U(1)_Y \rightarrow U(1)_{EM}$, gives mass to the W^+, W^- and Z^0 bosons while leaving the $U(1)$ symmetry of electromagnetism intact; so the photon remains massless.

The mass of the scalar Higgs particle is then responsible for giving mass to the other fundamental bosons that have been measured already. Furthermore, the Higgs field is the medium in which all massive particles permeate to gain mass through their interaction with it. The massive scalar Higgs particle has long been missing from experimental results. Although its unknown mass allowed a large number of production channels for investigation, the Higgs decay cascades in most cases to the Standard Model particles of QCD. Therefore no direct detection of the Higgs boson is possible; it may be inferred from excesses in certain branching ratios away from the “background” of QCD. Finding the Higgs boson has been the major target of the CMS and ATLAS detector experiments at the LHC during its last two year run. The results published from both CMS and ATLAS collaborations have identified a new particle with mass at around 125GeV [5, 6], which is within the expected mass ranges and consistent with the Standard Model for it to be the Higgs particle. The latest results from CMS [7] have further verified it has spin 0, thus it is the first elementary scalar to be found in nature. However, more refined tests with electron-positron colliders would hopefully

prove the new particle is indeed the *fundamental* Higgs boson missing from the Standard Model. If it is not, the experimental community have found a new particle that needs explanation outside the current Standard Model generalisations that contain the Higgs boson. The theorists therefore are still very enthused in model building for particle interactions and not just for QCD (see Chapter 4).

The final symmetry of the Standard Model concerns the strong force, governed by the $SU(3)_C$ part of the gauge group. The charges associated with this group are named for three colors which are *red*, *green* and *blue*, including three anti-colors that are mediated in combinations of pairs by massless gluons. The theory deals with quarks of varying mass that exist in six flavours (up, down, charm, strange, top and bottom), which carry one of the three types of color or anti-color. The quarks combine to form color neutral hadrons such as *red – antired* or *red – green – blue* combinations. The $SU(3)_C$ gauge group defines a *local* symmetry that once gauged, gives rise to QCD. The eight gluons are unlike other gauge bosons as they interact with themselves. QCD is therefore a non-linear theory known as a special kind of non-Abelian gauge theory, which cannot be solved analytically.

However, QCD is of phenomenological interest for a variety of reasons. One is confinement: physical states are only ever observed in a color singlet; free quarks or gluons are never observed. It is not clear why QCD should be confining, but it is the current opinion that it is due to gluons carrying charge combinations themselves. When separating a quark anti-quark meson, gluon fields or “color tubes” behave like rubber bands between them that increases in potential energy with their separation. At some point it is more energetically favourable to pull a quark and anti-quark out of the vacuum and the distant original quarks pair off with one each of the generated pair. This hadronisation is seen in detectors at the LHC for example. As protons are accelerated to high enough energies, their head on collisions pull apart the constituent quarks which creates new, high energy hadrons. These cascade down to lower energy hadrons, by pulling new quark anti-quark pairs out of the vacuum. These “jets” of hadrons are seen in the detectors as sprays of particle tracks, which are difficult to resolve from the initial interaction point. It is difficult to even deduce the number of jets for some interactions. The quantum process of hadronisation is poorly understood, but is also an active experimental avenue of research and essential for identifying the number of jets in detectors [8–10].

Another interesting property of QCD is asymptotic freedom. At very high energies, the strength of the interactions between quarks is weak, characterised by the coupling constant α_s . For $\alpha_s \ll 1$, a Taylor expansion series in the coupling can be used to determine an exact formulation of QCD when expanded to infinite order in the coupling. Practically, this cannot be achieved, but for small enough couplings these processes can be approximated to within experimental uncertainty using the first few orders of the expansion. This requires expanding the Lagrangian interaction terms proportional to α_s in a power expansion such that interactions that happen at higher order in the coupling will be a correction to the α_s terms. The energy scale that the coupling becomes small enough to use this method is determined experimentally to be $\sim 200\text{MeV}$. We assume throughout the thesis to work in the high energy regime far above this scale. Below this energy the strong coupling is larger than one and one must resort to other techniques.

One such alternative includes the lattice approach; by putting spacetime on a four dimensional lattice with spacing a , while predictive results rely on taking the continuum limit $a \rightarrow 0$ at the end. Lattice QCD has come a long way in providing predictions on relevantly phenomenological quantities since its inception in the 70's with Wilson [11]. The pace of technology in supercomputers has helped drive the predictive power in the field, in areas like hadron spectroscopy [12].

One can also attack the problem by studying a dual theory in the weakly coupled regime to which the strongly coupled theory of interest can be related. This is usually via the AdS/CFT correspondence; which is an extremely popular area of work, built upon the original insights of Maldacena [13] and later Witten [14]. Both of these contrasting approaches are interesting and productive areas of research in their own right, as ways of tackling the non-perturbative regime of QCD and other phenomenologically and mathematically interesting theories.

Perturbation theory deals with the approximation of a quantum mechanical system by adding corrections to the solvable system, by “perturbing” the original simplest Hamiltonian. The perturbations are typically a weak disturbance to the simple system, so a character expansion in a small parameter α_s , will determine a quantum mechanical process to a desired degree of accuracy in $\mathcal{O}(\alpha_s)$. It was highlighted earlier that particle

interactions are characterised by a weak coupling at energies above $\sim 200\text{MeV}$, which lends perturbation theory as a valid application to high energy QCD.

The process of scattering particles off each other is computed in terms of matrix elements, as a function of the coupling of the theory. The matrix that takes us from an initial state $|i\rangle$ to a final state $|f\rangle$ is known as the \mathcal{S} -matrix, while the scattering cross section is a quantity built up of all possible ways that the process of getting from initial to final state occurs. The individual \mathcal{S} -matrix elements absolute value squared $|\mathcal{S}_{if}|^2$ are the transitional amplitudes or probabilities of that process occurring. The scattering process decomposes into an integral over Lorentz invariant phase space with leading initial state factors, multiplied by the absolute value squared of the \mathcal{S} -matrix. A quantum mechanical *amplitude*, is then just the elements of the \mathcal{S} -matrix $|\mathcal{S}_{if}|^2$ for some state $|i\rangle$ to some state $|f\rangle$ for specific momenta, which in principle have to be summed over all possible final states. This quantity is the one that theorists strive to calculate for interesting theories and large numbers of particles to as high a degree of accuracy as possible. An amplitude contains then, the description of the dynamics of the properties inherent in the initial and final states of the interactions, such as momentum, intrinsic spin, or color. The amplitudes at next to leading order is where the bulk of this thesis is concentrated.

The QCD part of the Standard Model Lagrangian will be used to motivate the types of interactions needed for deriving a high energy effective theory expanded in the coupling constant α_s . The coupling expansion in α_s from the well known Feynman path integral procedure [15], can be used to derive Feynman rules; a set of encoded diagrams for quantum mechanical processes. In Feynman rules, each vertex of interaction or propagating particle between vertices corresponds to an algebraic expression to be evaluated. Connections of the vertices and propagators without any closed loops create Feynman diagrams that encode at $O(\alpha_s)$ the leading order (LO) contributions to quark-quark, quark-gluon or gluon-gluon interactions. The next to leading order (NLO) terms of $O(\alpha_s^2)$ form Feynman diagrams with a loop in them, or contributions from real emissions. At higher orders there are more loops, while each loop corresponds to an internal virtual state of momentum that has to be integrated over. Summing all possible graphs at each order, to as many orders as possible, provides theoretical predictions that give us the most precise tests of QCD to date.

For most phenomenological predictions summing Feynman diagrams to NLO is enough to be accurate within 10%. However, to calculate the typical interaction seen at an LHC detector of two protons to W and Z bosons plus up to four jets of hadrons, just at NLO, is the limit of current technology [8] for real QCD. Focusing on the NLO calculations, rather than the entire cross sections of particle scattering is the focus for many theoretical field theorists. So developing the toolkit for the study of QCD through the interactions of quarks and gluons is crucial. The evolution of quantum states via scattering amplitudes in QCD at high energies, requires modelling primarily gluon-gluon \rightarrow gluons plus $q\bar{q}$ pairs. For high energy processes such as those that occur at the LHC at full beam energy, the gluons have much higher energy than the equivalent mass carried by any of the quarks. Therefore, one can treat the lighter quarks as approximately massless. The typical centre of mass energy for the last two years at the LHC reached 8TeV, while during the current shutdown the beam energy is being upgraded to fire beams capable of 7TeV each. In this type of interaction there are many gluons and quarks with a significant fraction of the centre of mass energy. The LHC produced many top quarks per day during its experimental runs at 8TeV per beam. Also a new particle around 125GeV [5, 6], was discovered as a new scalar boson. Resolving that from the QCD background data, of which the detectors are almost saturated, is an arduous task. Furthermore the mass for the new particle was exactly in a range dominated by the cross sections of decays from other Standard Model interactions that are dominant in certain channels of production, including W^+W^- and $t\bar{t}$ for example.

Therefore an explicit understanding of all interactions between gluons and quarks and how they scatter is essential. Writing down the Feynman rules is easy enough, but putting the toolkit into practice, particularly for QCD becomes an issue. Since gluons self interact via exchange of colour charge there are many terms that are generated just for one Feynman diagram. As the number of external gluons grows, the number of diagrams accelerates out of control such that for a $gg \rightarrow 8g$ process at LO over 10^7 Feynman diagrams are generated. Furthermore, the intermediate stages of evaluating all the algebraic expressions from the diagrams are gauge-dependent, and are individually much more complicated than the gauge invariant answer at the end. It has been the focus of many research groups to develop new computational tools to overcome these obstacles, particularly for QCD.

Yang and Mills' work [2] first popularised the study of non-Abelian gauge theory, of which the case with gauge group $SU(3)$ was later shown to describe QCD. Consequently the study of the color force interactions is known widely as Yang-Mills theory. These non-Abelian theories were proven to be renormalisable in four dimensions by t' Hooft in 1972 [16]. Since then, the study of Yang-Mills theory in the perturbative regime has been driving to a deeper understanding of the symmetries and simpleness of scattering amplitudes as a whole, despite the arduous calculations needed to reach them. It is unclear if there is a better formulation of quantum field theory or perturbation theory which captures the symmetries in the intermediate steps using different variables or states. However, the current route of development prefers to use gauge-invariant intermediate steps at every level of the calculation. Keeping as many symmetries manifest at every stage of the calculation simplifies the overall computation of scattering amplitudes.

Furthermore, most techniques developed for efficient calculation are born from working with theories with particles that have so called “super” partners. In a theory with supersymmetry, all bosons gain fermionic super partners, while the original fermions gain bosonic super partners, such that the entire particle content of the original theory is doubled. Despite the lack of experimental evidence, it is one of the most accepted frameworks for beyond the Standard Model physics [17]. Its origins were born out of considering discrete spacetime symmetries depending on quantum numbers being conserved, that were possible to formulate using anti-commuting generators. Those were symmetries such as charge, parity and time, under the name CPT, and invariance under Poincare transformations. Coleman and Mandula published a theorem in 1967 [18] that suggested the only conserved quantities were Lorentz scalar or commuting generators; the most trivial that can combine spacetime and internal symmetries. By allowing anti-commuting generators that transform in the spinor representation of the Lorentz group, Haag, Lopuszanski and Sohnius weakened the conditions in 1975 [19], that led to the postulation of supersymmetry. The extension of the Poincare algebra to anti-commuting generators or fermionic supercharges, allowed the interplay of translations in spacetime with the mixing of fermions and bosons. Theories of extended supersymmetry increase the copies of supersymmetric transformations (with $4N$ supercharges), that constrain the field theory content and interactions. In four dimensions, the spinor's four degrees of freedom with a maximal eight number of supersymmetries

demands 32 supersymmetric generators. This automatically generates a massless field of spin 2 called the graviton. Other theories of supersymmetry include for example, a chiral multiplet for $\mathcal{N} = 1$, hypermultiplet for $\mathcal{N} = 2$ and vector multiplet for $\mathcal{N} = 4$. Theories of particle interaction with more supersymmetry are the prime testing ground for generating efficient techniques, due to their simplified \mathcal{S} -matrix compared with that of QCD.

The focus of the research outlined in this thesis is to continue to develop the mathematical tools needed to study the computation of NLO scattering amplitudes. In particular, the use of complex momenta and a new approach to deriving on shell recursion relations at NLO plays a fundamental role. We shall apply our techniques in both Yang-Mills theory and pure Einstein gravity for amplitudes with a single negative helicity, where we use the graviton to mediate the force of gravity in a local context similar to the gluon in Yang Mills. The mathematical developments we outline in Yang-Mills are extended to graviton scattering to derive a previously unknown n -point recursion relation. It agrees with explicit results at $n = 5, 6$, for NLO graviton amplitudes with a single negative helicity.

The rest of the thesis is organised as follows. Chapter 2 firstly outlines the essentials of Yang-Mills theory. We then describe how the Feynman rules are derived from the vertices and propagators allowed in the theory. Finally, we present the construction of amplitudes via perturbation theory, dealing with infinities at NLO and the traditional techniques of Passarino-Veltman reduction. Furthermore, we discuss the techniques for reducing the rank of tensors in loop momenta for numerators of NLO integrals to a known “scalar” set of integrals with an example.

Chapter 3 builds upon more modern simplifications and techniques of development general to the field of research. Firstly we introduce the color decomposition of both LO and NLO amplitudes, then we substitute the use of Weyl spinors for the original four momenta via the spinor helicity formalism. We adopt a particular gauge choice that is utilised throughout the thesis, with an application through an example to compute the simplest infinite set of LO n -point amplitudes.

In Chapter 4 we build upon the concept of supersymmetry from the Introduction and also motivate graviton scattering, with comments on theories of supersymmetric

gravity as possible candidates for perturbative quantum models. We highlight the supersymmetric decomposition of NLO amplitudes, which significantly aids computations in beyond LO QCD. We also motivate a particular highly supersymmetric perturbative quantum gravity model in terms of gravitons, and describe how models of graviton scattering are built out of products of Yang-Mills amplitudes. There is also an analogous supersymmetric decomposition for gravity amplitudes that will be utilised at NLO.

Chapter 5 provides an overview of the various analytic properties of amplitudes. We discuss the multi-particle pole, collinear and soft behaviour of amplitudes at both LO and NLO level. We explain the application of unitarity based methods at NLO, which reuses the knowledge of on shell LO amplitudes to determine the parts of NLO amplitudes containing branch cuts. We illustrate the methods of recursion based algorithms for LO amplitudes and rational parts of NLO amplitudes with examples. Finally we highlight some issues when applying on shell recursion at NLO due to the double poles induced for complex momenta.

Chapter 6 introduces the notion of non-standard factorisations to deal with double poles and sub-leading or “pole under the pole” (PUP) terms in recursive techniques for the NLO Yang-Mills amplitude $A^{1\text{-loop}}(a^-, b^+, c^+, \dots, n^+)$. We define a new computational setup based on techniques described in Chapter 3, and a sum over NLO diagrams to be integrated over. The full calculation of the five-point case is demonstrated to fully explain the method. Then the case is applied to the n -point NLO amplitude, as developed in work pioneered in publication with supervisors [20]. The double pole and PUP pieces are eventually expressed in terms of simple MHV amplitudes, that demonstrate the pole behaviour of loop splitting amplitudes for complex momenta.

Chapter 7 re-applies the non-standard factorisations concept using the same method as described in Chapter 6 this time in the pure graviton case; $M^{1\text{-loop}}(a^-, b^+, c^+, \dots, n^+)$. Much of the same methodology and techniques learnt from Chapter 6 are utilised to demonstrate the calculation of the five-point non-standard factorisation. This highlights how the simplifications of the double pole and PUP contributions are achieved in gravity that differ from the Yang-Mills case. To discern $n > 5$ -point non-standard factorisations, an off-shell generalisation to a Yang-Mills current with a wandering negative helicity is derived, that will feed into the calculations for gravity. Then we derive the n -point recursion relation for the NLO pure graviton amplitude. The section on the n -point non-standard factorisations methodically identifies the types of terms

generated at the double pole and PUP level in terms of the Kawai-Lewellen-Tye relation [21]. The final result contains all the double pole and associated PUP behaviour in terms of products of the simplest gauge theory amplitudes, with sums over various permutations of legs. A better understanding for the behaviour of double poles in loop splitting amplitudes in pure gravity is demonstrated, as was achieved in Chapter 6.

Chapter 8 highlights the progress in the field of determining perturbative field theory techniques so far, while reiterating the new developments made in Chapters 6 and 7. The future of recursive techniques is discussed, when considering rational NLO amplitudes and beyond. Appendix A contains the details on handling loop integration, in both Yang-Mills and gravity. This is followed by Appendix B with the tedious simplifications by reorganisation of the off shell current with a wandering negative helicity leg in pure Yang-Mills.

Chapter 2

Gauge Theory

In this chapter, gauged symmetries in an Abelian theory such as Quantum Electrodynamics (QED) is introduced, before moving on to the full description of the non-Abelian generalisation. We describe another one of the fundamental forces of interaction; namely that of the color force in Quantum-Chromo-Dynamics (QCD) with gauge symmetry $SU(N_c)$ with N_c the number of colors. We then describe how scattering amplitudes are built using traditional Feynman diagram techniques. Furthermore, the issues with diagrams at next to leading order (NLO) in the gauge coupling with infinities are discussed. Finally, the integration that appears at NLO is described in terms of traditional techniques for dealing with large rank tensors in numerators of the integrands. The Passarino-Veltman reduction is described with an example to reduce the integrands to a known set of simpler master integrals.

2.1 Yang-Mills theory

As highlighted in Chapter one, part of the success of the Standard Model is down to the development of gauge theories. One includes the gauged symmetry of $SU(N)$ which forms a special kind of non-Abelian gauge theory first formulated by Yang and Mills [2] for $SU(2)$. The procedure presented up to (2.15) follows [15, 22].

Yang and Mills developed a formulation of a more generalised gauge theory than the existing field theory of the time, QED. Although their aim was to describe a theory of hadron interactions, their work did describe a fundamental theory; those of quark

interactions. They were described via the transfer of a new type of charge that comes in three colors. Both QED and Yang-Mills theory use the idea of gauging, or localising a symmetry transformation. The simplest global transformation of some complex field ψ can be written as

$$\psi \rightarrow e^{i\alpha} \psi, \quad (2.1)$$

where α is independent of space-time coordinates. This global symmetry can be promoted to a local symmetry by insisting the transformation hold with α now a function of the spacetime coordinates x . QED is invariant under local phase rotations, and so exhibits a local, or Abelian $U(1)$ gauge symmetry with the transformation,

$$\psi(x) \rightarrow e^{i\alpha(x)} \psi(x). \quad (2.2)$$

The dynamics of QED stem from this local symmetry behaviour and define the gauge covariant derivative

$$D_\mu \psi = (\partial_\mu + ieA_\mu) \psi, \quad (2.3)$$

where the vector A_μ is identified as the photon field and e is the gauge coupling.

The generalisation by Yang and Mills to non-Abelian symmetry groups is the fundamental difference to that of QED. These interactions describe a non-Abelian gauge theory, of which the simplest example was given the name Yang-Mills theory. Non-Abelian gauge theories of which Yang and Mills developed the first example in 1954 [2], deal with non-commutative groups such as $SU(N)$. For a non-Abelian group G , a local gauge symmetry is defined as

$$U = e^{i\alpha^a(x)T^a}, \quad (2.4)$$

with the generators T^a of the gauge group satisfying the commutation relation

$$[T^a, T^b] = if^{abc}T^c, \quad (2.5)$$

where f^{abc} are the structure constants for G . The normalisation is taken such that $\text{tr } T^a T^b = \frac{1}{2} \delta^{ab}$.

2.1 Yang-Mills theory

The theory is described by complex fields ψ and gauge fields A_μ^a , whose dynamics are governed by the gauge covariant derivative

$$D_\mu \psi = (\partial_\mu - ig T^a A_\mu^a) \psi, \quad (2.6)$$

where g is a coupling constant and the gauge fields $A_\mu = T^a A_\mu^a$ live in the adjoint representation of G . Indices a, b can be raised or lowered trivially ($f^{abc} = f_{abc}$), whereas raising or lowering the Greek indices μ, ν corresponds to the usual Lorentz signature $\eta_{\mu\nu} = \text{diag}(-+++)$.

So under the gauge transformation (2.4),

$$\psi \rightarrow U \psi, \quad D_\mu \psi \rightarrow U D_\mu \psi \quad (2.7)$$

and the gauge field transformations of A_μ are also fixed. They are applied by

$$A_\mu \rightarrow U A_\mu U^{-1} + \frac{i}{g} U \partial_\mu U^{-1}, \quad (2.8)$$

or in the component form,

$$A_\mu^a \rightarrow A_\mu^a + \frac{i}{g} \partial_\mu \alpha^a + f^{abc} A_\mu^b \alpha^c. \quad (2.9)$$

The field strength tensor $F_{\mu\nu} = F_{\mu\nu}^a T^a$ can be constructed as the commutator of two gauge covariant derivatives;

$$[D_\mu, D_\nu] = ig F_{\mu\nu}, \quad (2.10)$$

where

$$F_{\mu\nu} = \partial_\mu A_\nu - \partial_\nu A_\mu - ig [A_\mu, A_\nu], \quad (2.11)$$

or in component form

$$F_{\mu\nu}^a = \partial_\mu A_\nu^a - \partial_\nu A_\mu^a + g f^{abc} A_\mu^b A_\nu^c. \quad (2.12)$$

Under the gauge transformation (2.4)

$$F_{\mu\nu} \rightarrow U F_{\mu\nu} U^{-1}, \quad (2.13)$$

therefore $\text{tr}(F_{\mu\nu} F^{\mu\nu})$ is a gauge invariant quantity, lending itself for use in a lagrangian. A non-Abelian gauge theory can then be described with the lagrangian,

$$\mathcal{L} = -\frac{1}{2} \text{tr} F_{\mu\nu} F^{\mu\nu} + \bar{\psi}(i\gamma^\mu D_\mu - m)\psi, \quad (2.14)$$

dependent on the coupling g and the mass m , which for the non-Abelian group $SU(N_c)$ describes QCD for the number of colors $N_c = 3$. In the lagrangian (2.14), the A_μ fields become the gluon fields, of which there are eight due to the $N_c^2 - 1 = 8$ generators of $SU(3)$. The $\psi \rightarrow \psi_f$ and $\bar{\psi} \rightarrow \bar{\psi}_f$ where f denotes the six ‘flavours’ of quark and anti-quarks (u, d, c, s, t and b). The sum over f in the lagrangian yields;

$$\mathcal{L}_{\text{QCD}} = -\frac{1}{2} \text{tr} F_{\mu\nu} F^{\mu\nu} + \sum_f \bar{\psi}_f(i\gamma^\mu D_\mu - m_f)\psi_f, \quad (2.15)$$

where the T_{ij}^a ($i, j = 1, 2, 3, a = 1 \dots 8$) generators in the covariant derivative (2.6) are now the $SU(3)$ Gell-Mann matrices $\times \frac{1}{2}$.

Interactions in Yang-Mills theory concerned with QCD will constantly be referred to throughout as obeying this model, however the bulk of calculations will be conducted without including the quarks. In the absence of quarks the theory is still interesting, as the non-Abelian nature of the theory allows the gluons to self interact since they carry color charge, hence the terminology “pure” Yang-Mills. This will be the focus of study for the hard scattering events in high energy processes where the coupling $\alpha_s = g^2/4\pi$ is small enough that interactions between the gluons dominate. Here one can use perturbation theory, and easily generate Feynman rules for the pure gauge interactions of Yang-Mills theory. From this point one could generate all the required diagrams for any interaction using the standard Feynman diagram techniques. However, more efficient techniques that make use of gauge invariant building blocks rather than gauge dependent diagrams will be covered through Chapters 3–5.

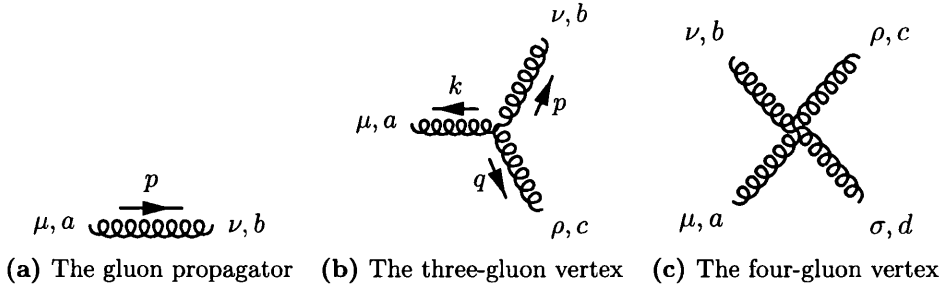


Figure 2.1: The Feynman rules for pure QCD. Figure 2.1a highlights the flow of color and momentum for the propagator. Figure 2.1b is the three-gluon vertex V_3 , with all indices and momenta labelled. Figure 2.1c indicates the four-gluon vertex V_4 with indices for color and the metric.

2.2 Feynman vertices

The basis for the modern techniques are still built on the bedrock of the Feynman vertices, which are essential in building diagrams that represent the particle interactions. The Feynman rules can be derived from the lagrangian of QCD (2.15), by the textbook of Peskin and Schroeder [15] for example. Expanding the lagrangian in terms of its component fields, and gauge fixing (conventionally in the Feynman gauge $\xi = 1$) defines a Feynman path integral. Although one must fix a gauge to define the gluon propagator, ghost terms must be introduced that cancel the unphysical degrees of freedom which would otherwise propagate in covariant gauges. The ghost fields will be neglected from the Feynman rules below as they can be decoupled from the theory with an axial gauge choice, albeit at the cost of increased technical difficulties.

We need not include the quark/anti-quark interaction via a gluon exchange (i.e. the vertex coupling of a gluon to two quarks), since we will be using pure Yang-Mills throughout. Therefore we only need the gluon self-interaction vertices and the propagator, defined for all momenta outgoing. The three ingredients needed to determine the Feynman rules for pure QCD are shown pictorially in figure 2.1, and taken from [23]. Firstly, the gluon propagator in figure 2.1a is given by

$$-\frac{i}{p^2 + i\epsilon} \delta^{ab} \left(g^{\mu\nu} + (\xi - 1) \frac{p^\mu p^\nu}{p^2 + i\epsilon} \right), \quad (2.16)$$

where the $i\epsilon$ factor is required be able to handle the integrals where poles in $p^0 =$

$\pm(E - i\epsilon)$ exist. There is a Feynman prescription for handling the poles by closing contours (that run below one pole and above the other) in the complex plane. The choice of closing the contour in the upper or lower half of the plane is determined by the time ordering of the propagation. One must also fix the gauge, where there exist many R_ξ gauge choices one can take. This breaks gauge invariance, however all final physical results after summation of all Feynman diagrams are independent of the gauge choice. Secondly, the three-gluon vertex in figure 2.1b is,

$$V_3 = g f^{abc} [g^{\mu\nu}(p - k)^\rho + g^{\nu\rho}(q - p)^\mu + g^{\rho\mu}(k - q)^\nu] \quad (2.17)$$

and finally the four-gluon vertex in figure 2.1c is

$$\begin{aligned} V_4 = & -ig^2 [f^{abe} f^{cde} (g^{\mu\rho} g^{\nu\sigma} - g^{\mu\sigma} g^{\nu\rho}) \\ & + f^{ace} f^{bde} (g^{\mu\sigma} g^{\nu\rho} - g^{\mu\nu} g^{\rho\sigma}) \\ & + f^{ade} f^{bce} (g^{\mu\nu} g^{\rho\sigma} - g^{\mu\rho} g^{\nu\sigma})] . \end{aligned} \quad (2.18)$$

All possible relevant Feynman graphs for any high energy gluon scattering process, such as those in high energy collisions in CMS and ATLAS experiments at the LHC, can be built out of these rules. Unfortunately, the task of computing even leading order (LO) $gg \rightarrow ng$ processes becomes computationally intensive; 220 diagrams for $n = 4$, increasing to 2485, 34300, 559405 and 10525900 diagrams through $n = 8$, from Table 1 in [24]. Furthermore, the self interactions of non-Abelian gauge bosons are so complicated that even the individual diagrams manifest a massively inflated number of terms generated from increasing indices. Also, the number of kinematic variables used to define all the required information from the outset generates arbitrarily complicated intermediate expressions. This illustrates the reason for the proliferation of computing time for modelling these types of gauge theory interactions.

It is surprising then, that the final expressions take a very simple form, especially when expressed in a more efficient framework. Even at NLO in perturbation theory, the final expressions do not grow in complexity as radically as the number of diagrams and terms to compute. This seems to hint that the way interactions of gauge theories are calculated through building Feynman diagrams from the lagrangian is not the best

2.3 Scattering amplitudes and their divergences

way to present scattering amplitudes. Therefore gauge theories have hidden structure that is not yet understood. Nevertheless, many computational techniques have been developed that will be discussed in the following chapters.

For the most part, the simplest next-to-NLO (NNLO) calculations match simple experimental processes to within a few per cent. Therefore the concentration on perturbative calculations is to categorise each order in the \mathcal{S} -matrix elements, up to experimental precision. As soon as one wishes to calculate NLO corrections in the perturbative expansion, there are infinities that fortunately can be regulated. These divergences are dealt with using renormalisability and dimensional regularisation.

2.3 Scattering amplitudes and their divergences

Perturbation theory allows the expansion of the Feynman path integral as a power series in the coupling constant g , from which one can determine the Feynman rules. These allow a basis of possible Feynman diagrams to be constructed and from then on, perturbative gauge theory is relatively simple. One simply draws all possible Feynman diagrams that contribute to a scattering amplitude to a desired order in the coupling $\alpha_s = g^2/4\pi$, to define the \mathcal{S} -matrix elements. The diagrams are then sums of shorthand graphical interpretations of algebraic expressions to be evaluated. The LO contributions at $\mathcal{O}(\alpha_s)$ in the perturbative expansion are classed as tree-level diagrams since all momenta along internal lines are determined by momenta of the external gluons. Higher order contributions allow for independent momenta arising in closed loops that have to be integrated over. They form the perturbations away from the solvable (classical) solution that is determined by the Hamiltonian of the theory. All NLO and higher corrections are then known as one-loop at $\mathcal{O}(\alpha_s^2)$, two-loop at $\mathcal{O}(\alpha_s^3)$, and so on, that is continued to ones desired degree of accuracy. However, these internal momenta dependent integrals tend to diverge in general, such that a cut-off ϵ in both IR or UV energy divergences is required.

As mentioned in Chapter 1, QCD exhibits UV asymptotic freedom, discovered in 1973 from the computation of the running of the coupling under the renormalisation group, by Gross and Wilczek [25], and independently by Politzer [26] and 't Hooft. See [15] section 17.2 for a thorough treatment of the QCD coupling by renormalisation. Asymptotic freedom allows calculations using perturbation theory to be performed in a

2.3 Scattering amplitudes and their divergences

high energy regime where the coupling constant $\alpha_s = g^2/4\pi$ is guaranteed to be much less than one. UV divergences occur in the building blocks of figure 2.1, which are reabsorbed into a renormalisation of the lagrangian such that all amplitudes are then finite in the UV. Hence the coupling α_s requires renormalisation defined at some mass scale μ to remove the UV divergences. The running of the coupling is determined by the universal beta function, taken from [27]

$$\mu^2 \frac{\partial^2 \alpha_s(\mu)}{\partial \mu^2} = \beta(\alpha_s(\mu)), \quad (2.19)$$

which has the expansion

$$\beta(\alpha_s) = -\alpha_s^2(\beta_0 + \beta_1 \alpha_s + O(\alpha_s^2)), \quad (2.20)$$

where β_0 and β_1 are calculated order by order in the coupling. Neglecting β_1 and higher coefficients, to one-loop order [27];

$$\alpha_s(\mu) = \frac{\alpha_s(\mu_0)}{1 + \alpha_s(\mu_0)\beta_0 \ln(\mu^2/\mu_0^2)}, \quad (2.21)$$

where μ_0 is a dimensionful parameter that is a constant of integration. This introduces a second arbitrary mass scale μ_0 upon which the coupling is dependent. For QCD, the running coupling at one-loop is given by a rewriting of (2.21), to eliminate μ_0 in favour of the experimentally observed $\Lambda_{\text{QCD}} \sim 200\text{MeV}$,

$$\alpha_s(\mu) = \frac{1}{\beta_0 \ln(\mu^2/\Lambda_{\text{QCD}}^2)}, \quad (2.22)$$

where β_0 was first calculated for $SU(N_c)$ pure gauge theory in [25], and for QCD with $N_c = 3$ is

$$\beta_0 = \frac{(33 - 2n_f)}{12\pi} \quad (2.23)$$

for n_f quark flavours. The parameter Λ_{QCD} marks the energy scale where α_s becomes greater than one as mentioned in Chapter 1. Therefore fall off of the coupling as the energy scale μ increases is clearly evident, revealing asymptotic freedom. The value of the coupling is normally determined at the mass of the Z^0 boson $\mu = m_{Z^0}$, which is a convenient reference scale to guarantee $\alpha_s(m_{Z^0})$ is in the perturbative domain.

QCD has IR singularities due to collinear or soft emission of gluons, dependent on the long range interactions or hadronisation of quarks. However, one can calculate IR safe or factorisable quantities due to asymptotic freedom and stay in the short-distance regime. The long range interactions correspond to hadronisation of quarks into jets, which are not amenable to perturbative study. Jet production and the analysis of parton distribution is an essential part of understanding the hadronisation process. Parton distribution functions determined from data that obey the DGLAP evolution equations [28–31], provide information on the long range dynamics. These factorise from the perturbative regime of QCD, which permits the emphasis on analysing the pure gauge theory interactions. IR divergences are dealt with via so-called dimensional regularisation, where divergences are replaced by powers of $1/\epsilon$. Reduction of dimensional tensor integrals in loop calculations to order ϵ is a common technique applied to the NLO loop integrals. A possible schematic setup of these integrals to reduce the order of loop momenta in the numerator is by Passarino-Veltman reduction.

2.4 Passarino-Veltmann reduction

Traditional techniques for computation of one-loop integrals include Passarino-Veltman reduction, based on work by Passarino and Veltman [32], and 't Hooft and Veltman [33], with numerous treatments of the method in [34]. The reduction procedure deals with 4-dimensional integrals of the following form [35],

$$I_n[\mathcal{P}(\ell)] = \int \frac{d^4\ell}{(2\pi^4)} \frac{\mathcal{P}(\ell)}{\prod_{i=1}^n ([\ell + p_{i-1}]^2 - m_i^2)}, \quad (2.24)$$

where n is the number of external particles with momentum k_j , where $p_i = \sum_{j=1}^i k_j$, and $p_0 = p_n = 0$ by momentum conservation. The m_i^2 are internal masses along the loop dependent propagators, which are more commonly zero $m_i^2 = 0$. The numerator contains a function of loop momenta $\mathcal{P}(\ell)$. The special case where the numerator $\mathcal{P}(\ell) = 1$ is known as a scalar integral. These are the known master integrals to which the original integrals are targeted.

Of course, in general $\mathcal{P}(\ell)$ is a polynomial function of various contractions of external momenta k_i , polarisation vectors and the loop momentum ℓ . From simple power counting, the n -point integral $I_n[\mathcal{P}(\ell)]$ manifests UV divergences for tensor integrals of

2.4 Passarino-Veltmann reduction

rank r contained in $\mathcal{P}(\ell)$ for $r \geq 2n - 4$. In QCD, the highest rank of an n -point one-loop diagram is $r = n$, hence only one-, two- three- and four-point one-loop integrals can be divergent in the UV region. Integrals of five-point or higher are then UV finite, while the former divergent integrands require regularisation. It is conventional to employ dimensional regularisation [16], where the computation is performed in $D = 4 - 2\epsilon$ dimensions, and the limit $\epsilon \rightarrow 0$ is taken at the end of the calculation. The integration therefore becomes D -dimensional and the measure is changed accordingly,

$$\frac{d^4\ell}{(2\pi)^4} \rightarrow \frac{d^D\ell}{(2\pi)^D}. \quad (2.25)$$

With ℓ now a D -dimensional vector, the integrals cannot in general diverge. Therefore, this modification regularises UV divergences in one-loop computations.

For propagators in the integrand going on shell simultaneously, non-integrable singularities are introduced. The most important examples of these are through soft and collinear singularities [36], however these can also be dimensionally regularised [37]. One can therefore define one-loop integrals in UV-divergent, renormalisable theories which contain massless particles with a single parameter $\epsilon = (4 - D)/2$.

It turns out that any one-loop integral $I_n[\mathcal{P}(l)]$ can be written as a linear combination of scalar integrals via the Passarino-Veltman prescription. Furthermore, in the limit $D \rightarrow 4$, any n -point one-loop amplitude $A_n^{1\text{-loop}}$ can be expressed with a basis of integrals. In a massless theory, the basis is made of so called bubble, triangle and box scalar integrals,

$$A_n^{1\text{-loop}} = \sum_{i=2,3,4} c_i I_n^i + R_n + O(\epsilon), \quad (2.26)$$

up to $O(\epsilon)$. The c_i can be computed in four dimensions, independent of R_n that is a rational part (i.e. no logarithmic or π^2 terms) which is a remnant of the dimensional regularisation procedure. For amplitudes that contain no branch cuts, only the rational function of kinematic invariants R_n survives. Keeping terms in higher order in ϵ leads to independent pentagons, and tadpoles only contribute in dimensionally regularised theories if one allows internal masses. All valid branch cuts allow complete knowledge of a one-loop amplitude purely from the rational coefficients c_i and the basis of loop integrals, when working in $(4 - 2\epsilon)$ -dimensions. One loop amplitudes of this type are

deemed entirely cut-constructible, explained in the unitarity section. In practice this is more difficult than evaluating the procedure in four dimensions. For most practical calculations, the c_i in (2.26) are computed in four dimensions, an example of which is shown in the unitarity section in Chapter 5. This forces the rational terms R_n to be computed separately.

The scalar integrals are known, so depending on what the theory of concern is, one will require a procedure for finding the rational term R_n and rational coefficients of the integrals c_i to determine any one-loop amplitude. The details for the tensor reduction of the numerator $\mathcal{P}(\ell)$ and the set of scalar integrals complete the chapter.

2.4.1 The reduction by example

Let us demonstrate the procedure of Passarino Veltman reduction with an example, taken from Appendix A.2 of [35]. Consider the three-point integral of rank one tensor in the numerator with internal masses set to zero (for simplicity), so that the integral takes the form of the triangle version of (2.24). Projecting on to a basis of the external momenta p_i ,

$$I_3[\ell^\mu] = \int \frac{d^4\ell}{(2\pi^4)} \frac{\ell^\mu}{\ell^2(\ell+p_1)^2(\ell+p_2)^2} = \sum_{i=1}^4 C_{n;i} p_i^\mu, \quad (2.27)$$

whilst recalling $p_i = \sum_{j=1}^i k_j$. Contracting both sides of the equation with firstly p_1^μ and then p_2^μ procures two linear equations to solve for the two unknowns $C_{3;1}$ and $C_{3;2}$,

$$\begin{aligned} \int \frac{d^4\ell}{(2\pi^4)} \frac{\ell \cdot p_1}{\ell^2(\ell+p_1)^2(\ell+p_2)^2} &= C_{3;1} p_1^2 + C_{3;2} p_1 \cdot p_2, \\ \int \frac{d^4\ell}{(2\pi^4)} \frac{\ell \cdot p_2}{\ell^2(\ell+p_1)^2(\ell+p_2)^2} &= C_{3;1} p_1 \cdot p_2 + C_{3;2} p_2^2. \end{aligned} \quad (2.28)$$

Using

$$\ell \cdot p_i = \frac{1}{2} ((\ell+p_i)^2 - \ell^2 - p_i^2), \quad (2.29)$$

the RHS can be substituted into (2.28). This allows for the re-expression of the integrals by cancellation of the numerators including ℓ dependent propagators with integrals of

2.4 Passarino-Veltmann reduction

one rank lower. These integrals contain the superscript (j) indicating the $(\ell + p_j)^2$ propagator that was cancelled,

$$\begin{aligned} C_{3;1} p_1^2 + C_{3;2} p_1 \cdot p_2 &= I_2^{(1)}[1] - I_2^{(0)}[1] - p_1^2 I_3[1], \\ C_{3;1} p_1 \cdot p_2 + C_{3;2} p_2^2 &= I_2^{(2)}[1] - I_2^{(0)}[1] - p_2^2 I_3[1]. \end{aligned} \quad (2.30)$$

Then a matrix equation can be formulated for the unknowns

$$\begin{pmatrix} p_1^2 & p_1 \cdot p_2 \\ p_2 \cdot p_1 & p_2^2 \end{pmatrix} \begin{pmatrix} C_{3;1} \\ C_{3;2} \end{pmatrix} = \begin{pmatrix} I_2^{(1)}[1] - I_2^{(0)}[1] - p_1^2 I_3[1] \\ I_2^{(2)}[1] - I_2^{(0)}[1] - p_2^2 I_3[1] \end{pmatrix}, \quad (2.31)$$

where to find the solution, the matrix to be inverted is known as the Gram matrix Δ_{ij} . For this simple case, the solution is

$$\begin{pmatrix} C_{3;1} \\ C_{3;2} \end{pmatrix} = \frac{1}{p_1^2 p_2^2 - (p_1 \cdot p_2)^2} \begin{pmatrix} p_2^2 & -p_1 \cdot p_2 \\ -p_2 \cdot p_1 & p_1^2 \end{pmatrix} \begin{pmatrix} I_2^{(1)}[1] - I_2^{(0)}[1] - p_1^2 I_3[1] \\ I_2^{(2)}[1] - I_2^{(0)}[1] - p_2^2 I_3[1] \end{pmatrix} \quad (2.32)$$

where the leading factor is known as the Gram determinant. The rank of the tensor integral was successfully reduced from one to zero, as a linear combination of scalar bubbles and triangle integrals. Care must be taken for cases where $n > 4$, since a basis must be chosen with four linearly independent momenta for which the Gram determinant does not vanish, and therefore UV finite. There will be some cases for $n \leq 4$ where the Passarino Veltman scheme will break down, however [34] has an alternative way of making the reduction for vanishing Gram determinants.

To evaluate integrals with tensors of higher rank, one must follow the same set of steps but project onto all possible Lorentz objects in the basis. So, for example

$$\begin{aligned} I_n[\ell^\mu \ell^\nu] &= C_{n;00} g^{\mu\nu} + \sum_{i,j} C_{n;ij} p_i^\mu p_j^\nu \\ I_n[\ell^\mu \ell^\nu \ell^\rho] &= \sum_{i=1}^4 C_{n;00i} g^{\{\mu\nu} p_i^{\rho\}} + \sum_{i,j,k=1}^4 C_{n;ijk} p_i^{\{\mu} p_j^\nu p_k^{\rho\}} \\ &\vdots \end{aligned} \quad (2.33)$$

where the curly braces indicate total symmetrisation of the indices. In the case of two powers of ℓ , one must also project on to the metric $g^{\mu\nu}$. However for $n > 4$, $DC_{n;00}$ becomes irrelevant, since it is also linearly dependent on the four chosen vectors. In

2.4 Passarino-Veltmann reduction

the case of three powers of ℓ , one needs to contract with $g^{\mu\nu}p_r^\rho$ and with $p_r^\mu p_s^\nu p_t^\rho$ to obtain a set of linear equations for the coefficients $C_{n;00i}$ and $C_{n;ijk}$. Beyond rank three projection with products of metrics is also included, and so the list for the basis accelerates. Therefore this process becomes more complicated as the power of ℓ grows, with the basis and various contractions growing rapidly. However, the reduction process guarantees to reduce the rank of the tensor in the numerator by one. From whatever rank tensor the integral is, one can iteratively repeat the process of projecting integrals on to combinations of external momenta in this fashion and building the set of matrix equations to find the Gram determinant. One can repeat this procedure until only a linear combinations of scalar integrals remain.

2.4.2 The scalar integrals

Scalar integrals fall into categories of bubbles $I_2[1]$, triangles $I_3[1]$, and boxes $I_4[1]$. The list of integral functions that can occur can be categorised as a set of functions \mathcal{F}_n with the argument $\mathcal{P}(\ell)$ dropped and there are no internal masses. The analytic results or computations are not included here, but are in Appendix I of [38], whose notation we shall adopt,

$$\mathcal{F}_n = \{I_{4:r,r',r'';i}^{4m}, I_{4:r,r';i}^{3m}, I_{4:r;i}^{2mh}, I_{4:r;i}^{2me}, I_{4:i}^{1m}, I_4^{0m}, I_{3:r,r';i}^{3m}, I_{3:r;i}^{2m}, I_{3:i}^{1m}, I_{2:r;i}\}. \quad (2.34)$$

The superscripts of this set \mathcal{F}_n define how many external masses exist, with clusters of external momenta labelled in clockwise direction for $r \rightarrow r' \rightarrow r''$ starting from i , depicted pictorially in figures 2.2, 2.3 and 2.4. The two mass boxes split into two cases, one hard and one easy, denoted by whether the masses are adjacent or not, respectively. The explicit computation of the integrals are detailed in the Appendix of [38].

2.4 Passarino-Veltmann reduction

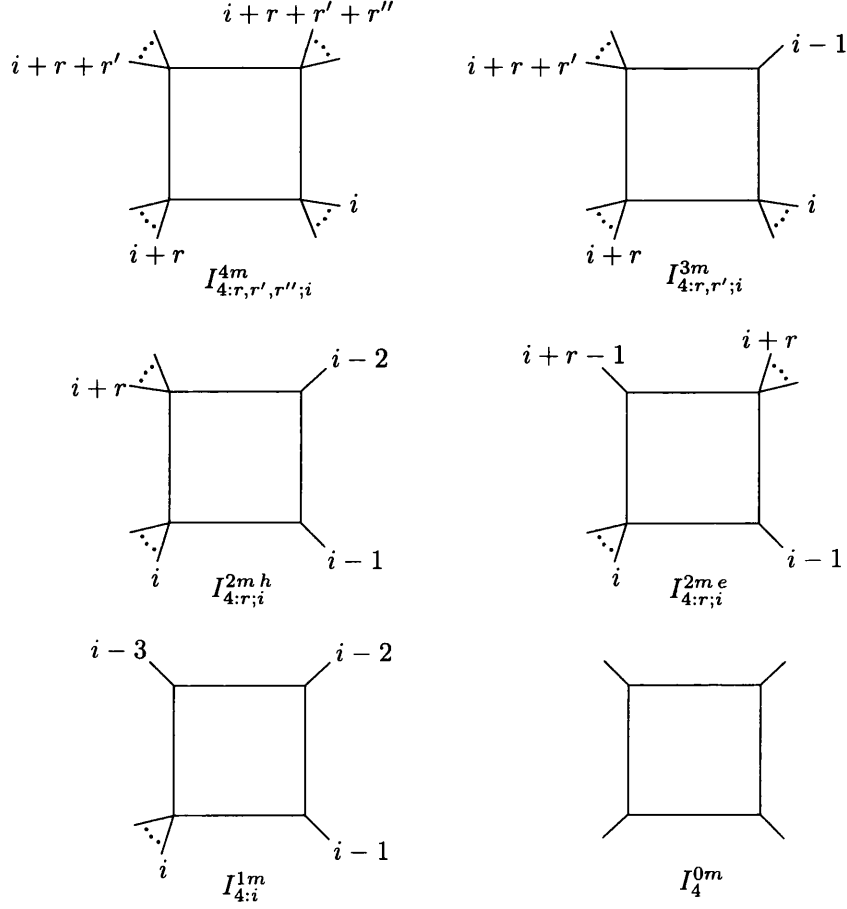


Figure 2.2: The box contributions, including the four-mass, three-mass, two-mass hard and two mass easy, the one-mass and zero-mass integrals.

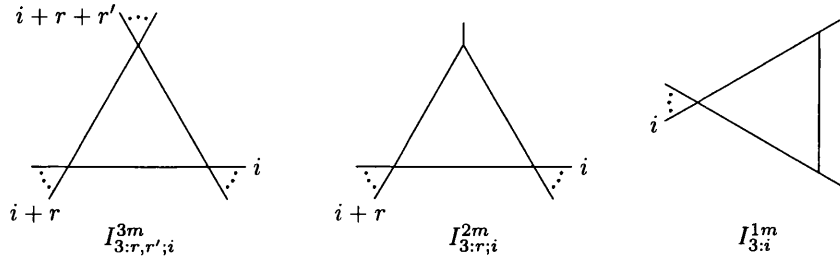


Figure 2.3: The three-mass, two-mass and one-mass triangle contributions.

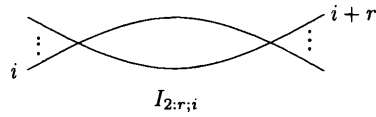


Figure 2.4: The two mass bubble contribution $I_{2:r,i}$.

Chapter 3

Organised amplitudes

In this chapter we describe the modern techniques for computing scattering amplitudes in massless non-Abelian gauge theories, that build on the standard techniques outlined in Chapter 2. Those include the consideration of color-ordered partial amplitudes for leading order and NLO, the spinor-helicity formalism and how this is used in a specific gauge to build the simplest tree-level amplitudes.

3.1 Color ordered amplitudes

Firstly, the factorisation of the color information for pure Yang Mills at both tree-level [24, 39–42] and one-loop [43, 44] is outlined, which is the first step towards healing the proliferation of Feynman diagrams.

3.1.1 Tree level

From the vertices of Yang Mills theory (2.17), (2.18), one finds either linear or quadratic factors of the gauge theory structure constants f^{abc} . These can be unpacked into traces over products of generators of the theory. The generators of $SU(N_c)$ in the fundamental representation are represented by T^a , where the index $a = 1 \dots N_c^2 - 1$ refers to the adjoint color index carried by the fermions, and N_c is the number of colors. The structure constants are then rewritten as a trace from their definition (2.5),

$$f^{abc} = \frac{i}{\sqrt{2}} \text{tr}(T^a T^b T^c - T^c T^b T^a). \quad (3.1)$$

3.1 Color ordered amplitudes

Unpacking this definition in two connected three-gluon vertices (2.17) for example, the T_c internal leg is replaced from the second vertex via $f^{cde}T^c = -i[T^d, T^e]$. This process is exhausted to leave all Feynman diagrams having vertices with a large number of traces over products of generators describing color information of the external gluons only. The traces appear in the form $\text{tr}(\dots T^a \dots) \text{tr}(\dots T^a \dots) \dots \text{tr}(\dots T^a \dots)$, which can be rearranged in to a single trace with $1/N_c$ suppressed terms using the $SU(N_c)$ Fierz identity [43],

$$\text{tr}(T^a X) \text{tr}(T^a Y) = \text{tr}(XY) - \frac{1}{N_c} \text{tr}(X) \text{tr}(Y). \quad (3.2)$$

By making the substitutions of equations (3.1) and (3.2), suppressing the $1/N_c$ terms where appropriate, all possible permutations of a single trace are left. This color information can now be factorised out to leave color-ordered Feynman rules [42] for massless QCD as follows.

Indices contracted together in the gluon propagator (2.16), leave us with the simplified color-ordered version

$$-\frac{i}{p^2} g^{\mu\nu}, \quad (3.3)$$

where we have used the Feynman gauge choice of $\xi = 1$. The color-ordered three-gluon vertex is simply,

$$V_3 = -\frac{ig}{\sqrt{2}} [g^{\mu\nu}(p-k)^\rho + g^{\nu\rho}(q-p)^\mu + g^{\rho\mu}(k-q)^\nu] \quad (3.4)$$

and the color-ordered four-gluon vertex is

$$V_4 = -ig^2 (g^{\mu\rho} g^{\nu\sigma} - \frac{1}{2} [g^{\mu\sigma} g^{\nu\rho} + g^{\mu\nu} g^{\rho\sigma}]). \quad (3.5)$$

All color-ordered *partial* tree amplitudes A_n can be built out of the color-ordered rules (3.3), (3.4) and (3.5). Then by combining the traces over generators into a sum,

3.1 Color ordered amplitudes

the color decomposition for a full n -gluon tree amplitude \mathcal{A}_n is [39–41],

$$\mathcal{A}_n^{\text{tree}}(\{k_i, \lambda_i, a_i\}) = g^{n-2} \sum_{\sigma \in S_n/Z_n} \text{Tr}(T^{a_{\sigma(1)}} \dots T^{a_{\sigma(n)}}) A_n^{\text{tree}}(\sigma(k_1^{\lambda_1}), \dots, \sigma(k_n^{\lambda_n})). \quad (3.6)$$

The leading g is the gauge coupling given by $\alpha_s = g^2/4\pi$ and the $\sigma \in S_n/Z_n$ are all possible distinct cyclic permutations of color orderings that appear in the trace. A_n is a function dependent on the momenta k_i and helicity λ_i of the gluons and contains one cyclically arranged configuration, such that kinematic singularities are restricted to the cyclically adjacent momentum channels, i.e. $s_{12} = (k_1 + k_2)^2$. The remaining partial amplitudes are now the focus of our attention, since after calculation one can recover the full amplitude via (3.6).

By construction these partial amplitudes $A_n^{\text{tree}}(1^{\lambda_1} \dots n^{\lambda_n})$ are much simpler, as they only receive contributions from a particular color ordering. They also benefit from a number of important properties and relationships. They are individually gauge invariant, so we have free gauge choice between different partial amplitudes. The number of partial amplitudes to be computed is reduced because they exhibit symmetries such as parity, where all helicities in an amplitude can be flipped simultaneously. They observe reflection of the arguments:

$$A_n^{\text{tree}}(1^{\lambda_1} \dots n^{\lambda_n}) = (-1)^n A_n^{\text{tree}}(n^{\lambda_n} \dots 1^{\lambda_1}). \quad (3.7)$$

They also permit dual Ward identities, which provide relations between partial amplitudes where two negative helicities are adjacent or not for example [42]. Given these relations and symmetries, the calculations of partial tree amplitudes still require much work.

3.1.2 Loop level

At one-loop, the color stripped decomposition includes non-planar graphs. For the planar pieces the leading color structure still incorporates a sum of traces, but now multiplied by a factor of N_c :

$$\text{Gr}_{n;1} = N_c \text{Tr}(T^{a_{\sigma(1)}} \dots T^{a_{\sigma(n)}}). \quad (3.8)$$

3.2 Spinor helicity formalism

Non-planar graphs contribute sub-leading color structures given by

$$\text{Gr}_{n;c} = N_c \text{Tr}(T^{a_{\sigma(1)}} \dots T^{a_{\sigma(c-1)}})(T^{a_{\sigma(c)}} \dots T^{a_{\sigma(n)}}), \quad (3.9)$$

where $c > 1$. Equations (3.8) and (3.9) combine to form the one-loop color-ordered decomposition formula [43], using $\lfloor x \rfloor$ as the largest integer less than or equal to x

$$\mathcal{A}_n^{1\text{-loop}}(\{k_i, \lambda_i, a_i\}) = \sum_{c=1}^{\lfloor n/2 \rfloor + 1} \sum_{\sigma \in S_n / S_{n;c}} \text{Gr}_{n;c}(\sigma) A_{n;c}^{1\text{-loop}}(\sigma), \quad (3.10)$$

where S_n is the set of all permutations of n objects, and $S_{n;c}$ is the subset leaving $\text{Gr}_{n;c}$ invariant. It turns out that *non-planar* partial amplitudes $A_{n;c}^{1\text{-loop}}$ for $c > 1$ can be expressed as sums over permutations of leading color *planar* amplitudes $A_{n;1}^{1\text{-loop}}$ [44]. So we will only compute $A_{n;1}^{1\text{-loop}}(1^{\lambda_1}, 2^{\lambda_2}, \dots, n^{\lambda_n})$, the *planar* also known as *primitive*, partial amplitudes at one-loop, where the $n;1$ subscripts will be dropped throughout.

For the purposes of the work discussed, we will not consider calculations beyond one-loop, hence further generalisations are not required. Calculating any two-loop amplitudes in pure Yang-Mills theory is beyond most of current technology, other than to simplify the calculation by considering only a low number of points or theories with more symmetries built in, namely supersymmetry (see Chapter 4). Staying with pure Yang-Mills theory, a compact representation for tree-level and one-loop amplitudes via the spinor helicity formalism follows.

3.2 Spinor helicity formalism

Here we review the notation to be used throughout the thesis when presenting calculations of partial amplitudes and primitive one-loop amplitudes. A thorough exposition of the spinor notation can be found in [45–52] that we shall utilise. In general the four momentum k_i^μ upon which the amplitudes are dependent are contracted with either polarisation vectors or other four-vectors in Lorentz invariants such as $s_{ij} = (k_i + k_j)^2$. For on-shell or massless momenta $s_{ij} = 2k_i \cdot k_j$, that we shall indeed restrict ourselves to in this formalism, for lowercase letters ($k_i^2 = 0$).

The restricted Lorentz group, denoted $SO^\dagger(1, 3)$ refers to the symmetries preserved in the flat metric, i.e. direction of time and orientation of space. This is locally iso-

3.2 Spinor helicity formalism

morphic to the Möbius group $SL(2; \mathbb{C}) \times SL(2; \mathbb{C})$. This observation was developed by Penrose into twistor theory [53]. The $SO^\dagger(1, 3)$ group has vector representations that may be classified as (m, n) , where m and n are half-integers describing the spin of the representation. One can then decompose four momenta k^μ into a choice of two or bi-spinor representations.

It is conventional to use Dirac spinors, which decompose into $(\frac{1}{2}, 0)$ and $(0, \frac{1}{2})$, that are the left- and right-handed chiral Weyl spinors, respectively. The complexified Lorentz group can then be used to project four-vectors on to a $(\frac{1}{2}, \frac{1}{2})$ bi-spinor $p_{\alpha\dot{\alpha}}$ where $\alpha, \dot{\alpha} = 1, 2$. One can then map from Minkowski coordinates (t, x, y, z) into this representation using

$$p_{\alpha\dot{\alpha}} = p_\mu (\sigma^\mu)_{\alpha\dot{\alpha}} = \begin{pmatrix} p^t + p^z & p^x - ip^y \\ p^x + ip^y & p^t - p^z \end{pmatrix}, \quad (3.11)$$

where the four-vector Pauli matrices are defined as

$$(\sigma^\mu)^{\alpha\dot{\alpha}} = (1, \boldsymbol{\sigma}) \quad \text{and} \quad (\bar{\sigma}^\mu)_{\alpha\dot{\alpha}} = (1, -\boldsymbol{\sigma}) \quad (3.12)$$

and $\boldsymbol{\sigma}$ is the three-vector Pauli matrices. Since $\det p_{\alpha\dot{\alpha}} = p^2 = 0$, then $p_{\alpha\dot{\alpha}}$ may be factorised as two Weyl spinors. The spinor indices $(\alpha, \dot{\alpha})$ highlight the distinctive two component label for each chiral spinor, to be identified as follows.

The positive and negative energy solution to the massless Dirac equation, $u_\pm(p)$ and $v_\pm(p)$ respectively, are identical up to normalisation conditions $u_\pm(p) = v_\mp(p)$, where the \pm sign identifies the helicity. The helicity states can be defined by acting with the chiral projection operators

$$u_\pm(p) = \frac{1}{2}(1 \pm \gamma_5)u(p), \quad (3.13)$$

where the positive and negative helicity states are identified as positive and negative chirality spinors $\lambda_i, \bar{\lambda}_i$ [54],

$$(\lambda_i)_\alpha \equiv [u_+(p_i)]_\alpha, \quad (\bar{\lambda}_i)_{\dot{\alpha}} \equiv [u_-(p_i)]_{\dot{\alpha}}. \quad (3.14)$$

Now the bi-spinor is defined as

$$(\sigma_\mu)_{\alpha\dot{\alpha}} p_i^\mu = (\lambda_\alpha)_i (\bar{\lambda}_{\dot{\alpha}})_i, \quad (3.15)$$

3.2 Spinor helicity formalism

where λ_α , and $\bar{\lambda}_{\dot{\alpha}}$ are holomorphic and anti-holomorphic spinors in the left- and right-handed half-integer spin representations. This reflects the property that a massless four-vector, when expressed as a bi-spinor, is simply the product of a left- and right-handed Weyl spinor.

With this notation, one can build Lorentz invariant spinor products using shorthand “ $\langle \ , \ \rangle$ ” and “[$\ , \]$ ” identifications [54],

$$\begin{aligned}\langle ij \rangle &\equiv \langle i^- | j^+ \rangle = \overline{u_-(p_i)} u_+(p_j) = \epsilon^{\alpha\beta} (\lambda_i)_\alpha (\lambda_j)_\beta, \\ [ij] &\equiv \langle i^+ | j^- \rangle = \overline{u_+(p_i)} u_-(p_j) = \epsilon^{\dot{\alpha}\dot{\beta}} (\bar{\lambda}_i)_{\dot{\alpha}} (\bar{\lambda}_j)_{\dot{\beta}},\end{aligned}\tag{3.16}$$

where the ϵ are $SU(2)$ antisymmetric tensors. These are used for raising and lowering the spinor indices, given by

$$\epsilon_{\alpha\beta} = \begin{pmatrix} 0 & 1 \\ -1 & 0 \end{pmatrix} \quad \text{and} \quad \epsilon_{\dot{\alpha}\dot{\beta}} = \begin{pmatrix} 0 & -1 \\ 1 & 0 \end{pmatrix},\tag{3.17}$$

such that $\epsilon^{\alpha\beta} \epsilon_{\beta\gamma} = \delta_\gamma^\alpha$. Likewise the same occurs for the case with dotted indices. The spinor products behave anti-symmetrically

$$\langle ij \rangle = -\langle ji \rangle, \quad [ij] = -[ji], \quad \langle ii \rangle = [ii] = 0,\tag{3.18}$$

and one can use the projection operator

$$|i^\pm\rangle\langle i^\pm| = \frac{1}{2}(1 \pm \gamma_5) \not{k}_i, \quad \not{k}_i = |i^+\rangle\langle i^+| + |i^-\rangle\langle i^-|,\tag{3.19}$$

to define Lorentz invariant products:

$$\langle ij \rangle [ji] = \text{tr} \left(\frac{1}{2} (1 - \gamma_5) \not{k}_i \not{k}_j \right) = 2k_i \cdot k_j = (k_i + k_j)^2 \equiv s_{ij}.\tag{3.20}$$

This can also be shown from the bi-spinors of two momenta p and q , by noticing that $(\bar{\sigma}^\mu)^{\alpha\dot{\alpha}} = (\sigma^\mu)^{\alpha\dot{\alpha}}$ and application of (3.11),

$$p^{\alpha\dot{\alpha}} q_{\alpha\dot{\alpha}} = 2p \cdot q.\tag{3.21}$$

We denote sums of cyclically adjacent momenta as

$$P_{i,j} = p_i + p_{i+1} + \dots + p_{j-1} + p_j\tag{3.22}$$

3.2 Spinor helicity formalism

with indices mod n for an n -gluon amplitude. The general invariant mass of the vector is $P_{i,j}^2$, of which (3.20) is a special case.

We will also use spinor strings such as

$$\langle a^- | P_{i,j} | b^- \rangle = [a | P_{i,j} | b] = \sum_{p \in i,j} [ap] \langle pb \rangle \quad (3.23)$$

which vanishes for $i = 1, j = n$ and $a, b \neq i, j$ in an n -gluon amplitude, where

$$\begin{aligned} [a | i + j | b] &= [ai] \langle ib \rangle + [aj] \langle jb \rangle, \\ \langle a | (i + j)(k + l) | b \rangle &= \langle ai \rangle [i | k + l | b] + \langle aj \rangle [j | k + l | b]. \end{aligned} \quad (3.24)$$

As well as antisymmetry, there are other useful identities, the Gordon identity;

$$\langle i^\pm | \gamma^\mu | i^\pm \rangle = 2k_i^\mu, \quad (3.25)$$

Fierz rearrangement;

$$\langle i^+ | \gamma^\mu | j^+ \rangle \langle k^+ | \gamma^\mu | l^+ \rangle = 2[ik] \langle lj \rangle, \quad (3.26)$$

and charge conjugation of current;

$$\langle i^+ | \gamma^\mu | j^+ \rangle = \langle j^- | \gamma^\mu | i^- \rangle. \quad (3.27)$$

However, the most useful identities that can be derived from those above, used for practical manipulations are;

$$\begin{aligned} \langle i | pq | j \rangle + \langle i | qp | j \rangle &= 2p \cdot q \langle ij \rangle, & \langle i | pp | j \rangle &= p^2 \langle ij \rangle, \\ \langle i | j | p \rangle \langle j | p | i \rangle &= (2k_i \cdot p)(2k_j \cdot p) - p^2(2k_i \cdot k_j), \end{aligned} \quad (3.28)$$

and lastly but by no means least the Schouten identity for spinors;

$$\langle ij \rangle \langle kl \rangle = \langle ik \rangle \langle jl \rangle + \langle il \rangle \langle kj \rangle, \quad (3.29)$$

which can be identically expressed for the anti-holomorphic spinors.

3.2.1 Complex momenta

The notion of complex momenta in quantum field theories is by no means a new one. As we shall explore in Chapter 5, complex momenta are vital ingredients in deriving recursion based relations and as parts of one-loop amplitudes via generalised unitarity cuts.

Complex momenta are extremely useful in computing non-vanishing three-point amplitudes in a massless theory, despite $s_{ij} = 0$ imposing collinearity for all three massless momenta of legs i , j and k . Recall from (3.15) that for *real* momenta the null spinors obey $\lambda = \pm \bar{\lambda}^*$, such that spinor products are complex square roots of the Lorentz invariants [42]

$$\langle ab \rangle = \pm \sqrt{s_{ab}} e^{i\phi_{ab}}, \quad [ab] = \pm \sqrt{s_{ab}} e^{-i\phi_{ab}}. \quad (3.30)$$

So, for vanishing s_{ij} the spinor products must vanish too. However, under continuation to complex momenta (3.30) no longer holds. To illustrate this, let us consider the momentum conservation upon a three-point amplitude, or equivalently the three-point vertex for spinors (where the α, β indices are dropped) [55],

$$\lambda_1 \bar{\lambda}_1 = \lambda_2 \bar{\lambda}_2 + \lambda_3 \bar{\lambda}_3. \quad (3.31)$$

For complex momenta, either the holomorphic or anti-holomorphic spinors are chosen to be proportional. For the choice of holomorphic spinors λ ,

$$\lambda_1 = c_1 \lambda_2, \quad \lambda_3 = c_2 \lambda_2, \quad (3.32)$$

which imposes that

$$\langle 12 \rangle = \langle 23 \rangle = \langle 31 \rangle = 0, \quad (3.33)$$

for some complex c_1 and c_2 . However, this does not prevent a definition of the three-point amplitude in terms of the anti-holomorphic spinors, although all momenta invariants s_{ij} still vanish. Indeed, for the case of the three-gluon tree-level amplitude with two positive helicities and one negative, it is expressed in one term with anti-holomorphic

spinors only [55],

$$A_3^{\text{tree}}(1^+, 2^+, 3^-) = -i \frac{[12]^3}{[23][31]}. \quad (3.34)$$

Therefore the parity reversed analog for two negative helicities and one positive is [55]

$$A_3^{\text{tree}}(1^-, 2^-, 3^+) = i \frac{\langle 12 \rangle^3}{\langle 23 \rangle \langle 31 \rangle}. \quad (3.35)$$

These are the two simplest kind of tree amplitudes, known as maximally helicity violating (MHV) for the holomorphic version and $\overline{\text{MHV}}$ or googly for the anti-holomorphic version. They are built from the color-ordered three-gluon vertex and polarisation vectors to be defined in the next section. One can build $n > 3$ -point amplitudes using these simple three-point amplitudes and their generalisations in section 3.5.

3.2.2 Polarisation vectors for massless particles

From the standard Feynman rules, scattering amplitudes are expressed as products of external momenta and polarisation vectors for the external particles. The massless polarisation vectors for gauge bosons can be expressed in terms of Weyl spinors. Using the Gordon identity; one can define circularly polarised gluons for definite helicities \pm in the bi-spinor notation [45],

$$\varepsilon_{\alpha\dot{\alpha}}^+(p, q) = \frac{(\lambda_q)_\alpha (\bar{\lambda}_p)_{\dot{\alpha}}}{\sqrt{2}\langle qp \rangle}, \quad \varepsilon_{\alpha\dot{\alpha}}^-(p, q) = \frac{(\lambda_p)_\alpha (\bar{\lambda}_q)_{\dot{\alpha}}}{\sqrt{2}[qp]}, \quad (3.36)$$

for a gluon with momentum $p_{\alpha\dot{\alpha}}$, where q is an arbitrary reference momenta, not proportional to p and whose choice does not affect the partial amplitude.

The polarisation vectors obey the relations

$$\begin{aligned} \varepsilon_{\alpha\dot{\alpha}}^\pm(p, q)p^{\alpha\dot{\alpha}} &= 0, & \varepsilon_{\alpha\dot{\alpha}}^\pm(p, q)q^{\alpha\dot{\alpha}} &= 0, \\ \varepsilon_{\alpha\dot{\alpha}}^\pm(p_1, q)\varepsilon^{\pm, \alpha\dot{\alpha}}(p_2, q) &= 0, & \varepsilon_{\alpha\dot{\alpha}}^\mp(p, q)\varepsilon^{\pm, \alpha\dot{\alpha}}(p, q) &= -1, \end{aligned} \quad (3.37)$$

using (3.21) and (3.26), while the latter relation in (3.37) identifies the renormalisation.

Any A_n contains contractions of $\varepsilon(p_i, q) \cdot p_j$ and $p_i \cdot p_j$ for gluons with momenta p_i, p_j and reference spinor q . These products, along with propagators $P_{i\dots j}^2$, are all that is required to build A_n . One common method at tree-level and one-loop, uses the Cachazo, Svrček and Witten (CSW) construction built from MHV vertices. We

shall incorporate the non-null extensions to momenta when required, in an axial gauge to illustrate the prescription with an example. The details of this construction are described once the choice of gauge has been made.

3.3 Axial gauge rules

We consider an extension to off-shell momenta which lends our choice of gauge to an axial one as used by Schwinn and Wienzierl [56]. Any massive four-vector K , can be expressed as a sum of two null vectors: K^b and reference vector q , on which the final amplitude is not dependent. One can associate a massless four-vector K^b to any four-vector K by [57]

$$K^b = K - \frac{K^2}{2K \cdot q} q, \quad (3.38)$$

so that if $K^2 = 0$ (null condition) $K = K^b$ is retrieved (and $2K^b \cdot q = 2K \cdot q$, always holds). Via the projection onto K^b the on-shell spinor formalism can be utilised in its spinor notation

$$\begin{aligned} |K\pm\rangle &\rightarrow |K^b\pm\rangle, \\ \langle K\pm| &\rightarrow \langle K^b\pm|. \end{aligned} \quad (3.39)$$

We can then use the following abbreviations

$$\begin{aligned} \langle ab \rangle &= \langle K_a^b - |K_b^b + \rangle, & [ab] &= \langle K_a^b + |K_b^b - \rangle, \\ \langle a - | b \pm c | d - \rangle &= \langle K_a^b - |K_b^b \pm K_c^b | K_d^b - \rangle, \end{aligned} \quad (3.40)$$

where the massless spinors can be promoted to their full off-shell momenta using (3.38). Furthermore, the gluon polarisation vectors can be expressed in a similar way (for $K^2 \neq 0$), by using the projection on to K^b . This essentially generates the same polarisation vectors as before, now expressed as four-momenta [56]:

$$\varepsilon_\mu^+(K, q) = \frac{\langle q - | \gamma_\mu | K^b - \rangle}{\sqrt{2} \langle q - | K^b + \rangle}, \quad \varepsilon_\mu^-(K, q) = \frac{\langle q + | \gamma_\mu | K^b + \rangle}{\sqrt{2} \langle K^b + | q - \rangle}, \quad (3.41)$$

that satisfy the same relations as (3.37).

3.3 Axial gauge rules

To incorporate off-shell momenta into the axial gauge one requires a modification of the expansion of the sum of polarisation vectors. The polarisation sum is [56]

$$\sum_{\lambda=+/-} \varepsilon_{\mu}^{\lambda}(K, q) \varepsilon_{\nu}^{-\lambda}(K, q) = -g_{\mu\nu} + 2 \frac{K_{\mu}^b q_{\nu} + q_{\mu} K_{\nu}^b}{2K \cdot q}. \quad (3.42)$$

Since the gluon propagator in the axial gauge is given by [56]

$$\frac{i}{K^2} d_{\mu\nu} = \frac{i}{K^2} \left(-g_{\mu\nu} + 2 \frac{K_{\mu} q_{\nu} + q_{\mu} K_{\nu}}{2Kq} \right), \quad (3.43)$$

one can identify (3.42) up to a factor of K^{-2} with the gluon propagating in the axial gauge if one introduces an unphysical polarisation into the sum:

$$\varepsilon_{\mu}^0(K, q) = 2 \frac{\sqrt{K^2}}{2Kq} q_{\mu}. \quad (3.44)$$

So the full propagator can be expressed in terms of the polarisation vectors [56],

$$\frac{i}{K^2} d_{\mu\nu} = \frac{i}{K^2} (\varepsilon_{\mu}^{+} \varepsilon_{\nu}^{-} + \varepsilon_{\mu}^{-} \varepsilon_{\nu}^{+} + \varepsilon_{\mu}^0 \varepsilon_{\nu}^0) \quad (3.45)$$

and the color-ordered propagator is dependent on the scalar propagator times a sum over polarisations as desired. The additional ε^0 can be absorbed into a redefinition of the four-gluon vertex. The four-gluon vertex must have at least one external leg with negative helicity m^{-} , which we can choose to identify with the reference momentum q . This will cause the contribution from those diagrams to vanish, due to leading $\langle mq \rangle / [mq]$ factors. Therefore, with a judicious choice of reference momentum q for our off-shell continuation we will only be using three-gluon vertices in our calculations.

From the properties of the polarisation vectors (3.37) it follows that $V_3(a^{-}, b^{-}, c^{-})$ and $V_3(a^{+}, b^{+}, c^{+})$ vanish. One need only use the color-ordered three-gluon vertex (3.4) along with the polarisation vectors (3.41) to build a vertex with two negative helicities and one positive, and its parity flipped version. These are the only two vertices that will be used,

$$\begin{aligned} V_3(a^{-}, b^{-}, c^{+}) &= i \frac{\langle ab \rangle [cq]^2}{[aq][bq]} = i \frac{\langle ab \rangle^3}{\langle bc \rangle \langle ca \rangle}, \\ V_3(a^{+}, b^{+}, c^{-}) &= i \frac{[ba] \langle cq \rangle^2}{\langle aq \rangle \langle bq \rangle} = i \frac{[ba]^3}{[bc][ca]} \end{aligned} \quad (3.46)$$

and are identical to the three-point maximally helicity violating, MHV (3.35) and $\overline{\text{MHV}}$ (3.34) amplitudes respectively. As highlighted via the equality, the vertices and hence all amplitudes are independent of the choice of reference spinor q which can itself be complex.

3.4 CSW construction from axial gauge

Cachazo, Svrček, and Witten (CSW) proposed a prescription [58] for building n -point color-ordered partial tree amplitudes out of MHV diagrams, that grow no faster than n^2 . In the CSW construction [58], one constructs partial amplitudes A_n by stitching all possible orderings of lower point MHV amplitudes together. By our choice of gauge and reference momenta, (and for the following example) we need only the simplest three-point MHV amplitudes. Also, we shall use examples later with off-shell three-point vertices (3.46) and off-shell MHV currents in Chapter 6.

The general construction for A_n obeys the following rules:

1. Use off-shell three-point MHV vertices (in terms of an arbitrary vector q) or $m < n$ -point MHV vertices.
2. Join the vertices together, helicities \pm to \mp (as the helicities are always considered outgoing and flip from the point of view of an incoming vertex). Between vertices a scalar propagator i/P^2 for momentum P is used.
3. For cases of non-null momenta, we can promote massless spinors $K_{\alpha\dot{\alpha}}^b$ to four momenta K_μ via,

$$|K^b\rangle \equiv K|q], \quad |K^b] \equiv -\frac{K|q\rangle}{2K \cdot q}. \quad (3.47)$$

4. Build A_n using all possible arrangements of scalar propagators between vertices, while summing over possible internal helicity arrangements.

The final result is q independent, but for a judicious choice of q early on, significantly simplifies the computations.

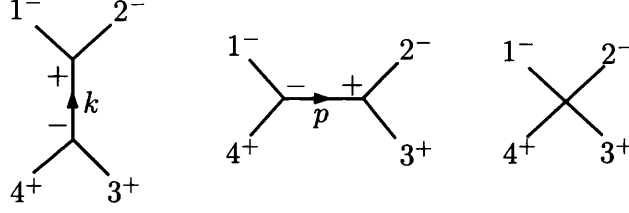


Figure 3.1: Contributions to the partial amplitude $A_4(1^-, 2^-, 3^+, 4^+)$ include three diagrams of which two vanish by gauge choice and judicious choice of vector q .

3.5 n -point MHV amplitudes as an example

Using the rules defined in the section above, we shall build the simplest four-gluon tree-level partial amplitude as a starting point to illustrate the process of computation in the CSW construction. Let us first consider the all positive helicity tree amplitude, $A_n(1^+, 2^+, \dots, n^+)$, which must sum all diagrams that are allowed by attaching at least the $\overline{\text{MHV}}$ vertices only. However, there is no way of ending the process without a spare external negative helicity, and so these amplitudes are zero by construction.

For the case of one negative helicity, then one can repeat the process as before with entirely $\overline{\text{MHV}}$ vertices and construct diagrams where the external vertex with the k_1^- attached contributes a $\langle 1q \rangle^2$ to every diagram. We are free to choose $\lambda_q = \lambda_1$ and all these diagrams vanish and these amplitudes do not contribute.

The first general n -point tree amplitude result that was derived are the MHV amplitudes [59], of which the three-points (3.46) are the simplest case. We will build the four-point color-ordered amplitude $A_4(1^-, 2^-, 3^+, 4^+)$ as an example using the CSW prescription for computing scattering amplitudes. The possible cyclically ordered diagrams available are included in figure 3.1. The two propagators $1/k^2$ and $1/p^2$ in diagrams one and two readily reduce to the special case of a Lorentz invariant, using (3.20). We sum over possible internal helicity configurations, but since we shall make the choice $\lambda_q = \lambda_1$, this requires that vertices with k_1 in them must enter on a diagram with an $(--+)$ vertex. As mentioned before, the choice of reference momentum for q causes the final four-vertex to vanish due to leading $\langle 1q \rangle/[1q]$ factors so we ignore the final contribution.

3.5 n -point MHV amplitudes as an example

The contributions from diagram one and two in figure 3.1 are then

$$A_4(1^-, 2^-, 3^+, 4^+) = \frac{\langle 12 \rangle [(-k)q]^2}{[1q][2q]} \frac{i^3}{k^2} \frac{[43] \langle kq \rangle^2}{\langle 3q \rangle \langle 4q \rangle} + \frac{\langle 1p \rangle [4q]^2}{[1q][pq]} \frac{i^3}{p^2} \frac{[(-p)3] \langle 2q \rangle^2}{\langle 3q \rangle \langle (-p)q \rangle}. \quad (3.48)$$

If we choose an orientation for $k = k_1 + k_2$ and $p = k_2 + k_3$ as off-shell momenta products, we can promote the k^b and p^b spinors to their full momenta via the q -capping procedure used in (3.47). Also, we choose the negative contributions of p and k to only affect the $\bar{\lambda}$ spinors, which introduces a minus sign in the second term. Then the calculation left to evaluate is,

$$A_4(1^-, 2^-, 3^+, 4^+) = \frac{\langle 12 \rangle}{[1q][2q]} \frac{i^3}{s_{12}} \frac{[43]}{\langle 3q \rangle \langle 4q \rangle} [q|1 + 2|q\rangle^2 + \frac{[4q]^2}{[1q]} \frac{i^3}{s_{23}} \frac{\langle 2q \rangle^2}{\langle 3q \rangle} \frac{[3|2 + 3|1\rangle}{[q|2 + 3|q\rangle}. \quad (3.49)$$

Now plugging in our choice for q to reduce the calculation further, we can take $\bar{\lambda}_q = \bar{\lambda}_4$ which will cancel the final term altogether. There is no dependence on $\bar{\lambda}_q$ or λ_q in the final amplitude due to the contractions of polarisation vectors having no overall spinor weight in $\bar{\lambda}_q$ or λ_q . Thus one can freely assign any suitable momentum choice to either part of q . Also, the restricted helicity configuration due to $\lambda_q = \lambda_1$ leaves us with,

$$\begin{aligned} A_4(1^-, 2^-, 3^+, 4^+) &= \frac{\langle 12 \rangle}{[14][24]} \frac{i^3}{s_{12}} \frac{[43]}{\langle 31 \rangle \langle 41 \rangle} [4|1 + 2|1\rangle^2 \\ &= i \frac{\langle 12 \rangle^4}{\langle 12 \rangle \langle 23 \rangle \langle 34 \rangle \langle 41 \rangle} \frac{[24][43] \langle 23 \rangle \langle 34 \rangle}{[21][14] \langle 12 \rangle \langle 31 \rangle} \\ &= i \frac{\langle 12 \rangle^4}{\langle 12 \rangle \langle 23 \rangle \langle 34 \rangle \langle 41 \rangle}. \end{aligned} \quad (3.50)$$

This is the four-point MHV tree-level partial amplitude, and the parity flipped $\overline{\text{MHV}}$ version is found by changing $\langle \rangle \rightarrow []$ and $i \rightarrow -i$. The n -point MHV tree-level amplitudes follow this simple pattern of denominator with cyclic combinations of spinors. This carries the “spinor-weight” of identifying the gluons with positive helicity, while the negative helicity gluons have inverse “spinor-weight” in the numerator to counterbalance the denominator. We review the simplest results for n -gluon tree-level

amplitudes:

$$A(1^\pm, 2^+, \dots, n^+) = 0,$$

$$A(1^+, \dots, i^-, \dots, j^-, \dots, n^+) = \frac{\langle ij \rangle^4}{\langle 12 \rangle \langle 23 \rangle \dots \langle n-1, n \rangle \langle n1 \rangle}, \quad (3.51)$$

where the “...” indicate continuation of cyclically ordered positive helicity gluons. This class of MHV amplitudes was first conjectured by Parke and Taylor [59], and later proven by Berends and Giele [60]. The n -point $\overline{\text{MHV}}$ amplitudes can be easily found by $\langle \rangle \rightarrow []$ and $i \rightarrow -i$ also, which means the parity flipped all-minus and single-plus tree amplitudes vanish too. This machinery has managed to reduce the summation over potentially millions of Feynman diagrams for massless QCD, resulting in six classes of n -point tree amplitudes, (albeit four vanish) in a compact notation. Finding amplitudes with more exotic helicity configurations can be complicated, but once one is found more are accessible via the dual Ward identities. Further enhancement to theories with supersymmetry follow, introducing some of the benefits this brings to tackling QCD, especially at one-loop.

Chapter 4

Utilising supersymmetry in Yang-Mills and Gravity

Although the main motivation touted previously in the introduction was to better understand perturbative QCD, techniques for developing scattering amplitudes in other, simpler theories have proven most useful. In this chapter, we highlight the benefits of constructing Yang-Mills amplitudes with more symmetries; specifically supersymmetry. Many of the efficient calculations of scattering amplitudes were first developed in the context of maximally supersymmetric Yang-Mills theory [44], that has a much simpler structure than real world QCD. They are sufficiently non-trivial however, in revealing many interesting mathematical structures governing the behaviour of the \mathcal{S} -matrix. Specifically, we will discuss the conformal and dual conformal symmetries of $\mathcal{N} = 4$ supersymmetric-Yang-Mills (sYM) theory and highlight the progress of the study of the \mathcal{S} -matrix in this theory. Later, we will also see how a supersymmetric decomposition is useful in calculations of one-loop QCD.

Furthermore, we shall promote our theories from Yang-Mills and gluons to describing graviton interactions, that require an understanding of amplitudes in maximal supergravity, using the Kawai-Lewellen-Tye (KLT) relations [21]. The motivation for analysing on-shell amplitudes of graviton scattering is predominantly to test the perturbative finiteness of quantum gravity. It's non-renormalizability is well known due to the dimensionful nature of Newton's constant, $G_N = M_{\text{Pl}}^{-2}$. String theory is one avenue that cures the UV divergences by introducing a length scale at which particles are no

longer point like. One can take the approach that a non-point like theory may not be necessary to describe a perturbatively finite quantum theory of gravity. The hope is that with enough symmetry, there may well exist a perturbative expansion of a point like theory of quantum gravity. In particular, the testing ground for probing on-shell UV divergences is maximal $\mathcal{N} = 8$ supergravity that admits particles of at most spin 2. We highlight the current state of the finiteness debate and possible counterterms. We also discuss a one-loop decomposition of the pure graviton scattering amplitude.

4.1 Supersymmetric field theories

As we established in the Introduction, combining the translations of spacetime and internal symmetries into supersymmetry is currently the only way to extend the space-time symmetries of particle physics [17].

The maximal number of symmetries \mathcal{N}_{max} that can be accommodated by a field theory or supergravity model originate from two requirements. Firstly, in the necessity of the symmetry transformations to act on the possible multiplets of physical states for the theory. Secondly, it must reflect the core description of the underlying theory. \mathcal{N}_{max} is then defined by either working in a renormalisable field theory in flat-space or in general relativity that permit different values of \mathcal{N}_{max} , despite the supersymmetry algebra admitting any number of symmetries.

The minimal range of spins contained in any supersymmetric multiplet increase with \mathcal{N} . Specifically, applying more than one symmetry transformation to one boson would not result in going back to the original boson due to the supersymmetry algebra delta functions. Furthermore, the new bosons have different spin. Any multiplet in \mathcal{N} -extended supersymmetry contains particles of spin at least as large as $\frac{1}{4}\mathcal{N}$ [61].

This dictates that theories of $\mathcal{N} > 4$ admit spins $\geq \frac{3}{2}$ and theories of $\mathcal{N} > 8$ admit spins $\geq \frac{5}{2}$. At a certain upper threshold that happens to be spin $\frac{3}{2}$, particles require coupling constants of negative mass dimensions. This makes field theories non-renormalisable. Thus $\mathcal{N}_{\text{max}} = 4$ for renormalisable flat-space field theories, which admits one unique multiplet whose spins span $0 \leq s \leq 1$. Furthermore, since gravity cannot consistently couple to particles of spin $\geq \frac{5}{2}$; $\mathcal{N}_{\text{max}} = 8$ for supergravity, also with a unique multiplet that admit spins of particles $0 \leq s \leq 2$.

Both of these maximally supersymmetric theories have been studied extensively due to their special properties, despite their albeit physically irrelevant particle interactions. $\mathcal{N} = 4$ super-Yang-Mills (sYM) is particularly special as we shall highlight, not least because it is not only renormalisable but perturbatively finite and has a uniquely determined spectrum. Hence the theory contains no free parameters.

4.1.1 $\mathcal{N} = 4$ sYM

Since the $\mathcal{N} = 4$ sYM spectrum contains particles of spin one, the superfield is restricted to a gauge multiplet. Therefore there is no matter multiplet and one only considers interactions of the non-Abelian gauge field A_μ with itself and its superpartners. The spectrum is composed of sixteen on-shell states, eight bosons and eight fermions. The bosonic states include the two helicity states of the gluon $G_{+/-}$ and six real scalars S_{AB} , (or three complex scalars) which transform in the adjoint representation of $SU(4)$. The fermionic superpartners are four gluinos Γ_A and four anti-gluinos $\bar{\Gamma}^A$, that transform in the anti-fundamental and fundamental representation of $SU(4)$ respectively. Uniquely, these sixteen on-shell states can be arranged into a PCT self-conjugate multiplet (see for example textbook [62]), described by one superfield Φ . The superfield is dependent on 4 Grassmann variables η^A , transforming in the fundamental representation of $SU(4)$ [63],

$$\Phi(\eta) = G_+ + \eta^A \Gamma_A + \frac{1}{2!} \eta^A \eta^B S_{AB} + \frac{1}{3!} \eta^A \eta^B \eta^C \epsilon_{ABCD} \bar{\Gamma}^D + \frac{1}{4!} (\eta)^4 G_- . \quad (4.1)$$

Assigning a helicity value of $\frac{1}{2}$ to η^A gives the total superfield a helicity of $+1$. The supersymmetry generators are expressed in terms of the original two component Weyl spinors λ_α , $\bar{\lambda}_{\dot{\alpha}}$ and the Grassmann variables η^A [63],

$$q_\alpha^A = \lambda_\alpha \eta^A , \quad \bar{q}_{\dot{\alpha}A} = \bar{\lambda}_{\dot{\alpha}} \frac{\partial}{\partial \eta^A} , \quad (4.2)$$

where the anti-commutator gives us the momentum generator [63],

$$\{q_\alpha^A, \bar{q}_{\dot{\alpha}B}\} = \delta_B^A \lambda_\alpha \bar{\lambda}_{\dot{\alpha}} = \delta_B^A p_{\alpha\dot{\alpha}} . \quad (4.3)$$

There are the further Lorentz and $SU(4)$ generators, listed in [64] that combine to fulfil a representation of the super Poincare algebra.

4.1.2 Twistor space

However there are further symmetries to explore, as $\mathcal{N} = 4$ sYM is also superconformal and even *dual* superconformal, which is related to the overwhelming evidence [65] that $\mathcal{N} = 4$ sYM theory is integrable in the planar limit. The (dual)-superconformal symmetry has a natural manifestation for amplitudes in (momentum)-twistor space, where the symmetry generators are all first order differential operators. By making the substitution for $\bar{\lambda}^{\dot{a}}$ into another two component object $\mu^{\dot{a}}$ [45],

$$\mu^{\dot{a}} = -i \frac{\partial}{\partial \bar{\lambda}_{\dot{a}}}, \quad \bar{\lambda}_{\dot{a}} = i \frac{\partial}{\partial \mu^{\dot{a}}}. \quad (4.4)$$

Thus the amplitude is homogeneous under twistor coordinates (λ, μ) , that satisfy an incidence relation [45]

$$\mu_{\dot{a}} + y_{a\dot{a}} \lambda^a = 0, \quad (4.5)$$

which geometrically identify between spacetime and twistor space. A fixed y determines a spacetime point and a line in twistor space, while a point in twistor space with fixed (λ, μ) defines a two dimensional plane of spacetime whose tangent vectors are all null. Two lines in twistor space exist on the same two dimensional plane, which satisfy the same incidence equation for different points in spacetime so two lines y and y' are null separated.

As detailed by Witten [45], amplitudes in twistor space are localised on an algebraic curve of degree $d + 1$ equal to the sum of the number of negative helicities plus the number of loops. They also have genus g less than or equal to the number of loops, similar to curves represented in the first part of figure 4.1. Specifically, the MHV amplitudes reduce to $d = 1, g = 0$; a line in twistor space with the particles of the interaction lying along the line, which occur “locally” on one spacetime point. This leads to the MHV diagram construction in twistor space as an analogue to the CSW prescription by intersecting different lines in twistor space; see the second part of figure 4.1. This prescription is identical to joining MHV vertices in spacetime; see the last part of figure 4.1. In this way curves of greater degree or equivalently non-MHV amplitudes are degenerate with some union of MHV twistor lines.

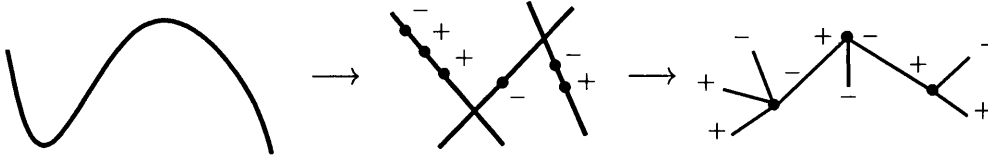


Figure 4.1: Firstly, an amplitude in twistor space of degree d , which is a union of MHV amplitudes, or $d = 1$ curves in twistor space. Two lines intersecting in twistor space is an MHV vertex in spacetime. Thus amplitudes can be written as connected lines in twistor space.

The twistor space setting is more natural for the superconformal symmetry to manifest, where the symmetry generators are all first order. The conformal group includes Lorentz transformations, translations and conformal inversions. All variables in the scattering amplitudes in $\mathcal{N} = 4$ sYM theory must be invariant under the superconformal transformations. The parametrisation of $\{\lambda_i, \bar{\lambda}_i, \eta_i\}$ defines the on-shell superspace upon which all tree-level amplitudes are superconformally invariant under the original physical superconformal algebra. There is an extended dual space $\{\lambda_i, x_i, \theta_i\}$ that makes the dual superconformal symmetry manifest under a new set of region momenta. It scales under conformal inversions $x_i^\mu \rightarrow -x_i^\mu/x_i^2$, and in transforming to a new copy of momentum-twistor space it has its own incidence relation similar to (4.5). It has its own parametrisation and its own entirely new superconformal algebra, (see [64] for a comprehensive list of all the generators) where all tree-level amplitudes behave covariantly under the new superconformal transformations. That is the natural home of Wilson loops, whose relationship to scattering amplitudes is an especially active area in recent years, e.g. [64, 66–69]. Thus the theory is *dual* superconformally invariant.

4.1.3 Superamplitudes

The PCT self-conjugate nature of the superfield in $\mathcal{N} = 4$ allows all n -particle scattering amplitudes to arrange themselves into a single superamplitude. The general form for the superamplitude is

$$\mathcal{A}_n = \frac{\delta^{(4)}(\sum_i \lambda_i^\alpha \bar{\lambda}_i^{\dot{\alpha}}) \delta^{(8)}(\sum_i \lambda_i^\alpha \eta_i^A)}{\langle 12 \rangle \langle 23 \rangle \cdots \langle n-1, n \rangle \langle n1 \rangle} \mathcal{P}_n(\lambda, \bar{\lambda}, \eta), \quad (4.6)$$

where the first delta function comes from the momentum conservation of $p^{\alpha\dot{\alpha}}$, and

4.1 Supersymmetric field theories

supersymmetry provides its counterpart q -symmetry as the second delta function: $\delta^{(8)}(\sum_i q_i)$. The fact this extra delta function appears gives some insight into the vanishing of certain pure gluon scattering amplitudes. There must be at least eight η variables in (4.6), which will cause all component amplitudes with less than two negative helicity gluons to vanish purely by supersymmetry. It determines the vanishing of certain pure gluon tree-level amplitudes in *all* gauge theories because such amplitudes are common to every gauge theory regardless of the matter content. This reveals that all gauge theories exhibit effects of $\mathcal{N} = 4$ supersymmetry, even if they are not supersymmetric. In $\mathcal{N} = 4$ sYM the statement continues to hold beyond tree-level due to this extra delta function, while in other theories such as pure QCD for example, the all-plus amplitudes do not vanish at loop level.

The denominator carries the helicities of the superparticles such that the function \mathcal{P}_n contains no overall helicity. The final supersymmetry generator listed in (4.2) further constrains \mathcal{P}_n by generating a translation of η^A proportional to $\bar{\lambda}^{\dot{a}}$. Therefore, there is an invariance under [64]

$$\mathcal{P}_n(\eta_i) = \mathcal{P}_n(\eta_i + [\bar{\lambda}_i \bar{\xi}]) . \quad (4.7)$$

This symmetry can be used to fix any two of the η_j, η_k to zero, by choosing

$$\bar{\xi}_{jk} = \frac{\bar{\lambda}_j \eta_k - \bar{\lambda}_k \eta_j}{[\bar{\eta}_j \bar{\eta}_k]} . \quad (4.8)$$

This becomes important when considering recursion relations among tree-level amplitudes in $\mathcal{N} = 4$ sYM theory.

The simplest example of a superamplitude is the MHV class with two negative helicities, for which $\mathcal{P}_n(\lambda, \bar{\lambda}, \eta) = 1$ [70],

$$\mathcal{A}_n^{\text{MHV}} = \frac{\delta^{(4)}(\sum_i \lambda_i^\alpha \bar{\lambda}_i^{\dot{\alpha}}) \delta^{(8)}(\sum_i \lambda_i^\alpha \eta_i^A)}{\langle 12 \rangle \langle 23 \rangle \cdots \langle n-1, n \rangle \langle n1 \rangle} . \quad (4.9)$$

The MHV helicity configuration is encoded in the second delta function, since the delta function of a Grassmann variable is the variable itself. So one can expand the superamplitude in terms of the η variables like the superfield. Thus the components of the superamplitude can be found by multiplying out the various Grassmann polynomials.

To illustrate a small number of the terms,

$$\begin{aligned} \mathcal{A}_n^{\text{MHV}} = & (\eta_1)^4 (\eta_2)^4 A(G_1^-, G_2^-, G_3^+, G_4^+, \dots, G_n^+) + \dots \\ & + (\eta_1)^4 (\eta_2)^3 (\eta_3) A(G_1^-, \bar{\Gamma}_2, \Gamma_3, \dots, G_n^+) + \dots \end{aligned} \quad (4.10)$$

In the expansion of the Grassmann delta function, the $\eta_1 \eta_2$ products yield the coefficient $\langle 12 \rangle$, and so the first term in (4.10) provides the MHV gluonic contribution for gluons one and two of negative helicity. The latter term is an MHV amplitude with two fermionic states of which the coefficient yields $\langle 12 \rangle^3 \langle 13 \rangle$.

Thus there is no need to specify which of the particles are special in the numerator for the superamplitude, as it includes all possible MHV amplitudes including those with mixed helicity configurations and also those where fermions or scalars are involved.

4.1.4 Supersymmetric ward identities

There are also supersymmetric ward identities (SWI) among different superamplitudes or in general gauge theory amplitudes, first realised from $\mathcal{N} = 2$ supersymmetry. One example, given in [42] is

$$A(1^-, 2_P^-, 3_P^+, 4^+, \dots, n^+) = \left(\frac{\langle 12 \rangle}{\langle 13 \rangle} \right)^{2h_P} A(1^-, 2_s^-, 3_s^+, 4^+, \dots, n^+) \quad (4.11)$$

where no subscript indicates gluons, s is for a scalar particle and P is for a particle with helicity h_P . There is also an implicit continuation of positive helicity gluons in "...", while h_P is 0 for a scalar, $\frac{1}{2}$ for a fermion and 1 for a gluon. The relation can be similarly derived from the two component amplitudes highlighted in the expansion (4.10).

4.1.5 One-loop SUSY decomposition for QCD

Color-ordered QCD at tree-level is “effectively” supersymmetric, that has been highlighted before. Thus, one only needs to consider diagrams of the interactions between the gluons, and any superpartner contributions would only enter at loop level. However, pure QCD at one-loop can be described by interactions of other supersymmetry multiplets which are much simpler to calculate than pure gluons in the loop [71–73].

4.1 Supersymmetric field theories

The following is a decomposition of one-loop QCD, to determine the contribution of a gluon or fermion in the loop by substitution for supersymmetric one-loop calculations.

Decomposing the color-ordered one-loop amplitude requires sums over contributions from a variety of supersymmetric multiplets including $\mathcal{N} = 4$ sYM, the chiral $\mathcal{N} = 1$ matter multiplet and a scalar loop computation. Maximal $\mathcal{N} = 4$ sYM contains (combining the doubling up of states earlier) one gluon, four gluinos and three scalars in its multiplet,

$$A_n^{\mathcal{N}=4} = A_n^{[1]} + 4A_n^{[1/2]} + 3A_n^{[0]}, \quad (4.12)$$

where $A_n^{[J]}$ represents the loop contribution to an n -gluon amplitude with internal particles of spin J in the loop. $J = 0$ is the non-supersymmetric (complex) scalar contribution. The chiral $\mathcal{N} = 1$ matter multiplet contains one fermion and one complex scalar,

$$A_n^{\mathcal{N}=1 \text{ chiral}} = A_n^{[1/2]} + A_n^{[0]}. \quad (4.13)$$

A rearrangement of these matter multiplets can give us the contribution to the pure QCD one-loop amplitude [42],

$$g = (g + 4f + 3s) - 4(f + s) + s = A_n^{\mathcal{N}=4} - 4A_n^{\mathcal{N}=1 \text{ chiral}} + A_n^{[0]}, \quad (4.14)$$

by calculating the simpler contributions from the supersymmetric theories (4.12,4.13) and a non-supersymmetric scalar term. Despite the lack of supersymmetry, the scalar contribution does not carry any spin information around the loop, and so the calculation is still simplified significantly.

Furthermore, to consider just a quark in the loop, one can combine the chiral $\mathcal{N} = 1$ contribution and the scalar contribution in the following way [42],

$$f = (f + s) - s = A_n^{\mathcal{N}=1 \text{ chiral}} - A_n^{[0]}. \quad (4.15)$$

There also exists a relation between the $\mathcal{N} = 1$ vector multiplet that contains a gluon and a fermion, and the $\mathcal{N} = 1$ chiral multiplet, given the knowledge of the

simplest non-trivial $\mathcal{N} = 4$ contribution. Thus,

$$(g + f) = (g + 4f + 3s) - 3(f + s), \quad (4.16)$$

and therefore the calculations satisfy the relation,

$$A_n^{\mathcal{N}=1 \text{ vector}} = A_n^{\mathcal{N}=4} - 3A_n^{\mathcal{N}=1 \text{ chiral}} \quad (4.17)$$

such that one need only know the $\mathcal{N} = 4$ calculation, one of the $\mathcal{N} = 1$ multiplet calculations and the scalar calculation to complete the desired contributions to one-loop QCD.

4.2 Supergravity theories

As mentioned earlier the maximally supersymmetric theory that admits a graviton in four dimensions is $\mathcal{N} = 8$ supergravity. However, part of the original revolution of supergravity was its generalisability to various numbers of dimensions. Particularly, a cause of initial excitement was eleven dimensional maximal supergravity, which was the first candidate for a theory of everything. The excitement was due in part to the fact it was the smallest number of dimensions large enough to contain all the gauge groups of the Standard Model and largest number of dimensions consistent with a single graviton. It is possible to dimensionally reduce the theory on an S_7 to maximal supergravity in four dimensions. However, its drawbacks such as an unrealistically large cosmological constant and the unsuccessful attempts to assimilate massless neutrinos into the theory by generating massless chiral fermions from a compactification, lead to disinterest for some years. These days it is seen as an effective theory, describing the low-mass degrees of freedom of a fundamental underlying theory.

Other alternative areas of research include loop quantum gravity [74–76], that aims to make this consistent with the Standard Model, but has yet to be realised. There are recent studies on causal dynamical triangulations that evaluate the path integral over space-time geometries using a lattice regularization with a discrete proper time, whose transfer matrix uniquely determines a theory [77, 78]. In two dimensions, this has been shown to provide a lattice regularisation of Horava-Lifshitz gravity [79]. Some

other areas includes those based upon extended theories of gravity [80], compactifications of higher dimensional theories [81] and brane-worlds [82]. Recently, the study of superstring theory or M-theory and its compactifications to lower dimensions has revived supergravity's popularity [81]. Supersymmetry is the driving force behind the developments, since it controls the dynamics and allows precise predictions based on non-renormalisation theorems, normally relating strong- to weak-coupling regimes.

4.2.1 The finiteness of $\mathcal{N} = 8$ supergravity debate

$\mathcal{N} = 8$ supergravity in four dimensions provides tantalising hints that it is perturbatively no more badly behaved than maximal $\mathcal{N} = 4$ sYM. It is a current area of research to determine possible counterterms by symmetry constraints [83], checked by multi-loop calculations of graviton scattering amplitudes [84]. $\mathcal{N} = 4$ sYM is known to be finite to all loop orders in perturbation theory in four dimensions. However, in $D > 4$ it does diverge, with the critical dimension D_c depending on the number of loops,

$$D_c(L)_{\mathcal{N}=4 \text{ sYM}} = 4 + \frac{6}{L} \quad (L > 1). \quad (4.18)$$

Through every computation to date [84], the ultraviolet behaviour of $\mathcal{N} = 8$ supergravity obeys the same relation,

$$D_c(L)_{\mathcal{N}=8 \text{ SUGRA}} = 4 + \frac{6}{L} \quad (L = 2, 3, 4). \quad (4.19)$$

Divergences in the critical dimension in $\mathcal{N} = 4$ for $L > 1$ are all associated with the $\mathcal{D}^2 F^4$ term, where F is the field strength that captures the covariant nature of the divergences that survive in Yang-Mills theories. However, the corresponding counterterm in $\mathcal{N} = 8$ supergravity has dimensionful coupling such that order by order L -loop counterterms have the form $\mathcal{D}^{2(L+1-p)} R^p$, where R is the Riemann tensor that captures the covariant nature of divergences in theories of gravity. Terms involving R^2 and R^3 at one- and two-loops respectively have been analysed and shown pure supergravity to be finite at both these orders [83]. In pure supergravity the first potential counterterm R^4 appears at three-loops, that was ruled out by analysing the UV behaviour of the three-loop four-graviton amplitude [85, 86]. Further calculations in this manner are underway to test higher-loop possible counterterms. Currently, there are several

arguments [87,88] that favour the existence of a counterterm at seven loops of the form $\mathcal{D}^8 R^4$. This is because it would correspond to the divergence of the four-loop four graviton amplitude in critical dimension $D_c = 5.5$, where it is only known not to diverge in $D = 4$ [83]. When the divergence in the five-loop amplitude is computed either the equality of (4.18) and (4.19) will break down or the required term for describing the five-loop divergence in the critical dimension must have higher order derivatives, namely $\mathcal{D}^{10} R^4$. This has two more derivatives on it than the proposed *seven*-loop counterterm in $D = 4$: $\mathcal{D}^8 R^4$ [83]. Thus if a $\mathcal{D}^{10} R^4$ counterterm in the critical dimension is found it suggests there is no seven-loop counterterm of the form $\mathcal{D}^8 R^4$. Hence the UV behaviour of the five-loop calculation will shed light on the potential seven loop divergence of $\mathcal{N} = 8$ supergravity in four dimensions [83].

4.2.2 KLT Relations for Gravity

Currently, no consistent quantum field theory for gravity has been constructed. However, the Maldacena conjecture [13] relates the weak coupling limit of gravity in anti de-Sitter space to a strong coupling limit of $\mathcal{N} = 4$ sYM theory. Further relationships including one between the weak coupling limits of both gravity and gauge theories [89] in the semi-classical regime has proven extremely useful. It has allowed gauge theories to be used as the direct ingredients for computations in perturbative quantum gravity. At the semi-classical level, or tree-level in perturbation theory, there is the remarkably suggestive property that heuristically,

$$\text{gravity} \sim (\text{gauge theory}) \times (\text{gauge theory}). \quad (4.20)$$

Thus, tree-level amplitudes in gravity can be written in terms of a bilinear combination of tree-level gauge theory amplitudes. By the fortune of generalised unitarity, one can extend this to the multi-loop level by cutting the gravity loop level amplitudes into products of gravity trees. Then the gravity-gauge relations can be applied to write everything in terms of tree-level gauge theory amplitudes, identical to cuts that appear in gauge theory loop amplitudes.

The original gauge-gravity relations for tree amplitudes were found by Kawai, Lewellen and Tye [21]. They recognised that the world sheet integrands for tree-level amplitudes in closed type II superstring theory matched the square of the integrands

4.2 Supergravity theories

from the open superstring tree-level amplitudes. As the string tension goes to infinity, closed type II superstring theory in $D = 4$ is $\mathcal{N} = 8$ supergravity, while the open string setup is $\mathcal{N} = 4$ sYM. Hence in the perturbative or low energy limit of the string theories, the KLT relations express any $\mathcal{N} = 8$ supergravity tree amplitude as a product of two copies of $\mathcal{N} = 4$ sYM,

$$[\mathcal{N} = 8] = [\mathcal{N} = 4]_L \otimes [\mathcal{N} = 4]_R. \quad (4.21)$$

The Fock space of $\mathcal{N} = 8$ supergravity naturally factorises into a product of left- and right-moving $\mathcal{N} = 4$ sYM Fock spaces.

The KLT relations satisfy a unique association between a pair of the 16 (color stripped) massless states of $\mathcal{N} = 4$ sYM [90] (centred around the zero helicity column in the bottom half of table 4.1) and one of the $256 = 16^2$ massless states of the supergravity multiplet, (organised in the top half of table 4.1). For example, the eight helicity $-\frac{3}{2}$ anti-gravitino states are products of helicity -1 gluons and and helicity $-\frac{1}{2}$ anti-gluinos in two possible ways,

$$\psi_A^- = G^- \otimes \lambda_A^-, \quad \psi_{A+4}^- = \lambda_A^- \otimes G^-. \quad (4.22)$$

where $A = 1, 2, 3, 4$.

$\mathcal{N} = 8$ supergravity									
h	-2	$-\frac{3}{2}$	-1	$-\frac{1}{2}$	0	$\frac{1}{2}$	1	$\frac{3}{2}$	2
# of states	1	8	28	56	70	56	28	8	1
field	h^-	ψ_i^-	v_{ij}^-	χ_{ijk}^-	s_{ijkl}	χ_{ijk}^+	v_{ij}^+	ψ_i^+	h^+
$\mathcal{N} = 4$ super-Yang-Mills									
h			-1	$-\frac{1}{2}$	0	$\frac{1}{2}$	1		
# of states			1	4	6	4	1		
field			G^-	λ_A^-	S_{AB}	λ_A^+	G^+		

Table 4.1: A table of the on-shell states for the two maximally symmetric multiplets of $\mathcal{N} = 8$ supergravity and $\mathcal{N} = 4$ sYM, organised by helicity.

4.2 Supergravity theories

There is no relation between the full color dressed amplitudes \mathcal{A}_n on the gauge theory side in the open string to the closed string side, thus the KLT relations refers to the color stripped partial amplitudes A_n only. For the supergravity tree amplitudes $\mathcal{M}_n^{\text{tree}}$, the powers of the gravitational coupling κ are stripped away, where κ is related to Newton's gravitational constant by $\kappa^2 = 32\pi G_N$. The partial gravity amplitudes M_n are then related to \mathcal{M}_n by [90],

$$\mathcal{M}_n^{\text{tree}}(1, 2, \dots, n) = \left(\frac{\kappa}{2}\right)^{n-2} M_n^{\text{tree}}(1, 2, \dots, n). \quad (4.23)$$

The first few KLT relations have the form [90],

$$\begin{aligned} M_3^{\text{tree}}(1, 2, 3) &= i A_3^{\text{tree}}(1, 2, 3) A_3^{\text{tree}}(1, 2, 3), \\ M_4^{\text{tree}}(1, 2, 3, 4) &= -i s_{12} A_4^{\text{tree}}(1, 2, 3, 4) A_4^{\text{tree}}(1, 2, 4, 3), \\ M_5^{\text{tree}}(1, 2, 3, 4, 5) &= i s_{12} s_{34} A_5^{\text{tree}}(1, 2, 3, 4, 5) A_5^{\text{tree}}(2, 1, 4, 3, 5) + \mathcal{P}(2, 3), \end{aligned} \quad (4.24)$$

where $\mathcal{P}(m)$ indicates a sum over the $m!$ permutations of the m arguments of \mathcal{P} . The n -point version of the KLT relation will be beneficial later on, and so we present them now.

The KLT relations between gravity and gauge amplitudes as presented in appendices of [91], in the field theory limit for an arbitrary number $n \geq 3$ of external particles is

$$\begin{aligned} M_n^{\text{tree}}(1, 2, \dots, n) &= i(-1)^{n+1} \left[A_n^{\text{tree}}(1, 2, \dots, n) \sum_{\text{perms}} f(i_1, \dots, i_j) \bar{f}(l_1, \dots, l_{j'}) \right. \\ &\quad \times A_n^{\text{tree}}(i_1, \dots, i_j, 1, n-1, l_1, \dots, l_{j'}, n) \Big] \\ &\quad + \mathcal{P}(2, 3, \dots, n-2), \end{aligned} \quad (4.25)$$

where ‘perms’ are $(i_1, \dots, i_j) \in \mathcal{P}(2, \dots, n/2)$, $(l_1, \dots, l_{j'}) \in \mathcal{P}(n/2 + 1, \dots, n-2)$, $j = n/2 - 1$, $j' = n/2 - 2$, giving a total of $(n/2 - 1)! \times (n/2 - 2)!$ terms in the square brackets. Here n is assumed to be even; the case of odd n is completely analogous. The

functions f and \bar{f} are given by

$$\begin{aligned} f(i_1, \dots, i_j) &= s(1, i_j) \prod_{m=1}^{j-1} \left(s(1, i_m) + \sum_{k=m+1}^j g(i_m, i_k) \right), \\ \bar{f}(l_1, \dots, l_{j'}) &= s(l_1, n-1) \prod_{m=2}^{j'} \left(s(l_m, n-1) + \sum_{k=1}^{m-1} g(l_k, l_m) \right), \end{aligned} \quad (4.26)$$

where

$$g(i, j) = \begin{cases} s(i, j) \equiv s_{ij}, & i > j, \\ 0, & \text{otherwise.} \end{cases} \quad (4.27)$$

The form as presented here picks out leg 1 as special; it does not appear in any of the products or permutations by virtue of (4.25). Also, one of the Yang-Mills gauge theory amplitudes $A(\dots, i_j, 1, \dots)$ will always come multiplied by a factor of s_{1i_j} which will be beneficial later on.

Recently, there has been developments including new KLT-type relations, that describes a color-kinematic duality satisfied by gauge theory amplitudes presented by Bern, Carrasco and Johansson [92]. The BCJ relations use Jacobi identities to replace color factors in Yang-Mills by a copy of kinematic numerators to generate a variety of supergravity amplitudes. They will not be used here but have been fruitful in computing many parts of supergravity multi-loop amplitudes [93].

4.2.3 One-loop SUSY decomposition for graviton amplitudes

In a one-loop graviton scattering amplitude there may be one of five states circulating in the loop; a scalar, a Weyl fermion, a vector, a gravitino or the graviton itself. These can be targeted individually from string based rules, but it proves more convenient to calculate the contributions from supersymmetric multiplets instead, as we described for QCD at one-loop.

By the same convention as before we identify the contribution for a particle of spin J to the graviton scattering amplitude as $M_n^{[J]}$, where $M_n^{[0]}$ represents a real scalar contribution. A supergravity theory can in general admit minimally coupled

4.2 Supergravity theories

matter multiplets. The contributions from the various supergravity multiplets can be summarised as [94]

$$\begin{aligned}
M_n^{\mathcal{N}=8} &= M_n^{[2]} + 8M_n^{[3/2]} + 28M_n^{[1]} + 56M_n^{[1/2]} + 70M_n^{[0]}, \\
M_n^{\mathcal{N}=6 \text{ matter}} &= M_n^{[3/2]} + 6M_n^{[1]} + 15M_n^{[1/2]} + 20M_n^{[0]}, \\
M_n^{\mathcal{N}=4 \text{ matter}} &= M_n^{[1]} + 4M_n^{[1/2]} + 6M_n^{[0]}, \\
M_n^{\mathcal{N}=1 \text{ matter}} &= M_n^{[1/2]} + 2M_n^{[0]}.
\end{aligned} \tag{4.28}$$

Thus the inversions can be used to construct the amplitudes for specific particles in the loop as follows

$$\begin{aligned}
M_n^{scalar} &= 2M_n^{[0]}, \\
M_n^{[1/2]} &= M_n^{\mathcal{N}=1 \text{ matter}} - M_n^{scalar}, \\
M_n^{[1]} &= M_n^{\mathcal{N}=4 \text{ matter}} - 4M_n^{\mathcal{N}=1 \text{ matter}} + M_n^{scalar}, \\
M_n^{[3/2]} &= M_n^{\mathcal{N}=6 \text{ matter}} - 6M_n^{\mathcal{N}=4 \text{ matter}} + 9M_n^{\mathcal{N}=1 \text{ matter}} - M_n^{scalar}, \\
M_n^{[2]} &= M_n^{\mathcal{N}=8} - 8M_n^{\mathcal{N}=6 \text{ matter}} + 20M_n^{\mathcal{N}=4 \text{ matter}} - 16M_n^{\mathcal{N}=1 \text{ matter}} + M_n^{scalar},
\end{aligned} \tag{4.29}$$

where the final relation is the contribution to the pure graviton scattering amplitude.

Chapter 5

Analytic Properties of Amplitudes

In this Chapter, we describe the analytic properties of amplitudes with applications to deriving new results in cases of tree-level and one-loop. Scattering amplitudes at both tree and loop level have a number of properties that have driven techniques for making calculations easier. In general, the analytic properties are not only powerful consistency checks on results but can also be used to derive information about amplitudes. For example, recursive algorithms for any number of external legs provide powerful non-trivial relations. General forms for some amplitudes can be derived in this way, combined with what symmetries they must obey and that they be gauge invariant also. We present the splitting and factorisation properties of amplitudes, leading to the unitarity method and recursive relations for both tree-level and one-loop amplitudes.

5.1 Multi-particle poles, collinear and soft limits

5.1.1 Tree level

The tree-level amplitudes display well understood factorisation properties that occur as kinematic invariants vanish, known as a pole where $P_{i,j}^2 \rightarrow 0$ for $P_{i,j}$ defined as the sum of null momenta from i to j (3.22). As mentioned in Chapter 3 via our color-ordered restriction to partial amplitudes, we are restricted to poles in channels of cyclically

5.1 Multi-particle poles, collinear and soft limits

adjacent momenta. Channels containing a sum of three or more null momenta are referred to as a multi-particle pole, whereas if only two momenta contribute to the channel then it is a collinear pole.

For tree-level amplitudes as $P_{1,r}^2 \rightarrow 0$, a multi-particle pole can be expressed as [42]

$$A_n^{\text{tree}} \xrightarrow{P_{1,r}^2 \rightarrow 0} \sum_{\lambda} A_{r+1}^{\text{tree}}(1, \dots, r, -P_{1,r}^{\lambda}) \frac{i}{P_{1,r}^2} A_{n-r+1}^{\text{tree}}(r+1, \dots, n, P_{1,r}^{-\lambda}), \quad (5.1)$$

where the intermediate state has momentum $P_{1,r}$ with helicity λ , while r can take values from $3 \rightarrow n-3$. The helicity λ is reversed when going from one side of the pole to the other, due to the convention of always writing the helicity as that of an outgoing particle.

The MHV tree-level amplitudes (3.51) do not have multi-particle poles. This is because apart from one negative helicity guaranteed from the internal state λ , one must have at least three negative helicity states from the parent amplitude to distribute down to the two factorised descendant amplitudes for those to be MHV amplitudes themselves. Therefore, for the special cases of MHV and $\overline{\text{MHV}}$ amplitudes, only collinear poles exist.

Any collinear pole at tree-level reduces more simply to a tree-level amplitude with one less leg, multiplied by a splitting amplitude $\text{Split}_{-\lambda}^{\text{tree}}$ governed by the helicities of the two momenta going collinear, and the helicity λ of the connecting leg with momentum K . As two neighbouring legs (i, j) , (with helicities λ_i and λ_j respectively) of any tree-level amplitude become collinear the resultant pole is [42],

$$A_n^{\text{tree}}(\dots, i^{\lambda_i}, j^{\lambda_j}, \dots) \xrightarrow{i \parallel j} \sum_{\lambda=\pm} \text{Split}_{-\lambda}^{\text{tree}}(z, i^{\lambda_i}, j^{\lambda_j}) A_{n-1}^{\text{tree}}(\dots, K^{\lambda}, \dots), \quad (5.2)$$

where the intermediate null state K is the sum of the momenta of the collinear legs $K = p_i + p_j$. The collinear limit is defined by $p_i = zK$ and $p_j = (1-z)K$.

The form of the splitting amplitudes in (5.2) can be derived from the collinear limits of the known five-point MHV amplitudes. As an example [42], we consider the $p_4 \parallel p_5$

5.1 Multi-particle poles, collinear and soft limits

limit of the tree-level five-point amplitude

$$A_5^{\text{tree}}(1^-, 2^-, 3^+, 4^+, 5^+) = i \frac{\langle 12 \rangle^4}{\langle 12 \rangle \langle 23 \rangle \langle 34 \rangle \langle 45 \rangle \langle 51 \rangle}, \quad (5.3)$$

to derive one of the splitting amplitudes. Thus, in the limit of particles p_4 and p_5 going collinear

$$\begin{aligned} A_5^{\text{tree}}(1^-, 2^-, 3^+, 4^+, 5^+) &\xrightarrow{4\parallel 5} \frac{1}{\sqrt{z(1-z)}\langle 45 \rangle} \times i \frac{\langle 12 \rangle^4}{\langle 12 \rangle \langle 23 \rangle \langle 3K \rangle \langle K1 \rangle}, \\ &= \text{Split}_-^{\text{tree}}(z, 4^+, 5^+) \times A_4^{\text{tree}}(1^-, 2^-, 3^+, K^+). \end{aligned} \quad (5.4)$$

With application of various limits on the five-point amplitude, and parity flipped versions where required, all $g \rightarrow gg$ splitting amplitudes can be derived, which are given by [24, 59, 60, 95],

$$\begin{aligned} \text{Split}_-^{\text{tree}}(z, i^-, j^-) &= 0, \\ \text{Split}_-^{\text{tree}}(z, i^+, j^+) &= \frac{1}{\sqrt{z(1-z)}\langle ij \rangle}, \\ \text{Split}_+^{\text{tree}}(z, i^+, j^-) &= \frac{(1-z)^2}{\sqrt{z(1-z)}\langle ij \rangle}, \\ \text{Split}_-^{\text{tree}}(z, i^+, j^-) &= -\frac{z^2}{\sqrt{z(1-z)}[ij]}. \end{aligned} \quad (5.5)$$

Supersymmetric ward identities for amplitudes can be used to obtain splitting amplitudes for factorisations involving fermions.

The behaviour of gluon amplitudes as one of the momentum vectors p_i goes to zero is known as the *soft* limit. The behaviour of this limit factorises out a soft factor [42],

$$A_n^{\text{tree}}(\dots, a, i^+, b, \dots) \xrightarrow{p_i \rightarrow 0} \text{Soft}^{\text{tree}}(a, i^+, b) A_{n-1}^{\text{tree}}(\dots, a, b, \dots) \quad (5.6)$$

where the soft factor is,

$$\text{Soft}^{\text{tree}}(a, i^+, b) = \frac{\langle ab \rangle}{\langle ai \rangle \langle ib \rangle} \quad (5.7)$$

5.1 Multi-particle poles, collinear and soft limits

which is dependent on the neighbouring states, a and b , and of the soft gluon i^+ . For legs with negative helicity i^- going soft, one swaps $\langle \rangle$ with $[]$ in (5.7) and gains a minus sign. The neighbouring states a and b are precisely color-ordered in the original partial tree-level amplitude, however the soft behaviour is independent of their helicity and also independent of whether they are gluons or quarks.

5.1.2 Loop level

One-loop amplitudes factorise to lower leg one-loop amplitudes in an analogous way to the tree-level amplitudes. However, both the splitting amplitudes for collinear limits and factorisation over multi-particle poles at one-loop are not as simple as at tree-level. Loop level factorisation does not discriminate against loop momenta flowing on either side of the vanishing propagator, and so one must sum over the possibilities of it appearing on either side of the channel. The factorisation properties of one-loop amplitudes provide powerful consistency checks on calculations, see [44, 96, 97]. Also, these are the only factorisations that can occur for real momenta. Cases of complex momenta developing poles are addressed in Chapters 6 and 7 to introduce new non-standard or complex factorisations.

For multi-particle poles, the one-loop amplitudes factorise as the channel $(p_i + p_{i+1} + \dots + p_{i+r-1})^2 = K^2 \rightarrow 0$ for real momenta via the following prescription [97],

$$\begin{aligned}
 A_n^{1\text{-loop}} \xrightarrow{K^2 \rightarrow 0} & \sum_{\lambda=\pm} \left[A_{r+1}^{1\text{-loop}}(p_i, \dots, p_{i+r-1}, -K^\lambda) \frac{1}{K^2} A_{n-r+1}^{\text{tree}}(K^{-\lambda}, p_{i+r}, \dots, p_{i-1}) \right. \\
 & + A_{r+1}^{\text{tree}}(p_i, \dots, p_{i+r-1}, -K^\lambda) \frac{1}{K^2} A_{n-r+1}^{1\text{-loop}}(K^{-\lambda}, p_{i+r}, \dots, p_{i-1}) \\
 & \left. + A_{r+1}^{\text{tree}}(p_i, \dots, p_{i+r-1}, -K^\lambda) \frac{1}{K^2} A_{n-r+1}^{\text{tree}}(K^{-\lambda}, p_{i+r}, \dots, p_{i-1}) c_\Gamma F_n(K^2; p_1, \dots, p_n) \right],
 \end{aligned} \tag{5.8}$$

where F_n is the one-loop factorisation function, and the factor c_Γ is given by

$$c_\Gamma = \frac{1}{(4\pi)^{2-\epsilon}} \frac{\Gamma(1+\epsilon)\Gamma^2(1-\epsilon)}{\Gamma(1-2\epsilon)}, \tag{5.9}$$

5.1 Multi-particle poles, collinear and soft limits

dependent on Gamma functions with factors of ϵ remnant from the integrals computed in $D = 4 - 2\epsilon$ dimensions. The two cases where the loop momenta is entirely confined to either side of the channel contribute to the first two terms of (5.8), as tree-level amplitudes multiplied by one-loop amplitudes. The factorisation function F_n , reflects that momenta on either side of the pole still interact at one-loop, since it is a function of all the momenta p_1, \dots, p_n . It can contain logarithmic terms containing momenta from both side of the pole.

The behaviour of a one-loop amplitude in a collinear limit is analogous to the tree-level case, in that an n -point amplitude is reduced to a sum of $(n - 1)$ -point amplitudes dressed by splitting functions as two external legs go collinear. As with the multi-particle poles at one-loop, one must include lower point tree-level amplitudes multiplied by one-loop splitting functions and lower point one-loop amplitudes multiplied by tree-level splitting functions.

The collinear limit for a color-ordered one-loop amplitude can then be written as [97],

$$A_{n;1}^{1\text{-loop}}(\dots, i^{\lambda_i}, j^{\lambda_j}, \dots) \xrightarrow{i||j} \sum_{\lambda=\pm} \left[\text{Split}_{-\lambda}^{\text{tree}}(z, i^{\lambda_i}, j^{\lambda_j}) A_{n-1;1}^{1\text{-loop}}(\dots, K^\lambda, \dots) \right. \\ \left. + \text{Split}_{-\lambda}^{\text{loop}}(z, i^{\lambda_i}, j^{\lambda_j}) A_{n-1}^{\text{tree}}(\dots, K^\lambda, \dots) \right], \quad (5.10)$$

where the collinear limit is defined by $p_i = zK$ and $p_j = (1 - z)K$ with $K = p_i + p_j$, as in the tree-level case. K and λ are the momentum and helicity of the internal state respectively. For particular multiplets, i.e. a chiral theory of $\mathcal{N} = 1$ supersymmetry, the loop splitting amplitudes vanish, to leave only the former term in eq. (5.10).

Defining $\text{Split}^{\text{loop}}$ is much more subtle (see [97] for a thorough treatment), since individual diagrams may not smoothly factorise as momenta become collinear in an IR divergent massless theory. $\text{Split}^{\text{loop}}$ will receive corrections once renormalised for UV divergences, but first one must take account of the singularities in an IR divergent theory. Consider an IR singularity containing a logarithmic term [97],

$$-c_\Gamma \frac{1}{\epsilon^2} (-s_{jl})^{-\epsilon} A_n^{\text{tree}} = -c_\Gamma \left[\dots - \frac{1}{\epsilon} \ln(-s_{jl}) + \dots \right] A_n^{\text{tree}}. \quad (5.11)$$

5.1 Multi-particle poles, collinear and soft limits

In the collinear limit (5.2), $k_i = zK$ and $k_j \rightarrow (1-z)K$, sending

$$\frac{1}{\epsilon} \ln(-s_{jl}) \rightarrow \frac{1}{\epsilon} \ln(-(1-z)s_{Kl}). \quad (5.12)$$

The limit introduces a $\ln(1-z)/\epsilon$ factor that does not belong to either set of terms in (5.10) and so cannot be interpreted as a factorising contribution. Thus we distinguish non-factorising terms contributing to the one-loop splitting amplitude [97],

$$\text{Split}^{\text{loop}} = \left(1 + \frac{n_s}{N_c} - \frac{n_f}{N_c}\right) \text{Split}^{\text{fact}} + \text{Split}^{\text{non-fact}}, \quad (5.13)$$

where the latter term includes contributions from diagrams whose loop integrals generate singularities. The former term is dressed with a factor that accounts for n_s scalars, n_f fermions in an N_c -color gauge theory, flowing in the loop for the $g \rightarrow gg$ factorisable loop splitting amplitudes. Those are given by [97]

$$\begin{aligned} \text{Split}_{\pm}^{\text{fact}}(z, i^+, j^-) &= \text{Split}_{\pm}^{\text{fact}}(z, i^-, j^+) = 0, \\ \text{Split}_{+}^{\text{fact}}(z, i^+, j^+) &= -\frac{1}{48\pi^2} \sqrt{z(1-z)} \frac{[ij]}{\langle ij \rangle^2}, \\ \text{Split}_{-}^{\text{fact}}(z, i^+, j^+) &= \frac{1}{48\pi^2} \sqrt{z(1-z)} \frac{1}{\langle ij \rangle}. \end{aligned} \quad (5.14)$$

The non-factorising contributions are proportional to the tree-level splitting functions, such that

$$\text{Split}_{-\lambda}^{\text{non-fact}}(z, i^{\lambda_i}, j^{\lambda_j}) = c_{\Gamma} \times \text{Split}_{-\lambda}^{\text{tree}}(z, i^{\lambda_i}, j^{\lambda_j}) \times r_S(i, j), \quad (5.15)$$

where r_S collects all contributions of singularities and their coefficients (see Table 1 of [97]) from the kind of substitutions in (5.11). For the $g \rightarrow gg$ loop splitting functions, the non-factorising contributions are [97],

$$\text{Split}_{-\lambda}^{\text{non-fact}}(i, j) = c_{\Gamma} \text{Split}_{-\lambda}^{\text{tree}}(i, j) \left[-\frac{1}{\epsilon^2} \left(\frac{\mu^2}{z(1-z)(-s_{ij})} \right)^{\epsilon} + 2 \ln z \ln(1-z) - \frac{\pi^2}{6} \right]. \quad (5.16)$$

Combining (5.14) and (5.16) into (5.13) yields the entire contribution to the $g \rightarrow gg$ loop splitting amplitudes. As is the case at tree-level, these loop level splitting functions

can be extracted from the collinear behaviour of known results for one-loop gluon amplitudes.

5.2 Unitarity

We now present the unitarity method, which makes use of recycling knowledge of tree-level amplitudes to calculate dispersive parts of one-loop amplitudes. We describe the optical theorem and use Cutkosky rules to compute the discontinuity of amplitudes by replacing propagators by delta functions, known as *cutting* the amplitude. The procedure is then turned around in the unitarity method, such that given the discontinuity in some channel it is possible to reconstruct the dispersive loop integrals using entirely on-shell information.

We present unitarity in various dimensions along with generalised unitarity, that allow representation of dispersive integrals in ultimately simple forms that are sometimes reduced to algebraic exercises. Some examples will be used to illustrate the use of this method, to read off coefficients from the basis of scalar integrals in (2.26).

5.2.1 Optical theorem

The conservation of probability is a fundamental requirement of any consistent field theory, and as such implies unitarity of the scattering matrix $\mathcal{S}^\dagger \mathcal{S} = \mathbb{1}$. By analysing the non-forward part of the scattering matrix, $T = -i(\mathcal{S} - \mathbb{1})$, unitarity implies that

$$-i(T - T^\dagger) = T^\dagger T. \quad (5.17)$$

This will lead to a powerful statement about the relation between absorptive and dispersive parts of amplitudes encoded in the LHS and RHS of (5.17) respectively. See [15] for a full treatment.

Firstly, one can think of the LHS of (5.17) in terms of initial p_{ini} incoming and final

p_{fin} outgoing states,

$$\begin{aligned}
 -i \left(\langle p_{\text{fin}} | T | p_{\text{ini}} \rangle - \langle p_{\text{fin}} | T^\dagger | p_{\text{ini}} \rangle \right) &= -i \left(\langle p_{\text{fin}} | T | p_{\text{ini}} \rangle - \overline{\langle p_{\text{ini}} | T | p_{\text{fin}} \rangle} \right) \\
 &= -i (2\pi)^4 \delta^{(4)} \left(\sum (p_{\text{fin}} - p_{\text{ini}}) \right) \\
 &\quad \times [\mathcal{M}(p_{\text{ini}} \rightarrow p_{\text{fin}}) - \mathcal{M}^*(p_{\text{fin}} \rightarrow p_{\text{ini}})] \\
 &= -i (2\pi)^4 \delta^{(4)} \left(\sum (p_{\text{fin}} + p_{\text{ini}}) \right) \text{Disc } \mathcal{M}(p_{\text{fin}}; p_{\text{ini}})
 \end{aligned} \tag{5.18}$$

where we have used

$$\langle p_{\text{fin}} | T | p_{\text{ini}} \rangle = (2\pi)^4 \delta^{(4)} \left(\sum (p_{\text{fin}} - p_{\text{ini}}) \right) \mathcal{M}(p_{\text{ini}} \rightarrow p_{\text{fin}}). \tag{5.19}$$

to replace T-matrix elements with invariant matrix elements \mathcal{M} (of real momenta) multiplied by momentum conserving delta functions.

Therefore, the LHS of (5.17) represents a discontinuity of an amplitude, which comes from a branch cut in complex momenta. The RHS of (5.17) can be found from a loop amplitude via a *cut*. This can be shown by inserting an entire set of intermediate states $\{q_i\}$ [15],

$$\mathbb{1} = \prod_i \int \frac{d^4 q_i}{(2\pi)^4} \delta^{(+)}(q_i^2 - m_i^2) |q_i\rangle \langle q_i|, \tag{5.20}$$

into the RHS of (5.17), so that

$$\begin{aligned}
 \langle p_{\text{fin}} | T^\dagger T | p_{\text{ini}} \rangle &= \sum_i \left(\prod_i \int \frac{d^4 q_i}{(2\pi)^4} \delta^{(+)}(q_i^2 - m_i^2) \right) \langle p_{\text{fin}} | T^\dagger | q_i \rangle \langle q_i | T | p_{\text{ini}} \rangle \\
 &= (2\pi)^4 \delta^{(4)} \left(\sum (p_{\text{fin}} + p_{\text{ini}}) \right) \sum_i \int d\text{LIPS } \mathcal{M}^*(p_{\text{fin}} \rightarrow q_i) \mathcal{M}(p_{\text{ini}} \rightarrow q_i),
 \end{aligned} \tag{5.21}$$

$$2\text{Im} \left(\text{Diagram} \right) = \sum_i \int \prod_i \left(\text{Diagram}_1 \right) \left(\text{Diagram}_2 \right)$$

Figure 5.1: The optical theorem: the imaginary part of a forward scattering one-loop amplitude arises as a sum over contributions of products of on-shell tree-level amplitudes from all possible intermediate particles i .

where $d\text{LIPS}$ is the multi-particle Lorentz-Invariant-Phase-Space measure,

$$d\text{LIPS} = \prod_i d^4 q_i \delta^{(+)}(q_i^2 - m_i^2) \delta^{(4)} \left(p_{\text{fin}} + p_{\text{ini}} - \sum_i q_i \right). \quad (5.22)$$

Combining the LHS and RHS again from (5.18) and (5.21) we arrive at the optical theorem

$$-i\text{Disc } \mathcal{M}(p_{\text{fin}}; p_{\text{ini}}) = \sum_i \int d\text{LIPS} \mathcal{M}^*(p_{\text{fin}} \rightarrow q_i) \mathcal{M}(p_{\text{ini}} \rightarrow q_i), \quad (5.23)$$

depicted pictorially in figure 5.1. The sum over i on the right hand side goes over all possible physical states q_i , intermediate between the process described by T^\dagger and T .

For any amplitudes \mathcal{M} of real momenta, the relation can be expressed in the sum of Feynman diagrams, which provide the discontinuities in the vanishing of loop propagators in the $i\epsilon$ prescription. This relation must hold order by order in perturbation theory, despite the discontinuity in a matrix element being related to a product of matrix elements on the right hand side. This means that at $\mathcal{O}(\alpha_s^2)$, the left hand side represents a discontinuity of a one-loop amplitude, while the RHS is a product of on-shell tree-level amplitudes. They are connected via two on-shell propagators, which is enforced by the momentum conserving delta functions. One must also sum over a discrete sum of all the allowed particle types to calculate the one-loop contribution.

5.2.2 Cutkosky Rules

A consequence of the optical theorem is that discontinuities of loop amplitudes may be found by “cutting” them. This is embodied by the Cutkosky rules [98], that are used to replace propagators (in Minkowski space using Feynman’s $i\epsilon$ prescription) by delta

functions. Then instead of computing Feynman integrals the problem is reduced to a LIPS integral. The rules are as follows:

1. For a given kinematic invariant, pick out the two internal propagators separating the external states in that kinematic invariant from the rest of the diagram.
2. Then “cut” each propagator, which means replacing each one by a delta function:

$$\frac{i}{p^2 + i\epsilon} \rightarrow 2\pi\delta^{(+)}(p^2), \quad (5.24)$$

where $(+)$ indicates a restriction to the future light-cone.

3. Perform the integral in Lorentz invariant phase space over the two intermediate, now on-shell states ℓ_1 and ℓ_2 using

$$d\text{LIPS}(\ell_2, -\ell_1; P_\ell) = d^4\ell_1\delta^{(+)}(\ell_1^2)d^4\ell_2\delta^{(+)}(\ell_2^2)\delta^{(4)}(\ell_2 - \ell_1 + P_\ell) \quad (5.25)$$

to identify the discontinuity in the branch cut, where P_ℓ is the momenta across the cut.

The Cutkosky rules tell us that we can turn the cutting process around, and sew two on-shell diagrams together to create one-loop Feynman integrals,

$$\begin{aligned} \text{Disc}A_n^{1\text{-loop}} &= \sum_{\text{spin}} \int d\text{LIPS}(\ell_2, -\ell_1; P_\ell) A^{\text{tree}}(\ell_1, \dots, -\ell_2) A^{\text{tree}}(-\ell_1, \dots, \ell_2) \\ &\rightarrow \sum_{\text{spin}} \int \frac{d^D\ell_1}{(2\pi)^D} \frac{d^D\ell_2}{(2\pi)^D} \frac{1}{\ell_1^2} \frac{1}{\ell_2^2} A^{\text{tree}}(\ell_1, \dots, -\ell_2) A^{\text{tree}}(-\ell_1, \dots, \ell_2) \end{aligned} \quad (5.26)$$

where $d\text{LIPS}(\ell_2, -\ell_1; P_\ell)$ is defined in (5.25), and one must sum over the types of spin of the internal states, which are taken to be D -dimensional. We discuss what this means for the notion of our physical state to extend in D -dimensions, and how we approach the calculation as we explain the unitarity method.

5.2.3 Unitarity method

The Cutkosky rules [98] apply at the level of diagrams. Consider a cut of a one-loop amplitude where diagrams with one or both of the required cut propagators missing are omitted. The sum of all possible tree-level diagrams on either side of the cut are on-shell tree-level amplitudes. This determines the coefficient of a single Feynman integral. Therefore, cuts in all kinematic invariants must be considered to generate all the required Feynman integrals in any one-loop amplitude. Thus, the application of unitarity as an on-shell method of calculating one-loop amplitudes turns the cutting step around. Instead of cutting one-loop amplitudes, tree-level amplitudes are sewn together to form the coefficients of integrals that arise at one-loop.

Unitarity was first used as an efficient tool to calculate the supersymmetric or *cut-constructible* parts of QCD loop amplitudes in [44]. Supersymmetric one-loop amplitudes are known to be entirely determined by their branch cuts [38]. So knowing all cuts available for a given kinematic point, the entire supersymmetric contribution to a one-loop amplitude can be determined:

$$\text{Im}A_n^{1\text{-loop}} = \sum_{\text{cuts}} \sum_{\text{spin}} \int \frac{d^D \ell_1}{(2\pi)^4} \frac{d^D \ell_2}{(2\pi)^4} A^{\text{tree}} \frac{1}{\ell_1^2} \frac{1}{\ell_2^2} A^{\text{tree}} = \sum_i c_i \mathcal{J}_i. \quad (5.27)$$

We highlight that the final result is in terms of linear combinations of a set of cut integrals \mathcal{J}_i with rational coefficients c_i .

The unitarity method has then recycled perturbative techniques from tree-level, as the integrals left to compute retain the use of the on-shell spinor formalism and compact tree-level amplitudes in their coefficients c_i . We do not want to explicitly compute these integrals, but one can make use of the previously defined basis of scalar integrals (2.34). This basis is what the integrals \mathcal{J}_i are ultimately targeted via tensor reduction techniques, such that one can read off their rational coefficients c_i in (2.26). In practice, applying a full Passarino-Veltman style reduction ($c_i \mathcal{J}_i \rightarrow \sum_i c_i I^i[1]$) is not always necessary; appropriate partial-fractioning of the integrand with respect to the loop momentum accomplishes the same goal in many cases.

Calculations such as (5.27) are of most benefit where the cut momenta exist in $D = 4$ dimensions. As pioneered by Bern, Dixon, Dunbar and Kosower in [44] where the $\mathcal{N} = 4$ and $\mathcal{N} = 1$ supersymmetric contributions to Yang-Mills theories were computed via cuts that utilised four dimensional on-shell tree-level amplitudes. Furthermore, in

$\mathcal{N} = 1$ super Yang-Mills (sYM) theory one-loop amplitudes are entirely determined by cuts in integrals contributing to boxes, triangles and bubbles, while $\mathcal{N} = 4$ sYM theory only receives contributions from boxes. In general, the cut momenta should be in $4 - 2\epsilon$ dimensions, but four dimensional tree-level amplitudes suffice to determine all of the integrals' coefficients c_i . Hence the cut-constructible pieces are the simplest to determine for supersymmetric theories.

In theories such as pure Yang-Mills, one receives contributions at one-loop that are not proportional to any logarithms or dilogarithms; the rational terms R_n that are a remnant of working to $O(\epsilon)$. Hence these terms are not found by four dimensional cutting techniques. The supersymmetric decomposition of one-loop QCD (4.14) showed that besides supersymmetric contributions one requires a scalar loop contribution, which yields rational terms as well as box, triangle and bubble integrals. Despite no supersymmetry, the scalar loop is still simpler than the full gluon amplitude, as the scalar does not propagate spin information. One can still utilise unitarity to determine the coefficients of these integrals for the scalar contribution. However, one must work in $4 - 2\epsilon$ -dimensions [99–101] or use on-shell recursion [102–106], or consider other analytic approaches [107, 108] to determine the rational terms.

5.2.3.1 An example of unitarity

In this subsection, we introduce a basic example of unitarity in cutting a loop amplitude to generate the required Feynman integrals [38] from a LIPS integral utilising on-shell tree-level amplitudes. As we have noted, $\mathcal{N} = 4$ sYM can be characterised in terms of only box integrals in the set of integrals \mathcal{F}_n from (2.34),

$$A_n^{1\text{-loop}, \mathcal{N}=4} = \sum_{i \in \mathcal{F}_n} d_i I_4^i \quad (5.28)$$

and so we consider the unitarity cut of an $\mathcal{N} = 4$ multiplet of the leading color MHV amplitude for n legs, first calculated in [44]. The Cutkosky rules are applied at the amplitude level, such that the sum of all diagrams on either side of the cut correspond to a product of two tree-level amplitudes. The double cut used in the one-loop amplitude is given by the integral over a two body phase space of the two possible orientations of products of MHV tree-level amplitudes, depicted in figure 5.2. These are summed over each intermediate helicity configuration that contributes, while the convention of

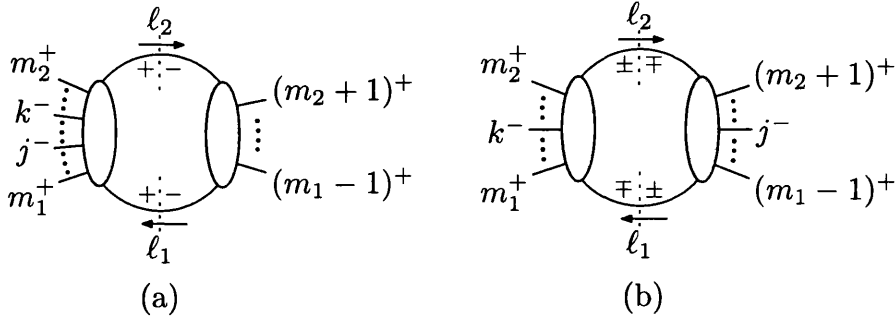


Figure 5.2: The two arrangements of negative helicities on either side of the cut, using MHV tree-level amplitudes. There is one helicity configuration non-vanishing in (a), while (b) allows both cases.

using outgoing helicities for all states requires intermediate particles reverse helicity on crossing the cut.

The first case to consider is the two negative helicity gluons on the same side of the cut, depicted in figure 5.2(a). We see the intermediate helicity configuration falls to the only non-vanishing case, such that the tree-level amplitudes sewn together are MHV also. We note also that, there are no helicity configurations one can assign for intermediate fermions or scalars (using particle/anti-particle assignment) such that the tree-level amplitudes on either side of the cut do not vanish. Thus for case (a) we can use pure gluon MHV tree-level amplitudes, where we shall denote the negative helicity arguments in the subscript. We consider cut in the channel indicated in figure 5.2(a) of momenta $(k_{m_1} + k_{m_1+1} + \dots + k_{m_2-1} + k_{m_2})^2$, where $m_1 \leq j < k \leq m_2$. The cut can be expressed as the Lorentz invariant phase space integral,

$$\begin{aligned} & \int d\text{LIPS}(-\ell_1, \ell_2) A_{jk}^{\text{tree MHV}}(-\ell_1, m_1, \dots, m_2, \ell_2) A_{(-\ell_2)\ell_1}^{\text{tree MHV}}(-\ell_2, m_2 + 1, \dots, m_1 - 1, \ell_1) \\ &= -i A_{jk}^{\text{tree MHV}}(1, 2, \dots, n) \int d\text{LIPS}(-\ell_1, \ell_2) \frac{\langle m_1 - 1, m_1 \rangle \langle \ell_1 \ell_2 \rangle^2 \langle m_2, m_2 + 1 \rangle}{\langle m_1 - 1, \ell_1 \rangle \langle \ell_1 m_1 \rangle \langle m_2 \ell_2 \rangle \langle \ell_2, m_2 + 1 \rangle}, \end{aligned} \quad (5.29)$$

which turns out to be the same result as that from case (b) in 5.2, even though that must include contributions from gluons, fermions and scalars in the $\mathcal{N} = 4$ multiplet. Despite an n -leg computation, only a few factors depend on the loop momenta and therefore the Feynman integral is simple to construct. Using the on-shell condition

$\ell_1^2 = \ell_2^2 = 0$ allows us to promote the ℓ -dependent denominator spinor products to scalar propagators,

$$\frac{1}{\langle \ell_x y \rangle} = \frac{[y \ell_x]}{2\ell_x \cdot y} = \frac{[y \ell_x]}{(\ell_x - y)^2}. \quad (5.30)$$

Furthermore, applying the reverse Cutkosky transformation (5.26) invokes the two propagators $\ell_1^2 \ell_2^2$, such that we are left with a cut hexagon with a loop-dependent numerator.

The hexagon integrand can be broken up into a sum of four cut box integrands via a partial fraction decomposition. The resulting boxes can be decomposed to a set of scalar boxes triangles and bubbles using Passarino-Veltman reduction. That leads to the contributions from the triangles and bubbles vanishing, to leave the result for the $\mathcal{N} = 4$ sYM one-loop MHV amplitude in terms of tree-level MHV amplitudes multiplied by scalar boxes. These are dimensionally regularised for both IR and UV divergences.

5.2.4 Generalised Unitarity

The unitarity method as presented currently, selects only those contributions in a one-loop amplitude with two propagators present. In terms of the Feynman integrals generated, one must sum over a large variety of cuts to account for all the integrals where only the two propagators present are determined by the discontinuity in a certain channel. This can also be thought of in terms of the scalar integral basis. Only those unitarity cuts whose result contains both cut propagators contribute to the coefficient of those integrals. As discussed in the previous subsection, analytic simplifications are required on cut expressions to isolate contributions to coefficients of different integrals. The procedure sorts terms into contributions to any integrals with the propagator denominators present in the cut channel, and removes contributions to lower point integrals. Requiring the cut across additional propagators beyond the original pair reduces the number of integrals that can contribute. Cutting more than just a pair of propagators goes under the name “generalised unitarity” that isolates a smaller subset of integrals to consider. This means two tree-level amplitudes in a single cut get split into more tree-level amplitudes with less external legs that will ultimately be simpler, hence there is less work to perform to extract coefficients of the integrals.

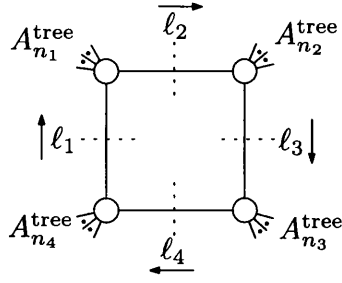


Figure 5.3: The maximal cuts for a box that isolates the integral's coefficient precisely, as the product of four on-shell tree-level amplitudes.

The ultimate refinement of this procedure is cutting enough propagators such that an integral from our basis in (2.26) is entirely isolated. It is also known as extracting the leading discontinuity of an amplitude [109]. This is possible for the boxes, using maximal generalised unitarity, which involves the cutting of all four propagators ℓ_i^2 for $i = 1 \dots 4$. This isolates the coefficient of a single box integral as a product of four tree-level amplitudes, as illustrated in figure 5.3. Furthermore, when considering supersymmetric theories one can take the cut momenta to be in four dimensions, such that the four delta functions freeze the loop momentum entirely [110],

$$\int \frac{d^D \ell}{(2\pi)^D} \frac{f(\ell_i)}{\ell_1^2 \ell_2^2 \ell_3^2 \ell_4^2} \Big|_{\ell^D \rightarrow \ell^4} \rightarrow \int \frac{d^D \ell}{(2\pi)^D} \delta^{(+)}(\ell_1^2) \delta^{(+)}(\ell_2^2) \delta^{(+)}(\ell_3^2) \delta^{(+)}(\ell_4^2) \Big|_{\ell^D \rightarrow \ell^4} = \frac{1}{2} \sum_{\text{sol}^{\text{B}}_{\text{s}}} f(\ell_i) \quad (5.31)$$

The four dimensional delta functions uniquely determine a discrete set of simultaneous on-shell equations, that are summed over. Hence the coefficients of the box integrals are reduced to the algebraic exercise of multiplying four tree-level amplitudes, summed over the solutions of various helicity configurations λ , for the cut momenta ℓ_i^λ ,

$$c_4 = \frac{1}{2} \sum_{\lambda=\pm} A_{n_1}^{\text{tree}}(-\ell_1^\lambda, \dots, \ell_2^{-\lambda}) A_{n_2}^{\text{tree}}(-\ell_2^\lambda, \dots, \ell_3^{-\lambda}) A_{n_3}^{\text{tree}}(-\ell_3^\lambda, \dots, \ell_4^{-\lambda}) A_{n_4}^{\text{tree}}(-\ell_4^\lambda, \dots, \ell_1^{-\lambda}), \quad (5.32)$$

where the external momenta are here implicit, and $\sum_i n_i = n + 8$. The sum is restricted to two solutions, hence the fractional normalisation, including those for which $f(\ell_i)$ may vanish. The frozen loop momenta (5.31) leads to direct extraction of the loop

coefficients using entirely four dimensional on-shell tree-level amplitudes. Since it is possible to use massless three-point amplitudes in the sewing process, one must use complex momenta so that these cuts do not vanish. Then the process is ultimately recycling the spinor-helicity method algebra for simple tree-level amplitudes at one-loop level.

In the maximal approach of generalised unitarity, a larger set of cuts including quadruple, triple and double cuts are required; but each one is simple and directly yields the coefficient of a single integral. Firstly, all possible quadruple cuts are computed for each type of box integral. Then one moves to three mass triangles, isolated using triple cuts, as used in [111]. Integrands coming from triple cuts in general also contain contributions to those same cuts appearing in some of the box integrals. These must be removed, along with box-like terms that vanish upon loop integration, to extract the coefficient of the three mass triangle. One way of achieving this, is using the decomposition of Ossola et al [112]. The remaining terms come from two- and one-mass triangles, and finally bubble integrals that make use of the standard cuts. The one- and two-mass triangles can be written as sums of bubble integrals, and so also fall under the umbrella of standard cut techniques. Further developments include direct extraction of loop integral coefficients [113] as one example; unitarity with massive propagators [114, 115]; while bringing rational terms into the fold of generalised unitarity was used here [116–118].

For dimensionally regularised theories, unitarity cuts must be evaluated where the loop momenta flows in $4 - 2\epsilon$ -dimensions. If one expands the amplitude in powers of ϵ as before, keeping terms of higher order than $O(\epsilon^0)$, rational terms R_n will contain invariants $(-s)^{-\epsilon}$. These will give rise to a term,

$$1 - \epsilon \ln(-s) + \dots, \quad (5.33)$$

which is discontinuous for $s > 0$ and hence detectable via a unitarity cut in the s channel. Rational terms can then be obtained on truncation to $O(\epsilon^0)$. In general a D -dimensional unitarity procedure will provide the result to all orders in ϵ , however this is beyond what is needed for practical applications. The spinor helicity formalism cannot be utilised as readily in D -dimensions, although being on-shell is beneficial. Hence D -dimensional unitarity is more of a computational effort than the combination of four

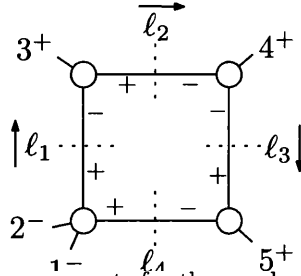


Figure 5.4: One of the five arrangements for the quadruple cut integral with massive leg K_{12} .
Figure 5.4: One of the five arrangements for the quadruple cut integral with massive leg K_{12} .

dimensional unitarity with additional techniques for rational parts, to be discussed in the following section. However, this method has been utilised in spinor integration methods [119–121], and is very useful when one needs to compute a process to high order in ϵ such as a loop splitting function.

The application of generalised unitarity works equally well beyond one-loop too; some applications can be found in [122–132].

5.2.5 A Box example

As an example [55], we compute the coefficient of a box integral in the pure gauge theory amplitude $A_5^{1\text{-loop}}(1^-, 2^-, 3^+, 4^+, 5^+)$. The possible box integrals will include precisely one massive external leg, $K_{ij} = k_i + k_j$, and three massless external legs. There are five boxes available for the arrangements of the massive leg K_{12} , K_{23} , K_{34} , K_{45} and K_{51} . The amplitude is symmetric under reflection $(12345) \rightarrow (21543)$, which relates the coefficients of the one-mass boxes between the integrals of K_{51} to K_{23} and that of K_{45} to K_{34} .

We shall compute the coefficient of the first one-mass box integral with massive leg at K_{12} ,

$$I_{4:1}^{1m} = \int \frac{d^{4-2\epsilon}\ell}{(2\pi)^{4-2\epsilon}} \frac{1}{\ell^2(\ell - K_{12})^2(\ell - K_{123})^2(\ell + K_4)^2} \quad (5.34)$$

using maximal generalised unitarity. When all four propagators are cut, as shown in figure 5.4, and the loop momenta is restricted to four dimensions, we are left with one four-point tree-level amplitude and three three-point tree-level amplitudes.

We see that we are restricted to complex loop momenta for non-vanishing results to exist, as possible solutions require distinct parametrisation for both the holomorphic and anti-holomorphic spinors. Specifically, the on-shell conditions on the top left vertex require that either

$$\lambda_{\ell_2} \propto \lambda_3 \quad \text{or} \quad \bar{\lambda}_{\ell_2} \propto \bar{\lambda}_3, \quad (5.35)$$

while the on-shell conditions of the top right vertex require that

$$\lambda_{\ell_2} \propto \lambda_4 \quad \text{or} \quad \bar{\lambda}_{\ell_2} \propto \bar{\lambda}_4. \quad (5.36)$$

However, we must maintain that for generic external momenta, momentum invariants such as s_{34} do not vanish. Therefore we combine the compatible solutions that are permitted:

$$\lambda_{\ell_2} \propto \lambda_3 \text{ and } \bar{\lambda}_{\ell_2} \propto \bar{\lambda}_4, \quad \text{or} \quad \lambda_{\ell_2} \propto \lambda_4 \text{ and } \bar{\lambda}_{\ell_2} \propto \bar{\lambda}_3, \quad (5.37)$$

which in turn forces neighbouring three point vertices to be of alternating type (from MHV to $\overline{\text{MHV}}$) as we circle the diagram. The helicity ordering is further constrained by the helicities attached at the massive leg, which requires negative helicity states for both cut momenta at that vertex, since we require a non-vanishing four point amplitude. These two requirements entirely fixes the contribution of the cut to the case depicted in figure 5.4, which means we must pick the first case in (5.37).

This such a configuration only exists for internal gluonic states, the massless quark/anti-quarks and scalars/anti-scalars circulating in this setup give a vanishing contribution. Hence we will use entirely pure gluon tree-level amplitudes to write the coefficient of the box integral, however we must first evaluate the on-shell conditions to solve for ℓ_2 explicitly. Three of the on-shell conditions,

$$\ell_2^2 = 0, \quad \ell_1^2 = (\ell_2 + k_3)^2 = 0, \quad \ell_3^2 = (\ell_2 - k_4)^2 = 0, \quad (5.38)$$

allow us to satisfy the first case of (5.37), by expanding out the possible parametrisation for ℓ_2^μ that is non-vanishing from the relations in (5.38);

$$\therefore \ell_2^\mu = \alpha_2 \langle 3 | \gamma^\mu | 4 \rangle. \quad (5.39)$$

Using a fourth condition for ℓ_2 , α_2 is fixed

$$\ell_4^2 = (\ell_2 - K_{45})^2 = 0, \quad \rightarrow \quad s_{45} - \alpha_2[4|5|3] = 0, \quad (5.40)$$

to be $\alpha_2 = \langle 45 \rangle / \langle 35 \rangle$. The coefficient of the box integral with massive leg K_{12} is then [55],

$$\begin{aligned} c_{12} &= \frac{1}{2} A_4^{\text{tree}}(-\ell_4^+, 1^-, 2^-, \ell_1^+) A_3^{\text{tree}}(-\ell_1^-, 3^+, \ell_2^+) A_3^{\text{tree}}(-\ell_2^-, 4^+, \ell_3^-) A_3^{\text{tree}}(-\ell_3^+, 5^+, \ell_4^-) \\ &= \frac{1}{2} \frac{\langle 12 \rangle^3}{\langle (-\ell_4)1 \rangle \langle 2\ell_1 \rangle \langle \ell_1(-\ell_4) \rangle} \frac{[\ell_2 3]^3}{[(-\ell_1)3][\ell_2(-\ell_1)]} \frac{\langle \ell_3(-\ell_2) \rangle^3}{\langle (-\ell_2)4 \rangle \langle 4\ell_3 \rangle} \frac{[5(-\ell_3)]^3}{[5\ell_4][\ell_4(-\ell_3)]} \\ &= -\frac{1}{2} \frac{\langle 12 \rangle^3 [5|\ell_3 \ell_2|3]^3}{\langle 4|\ell_3 \ell_4|1 \rangle \langle 2|\ell_1|3 \rangle \langle 4|\ell_2 \ell_1 \ell_4|5 \rangle} \end{aligned} \quad (5.41)$$

We can eliminate all loop momenta dependence using momentum conservation at each vertex and the solution for ℓ_2 (5.39), to simplify the expression to [55],

$$c_{12} = -\frac{1}{2} \frac{\langle 12 \rangle^3}{\langle 23 \rangle \langle 34 \rangle \langle 45 \rangle \langle 51 \rangle} s_{34} s_{45} = \frac{i}{2} A_5^{\text{tree}}(1^-, 2^-, 3^+, 4^+, 5^+) s_{34} s_{45}. \quad (5.42)$$

This is the coefficient to the box integral defined in (5.34) with massive leg K_{12} which is given by [55],

$$\begin{aligned} I_{4:1}^{1m} &= \frac{-2ic_\Gamma}{s_{34}s_{45}} \left\{ -\frac{1}{\epsilon^2} \left[\left(\frac{\mu^2}{-s_{34}} \right)^\epsilon + \left(\frac{\mu^2}{-s_{45}} \right)^\epsilon - \left(\frac{\mu^2}{-s_{12}} \right)^\epsilon \right] \right. \\ &\quad \left. + \text{Li}_2 \left(1 - \frac{s_{12}}{s_{34}} \right) + \text{Li}_2 \left(1 - \frac{s_{12}}{s_{45}} \right) + \frac{1}{2} \ln^2 \left(\frac{s_{34}}{s_{45}} \right) + \frac{\pi^2}{6} \right\} + O(\epsilon) \end{aligned} \quad (5.43)$$

where c_Γ is from (5.9). This and the other required box integrals with masses at legs K_{34} and K_{45} can be found in [97]. The resulting coefficients of those procure the exact same tree-level amplitude with the correct momentum invariant prefactors to cancel those coming from the denominators of the corresponding box integrals as in the first

case we evaluated. Thus the entire gluon-loop contribution to the five point one-loop amplitude is [55],

$$\begin{aligned}
 A_5^{1\text{-loop}}(1^-, 2^-, 3^+, 4^+, 5^+) = A_5^{\text{tree}}(1^-, 2^-, 3^+, 4^+, 5^+) c_{\Gamma} \Bigg\{ & \\
 - \frac{1}{\epsilon^2} \left[\left(\frac{\mu^2}{-s_{34}} \right)^\epsilon + \left(\frac{\mu^2}{-s_{45}} \right)^\epsilon - \left(\frac{\mu^2}{-s_{12}} \right)^\epsilon \right] & \\
 + \text{Li}_2 \left(1 - \frac{s_{12}}{s_{34}} \right) + \text{Li}_2 \left(1 - \frac{s_{12}}{s_{45}} \right) + \frac{1}{2} \ln^2 \left(\frac{s_{34}}{s_{45}} \right) + \frac{\pi^2}{6} & \\
 + \text{cyclic permutations} \Bigg\} + \text{triangles} + \text{bubbles}. & \\
 \tag{5.44} &
 \end{aligned}$$

Hence when working in $\mathcal{N} = 4$ sYM there are no contributions from triangles or bubbles, and this is the entire amplitude. The MHV one-loop amplitude bears a very similar resemblance to its tree-level counterpart, albeit with a sum over cyclic permutations and regulated against IR and UV divergences.

5.3 On-shell recursion

We have seen the benefit of continuing to complex momenta to define the three-point amplitude, and its applications in unitarity based methods in the previous sections. More significantly however, complex kinematics have been exploited to probe generic factorisation singularities of on-shell amplitudes. The use of the factorisations of amplitudes to reconstruct them via a shift into the complex plane, was developed for tree-level amplitudes by Britto, Cachazo, Feng and Witten (BCFW) [133]. Now the BCFW recursion relations are widely used, which we shall outline with an example by proving the n -leg MHV tree-level amplitudes.

Furthermore, loop level rational terms can be found by knowledge of their factorisations and determined via on-shell recursion also. We motivate the need to deal with these non-standard factorisations and elucidate through the verifying of the one-loop pure Yang-Mills amplitudes with a single negative helicity in the following Chapter.

5.3.1 Tree-level amplitudes by recursion

We now study the BCFW deformation of an amplitude, such that it depends upon a complex parameter z , introduced by the selection of two momenta to be deformed, typically by hatting the variables

$$\begin{aligned}\hat{p}_a(z) &= p_a - zq, \\ \hat{p}_b(z) &= p_b + zq,\end{aligned}\tag{5.45}$$

such that momentum conservation is still manifest. To maintain on-shell conditions for arbitrary z , we require:

$$q^2 = q \cdot \hat{p}_a = q \cdot \hat{p}_b = 0.\tag{5.46}$$

These equations are best solved by turning to the spinor notation, such that we can express $q = \lambda_a \bar{\lambda}_b$ and the deformation becomes

$$\begin{aligned}\hat{\lambda}_a &\rightarrow \lambda_a, \\ \hat{\bar{\lambda}}_a &\rightarrow \bar{\lambda}_a - z\bar{\lambda}_b, \\ \hat{\lambda}_b &\rightarrow \lambda_b + z\lambda_a, \\ \hat{\bar{\lambda}}_b &\rightarrow \bar{\lambda}_b.\end{aligned}\tag{5.47}$$

In this case for hatted \hat{p}_a and \hat{p}_b the deformation is known as the $[a, b)$ -shift [133]. Under the $A(p_a, p_b) \rightarrow A(z)$ deformation the shifted amplitude $A(z)$ can be studied using complex analysis. We can consider the following contour integration

$$I = \int_C \frac{dz}{z} A(z)\tag{5.48}$$

where the contour C is pushed to infinity and hence encircles all poles. Thus if $A(z)$ is rational, has simple poles at z_i and vanishes at large $|z|$, the boundary contribution vanishes and we can use Cauchy's theorem to reconstruct the unshifted tree-level

amplitude $A(z=0)$ as a sum of residues,

$$I = A(0) + \sum_{z_i} \text{Res} \left(\frac{A(z)}{z}, z_i \right) = 0. \quad (5.49)$$

Hence this is only useful if we can interpret the computation of the residues, and therefore an understanding of the singularity structure of the amplitude is essential.

We use factorisation properties of amplitudes to determine the residues in terms of known lower point amplitudes. At tree-level the factorisation of amplitudes occurs along collinear or multi-particle poles, see (5.1) and (5.2). The residues highlight instances where particular kinematic invariants vanish, $K_{i,j}^2(z) \rightarrow 0$ where $K_{i,j}^\mu = (k_i + k_{i+1} + \dots + k_j)^\mu$. For example on a multi-particle pole with two partitions of momenta $(S_{\mathcal{L}}, S_{\mathcal{R}})$ with one of the shifted momenta either side,

$$A_n^{\text{tree}} \xrightarrow{K_{i,j}^2 \rightarrow 0} \sum_{\sigma} \left[A_{r+1}^{\text{tree}}(k_i \in S_{\mathcal{L}}, K_{i,j}^\sigma) \frac{i}{K_{i,j}^2} A_{n-r+1}^{\text{tree}}((-K_{i,j})^{-\sigma}, k_i \in S_{\mathcal{R}}) \right] \quad (5.50)$$

The shifted amplitude $A(z)$ contains poles for values of z where $K_{i,j}^2(z) = 0$. Only the propagators containing one of \hat{k}_a or \hat{k}_b will be z dependent. So for $K_{i,j}$ containing \hat{k}_b , the shifted momentum along the channel is $\hat{K}_{i,j}^\mu(z) = K_{i,j}^\mu + z\lambda_a\bar{\lambda}_b$. Then the z -dependent propagator is

$$\hat{K}_{i,j}^2(z) = K_{i,j}^2 + z\langle\lambda_a|K_{i,j}|\lambda_b\rangle. \quad (5.51)$$

So the poles at z_i that cause the internal propagator $\hat{K}_{i,j}^2(z)$ to vanish are given by,

$$z_i = -\frac{K_{i,j}^2}{[b|K_{i,j}|a\rangle].} \quad (5.52)$$

We evaluate the residue at $A(z)/z$ for any z_i such that the intermediate propagator is put on-shell,

$$-\text{Res} \left[\frac{1}{z} \frac{1}{\hat{K}_{i,j}(z)^2} \right]_{z_i} = \frac{1}{K_{i,j}^2} \quad (5.53)$$

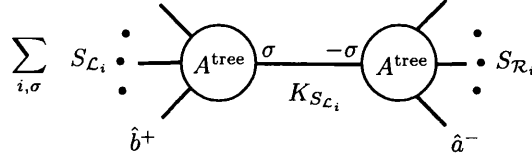


Figure 5.5: The factorisations that occur for tree-level recursion, summing over all i partitions of momenta on the left, \mathcal{L}_i and right \mathcal{R}_i and internal helicity configurations σ .

and reverts to its form in the unshifted kinematics. Hence the residues will be the products of lower point amplitudes defined at $z = z_i$, defined pictorially in figure 5.5,

$$A(z=0) = - \sum_{z_i} \text{Res} \left(\frac{A(z)}{z}, z_i \right) = \sum_{i, \sigma} A_{S_{\mathcal{L}_i+1}}^{\text{tree}, \sigma}(z_i) \frac{i}{K_{S_{\mathcal{L}}}^2} A_{S_{\mathcal{R}_i+1}}^{\text{tree}, \sigma}(z_i), \quad (5.54)$$

where the propagator is not evaluated on the pole, to recover the unshifted tree-level amplitude in terms of known lower point amplitudes. The summation over i only includes factorisations where the legs \hat{k}_a and \hat{k}_b are split across either $S_{\mathcal{L}}$ or $S_{\mathcal{R}}$.

5.3.1.1 Example of tree-level recursion - MHV amplitudes

We shall prove the n -point recursion relation for tree-level MHV amplitudes, which is a particularly simple example [55] to illustrate the method. There exist only collinear poles, due to the restricted assignments of helicity to yield non-vanishing amplitudes on either side of the pole. Indeed for any choice of two shifted momenta, there will only be two possible poles generated in this setup. Suppose we apply the $[n, 1]$ -shift,

$$\begin{aligned} \hat{\lambda}_1 &= \lambda_1 + z \lambda_n \\ \hat{\bar{\lambda}}_n &= \bar{\lambda}_n - z \bar{\lambda}_1 \end{aligned} \quad (5.55)$$

to the n -leg MHV amplitude,

$$A_{jn}^{\text{tree MHV}}(z) = i \frac{\langle jn \rangle^4}{(\langle 12 \rangle + z \langle n2 \rangle) \langle 23 \rangle \dots \langle n-1, n \rangle \langle n1 \rangle}. \quad (5.56)$$

The two z -dependent collinear poles that are possible, occur in the momentum invariants, $(\hat{k}_1 + k_2)^2$ and $(k_{n-1} + \hat{k}_n)^2$. The three-point amplitude on the latter pole is

an $\overline{\text{MHV}}$ amplitude which vanishes under the shift, hence the former pole is the only invariant to consider, as highlighted via the one shifted spinor product in eq. (5.56),

$$z_{12} = -\frac{s_{12}}{[1|K_{12}|n\rangle} = -\frac{[12]\langle 21\rangle}{[12]\langle 2n\rangle} = -\frac{\langle 12\rangle}{\langle n2\rangle} \quad (5.57)$$

that induces the pole in $A(z)$. The quotient $A(z)/z$ behaves like $1/z^2$ as $z \rightarrow \infty$, so the integral around the contour at infinity vanishes as required,

$$0 = \int \frac{A_{jn}^{\text{tree MHV}}(z)}{z} dz. \quad (5.58)$$

Thus we can utilise (5.54) as the amplitude at the pole $z = 0$ is equal and of opposite sign to the residue at the pole (5.57). So by using the fact that intermediate states going on-shell cause the amplitude to factorise over the diverging propagator, we have the un-shifted amplitude in terms of the residue at $z = z_{12}$,

$$\begin{aligned} A_n^{\text{tree}} &= - \sum_{\lambda=\pm} A_{n-1}^{\text{tree}}(\hat{K}_{12}^\lambda, 3^+, \dots, j^-, \dots, \hat{n}^-) \text{Res} \left[\frac{1}{z} \frac{i}{\hat{K}_{12}^2(z)} \right]_{z_{12}} A_3^{\text{tree}}(\hat{1}^+, 2^+, -\hat{K}_{12}^{-\lambda}) \\ &= A_{n-1}^{\text{tree}}(\hat{K}_{12}^\lambda, 3^+, \dots, j^-, \dots, \hat{n}^-) \frac{i}{s_{12}} A_3^{\text{tree}}(\hat{1}^+, 2^+, -\hat{K}_{12}^-), \end{aligned} \quad (5.59)$$

where the sum over the helicity of the intermediate state λ reduces to one non-vanishing contribution in this case. Inputting the MHV amplitudes, we evaluate the hatted variables according to the shift (5.55) at the residue (5.57),

$$\begin{aligned} A_n^{\text{tree}} &= \frac{i\langle j\hat{n}\rangle^4}{\langle \hat{K}_{12}3\rangle\langle 34\rangle\dots\langle n-1,\hat{n}\rangle\langle \hat{n}\hat{K}_{12}\rangle} \frac{i}{s_{12}} \frac{-i[\hat{1}2]^3}{[2(-\hat{K}_{12})][(-\hat{K}_{12})\hat{1}]} \\ &= i \frac{\langle jn\rangle^4[12]^3}{[2|\hat{K}_{12}|n\rangle s_{12}[1|\hat{K}_{12}|3\rangle\langle 34\rangle\dots\langle n-1,n\rangle]} \\ &= i \frac{\langle jn\rangle^4}{\langle 12\rangle\langle 23\rangle\langle 34\rangle\dots\langle n-1,n\rangle\langle n1\rangle}. \end{aligned} \quad (5.60)$$

Thus we have proven the n -point MHV tree-level amplitude recursively, matching the form (3.51).

5.3.2 The tree-level \mathcal{S} -matrix of $\mathcal{N} = 4$ sYM theory

Recursion relations have been developed in many theories, those with more supersymmetry with the most success. Particularly, we present the general construction for the entire tree-level \mathcal{S} -matrix in $\mathcal{N} = 4$ sYM theory [134].

Consider the BCFW recursion procedure, in a $[n, 1\rangle$ -shift. The behaviour of $A(z)$ for large z depends on the helicity of the shifted legs, such that for particles $(1, n)$ [64],

$$A(+-) \sim \frac{1}{z}, \quad A(++) \sim z, \quad A(--) \sim z, \quad A(-+) \sim z^3. \quad (5.61)$$

By the arguments of Arkani-Hamed and Kaplan [135], it can be shown that in certain cases, cancellations among diagrams contribute to a soft enough large z behaviour for the $(++)$ and $(--)$ cases, such that the z dependence becomes $A(z) \rightarrow z^{-1}$. Importantly, one can make use of the \bar{q} -symmetry (4.7) to shift the η variables for any two legs to zero, thus one can shift the two η variables related to the shifted legs. Hence the full superamplitude with the shifted η variables can be related to the $(++)$ amplitude. Recall that the \bar{q} -symmetry (4.7) relates η and $\bar{\lambda}$ variables, so to preserve the symmetry then one must shift η whenever $\bar{\lambda}$ is shifted. Hence the full z -dependent shift for the recursion to perform in $\mathcal{N} = 4$ theory is [134],

$$\begin{aligned} \hat{\lambda}_1(z) &= \lambda_1 - z\lambda_n, \\ \hat{\bar{\lambda}}_n(z) &= \bar{\lambda}_n - z\lambda_1, \\ \hat{\eta}_n(z) &= \eta_n + z\eta_1. \end{aligned} \quad (5.62)$$

With this modified shift, the $\bar{\xi}$ parameter from (4.8) of the \bar{q} transformation required to set η_1 and $\hat{\eta}_n(z)$ to zero is independent of z ,

$$\bar{\xi}^A = \frac{\bar{\lambda}_1 \hat{\eta}_n^A(z) - \hat{\bar{\lambda}}_n(z) \eta_1^A}{[\bar{\eta}_1 \hat{\eta}_n(z)]} = \frac{\bar{\lambda}_1 \eta_n^A - \bar{\lambda}_n \eta_1^A}{[\bar{\eta}_1 \eta_n]}. \quad (5.63)$$

Thus $\eta_1 = \eta_n = 0$ is kept throughout, and the shift is valid for the full superamplitude. The recursion is setup as a sum over residues over factorised amplitudes on diverging propagators as before. However, rather than summing over internal states, one must

instead integrate over the Grassmann variable associated to the internal line joining the two sub-amplitudes. The recursion relation for $\mathcal{N} = 4$ super Yang-Mills theory at tree level is then constructed as [64],

$$A_n = \sum_i \int \frac{d^4 \eta_{\hat{P}_i}}{P_i^2} A_L(\hat{1}(z_{p_i}), 2, \dots, i-1, -\hat{P}(z_{p_i})) A_R(\hat{P}(z_{p_i}), i, \dots, n-1, \hat{n}(z_{p_i})). \quad (5.64)$$

We will not prove any cases here as the MHV case is a single term computation very similar to that calculated before for the tree-level recursion example in pure gluon amplitudes, but instead refer readers to [134] where the explicit derivations of all tree-level amplitudes in $\mathcal{N} = 4$ super Yang-Mills is presented starting from three point vertices and terms of recurring structure in an R invariant. The solution to $\mathcal{N} = 4$ Yang-Mills is not a restriction though, as the tree-level gluon amplitudes are the same in any gauge theory. The simplicity of the expressions arising from the recursive structure applies to all gauge theories and not just the maximally supersymmetric solution presented by Drummond and Henn [134]. Furthermore, the entire tree-level S -matrix for massless QCD has now been categorised utilising these techniques [136], with computer code packages.

The recursive technique used here can be extended to supergravity [137]. Again it can be made manifestly supersymmetric of which maximal $\mathcal{N} = 8$ is the simplest [138], admitting an explicit solution [139]. Also, pure graviton amplitudes have been considered using recursion relations [140, 141].

Various shifts on multiple legs have proven useful [142], as they can lead to improved behaviour of the shifted amplitudes as $z \rightarrow \infty$ [102]. The BCFW deformation was extended to Yang-Mills amplitudes with massless external quarks as well as gluons in [143–146]. Recursion relations were utilised for tree-level amplitudes containing massive external particles, such as electroweak vector bosons, Higgs bosons, heavy quarks and squarks in [147–151]. Even Abelian theories such as QED can also be solved recursively [152].

5.3.3 Recursion for rational terms at one-loop

Beyond tree-level there are three concerns in continuing with recursion. Firstly, there are non-rational functions such as logarithms and dilogarithms; secondly, the amplitudes may include poles of higher order for complex momenta and finally; the amplitudes may not vanish asymptotically with z . However, techniques have been developed that make use of unitarity methods [99–101] and on-shell recursion [102–106] combined.

If we consider the parts pertaining to branch cuts C_n in our one-loop amplitudes as having been dealt with previously in the unitarity section, then the rational part R_n can be found if sufficient knowledge of its singularity structure is known. The rational terms R_n make up the contribution to one-loop amplitudes with all logarithmic and π^2 terms set to zero. By shifting into the complex plane, $R_n(z)$ may be found as a sum of residues,

$$A_n - C_n = R_n = \sum_{z_i} \text{Res} \left(\frac{R_n(z)}{z}, z_i \right) \quad (5.65)$$

similar to the tree-level case of (5.54). The factorisation of one-loop amplitudes (5.8) provides the possible simple poles over which residues are constructed corresponding to the diagrams in figure 5.6, under a suitable shift. Other deformations such as shifting more than two spinors [102] may be required to ensure proper large z behaviour. Knowledge of the three- and four-point rational terms and tree-level amplitudes lead us to the formula (depicted pictorially in figure 5.6) for an n -point rational contribution to a one-loop amplitude [106],

$$R_n = \sum_{i,\lambda} \left(R_{S_{\mathcal{L}_i}+1}(z_i) \frac{i}{K_{S_{\mathcal{L}_i}}^2} A_{S_{\mathcal{R}_i}+1}^{\text{tree}}(z_i) + A_{S_{\mathcal{L}_i}+1}^{\text{tree}}(z_i) \frac{i}{K_{S_{\mathcal{L}_i}}^2} R_{S_{\mathcal{R}_i}+1}(z_i) \right. \\ \left. + A_{S_{\mathcal{L}_i}+1}^{\text{tree}}(z_i) \frac{i\mathcal{F}_n}{K_{S_{\mathcal{L}_i}}^2} A_{S_{\mathcal{R}_i}+1}^{\text{tree}}(z_i) \right) \quad (5.66)$$

where there are sums over the internal intermediate helicity λ of state K , and i partitions of momenta $S_{\mathcal{L}}$ and $S_{\mathcal{R}}$ containing at least one of the shifted momenta on either side. The recursion relation also receives contribution from a one-loop factorisation

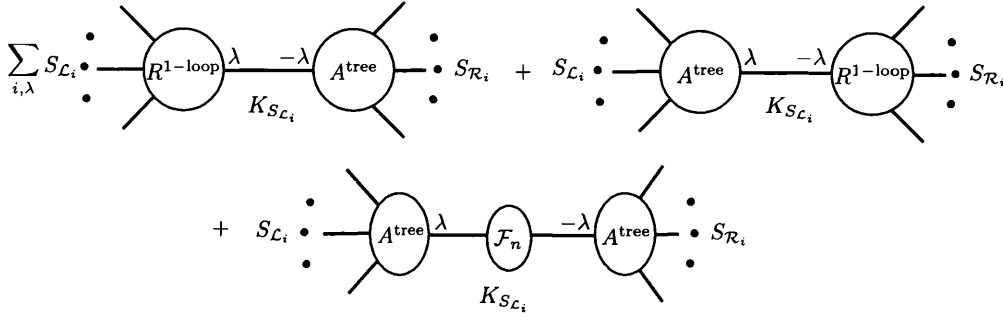


Figure 5.6: The factorisations that occur for the rational terms R_n at one-loop on-shell recursion. For a particular shift, the factorisations include those with lower point tree-level amplitudes connected to lower point rational terms, and the swap for the shifted momenta attached to the opposite functions. The one-loop factorisation function \mathcal{F}_n contributes only in amplitudes with multiparticle poles. Sums over i partitions of momenta on the left \mathcal{L}_i and right \mathcal{R}_i , and internal helicity configurations λ are required.

function \mathcal{F}_n , similar to that in the case of standard factorisations of one-loop amplitudes (5.8). Terms contained in \mathcal{F}_n only contribute for multi-particle channels, provided the tree-level amplitude contains a pole in that channel. Thus for one-loop amplitudes with either one or two helicities different from the rest, there is no contribution from \mathcal{F}_n .

The complication not addressed is when complex momenta in one-loop amplitudes develop higher order singularities. While these do not prohibit the use of recursion, they do necessitate an understanding of factorisation beyond leading order. Suppose a rational term has a double pole so that

$$R(z) = \frac{\alpha}{(z - z_i)^2} + \frac{\beta}{(z - z_i)} + \dots \quad (5.67)$$

then

$$R(0) = \sum_i \left(\frac{\alpha}{z_i^2} - \frac{\beta}{z_i} \right). \quad (5.68)$$

As we can see, we need the coefficients of both the leading and sub-leading terms. The sub-leading poles here are independent of the normal simple poles from other factorisations, yet they must still be accounted for. In general the structure of the sub-leading pole or “pole under the pole” (PUP) which arises is poorly understood.

For complex momenta we can acquire higher order poles than the single poles in

5.3 On-shell recursion

the standard factorisations of one-loop amplitudes (5.8) for real momenta. For a two-particle pole $K^2 = (k_a + k_b)^2 = 2k_a \cdot k_b = \langle a b \rangle [b a]$. For real momentum $\langle a b \rangle = \pm [a b]^*$ and so both vanish at the pole. However for complex momenta we may have $\langle a b \rangle = 0$ but $[a b] \neq 0$. So terms such as $[a b]^2 / \langle a b \rangle^2$ which are finite for real momenta can have multiple poles in complex momenta. These can be interpreted within (5.8) as arising from the three-point one-loop amplitude acquiring a singularity. Specifically, the three-point all-plus one-loop amplitude has a pole

$$A_3^{1\text{-loop}}(K^+, a^+, b^+) = \frac{1}{K^2} V^{1\text{-loop}}(K^+, a^+, b^+) \quad (5.69)$$

where the three-point “loop-vertex” for pure Yang-Mills is

$$V^{1\text{-loop}}(K^+, a^+, b^+) = -\frac{i}{48\pi^2} [K a][a b][b K]. \quad (5.70)$$

For real momenta $A_3^{1\text{-loop}}(K^+, a^+, b^+)$ vanishes as $s_{ab} \rightarrow 0$ but it can be singular for complex momenta. Equation (5.69) specifies the double pole as $s_{ab} \rightarrow 0$ however, as discussed previously, we require the sub-leading pole in order to use recursion.

Further spurious poles in general appear in the rational terms, that cancel against those in the cut-containing parts C_n , but must be accounted for in the recursion relations for R_n . The coefficients of the integrals that appear at one-loop, contain a range of singularities that are not present in the full amplitude. There are *spurious singularities* of the form Δ^{-P} , where Δ is a Gram-determinant of an integral function in the coefficients, yet the entire amplitude is finite as $\Delta \rightarrow 0$. These singularities in the coefficients can be of high-order in Δ , examples have been encountered with a case of $P = 5$ in closely related work [20]. These spurious singularities cancel amongst the terms in C_n and also, crucially, with the rational term R_n . There are also singularities that occur at the same kinematic points as the physical singularities, but are of higher order. Again cancellations between the terms in C_n and R_n must remove these higher order poles from the whole amplitude.

In the recursive approach higher order poles can generate rational *descendants* from the terms in C_n . To evaluate the residue at a higher order pole the integral functions must be expanded to a corresponding order and the derivatives in this Taylor expansion

eventually yield rational terms. In this way one can obtain rational terms whose origins lie in both the box and bubble integral contributions to C_n .

Dealing with higher order poles and spurious poles has not stopped the use of on-shell recursion being used beyond tree-level, and we illustrate the case of determining the rational part of a five-point rational contribution to a one-loop amplitude with a single negative helicity in the example below, that will highlight the issue of higher order poles.

5.3.3.1 One-loop on-shell recursion – an example

For amplitudes of a single negative helicity (single-minus) or indeed all-plus, their one-loop computation is the first non-vanishing contribution. Furthermore, by virtue of their helicity structure they have no cut containing terms and as such are entirely rational functions. These amplitudes have been categorised completely for pure Yang-Mills using on-shell recursion techniques [102]. A single-minus one-loop amplitude allows a factorisation over a MHV tree-level amplitude multiplied by a collinear one-loop amplitude with all positive helicities. We shall see this gives rise to a double pole and coincident single pole from this contribution.

We now compute the recursive contributions to the entirely rational one-loop amplitude $A_5^{1\text{-loop}}(a^-, b^+, c^+, d^+, e^+)$ via on-shell recursion [102], using the $[a, b]$ -shift in (5.47). We can draw the recursive diagrams required to build this recurrence relation in the normal on-shell prescription as a sum of connected tree-level and one-loop amplitudes, as illustrated in figure 5.7.

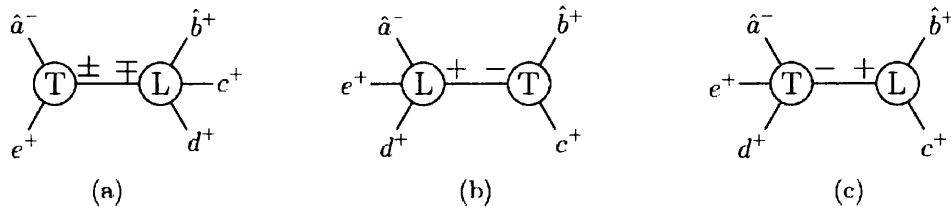


Figure 5.7: These are the possible connections of tree-level and one-loop amplitudes that contribute to the recursive expression for $A_5^{1\text{-loop}}(a^-, b^+, c^+, d^+, e^+)$, where T are trees and L are loops.

We have two contributions from simple poles in figure 5.7(a) and (b), while the double pole with its coincident single pole are contained in figure 5.7(c). For the

5.3 On-shell recursion

recursive construction we will require two one-loop four-point amplitudes as follows,

$$\begin{aligned} A_4^{1\text{-loop}}(a^+, b^+, c^+, d^+) &= -\frac{iN_p}{96\pi^2} \frac{[ab][cd]}{\langle ab \rangle \langle cd \rangle}, \\ A_4^{1\text{-loop}}(a^-, b^+, c^+, d^+) &= \frac{iN_p}{96\pi^2} \frac{\langle bd \rangle [bd]^3}{[ab] \langle bc \rangle \langle cd \rangle [da]} \end{aligned} \quad (5.71)$$

and the MHV and $\overline{\text{MHV}}$ n -gluon tree-level amplitudes (3.51).

Taking into account the two helicity configurations from figure 5.7(a), only one survives due to the requirement k_a must enter on an MHV amplitude to contribute a non-vanishing result. Therefore the expected form of the recurrence relation for the five-point one-loop amplitude is,

$$\begin{aligned} A_5^{1\text{-loop}}(a^-, b^+, c^+, d^+, e^+) &\sim A_3^{\text{tree}}(\hat{a}^-, -\hat{K}_{ae}^-, e^+) \frac{i}{K_{ae}^2} A_4^{1\text{-loop}}(\hat{b}^+, c^+, d^+, \hat{K}_{ae}^+) \\ &\quad + A_3^{\text{tree}}(\hat{b}^+, c^+, -\hat{K}_{bc}^-) \frac{i}{K_{bc}^2} A_4^{1\text{-loop}}(\hat{a}^-, \hat{K}_{bc}^+, d^+, e^+) \\ &\quad + A_3^{1\text{-loop}}(\hat{b}^+, c^+, -\hat{K}_{bc}^+) \frac{i}{K_{bc}^2} A_4^{\text{tree}}(\hat{a}^-, \hat{K}_{bc}^-, d^+, e^+). \end{aligned} \quad (5.72)$$

We shall take each term separately. Firstly, the helicity configuration that is non-vanishing in figure 5.7(a) that corresponds to the first term in (5.72) can be calculated as follows,

$$\begin{aligned} \text{figure 5.7(a)} &= A_3^{\text{tree}}(\hat{a}^-, \hat{K}_{ae}^-, e^+) \frac{1}{K_{ae}^2} A_4^{1\text{-loop}}(\hat{K}_{ae}^+, \hat{b}^+, c^+, d^+) \\ &= \frac{iN_p}{96\pi^2} \frac{\langle \hat{a}(-\hat{K}_{ae}) \rangle^3}{\langle \hat{a}e \rangle \langle e(-\hat{K}_{ae}) \rangle} \frac{1}{s_{ae}} \frac{[cd][\hat{b}\hat{K}_{ae}]}{\langle cd \rangle \langle \hat{b}\hat{K}_{ae} \rangle} \\ &= -\frac{iN_p}{96\pi^2} \frac{[be]^3}{\langle cd \rangle^2 [ab][ea]}. \end{aligned} \quad (5.73)$$

5.3 On-shell recursion

Secondly, the second term in (5.72) can be calculated from figure 5.7(b) as follows,

$$\begin{aligned}
\text{figure 5.7(b)} &= A_3^{\text{tree}}(\hat{b}^+, c^+, -\hat{K}_{bc}^-) \frac{i}{K_{bc}^2} A_4^{1\text{-loop}}(\hat{a}^-, \hat{K}_{bc}^+, d^+, e^+) \\
&= -\frac{iN_p}{96\pi^2} \frac{[\hat{b}c]^3}{[(-\hat{K}_{bc})\hat{b}][c(-\hat{K}_{bc})]} \frac{1}{s_{bc}} \frac{\langle \hat{K}_{bc}e \rangle [\hat{K}_{bc}e]^3}{[a\hat{K}_{bc}]\langle \hat{K}_{bc}d \rangle \langle de \rangle [ea]} \\
&= -\frac{iN_p}{96\pi^2} \frac{\langle ad \rangle^3 [de] \langle ce \rangle}{\langle ab \rangle \langle bc \rangle \langle cd \rangle^2 \langle de \rangle^2}.
\end{aligned} \tag{5.74}$$

Let us now concentrate on the last residue that contains the double and single poles as $\langle \hat{b}c \rangle \rightarrow 0$. The residue that is calculated requires the all-plus one-loop three-point amplitude connected to the four-point tree-level amplitude with K_{bc}^2 the on-shell propagator. The calculation is

$$\text{figure 5.7(c)} = A_3^{1\text{-loop}}(\hat{b}^+, c^+, -\hat{K}_{bc}^+) \frac{1}{K_{bc}^2} A_4^{\text{tree}}(\hat{a}^-, \hat{K}_{bc}^-, d^+, e^+). \tag{5.75}$$

We can use the three-point loop vertex defined in (5.69), for the legs k_b and k_c going collinear as follows,

$$A_3^{1\text{-loop}}(b^+, c^+, d^+) = -i \frac{N_p}{96\pi^2} \frac{[bc][cd][db]}{K_{bc}^2} = \frac{1}{K_{bc}^2} V_3^{1\text{-loop}}(b^+, c^+, d^+) \tag{5.76}$$

This is where the double pole appears from, since we retrieve the extra factor of $1/K_{bc}^2$ from the on-shell propagator in (5.75). However, this is not enough to define the behaviour arising from the pole under the double pole, and so the soft factors were introduced by Bern et al [102], such that the residue was modified to include the next to leading order behaviour in $O(K_{bc}^2)$.

$$\begin{aligned}
\text{figure 5.7(c)} &\rightarrow \frac{V_3^{1\text{-loop}}(\hat{b}^+, c^+, -\hat{P}_{bc}^+) A_4^{\text{tree}}(\hat{a}^-, \hat{P}_{bc}^-, d^+, e^+)}{(K_{bc}^2)^2} \\
&\quad \times \left(1 + K_{bc}^2 S^{\text{tree}}(\hat{a}, \hat{K}_{bc}^+, d) S^{\text{tree}}(c, -\hat{K}_{bc}^-, \hat{b}) \right) \\
&= -\frac{iN_p}{96\pi^2} \frac{\langle ac \rangle^2 \langle ab \rangle [bc]}{\langle bc \rangle^2 \langle cd \rangle \langle de \rangle \langle ea \rangle} \left(1 + \frac{\langle ad \rangle \langle bc \rangle}{\langle ab \rangle \langle cd \rangle} \right)
\end{aligned} \tag{5.77}$$

where the soft factors are given by

$$S^{\text{tree}}(a, s^+, b) = \frac{\langle ab \rangle}{\langle as \rangle \langle sb \rangle} \quad \text{and} \quad S^{\text{tree}}(a, s^-, b) = -\frac{[ab]}{[as][sb]}, \quad (5.78)$$

as introduced in (5.7). The modification is a combination of soft factors that include a sub-leading pole with explicit s_{bc} , but also carries no overall spinor weight. Thus the postulated terms of (5.72) are replaced by the calculations in (5.73), (5.74) and (5.77) first introduced by Bern et al [102]. The final result for the single-minus one-loop amplitude is

$$A_5^{1\text{-loop}}(a^-, b^+, c^+, d^+, e^+) = \frac{iN_p}{96\pi^2} \left[-\frac{[be]^3}{\langle cd \rangle^2 [ab][ea]} + \frac{\langle ad \rangle^3 [de] \langle ce \rangle}{\langle ab \rangle \langle bc \rangle \langle cd \rangle^2 \langle de \rangle^2} \right. \\ \left. - \frac{\langle ab \rangle [bc] \langle ca \rangle^2}{\langle bc \rangle^2 \langle cd \rangle \langle de \rangle \langle ea \rangle} - \frac{\langle ad \rangle [bc] \langle ca \rangle^2}{\langle bc \rangle \langle cd \rangle^2 \langle de \rangle \langle ea \rangle} \right] \quad (5.79)$$

which has to account for the pole under the pole (PUP) behaviour of double poles. We shall explore further in the following chapters the general behaviour of the leading and sub-leading terms coming from double poles in complex momenta.

Chapter 6

One-loop n -point single-minus Yang-Mills amplitudes

In this chapter, we present a recalculation of the n -point Yang-Mills one-loop amplitude $A^{1\text{-loop}}(a^-, b^+, c^+, \dots, n^+)$. We abbreviate the amplitude to one-loop *single-minus*, that we shall derive by on-shell recursion with sums over factorisations for the BCFW $[a, b]$ -shift:

$$\begin{aligned}\hat{\bar{\lambda}}_a &= \bar{\lambda}_a - z\bar{\lambda}_b, \\ \hat{\lambda}_b &= \lambda_b + z\lambda_a,\end{aligned}\tag{6.1}$$

with a new method for dealing with double poles. As discussed in Chapter 5, factorisations inducing double poles occur when considering the one-loop splitting amplitude (5.76) as $\langle \hat{b}c \rangle \rightarrow 0$ for on-shell recursion procedures. Previously, this factorisation was dealt with by implementing an evaluation on the pole with an ansatz introduced by Bern et al [102]. We summarise their application to the n -point amplitude that was also shown by the same authors [102], before setting up the non-standard factorisations in terms of an axial gauge summation of diagrams. We provide the explicit constructive derivation for the five-point amplitude to replicate (5.77), before moving on to the n -point amplitude. We show that the result has universal properties of interchange MHV amplitudes, that will feature in Chapter 7 for generalisations to pure gravity.

6.1 Complex factorisation

Factorisation in collinear channels, at least at one-loop has proven more subtle in complex kinematics than real kinematics. For real momenta, in the collinear limit $k_i \parallel k_j$, the spinor products $\langle ij \rangle$ and $[ij]$ vanish with the same rapidity. The additional complication in collinear channels with complex momenta, is due to the fact that one of the two spinor products remains non-zero in on-shell three-point kinematics. Thus when the case of an all-plus loop splitting amplitude arises in complex momenta, its associated collinear behaviour from (5.14) is,

$$\text{Split}_+^{1\text{-loop}}(i^+, j^+) \sim \frac{[ij]}{\langle ij \rangle^2}. \quad (6.2)$$

This behaviour does not manifest at tree-level, since all-plus splitting amplitudes vanish due to the vanishing three-point tree vertex. The typical tree-level collinear behaviour is $1/[ij]$ or $1/\langle ij \rangle$, that for real momenta is equivalently singular in magnitude, $A \sim 1/\sqrt{s_{ij}}$. However, for complex momenta poles can develop at which $\langle ij \rangle$ vanish but $[ij]$ do not.

This leads to double poles in the z parameter space when recursive techniques are used at the one-loop level coming from contributions such as (6.2). These are poorly understood due to the need to probe beyond the leading double pole when extracting the coefficients of the poles via the residue theorem. This is because Cauchy's theorem for the sum over residues includes all possible induced poles. So as a pole develops for $1/\langle ij \rangle^2$ in (6.2), the residue will in principle require a non-vanishing contribution from the sub-leading $1/\langle ij \rangle$ pole,

$$\text{Res} \left(\frac{1}{z} \frac{1}{\langle ij \rangle^2} \right)_{\langle ij \rangle \rightarrow 0} \sim \frac{A}{\langle ij \rangle^2} + \frac{B}{\langle ij \rangle}. \quad (6.3)$$

This sub-leading pole is exposing the pole structure of the one-loop splitting amplitudes under vanishing complex momenta. Thus the coefficient B in (6.3) is not related to any other factorisations for which $\langle ij \rangle \rightarrow 0$ might contribute, but must be found to compute the correct factorisation.

We shall motivate the need for a new kind of non-standard or *complex* factorisation that can automatically probe the sub-leading pole region. In general this would benefit on-shell recursion techniques by not requiring the addition of soft factors as seen in the

6.1 Complex factorisation

one-loop example computed in Chapter 5. To better understand how these factors arise without having to resort to introducing new factors by hand, axial gauge rules are used to build analytic functions for the single-minus one-loop amplitude in particular. We shall derive the coefficient of the sub-leading pole under the pole previously known as soft factors using the axial gauge formalism. This contains all the analytic behaviour to replicate the double pole and the coincident single pole. Therefore, we shall supplant the common factorisation with a new non-standard or *complex* factorisation arising because of the complex momenta inducing double poles.

In [102] the all-plus loop splitting factorisation of the single-minus Yang-Mills one-loop amplitude was considered and a universal form for the pole under the pole (PUP) proposed. The form of the PUP was postulated to be

$$\frac{1}{(K^2)^2} \left(1 + \sum_{a_i, b_i} S(a_1, \hat{K}^+, a_2) K^2 S(b_1, \hat{K}^-, b_2) \right), \quad (6.4)$$

where the soft factors were those used in the one-loop on-shell recursion example in Chapter 5; (5.78). With these additive factors the normal one-loop recursion correctly retrieves the known one-minus one-loop amplitudes. The consistency requirements for recursion in QCD were shown to be sufficient to determine these factors in [153] by exploiting Lorentz invariance.

The proposed form for the n -leg amplitude is

$$\begin{aligned} A_n^{1\text{-loop}}(a^-, b^+, \dots, n^+) &= A_{n-1}^{1\text{-loop}}(d^+, \dots, n^+, \hat{a}^-, \hat{K}_{bc}^+) \frac{i}{K_{bc}^2} A_3^{\text{tree}}(\hat{b}^+, c^+, -\hat{K}_{bc}^-) \\ &+ \sum_{i=4}^{n-1} A_{n-i+2}^{\text{tree}}((i+1)^+, \dots, n^+, \hat{a}^-, \hat{K}_{b\dots i}^-) \frac{i}{K_{b\dots i}^2} A_i^{1\text{-loop}}(\hat{b}^+, \dots, i^+, -\hat{K}_{b\dots i}^+) \\ &+ A_{n-1}^{\text{tree}}(d^+, \dots, n^+, \hat{a}^-, \hat{K}_{bc}^-) \frac{i}{(K_{bc}^2)^2} V^{1\text{-loop}}(\hat{b}^+, c^+, -\hat{K}_{bc}^+) \\ &\times \left(1 + K_{bc}^2 S^{\text{tree}}(\hat{a}, \hat{K}_{bc}^+, d) S^{\text{tree}}(c, -\hat{K}_{bc}^-, \hat{b}) \right) \end{aligned} \quad (6.5)$$

where hatted variables indicate they must be evaluated at $\hat{K}_{b\dots i}^2 = 0$ for the $[a, b]$ -shift (6.1). Expression (6.5) matches that of Mahlon [154] up to $n = 15$, found using off-shell quark currents and recursive techniques. The first form of the n -leg result was obtained

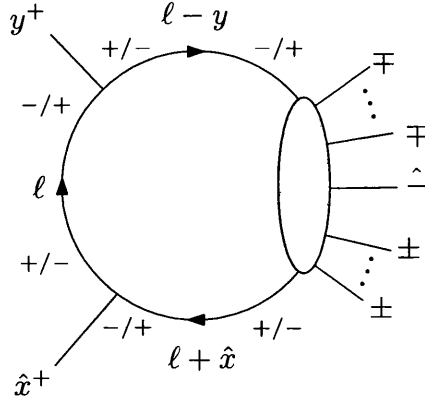


Figure 6.1: The modified all plus collinear loop splitting amplitude, written at the integrand level as an ℓ -dependent off-shell current, τ_n with a common LHS. The current can contain in principle any helicity configuration provided at least one external leg has negative helicity. Contributions required for on-shell recursion procedures require shifting the ‘hatted’ momenta on the residue after the integral.

using off-shell recursion [60]. In the next section we provide a constructive derivation of the sub-leading terms based on a diagrammatic analysis using axial gauge rules [20].

6.2 Computation setup

The schematic setup will be in general to replace collinear factorisations that occur along all-plus loop splitting amplitudes with a sum of diagrams that form an off-shell current τ_n . There are two common vertices that carry the loop momenta in every diagram, that also contain the two particles going collinear. Thus τ_n represents the diagrammatic sum of all tree-level diagrams with two legs off-shell. We show the general setup pictorially in figure 6.1, with the two common vertices, multiplied by a blob τ_n , connected by loop momentum dependent propagators. These complex factorisations require a loop integration over $d^d \ell$, which can in principle be performed before or after the residue theorem has been applied for $\langle \hat{x}y \rangle \rightarrow 0$.

The tree-level off-shell quantity or current τ_n , has two non-null legs and will contain at least two negative helicities in general, one coming from one of the off-shell legs denoted in figure 6.1. Herein lies the extra pole structure to be determined via the summation of beyond leading order contributions. For the case of the off-shell current appearing as an MHV current, at leading order it provides an overall $1/\langle xy \rangle$ factor,

and so we require diagrams that survive to order $O(\langle xy \rangle^0)$, which will be explained explicitly in the next section. Currents with more exotic mixtures of helicity structure such as $(---+++)$ will in principle yield sub-leading poles as both holomorphic and anti-holomorphic spinor products vanish, which is currently an open problem.

In general this current τ_n is a sum of tree-level diagrams that depend on the loop momenta ℓ , and as such we require that the on-shell recursion procedure is maintained by working in the limit that all loop propagators are close to null; $\ell^2, (\ell - y)^2, (\ell + x)^2 \rightarrow 0$. Sub-leading terms in the pole structure of the factorisation survive in this limit, such that we can simplify the contribution in the MHV case, as will be explicitly derived in the rest of the chapter. Throughout, we view the unshifted amplitude as a sum of functions, each of which corresponds to a Feynman diagram involving real momenta. Specifically, the loop momenta are real such that where diagrams are indicated with BCFW shifted legs, the shift applies to the function obtained by evaluating the diagram with real momenta.

The contribution from figure 6.1, using the axial gauge three-point vertices (3.46), is then

$$C^{n\text{-sf}} = \int d^d \ell \frac{[x|\ell|q][y|\ell|q]}{\langle xq \rangle \langle yq \rangle} \left(\frac{\langle \ell - y, q \rangle}{\langle \ell + x, q \rangle} \right)^{2h} \frac{\tau_n(\dots, (\ell + x)^{-h}, (y - \ell)^h, \dots, n)}{\ell^2 (\ell + x)^2 (\ell - y)^2}, \quad (6.6)$$

where q is a reference momenta that the final calculation is independent of. There are two helicity configurations to sum over, $h = \pm$ across the internal lines. The ℓ -dependent spinor products to the power $2h$ comes from the contribution of the scalar running in the loop. This is due to the overall single-minus amplitude having vanishing contributions from the other supersymmetric multiplets in the one-loop decomposition (4.14). The entire contribution to the gluon in the loop is then reduced in this example to just the scalar contribution. The sum over the two internal helicity configurations flowing in the loop can be thought of as an effective sum over two real scalars. The only remnant of the effect of the scalars in the loop come from the factor to the power $2h$ in (6.6), which arises when promoting null momenta to massive momenta (using (3.47)) for the two three-point vertices on the LHS of figure 6.1. All other loop-dependent quantities on the RHS of the figure contained in τ_n can be promoted to massive momenta too, leaving the prefactor $\left(\frac{\langle \ell - y, q \rangle}{\langle \ell + x, q \rangle} \right)^{-2h}$. Thus the factors to the power $2h$ and

6.2 Computation setup

$-2h$ from the LHS and RHS respectively cancel when combined. Therefore the integrals have full d -dimensional ℓ -momenta when all ℓ -nullified spinor dependencies are removed using (3.47).

We perform the integrals in $d = 4 - 2\epsilon$ dimensions, however the $d^{(-2\epsilon)}\ell$ integrals would yield a mass μ^2 in the dimensionally regularised integrals. At $\mathcal{O}(\epsilon)$ in the limit all propagators are null there are no masses induced and the $d^{(-2\epsilon)}\ell$ integrals do not appear. Therefore one can use $d = 4$ for the loop momenta ℓ , integrate over $d^4\ell$ and utilise on-shell methods as we saw in the unitarity examples in Chapter 5 (see Appendix A for full details on computing the integrals). We shall see that the leading factor of $\langle xy \rangle^{-1}$ comes from effectively integrating around the region $|\ell| = 0$. Specifically, since $(\ell + x)^2 = \ell^2 + 2\ell \cdot x + x^2 = \ell^2 + 2\ell \cdot x$, around $|\ell| = 0$ the integration region appears as

$$\sim \int_0 |\ell|^{d-1} d|\ell| \frac{\tau|_{\ell=0}}{|\ell|^2(|\ell|^2 + 2\ell \cdot x)(|\ell|^2 + 2\ell \cdot y)} \sim \int_0 |\ell|^{d-1} \frac{d|\ell|}{|\ell|^2(\ell \cdot x)(\ell \cdot y)} \sim \frac{1}{\langle xy \rangle}. \quad (6.7)$$

After integration, we compute the particular residue from Cauchy's theorem that exposes the poles from the complex shift

$$\text{Res} \left(\frac{1}{z} C^{n\text{-sf}}(\dots, \hat{-}, \dots, \hat{x}^+, y^+, \dots) \right) \Big|_{\langle \hat{x}y \rangle \rightarrow 0}, \quad (6.8)$$

that yields the desired coefficients of the double pole and any underlying PUP contribution. Thus we can show that this new factorisation successfully probes underneath the leading order pole behaviour, to determine the coefficients in (6.3). The work we present in this and the following chapter utilises this method to extract the correct coefficients of the poles induced in loop level recursion techniques. In this chapter specifically, we verify the n -point single-minus Yang-Mills one-loop amplitude (6.5) using this technique. Furthermore, we apply the technique to the corresponding single-minus one-loop amplitudes in pure Einstein gravity in Chapter 7.

The rest of the chapter deals with illustrating the uses of the complex factorisation to supplement on-shell recursion in pure Yang-Mills. We first introduce the method of summing the required diagrams in axial gauge for an MHV off-shell tree current with five legs τ_5 , to verify the calculation from (5.77) [102]. We then extend the method to n -point in the MHV case by forming compact expressions for the current τ_n , in the

$$C^{n-sf} = \sum_{\pm} \text{Diagram}$$

Figure 6.2: The MHV off-shell current $\tau_5(\hat{a}^-, (\hat{b}+\ell)^-, (c-\ell)^+, d^+, e^+)$, that contributes to the non-standard factorisation C^{n-sf} . The sum over the two internal helicity configurations generates an overall factor of two.

$\ell^2 \rightarrow 0$ limit. The n -point result of [102] is verified using this method that explains the form of the previously introduced soft factors (5.78).

6.3 The full axial gauge treatment at five-point

First consider the $[a, b]$ -shift (6.1) to apply on-shell recursion to derive the single-minus one-loop amplitude $A_5^{1\text{-loop}}(\hat{a}^-, \hat{b}^+, c^+, d^+, e^+)$. We are applying precisely the shift as it was in the example computed in the one-loop on-shell recursion example in Chapter 5. We substitute the contribution from the factorisation containing the three-point all-plus loop in figure 5.7(c) with the possible one-loop contributions to the residue at $\langle \hat{b}c \rangle \rightarrow 0$ that fall under the grouping in figure 6.1. Thus we are considering the set of diagrams that make the off-shell current $\tau_5(\hat{a}^-, (\hat{b}+\ell)^-, (c-\ell)^+, d^+, e^+)$ to the contribution C^{n-sf} as shown pictorially in figure 6.2.

Since there are off-shell momenta flowing into the RHS of figure 6.2, the momenta are capitalised to emphasise they are off-shell and are defined,

$$\begin{aligned} B &= \ell + b, \\ C &= \ell - c, \end{aligned} \tag{6.9}$$

such that $B - C = k_b + k_c$. The off-shell four-vectors can be redefined in the spinor language up to factors of B^2 or C^2 using our equation for massive momenta (3.38).

There will be ℓ -dependent propagators for some of the diagrams, indicating integrals of higher sided polygons required than just the standard three-point loop vertex from figure 5.7 that appeared before. See figure 6.3 for the groupings separated into two cases: with MHV like currents required for the first set and ℓ -dependent diagrams including two boxes and a pentagon in the second set. The first set of diagrams in figure 6.3 will

6.3 The full axial gauge treatment at five-point

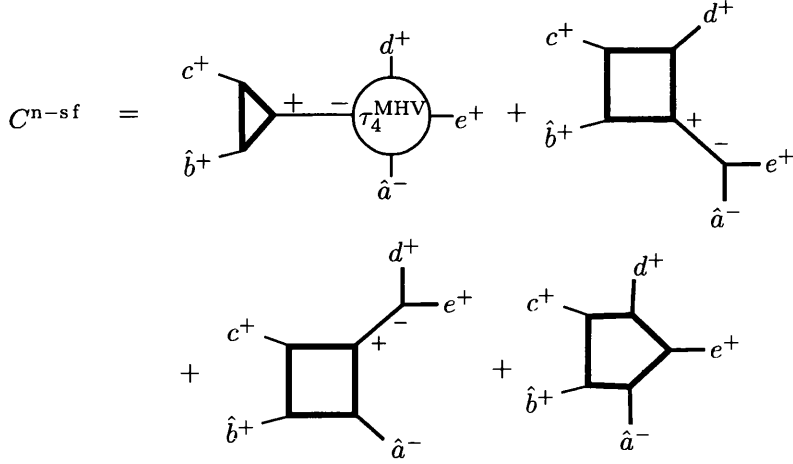


Figure 6.3: The two sets of diagrams that contribute to the integrals in C^{n-sf} . All original standard MHV diagrams are in the first set. Diagrams sub-leading in $O(s_{bc})$ include in this case two boxes and a pentagon.

contain the double pole term in the conventional MHV current, but in axial gauge will require the off-shell $(k_b + k_c)^-$ for the contributions to τ_4^{MHV} . It is possible to consider the next to leading order behaviour in $O(s_{bc})$ from a diagram by diagram approach to include not only the contribution where k_b and k_c are fused together, but also any possible loop diagram that contributes to the latter set of diagrams in figure 6.3.

Particles k_b and k_c are going collinear, such that the integrals are performed around $\ell^2 \rightarrow 0$, so all ℓ -dependent propagators (thick lines in figure 6.3) are close to null. This allows us to still make use of the residue theorem and compute the resulting contributions after integration for complex momenta on the $[a, b]$ -shift. We will be performing integrals around $\ell^2 = 0$, which means any full ℓ -dependent propagators will be easily decomposed into spinors using (3.38), with a vanishing contribution from B^2 or C^2 . An example of this is taking the first box term from the latter set of diagrams in figure 6.3, which has the ℓ -dependent propagator

$$(C - k_d)^2 = C^2 - [d|C|d\rangle = C^2 \left(1 - \frac{[d|q|d\rangle}{[q|C|q\rangle} \right) - [dC]\langle Cd\rangle. \quad (6.10)$$

Thus $O(B^2, C^2)$ in the propagators are sub-leading for the integrals and are effectively $O(\langle bc \rangle)$ corrections due to the integration around $|\ell| = 0$ in (6.7). This shall be of benefit later when simplifying the contributions to the current τ_5 .

6.3.1 Axial gauge diagrams

Recall the possible three-point vertices in the axial gauge (3.46) where q is a reference vector, but now generalised for two off-shell momenta, simulating momentum ℓ flowing through the vertex

$$\tau_3(x^+, B^+, C^-) = \frac{i}{\sqrt{2}} \frac{\langle Cq \rangle^2}{\langle Bq \rangle^2} \frac{[x|C|q]}{\langle xq \rangle}, \quad \tau_3(x^-, B^-, C^+) = \frac{i}{\sqrt{2}} \frac{[Cq]^2}{[Bq]^2} \frac{[q|B|x]}{[xq]}, \quad (6.11)$$

as a result of using 3.38 to promote all ℓ -dependent spinors to full momenta. Cases where one of the two off-shell momenta may also be null reduces to;

$$\tau_3(x^+, B^+, y^-) = \frac{i}{\sqrt{2}} \frac{1}{\langle Bq \rangle^2} \frac{[xy]\langle yq \rangle^3}{\langle xq \rangle}, \quad \tau_3(x^-, B^-, y^+) = -\frac{i}{\sqrt{2}} \frac{1}{[Bq]^2} \frac{\langle xy \rangle [yq]^3}{[xq]}, \quad (6.12)$$

which are all vertices that are required to build the diagrams appearing in τ_n . The vertices (6.11, 6.12) when combined for n -leg diagrams, each come with an associated off-shell propagator. After cleaning out the $\langle Cq \rangle^2$, $[Bq]^2$, etc. factors, terms are revealed that are of the form

$$\frac{[x|\ell - K_{i,j}|q]}{(\ell - K_{i,j})^2}, \quad \text{or} \quad \frac{[q|\ell + K_{m,n}|y]}{(\ell + K_{m,n})^2}, \quad (6.13)$$

per ℓ -dependent vertex, where $K_{i,j}$ or $K_{m,n}$ may include any cyclic ordering of the null momenta in the problem.

The process of summing all axial gauge diagrams can be simplified by choosing $\lambda_q = \lambda_a$ to nullify off-shell momenta for three reasons. Firstly, due to considerations in section 3.3 on axial gauge rules, all four gluon vertices have leading $\langle aq \rangle$ factors, and so vanish for our choice of q . Secondly, identifying q with the complex momenta shift in the recursion procedure only permits the shifted leg \hat{a}^- to appear in an MHV vertex and the other shifted leg \hat{b}^+ to enter on a googly vertex. Lastly, this also avoids any extra spurious $\langle \hat{a}q \rangle$ poles that would have been introduced. Thus it is also beneficial to select $\bar{\lambda}_q = \bar{\lambda}_b$ to match the recursion optimised choice for making the propagators in the standard factorisations null. Hence we can construct all necessary diagrams for this setup that contribute to the pole structures required in this one-loop amplitude

6.3 The full axial gauge treatment at five-point

using connected three-point $\overline{\text{MHV}}$ vertices and a single MHV three-point vertex (6.11) where the k_a enters into the diagram.

6.3.2 Contributions to the final residue diagrammatically

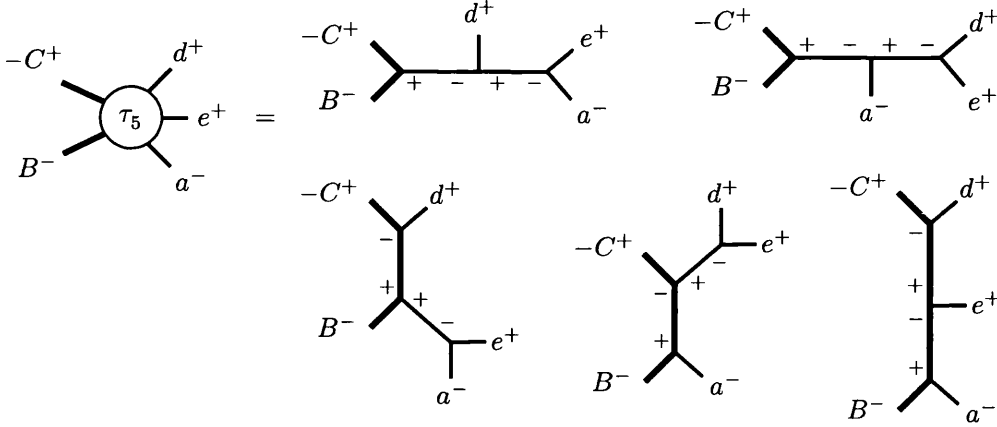


Figure 6.4: Five diagrams are included in building the off-shell amplitude τ_5 in figure 6.2, where the capital momenta indicate off-shell momenta, i.e. $B = l + b$ and $-C = c - l$. There is only one helicity configuration that is non-vanishing, that permits one MHV vertex where a^- enters, and two $\overline{\text{MHV}}$ vertices for the other legs.

The possible tree-level loop dependent diagrams that contribute to the integrals C^{n-sf} for the case of five external legs are given in figure 6.4. We see that the contribution to the sum of integrals includes two box integrals and a pentagon integral from the diagrams with extra ℓ -dependent propagators. The contribution to C^{n-sf} from figure 6.4 is then,

$$C^{n-sf} = \int d^4\ell \frac{[b|\ell|q][c|\ell|q]}{\langle bq\rangle\langle cq\rangle} \frac{\langle Cq\rangle^2}{\langle Bq\rangle^2} \frac{\tau_5(a^-, B^-, -C^+, d^+, e^+)}{\ell^2 B^2 C^2} \quad (6.14)$$

where we have picked out one helicity configuration in the figure. The second helicity configuration yields exactly the same computation, so we get a factor of two overall.

Bringing the correct spinor weight for the quantities B and C in the form $\langle Bq\rangle^2/\langle Cq\rangle^2$ outside of τ_5 , it cancels with the factor to the power -1 from the LHS. It also ensures that all other appearances of B and C are “q-capped”, such that ℓ -dependent factors can be promoted from massless spinors to the full off-shell momentum using (3.38).

6.3 The full axial gauge treatment at five-point

The off-shell current τ_5 is then the sum of the five diagrams on the RHS of figure 6.4,

$$\begin{aligned} \tau_5(a^-, B^-, -C^+, d^+, e^+) = & \frac{\langle Bq \rangle^2}{\langle Cq \rangle^2} \left(\frac{\langle a|(B-C)C|q\rangle [q|d+e|a]^2 [ed]}{\langle dq \rangle \langle eq \rangle [aq] [q|B-C|q] s_{bc} s_{de}} \right. \\ & + \frac{\langle q|BC|q\rangle [qe]^2 [de] \langle ea \rangle}{\langle dq \rangle [q|a+e|q] [aq] s_{bc} s_{ae}} - \frac{[d|C|q] \langle a|e(d-C)|q\rangle [qe]^2}{\langle dq \rangle [aq] [q|a+e|q] s_{ae} (C^2 - [d|C|d])} \\ & - \frac{[d|C|q] \langle e|d-C|q\rangle [q|B|a] [q|B+a|q]^2}{\langle dq \rangle \langle eq \rangle [aq] [q|B|q]^2 ([a|B|a] + B^2) (C^2 - [d|C|d])} \\ & \left. - \frac{\langle q|(d+e)C|q\rangle [q|B|a] [q|a+B|q]^2}{\langle dq \rangle \langle eq \rangle [aq] [q|B|q]^2 \langle ed \rangle ([a|B|a] + B^2)} \right), \end{aligned} \quad (6.15)$$

where momentum conservation is kept by $k_a + B - C + k_d + k_e = 0$. We can simplify this expression significantly by employing the recursion optimised choice for q at this stage. So, with $q \rightarrow \lambda_a \bar{\lambda}_b$, and using momentum conservation, the contribution of the five diagrams is,

$$\begin{aligned} \tau_5(a^-, B^-, -C^+, d^+, e^+) |_{q \rightarrow \lambda_a \bar{\lambda}_b} = & \frac{\langle Ba \rangle^2}{\langle Ca \rangle^2} \left(- \frac{\langle a|B(d+e)|a\rangle \langle ca \rangle}{\langle da \rangle \langle ea \rangle [ab] \langle ed \rangle \langle bc \rangle} \right. \\ & - \frac{\langle a|B(d+e)|a\rangle [be] [de]}{\langle da \rangle [ab] s_{bc} s_{ae}} - \frac{[d|C|a] \langle e|B|a\rangle [be]}{\langle da \rangle [ab] s_{ae} (C^2 - [d|C|d])} \\ & \left. + \frac{[d|C|a] \langle e|B|a\rangle [b|B|a]}{\langle da \rangle \langle ea \rangle [ab] (B^2 + [a|B|a]) (C^2 - [d|C|d])} - \frac{\langle a|B(d+e)|a\rangle [b|B|a]}{\langle da \rangle \langle ea \rangle [ab] \langle ed \rangle (B^2 + [a|B|a])} \right). \end{aligned} \quad (6.16)$$

The off-shell currents τ_n , will in general proliferate to calculating many diagrams as n grows, but we illustrate the method of employing the axial gauge rules to illustrate the reduction to a set of simple triangle integrals in the $\ell^2 \rightarrow 0$ limit. That will inevitably allow a rewriting of the off-shell current in this example in a more compact form, without the need for summing all diagrams as the number of legs n grows.

The first two terms fall into the first set of diagrams in figure 6.3 and are thus triangle integrals. An explicit $\langle bc \rangle^{-1}$ factor enters in these first two terms in (6.16), so they correspond to the double pole contribution, combining with the $\langle bc \rangle^{-1}$ from the LHS factor, as illustrated in (6.7). However there is also a z dependence on the shift of $[\hat{a}e]^{-1}$ that appears in the second term of (6.16). This requires the double pole term to be expanded to next to leading order in z , where $z = -\langle bc \rangle / \langle ac \rangle + \delta$ for small δ .

6.3 The full axial gauge treatment at five-point

The sub-leading term in the expansion of the series for small δ will contribute to part of the PUP contribution.

The three remaining terms when considered in the limit of B^2 and C^2 close to null define the rest of the PUP contribution. The ℓ -dependent propagators in the sub-leading terms, initially provide a problem of handling box and higher sided polygonal integrals in general. Furthermore, the integrands of boxes or higher sided polygons have no explicit pole as $\langle bc \rangle \rightarrow 0$ and only generates a pole after integration (6.7). Terms of $O(B^2, C^2)$ through integration around $|\ell| = 0$ in (6.7) are effectively $O(\langle bc \rangle^0)$ terms. Thus the denominators in the latter set of figure can freely apply vanishing B^2 and C^2 , while further manipulations can clear out all instances of B and C from the denominators to the same order.

We explicitly show the five-point simplification using spinor algebra, which in the B^2 and $C^2 \rightarrow 0$ limit reduces to a common set of triangle integrals. We perform the simplification to group together like terms,

$$\begin{aligned} \tau_5(a^-, B^-, -C^+, d^+, e^+) &= \frac{\langle Ba \rangle^2}{\langle Ca \rangle^2 \langle da \rangle \langle ea \rangle [ab]} \left(-\frac{\langle a|B(d+e)|a\rangle}{\langle bc \rangle} \left[\frac{\langle ca \rangle}{\langle cd \rangle} + \frac{[be][de]}{[cb][ae]} \right] \right. \\ &\quad \left. + \frac{[d|C|a][e|B|a][be]}{[ae][d|C|d]} - \frac{[b|B|a]}{[a|B|a]} \left[\frac{[d|C|a][e|B|a]}{[d|C|d]} - \frac{\langle a|BC|a\rangle}{\langle ed \rangle} \right] \right) + O(\langle bc \rangle^0). \end{aligned} \quad (6.17)$$

We shall now demonstrate how the factors of B and C can be cleaned right out of the denominator to the same order. Firstly, around the region of integration we can make the substitutions

$$\frac{[d|C|a]}{[d|C|d]} = \frac{\langle Ca \rangle}{\langle Cd \rangle} + O(\langle bc \rangle) = \frac{\langle ca \rangle}{\langle cd \rangle} + O(\langle bc \rangle), \quad (6.18)$$

such that the instances of C in the denominator can be cleaned out at will. To remove the $[a|B|a]$ from the denominator of the latter terms one must be more strategic. One can think of the last two diagrams in figure 6.4 as the two axial gauge diagrams required to build an off-shell current with a single negative helicity including legs $(-C^+, d^+, e^+, P^-)$. As $C^2 = 0$ there is only one massive leg P^- , and the contribution

6.3 The full axial gauge treatment at five-point

of this current is proportional to P^2 , as the summation yields

$$\tau(-C^+, d^+, e^+, P^-) = \frac{P^2 \langle Pq \rangle^2}{\langle Cq \rangle \langle Cd \rangle \langle de \rangle \langle eq \rangle}. \quad (6.19)$$

Thus the propagator $(a+B)^2$ from the last two diagrams in figure 6.4 cancels with P^2 contained in the off-shell current, $\tau(-C^+, d^+, e^+, (a+B)^-)$. We shall see a generalisation of this off-shell current with a single negative helicity later, that will help with writing the compact form for the n -point case. Thus, we put the final two terms in (6.17) over a common denominator using $B^2 = C^2 = 0$,

$$\begin{aligned} \tau_5(a^-, B^-, -C^+, d^+, e^+) &= \frac{\langle Ba \rangle^2}{\langle Ca \rangle^2 \langle da \rangle \langle ea \rangle [ab]} \left(-\frac{\langle a|B(d+e)|a \rangle}{\langle bc \rangle} \left[\frac{\langle ca \rangle}{\langle ed \rangle} + \frac{[be][de]}{[cb][ae]} \right] \right. \\ &\quad \left. + \frac{\langle Ca \rangle [e|B|a][be]}{[ae]\langle Cd \rangle} - \frac{[b|B|a] \langle Ca \rangle \langle a|B(e-C)|d \rangle}{[a|B|a] \langle Cd \rangle \langle ed \rangle} \right) + O(\langle bc \rangle). \end{aligned} \quad (6.20)$$

To manifest the cancellation of B in the denominator we require a manipulation using momentum conservation $e - C = -(a + B + d)$, and $B^2 = C^2 = 0$ again,

$$\begin{aligned} \tau_5(a^-, B^-, -C^+, d^+, e^+) &= \frac{\langle Ba \rangle^2}{\langle Ca \rangle^2 \langle da \rangle \langle ea \rangle [ab]} \left(-\frac{\langle a|B(d+e)|a \rangle}{\langle bc \rangle} \left[\frac{\langle ca \rangle}{\langle ed \rangle} + \frac{[be][de]}{[cb][ae]} \right] \right. \\ &\quad \left. + \frac{\langle Ca \rangle}{\langle Cd \rangle} \left[\frac{[e|B|a][be]}{[ae]} + \frac{[b|B|a] \langle da \rangle}{\langle de \rangle} \right] \right) + O(\langle bc \rangle), \end{aligned} \quad (6.21)$$

where the entire prefactor $\langle Ca \rangle / \langle Cd \rangle$ can be reduced using (6.18). So now we can write the entire contribution to C^{n-sf} dropping the $O(\langle bc \rangle)$ terms,

$$\begin{aligned} C^{n-sf} &= \int \frac{d^4 \ell}{\ell^2 B^2 C^2} \frac{[b|\ell|a][c|\ell|a]}{\langle ba \rangle \langle ca \rangle \langle da \rangle \langle ea \rangle [ab]} \left(-\frac{\langle a|B(d+e)|a \rangle}{\langle bc \rangle} \left[\frac{\langle ca \rangle}{\langle ed \rangle} + \frac{[be][de]}{[cb][ae]} \right] \right. \\ &\quad \left. + \frac{\langle ca \rangle}{\langle cd \rangle} \left[\frac{[e|B|a][be]}{[ae]} + \frac{[b|B|a] \langle da \rangle}{\langle de \rangle} \right] \right), \end{aligned} \quad (6.22)$$



6.3 The full axial gauge treatment at five-point

where we have reduced the problem to set of triangle integrals of the form,

$$\mathcal{J} = \int \frac{d^4 \ell}{(2\pi)^4} \frac{[b|\ell|a][c|\ell|a][X|B|a]}{\ell^2 B^2 C^2}. \quad (6.23)$$

Using the result from (A.13) that is calculated in Appendix A, we see that at five-point all triangle integrals (6.23) are readily evaluated to,

$$\mathcal{J} = \frac{i}{96\pi^2} \frac{\langle a|bc|a \rangle}{\langle bc \rangle} [X|2b + c|a]. \quad (6.24)$$

6.3.3 The five-point result

Using (6.24) we are left with the contribution to the integrated non standard factorisation,

$$C^{\text{n-sf}} = -\frac{i}{96\pi^2} \frac{[bc]}{\langle bc \rangle \langle da \rangle \langle ea \rangle [ab]} \left(-\frac{\langle a|(2b+c)(d+e)|a \rangle}{\langle bc \rangle} \left[\frac{\langle ca \rangle}{\langle ed \rangle} + \frac{[be][de]}{[cb][ae]} \right] + \frac{\langle ca \rangle}{\langle cd \rangle} \left[\frac{[e|2b+c|a][be]}{[ae]} + \frac{[b|c|a]\langle da \rangle}{\langle de \rangle} \right] \right), \quad (6.25)$$

Thus we evaluate the residue of the non-standard factorisation, using the $[a, b]$ -shift in (6.1), when $\langle \hat{b}c \rangle \rightarrow 0$. This yields a sub-leading term in $\langle bc \rangle$ when the shift encounters the $\langle \hat{b}c \rangle^{-2} [\hat{a}e]^{-1}$ term,

$$\text{Res} \left(\frac{1}{z} C^{\text{n-sf}}(\hat{a}^-, \hat{b}^+, c^+, d^+, e^+) \right) \Big|_{\langle \hat{b}c \rangle \rightarrow 0} = -\frac{i}{96\pi^2} \frac{[bc]}{\langle bc \rangle \langle da \rangle \langle ea \rangle [ab]} \left(\frac{\langle a|bc|a \rangle}{\langle bc \rangle} \left[\frac{\langle ca \rangle}{\langle ed \rangle} + \frac{[be][de]\langle ac \rangle}{[cb](\langle ac \rangle [ae] + \langle bc \rangle [be])} + \frac{[be]^2 [de] \langle ac \rangle \langle bc \rangle}{[cb](\langle ac \rangle [ae] + \langle bc \rangle [be])^2} \right] + \frac{\langle ca \rangle}{\langle cd \rangle} \left[\frac{[e|2b+c|a][be]\langle ac \rangle}{(\langle ac \rangle [ae] + \langle bc \rangle [be])} + \frac{[b|c|a]\langle da \rangle}{\langle de \rangle} \right] \right). \quad (6.26)$$

The sub-leading pole that was introduced cancels against one of the factors of k_b in the term $[e|2b+c|a]$, whilst the other factor of two is removed using, $\langle a|(2b+c)(d+e)|a \rangle = \langle a|b(d+e)|a \rangle$ by momentum conservation. This result matches the desired Bern et al double pole and corresponding sub-leading pole (5.77).

The five-point example highlights the cancellation between the factor of two coming from the integration around the loop by the sub-leading part of the expansion of the residue around the double pole. It can be shown that for an n -point calculation of this form, the contributions to these off-shell currents can always be reduced to triangle integrals multiplied by spinor coefficients in the $\ell^2 \rightarrow 0$ limit. Furthermore, since all integrals that appear are of the form (6.23), the problem reduces to finding a more compact expression for the off-shell current $\tau_n(a^-, B^-, -C^+, d^+, \dots, n^+)$.

6.4 n -point calculation

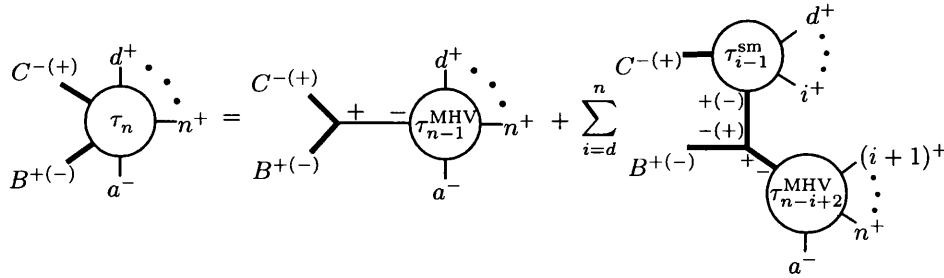


Figure 6.5: An organisation of the diagrams within τ_n showing triangle contributions to C^{n-sf} on the left with boxes, pentagons, etc., in the $B^2 = C^2 = 0$ case to the right.

We can expand τ_n in the desired $\ell^2 \rightarrow 0$ limit into two sub-currents, which are either MHV currents or currents with a single-minus as show in figure 6.5. The first structure in figure 6.5 gathers all the triangles, that we label τ_n^{tri} . This contains an explicit factor of $\langle bc \rangle^{-1}$ from the common s_{bc} propagator, and generates a further pole upon integration and so gives rise to the double pole contributions. The other structures only generate single poles, that come from the boxes, pentagons, and so on, as we saw with the five-point example earlier, and we label them τ_n^{b} . The diagrammatic expansion gives both of these contributions in terms of off-shell MHV tree currents τ_n^{MHV} . Furthermore, off-shell currents with a single negative helicity encountered earlier (6.19), now denoted τ^{sm} will be used for simplifying the boxes, pentagons and so on.

6.4.1 Useful off-shell currents

We can use the general results, specialised to $\lambda_q = \lambda_a$ for the currents with one off-shell momentum, and only P with negative helicity, since any currents with P positive helicity include the null leg a^- , which vanish. This is because the sum of any axial gauge diagrams that include leg a^- must have an MHV configuration, and since all other legs are positive helicity the leg P must therefore have negative helicity. The case of all null positive helicity legs only occur for the simplest off-shell current and so P has negative helicity to generate the sum of $\overline{\text{MHV}}$ axial gauge vertices. The results, given by [154, 155], include the case of all-plus helicity null legs, that we denote the single-minus current,

$$\tau^{\text{sm}}(P^-, 1^+, \dots, n^+) = -\frac{P^2 \langle Pa \rangle^2}{\langle a1 \rangle \langle 12 \rangle \dots \langle n-1, n \rangle \langle na \rangle}, \quad (6.27)$$

which was used in the explicit five-point computation (6.19). We also use the off-shell MHV current,

$$\tau^{\text{MHV}}(a^-, P^-, f^+ \dots n^+) = \frac{i \langle Pa \rangle^2 P^2}{\langle af \rangle \langle fg \rangle \dots \langle (n-1)n \rangle \langle na \rangle} \left(\frac{[qn]}{[aq][an]} - \sum_{j=f}^{n-1} \frac{\langle a|P_j j|a \rangle}{P_j^2 P_{j-1}^2} \right), \quad (6.28)$$

where $P_j \equiv k_{j+1} + \dots + k_n + k_a$. Although the last equation carries an explicit P^2 factor in the numerator, the $j = f$ term in the sum contains a $1/P^2$ since $P_{f-1} = -P$ which survives in the $P^2 \rightarrow 0$ limit. We will need a simple generalisation of (6.27),

$$\tau^{\text{sm}}(P^{-h}, f^{+h} \dots n^+) = \left(\frac{\langle fa \rangle}{\langle Pa \rangle} \right)^{2-2h} \tau^{\text{sm}}(P^-, f^+ \dots n^+). \quad (6.29)$$

This result follows diagram by diagram in τ^{sm} as only three-point $\overline{\text{MHV}}$ vertices are present. So every $\overline{\text{MHV}}$ vertex that the non-gluonic particle encounters introduces a factor of

$$\left(\frac{[\kappa p_{\text{in}}]}{[\kappa p_{\text{out}}]} \right)^{2-2h} = \left(\frac{\langle p_{\text{out}} a \rangle}{\langle p_{\text{in}} a \rangle} \right)^{2-2h} \left(\frac{[\kappa p_{\text{in}} | a]}{[\kappa p_{\text{out}} | a]} \right)^{2-2h} = \left(\frac{\langle p_{\text{out}} a \rangle}{\langle p_{\text{in}} a \rangle} \right)^{2-2h}, \quad (6.30)$$

where the product of these gives the factor in (6.29) for each diagram.

6.4.2 Diagrammatic contributions

For τ_n^{tri} we have,

$$\begin{aligned}\tau_n^{\text{tri}} &= \tau_3(P^+, B^+, -C^-) \frac{1}{P_{BC}^2} \tau_{n-1}^{\text{MHV}}(a^-, -P^-, d^+, \dots, n^+) \\ &= \frac{\langle Ca \rangle^2}{\langle Ba \rangle^2} \frac{\langle a|BC|a \rangle}{s_{bc}} \frac{\tau_{n-1}^{\text{MHV}}(a^-, (b+c)^-, d^+, \dots, n^+)}{\langle P_{b+c}a \rangle^2}.\end{aligned}\tag{6.31}$$

The dependence of τ^{tri} on the off-shell momenta B and C is very simple. Furthermore, it contains an explicit $1/s_{bc}$ factor which, together with the pole from integration, reproduces the double pole coefficient upon evaluation at the residue of $\langle \hat{b}c \rangle \rightarrow 0$. This also contributes to the sub-leading pole, due to further shifted variables in τ^{MHV} .

The remaining contributions to τ_n arise from the second class of diagram in figure 6.5. The integrand does not have an explicit pole as $\langle bc \rangle \rightarrow 0$ and only generates a single pole after integration. Since this arises at $C^2, B^2 \rightarrow 0$, we can take $C^2 = 0$ so that the τ^{sm} structures in figure 6.5 have only one massive leg. In this limit we can use the formulae of (6.27) and (6.28) for currents with a single massive leg, and to leading order in $\langle bc \rangle$, we obtain

$$\tau_n^b = \frac{\langle Ba \rangle^2}{\langle Ca \rangle^2} \left[\frac{\langle ca \rangle [b|\ell|a]}{\langle cd \rangle \langle de \rangle \dots \langle na \rangle [ab]} - \sum_{i=d}^{n-1} \frac{\langle ca \rangle \langle a|BK_i|a \rangle}{\langle cd \rangle \langle de \rangle \dots \langle ia \rangle} \frac{\tau^{\text{MHV}}(a^-, -K_i^-, (i+1)^+, \dots, n^+)}{\langle K_i a \rangle^2 K_i^2} \right]\tag{6.32}$$

where the $K_i = k_{i+1} + \dots + k_n + k_a$ are fixed by momentum conservation within the τ^{MHV} structures and we have made use of the simplification in the $\ell^2 \rightarrow 0$ limit,

$$\frac{\langle Ca \rangle}{\langle Cd \rangle} \rightarrow \frac{\langle ca \rangle}{\langle cd \rangle} + \mathcal{O}(\langle bc \rangle).\tag{6.33}$$

6.4.3 Integration and BCFW evaluation

In this form we see that all of the contributions to C^{n-sf} involve the same basic integral as we encountered at the five-point example calculated earlier, and so we use

$$\int d^4l \frac{[b|\ell|a][c|\ell|a][X|B|a]}{\ell^2 B^2 C^2} = \frac{i}{96\pi^2} \frac{\langle a|bc|a\rangle}{\langle bc\rangle} [X|2b+c|a], \quad (6.34)$$

leading to

$$\begin{aligned} & C^{n-sf}(a^-, b^+, c^+, d^+, e^+, \dots, n^+) \\ &= \frac{i}{96\pi^2} \frac{[bc]}{\langle bc\rangle} \left[\frac{\langle a|\beta(b+c)|a\rangle}{s_{bc}} \frac{\tau^{\text{MHV}}(a^-, (b+c)^-, d^+ \dots n)}{\langle P_{b+c}a\rangle^2} + \frac{\langle ca\rangle[b|\beta|a]}{\langle cd\rangle\langle de\rangle \dots \langle na\rangle[ab]} \right. \\ & \quad \left. - \sum_{i=d}^{n-1} \frac{\langle ca\rangle\langle a|\beta K_i|a\rangle}{\langle cd\rangle\langle de\rangle \dots \langle ia\rangle} \frac{\tau^{\text{MHV}}(a^-, -K_i^-, (i+1)^+, \dots, n^+)}{\langle K_i a\rangle^2 K_i^2} \right], \end{aligned} \quad (6.35)$$

where $\beta = 2b + c$. By introducing $\gamma = -b$ so that $\beta + \gamma = b + c$, we have

$$\frac{\langle \gamma a\rangle}{\langle \gamma d\rangle} = \frac{\langle ba\rangle}{\langle bd\rangle} \frac{\langle cd\rangle}{\langle cd\rangle} = \frac{\langle ca\rangle}{\langle cd\rangle} + \mathcal{O}(\langle bc\rangle). \quad (6.36)$$

The identification of β and γ come from the integration around the loop, that substitutes the two legs B and C with an off-shell β and null γ in the sum of axial gauge diagrams for τ_n . So to leading order in $\langle bc\rangle$ we have

$$\begin{aligned} & C^{n-sf}(a^-, b^+, c^+, d^+, e^+, \dots, n^+) \\ &= \frac{i}{96\pi^2} \frac{[bc]}{\langle bc\rangle} \left[\frac{\langle a|\beta(b+c)|a\rangle}{s_{bc}} \frac{\tau^{\text{MHV}}(a^-, (b+c)^-, d^+ \dots n)}{\langle P_{b+c}a\rangle^2} + \frac{\langle \gamma a\rangle[b|\beta|a]}{\langle \gamma d\rangle\langle de\rangle \dots \langle na\rangle[ab]} \right. \\ & \quad \left. + \sum_{i=d}^{n-1} \frac{\langle a|\beta \kappa_i|a\rangle \langle \gamma a\rangle^2}{K_i^2 \kappa_i^2} \frac{\tau^{\text{sm}}(-\kappa_i^-, \gamma^+, d^+ \dots i^+)}{\langle \kappa_i a\rangle^2} \frac{\tau^{\text{MHV}}(a^-, -K_i^-, (i+1)^+ \dots n)}{\langle K_i a\rangle^2} \right], \end{aligned} \quad (6.37)$$

where the internal momenta, κ_i , are specified by momentum conservation within the τ^{sm} currents, as the K_i were in (6.32). The quantity in the square brackets is now essentially a current for off-shell β , equivalent to $\tau_n(a^-, \beta^-, \gamma^+, d^+, \dots, n^+)$. This may

6.4 n -point calculation

seem an unorthodox step to express the amplitude purely in terms of β and γ , but it will be of great benefit in re-expressing the PUP contribution later on. The second term of (6.37) can be absorbed into the sum by adopting an appropriate definition for $\tau^{\text{MHV}}(a^-, K_n^-)$.

Using the explicit form for τ^{MHV} in the τ^{tri} contribution we have

$$C^{\text{n-sf}}(a^-, b^+, c^+, d^+, e^+, \dots, n^+) = \frac{i}{96\pi^2} \frac{[bc]}{\langle bc \rangle} \left[\frac{\langle a|\beta(b+c)|a\rangle}{\langle ad\rangle\langle de\rangle\cdots\langle(n-1)n\rangle\langle na\rangle} \left(\frac{[qn]}{[aq][an]} + \frac{\langle a|(b+c)d|a\rangle}{t_{bcd}s_{bc}} - \sum_{j=e}^{n-1} \frac{\langle a|K_{a,j+1..n}j|a\rangle}{s_{a,j+1..n}s_{a,j..n}} \right) + \sum_{i=d}^n \frac{\langle a|\beta\kappa_i|a\rangle\langle\gamma a\rangle^2}{K_i^2\kappa_i^2} \frac{\tau^{\text{sm}}(-\kappa_i^-, \gamma^+, d^+ \dots i^+)}{\langle\kappa_i a\rangle^2} \frac{\tau^{\text{MHV}}(a^-, -K_i^-, (i+1)^+ \dots n)}{\langle K_i a\rangle^2} \right], \quad (6.38)$$

where we have extracted the $j = d$ term from the τ^{MHV} to highlight the explicit $1/s_{bc}$ factor. As discussed previously, the quantity of interest is,

$$\text{Res}\left(\frac{1}{z} C^{\text{n-sf}}(\hat{a}^-, \hat{b}^+, c^+, d^+, e^+, \dots, n^+)\right) \Big|_{\langle\hat{b}c\rangle=0} \quad (6.39)$$

The residue of the double pole term is extracted using,

$$\text{Res}\left(\frac{[bc]}{\langle\hat{b}c\rangle} \frac{1}{z t_{bcd}s_{bc}}\right)_{\langle\hat{b}c\rangle=0} = \frac{1}{\langle bc\rangle\langle a|(b+c)d|c\rangle} \left(\frac{\langle ac\rangle}{\langle bc\rangle} - \frac{[b|c+d|a]\langle ac\rangle}{\langle a|(b+c)d|c\rangle} \right) \quad (6.40)$$

The first term here is precisely the double pole contribution of [102]

$$A_{n-1}^{(0)}(d^+, \dots, n^+, \hat{a}^-, \hat{K}_{bc}^-) \frac{i}{(K_{bc}^2)^2} V^{\text{1-loop}}(\hat{b}^+, c^+, -\hat{K}_{bc}^+) \\ = \frac{i}{96\pi^2} \frac{\langle ac\rangle}{\langle bc\rangle^2} \frac{\langle a|\beta(b+c)|a\rangle}{\langle cd\rangle\langle de\rangle\cdots\langle(n-1)n\rangle\langle na\rangle}. \quad (6.41)$$

The second term in (6.40) contains only a single factor of $\langle bc\rangle$ in the denominator such that it combines with the rest of the sub-leading pole terms. Its coefficient is unaffected

by the shift, so we can write the full sub-leading or PUP contribution as:

$$\begin{aligned}
 C^{\text{PUP}} = & \frac{i}{96\pi^2} \frac{[bc]}{\langle bc \rangle} \left[\frac{\langle a|\beta(b+c)|a\rangle}{\langle ad\rangle\langle de\rangle\cdots\langle(n-1)n\rangle\langle na\rangle} \right. \\
 & \times \left(\frac{[qn]}{[aq][an]} - \frac{\langle a|(b+c)d|a\rangle[b|c+d|a\rangle\langle ac\rangle}{[bc]\langle a|(b+c)d|c\rangle^2} - \sum_{j=e}^{n-1} \frac{\langle a|K_{a,j+1..n}j|a\rangle}{s_{a,j+1..n}s_{a,j..n}} \right) \\
 & \left. + \sum_{i=d}^n \frac{\langle a|\beta\kappa_i|a\rangle\langle\gamma a\rangle^2}{K_i^2\kappa_i^2} \frac{\tau^{\text{sm}}(-\kappa_i^-, \gamma^+, d^+ \cdots i^+)}{\langle\kappa_i a\rangle^2} \frac{\tau^{\text{MHV}}(a^-, -K_i^-, (i+1)^+ \cdots n)}{\langle K_i a\rangle^2} \right]_{\tilde{\dagger}}
 \end{aligned} \tag{6.42}$$

where $\tilde{\dagger}$ denotes that the quantity in square brackets is to be shifted and evaluated at $z = -\langle bc\rangle/\langle ac\rangle$.

6.4.4 Reinterpreting the PUP contribution

The sums in the PUP expression form most of the terms in the expansion of an on-shell MHV amplitude. We can use the simple interchange properties of the Parke-Taylor MHV amplitudes and τ^{sm} to gather many of these terms into a finite on-shell MHV amplitude, with a $\gamma \leftrightarrow d$ swap, that will form $\tau^{\text{MHV}}(a^-, \beta^-, d^+, \gamma^+, e^+ \cdots n^+)$ with β null. From a diagrammatic perspective we have,

$$\begin{aligned}
 \tau^{\text{MHV}}(a^-, \beta^-, d^+, \gamma^+, e^+, \dots, n^+) = & \frac{[d|K_1|a]\langle\beta a\rangle^2}{\langle da\rangle} \frac{\tau^{\text{MHV}}(a^-, -K_1^-, \gamma^+, e^+ \cdots n)}{\langle K_1 a\rangle^2 K_1^2} \\
 & + \langle a|\beta\kappa_2|a\rangle\langle\beta a\rangle^2 \frac{\tau^{\text{sm}}(-\kappa_2^-, d^+, \gamma^+)}{\langle\kappa_2 a\rangle^2 \kappa_2^2} \frac{\tau^{\text{MHV}}(a^-, -K_2^-, e \cdots n)}{\langle K_2 a\rangle^2 K_2^2} \\
 & + \sum_{i=e}^n \langle a|\beta\kappa_i|a\rangle\langle\beta a\rangle^2 \frac{\tau^{\text{sm}}(-\kappa_i^-, d^+, \gamma^+, e, \dots i^+)}{\langle\kappa_i a\rangle^2 \kappa_i^2} \frac{\tau^{\text{MHV}}(a^-, -K_i^-, (i+1)^+ \cdots n)}{\langle K_i a\rangle^2 K_i^2}.
 \end{aligned} \tag{6.43}$$

Interchanging the γ and d legs in the τ^{sm} amplitudes in the final sum introduces a simple prefactor $-\langle ad\rangle\langle\gamma e\rangle/(\langle a\gamma\rangle\langle de\rangle)$. We can then replace all but the first term of the final sum in (6.42) with $\tau^{\text{MHV}}(a^-, \beta^-, d^+, \gamma^+, e^+ \cdots n^+)$ and the first two terms in

the diagrammatic expansion (6.43),

$$\begin{aligned}
 C^{\text{PUP}} = & \frac{i}{96\pi^2} \frac{[bc]}{\langle bc \rangle} \left[\frac{\langle a|\beta(b+c)|a\rangle}{\langle ad\rangle\langle de\rangle\cdots\langle(n-1)n\rangle\langle na\rangle} \right. \\
 & \times \left(\frac{[qn]}{[aq][an]} - \frac{\langle a|(b+c)d|a\rangle[b|c+d|a\rangle\langle ac\rangle}{[bc]\langle a|(b+c)d|c\rangle^2} - \sum_{j=e}^{n-1} \frac{\langle a|K_{a,j+1..n}j|a\rangle}{s_{a,j+1..n}s_{a,j..n}} \right) \\
 & + \frac{\langle a|\beta\kappa_2|a\rangle\langle\gamma a\rangle^2}{K_2^2\kappa_2^2} \frac{\tau^{\text{sm}}(-\kappa_2^-, \gamma^+, d^+)}{\langle\kappa_2 a\rangle^2} \frac{\tau^{\text{MHV}}(a^-, -K_2^-, e^+ \cdots n^+)}{\langle K_2 a\rangle^2} \\
 & - \frac{\langle ad\rangle\langle\gamma e\rangle}{\langle a\gamma\rangle\langle de\rangle} \left(\frac{[d|K_1|a\rangle\langle\gamma a\rangle^2}{\langle da\rangle} \frac{\tau^{\text{MHV}}(a^-, -K_1^-, \gamma^+, e^+ \cdots n)}{K_1^2\langle K_1 a\rangle^2} \right. \\
 & \quad + \frac{\langle a|\beta\kappa_2|a\rangle\langle\gamma a\rangle^2}{K_2^2\kappa_2^2} \frac{\tau^{\text{sm}}(-\kappa_2^-, d^+, \gamma^+)}{\langle\kappa_2 a\rangle^2} \frac{\tau^{\text{MHV}}(a^-, -K_2^-, e^+ \cdots n^+)}{\langle K_2 a\rangle^2} \\
 & \quad \left. \left. - \frac{\langle\gamma a\rangle^2}{\langle\beta a\rangle^2} \tau^{\text{MHV}}(a^-, \beta^-, d^+, \gamma^+, e^+ \cdots n^+) \right) \right]_{\tilde{\Gamma}}. \tag{6.44}
 \end{aligned}$$

Once shifted and evaluated at $z = -\langle bc\rangle/\langle ac\rangle$, the final τ^{MHV} becomes an on-shell MHV amplitude and we can use the Parke-Taylor form for this term. Using (6.28) for the off-shell τ^{MHV} factors we see that all of these contain the following common term,

$$\frac{[qn]}{[aq][an]} - \sum_{j=e}^{n-1} \frac{\langle a|K_{a,j+1..n}j|a\rangle}{s_{a,j+1..n}s_{a,j..n}}. \tag{6.45}$$

The overall coefficient of this term vanishes before we apply the shift. The sum in (6.28) for the off-shell $\tau^{\text{MHV}}(a^-, K_1^-, \gamma^+, e^+ \cdots n)$ also contains an $j = \gamma$ term. On the pole this term cancels with the sub-leading second term in the residue of the double pole (6.40). Therefore we are left with just the $\tau^{\text{MHV}}(a^-, \beta^-, d^+, \gamma^+, e^+ \cdots n^+)$ term,

$$C^{\text{PUP}} = \frac{i}{96\pi^2} \frac{[bc]}{\langle bc \rangle} \times \left[\frac{\langle ad\rangle\langle\gamma e\rangle}{\langle a\gamma\rangle\langle de\rangle} \frac{\langle\gamma a\rangle^2}{\langle\beta a\rangle^2} \tau^{\text{MHV}}(a^-, \beta^-, d^+, \gamma^+, e^+ \cdots n^+) \right]_{\tilde{\Gamma}}. \tag{6.46}$$

In performing the shift, the variables $\lambda_\beta, \lambda_\gamma \rightarrow \lambda_c$ at the pole, and we obtain the on-shell

form of the MHV contribution,

$$C^{\text{PUP}} = \frac{i}{96\pi^2} \frac{[bc]}{\langle bc \rangle} \times \frac{\langle ad \rangle \langle ce \rangle}{\langle ac \rangle \langle de \rangle} A^{\text{MHV}}(a^-, c^-, d^+, c^+, e^+ \dots n^+) \quad (6.47)$$

that exactly reproduces the soft factor of [102] given in (6.5).

Thus, we have recalculated the Bern et al soft factor by interpreting the sub-leading contributions from off-shell currents to one-loop integrals that introduced off-shell momenta β and γ . Once evaluated on the pole $\lambda_\beta, \lambda_\gamma \rightarrow \lambda_c$, the currents reduce to the on-shell case that is highlighted here (6.47), in a simple interchange form of an MHV amplitude. This supplements the normal recursion procedure to complete a constructive derivation of the one-loop single-minus pure Yang-Mills amplitudes. This form for the PUP contribution will be useful for pure gravity as we shall demonstrate in the following chapter.

Chapter 7

One-loop n -point single-minus graviton amplitudes

In this chapter, we shall derive a modified on-shell recursion procedure for one-loop (pure Einstein) gravity amplitudes with a single negative helicity. We abbreviate this purely rational quantity to: single-minus one-loop graviton amplitudes. We utilise the machinery of BCFW recursion and the techniques developed in Chapter 6, with some generalisations. We shall propose a prescription for the non-standard factorisations we encounter, based on the KLT relations [21].

Rational amplitudes at one-loop in pure Yang-Mills have succumbed to BCFW shifts [102, 105]. Those shifts induce double poles and coincident single poles that modified the standard procedure, for cases of complex momenta going collinear in loop amplitudes. The factorisation of loop amplitudes containing complex momenta is only recently becoming clearer with the input of new non-standard factorisations, as we saw for pure Yang-Mills in Chapter 6. There specifically, we showed how to deal with Yang-Mills single-minus one-loop amplitudes. We derived the origin of the underlying pole under the double pole structure induced from the all positive loop splitting amplitude. The same technique translates to gravity amplitudes in a similar way that we shall recap from Chapter 6.

In contrast with Yang-Mills theory, very few of the one-loop graviton scattering amplitudes are known. Only for $n = 4$ [94, 156, 157] and recently $n = 5$ [20, 91, 158–162] has the computation of the full one-loop graviton scattering amplitude been completed.

Despite the supersymmetric decomposition (4.29), computations for more than four gravitons is difficult. Until very recently only the supersymmetric parts of the $n = 5$ MHV amplitude were known, however in [20] the concept of complex factorisation for complex momenta going collinear was used to obtain the last MHV scalar component $M_5^{[0]}$.

Previous work on the application of on shell recursion for *gravity* amplitudes includes the work of Brandhuber et al at tree [140] and loop level [163]. They defined the all positive helicity loop amplitudes up to $n = 6$, but highlighted the difficulties of applying the standard recursion procedure on the $n = 5$ single-minus one-loop amplitude.

The rational n -point one-loop gravity amplitudes can in principle be recast in a recursion procedure similar to the Yang-Mills case with standard and non-standard factorisations. Progress in computing the non-standard diagrams was first achieved in the single-minus case for $n = 5, 6$ in augmented procedures for recursion [158]. We shall use a generalisation of the Yang-Mills non-standard factorisation to derive a complete recursion procedure for the one-loop single-minus n -point graviton amplitudes.

7.1 The calculation

We now set out the calculation for the contributions to the gravity single-minus one-loop amplitude $M_n^{1\text{-loop}}(a^-, b^+, c^+, d^+, \dots, n^+)$, using on shell recursion with non-standard factorisations as we did in the Yang-Mills case (6.5). Specifically, we consider the $[a, b]$ -shift as before from (5.47), and analyse the standard and complex factorisations, shown pictorially in figure 7.1.

The pure Yang-Mills recursion relation (6.5) provides identical factorisations to the pure graviton case. However, we need to include the sum over permutations of the distinct orderings of the unshifted legs on each side of the factorisation. We denote this set of diagrams with permutations over $\mathcal{P}_D(x \in y)$, where arguments x are permuted through the possible choices in set y , with arguments not in x assigned accordingly (see figure 7.1). For example, a five-point factorisation over a collinear pole would contain a three-point amplitude on one side, that only has one free choice for the unshifted external leg. There are three ways of choosing the lone leg on the three-point side or equivalently three subsets of two legs possible for the other side of the factorisation.

7.1 The calculation

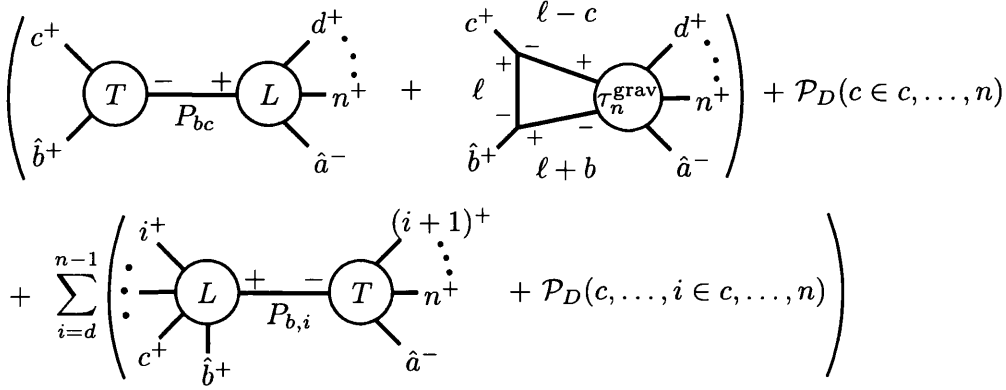


Figure 7.1: The factorisations that occur for $M_n^{1\text{-loop}}(\hat{a}^-, \hat{b}^+, c^+, d^+, \dots, n^+)$. T represents a tree-level MHV or $\overline{\text{MHV}}$ amplitude, while L represents a lower point rational one-loop graviton amplitude. The diagram containing τ_n^{grav} is the modified non-standard factorisation for the all positive helicity one-loop splitting amplitude. The $\mathcal{P}_D(x \in y)$ are permutations over the diagrams for the choices of assigning legs x through y .

Thus we can immediately write down the contribution from diagram 1 in figure 7.1 that contains $(n-1)$ -point one-loop single-minus graviton amplitudes,

$$M_{n-1}^{1\text{-loop}}(d^+, \dots, n^+, \hat{a}^-, \hat{K}_{bc}^+) \frac{i}{K_{bc}^2} M_3^{\text{tree}}(\hat{b}^+, c^+, -\hat{K}_{bc}^-) + \mathcal{P}_D(c \in c, \dots, n) \quad (7.1)$$

where there is an explicit sum over the permutations of external unshifted legs $\mathcal{P}_D(c \in c, \dots, n)$.

The set of factorisations including a sum over i in figure 7.1 includes all but one of the contributions involving lower point graviton all-plus loop amplitudes. We write in the compact form,

$$\sum_{i=d}^{n-1} \left[M_{n-i+2}^{\text{tree}}((i+1)^+, \dots, n^+, \hat{a}^-, \hat{K}_{b\dots i}^-) \frac{i}{K_{b\dots i}^2} M_i^{1\text{-loop}}(\hat{b}^+, c^+, \dots, i^+, -\hat{K}_{b\dots i}^+) + \mathcal{P}_D(c \dots i \in c, \dots, n) \right] \quad (7.2)$$

where there is an explicit sum over the ways of attaching the unshifted external legs. For example, the 6-point, $i = d$ contribution would include the sum over the $\frac{4!}{2!2!}$ ways

7.1 The calculation

of picking two of the unshifted legs from (c, d, e, f) for the 4-point MHV on one side of the factorisation. Specifically, the sum includes

$$M_4^{\text{tree}}(e^+, f^+, \hat{a}^-, \hat{K}_{bcd}^-) \frac{i}{K_{bcd}^2} M_4^{1\text{-loop}}(\hat{b}^+, c^+, d^+, -\hat{K}_{bcd}^+) \quad (7.3)$$

plus the contributions where the legs (c^+, d^+) can be either: (c^+, e^+) , (c^+, f^+) , (d^+, e^+) , (d^+, f^+) , or (e^+, f^+) , with the opposite pair for the other side. The unshifted results are obtained in (7.2) by applying the shift at the pole $\hat{K}_{b\dots i}^2 = 0$ at each instance of i in the sum.

Lastly, we must deal with the instance where, as $\langle \hat{b}c \rangle \rightarrow 0$, the loop splitting amplitude gives rise to double pole and pole under the pole (PUP) contributions in the on shell recursion. This occurs for gravitons in the same way as it did for gluons, where the all-positive helicity graviton one-loop amplitude:

$$M^{1\text{-loop}}(b^+, c^+, K^+) = -\frac{i\kappa^3}{1440\pi^2} \frac{([Kb][bc][cK])^2}{s_{bc}}, \quad (7.4)$$

has a pole for complex momenta with legs k_b and k_c collinear. This combines with the propagator $1/s_{bc}$ to provide the double pole, similar to the case in Yang-Mills (5.76). The diagram of figure 7.1 with the τ_n^{grav} blob would have occurred as a normal factorisation in (7.2) for $i = c$, but we shall modify it accordingly to probe further pole structure. It is now reinterpreted in a similar prescription to the Yang-Mills case in Chapter 6. We shall replace the case of the all-plus gravity split loop amplitude with a pair of gravity vertices including the null leg c^+ and shifted leg \hat{b}^+ connected via propagators dependent on a loop momentum ℓ . These are connected to an off shell gravity current τ_n^{grav} following the procedure of figure 6.1.

We ultimately compute all diagrams that contribute to the pure gravity off shell current τ_n^{grav} in figure 7.1, as the integral

$$C_{\text{grav}}^{\text{n-s f}} = \int d^d\ell \left(\frac{[b|\ell|a][c|\ell|a]}{\langle ba \rangle \langle ca \rangle} \frac{\langle Ca \rangle^2}{\langle Ba \rangle^2} \right)^2 \frac{\tau_n^{\text{grav}}(a^-, B^-, C^+, d^+, \dots, n^+)}{\ell^2 B^2 C^2}, \quad (7.5)$$

where the LHS of the expression comes from the Yang-Mills axial gauge three-point vertices in (3.46) squared. The non-standard factorisation will have to be shifted and its residue extracted as $\langle \hat{b}c \rangle \rightarrow 0$. The off shell current τ_n^{grav} is a summation of ℓ -dependent

7.1 The calculation

diagrams. Again, ℓ is the loop momentum over which we integrate, where we consider the off-shell momenta in the problem as

$$\begin{aligned} B &= \ell + b, \\ C &= \ell - c, \end{aligned} \tag{7.6}$$

that we have seen previously in (6.9). However, the difference between the pure gluon and pure gravity off shell current τ_n^{grav} , is that we will need to include all possible orderings allowed in gravity. Thus we also have to add to $C_{\text{grav}}^{n-s f}$ the permutations over diagrams $\mathcal{P}_D(c \in c \dots n)$ that will be included at the end.

We utilise the KLT relations to build the required products of off shell diagrams as products of Yang-Mills currents we have already described. The extension of the KLT relations to off-shell currents has been used before [20] but requires some motivation considering the statements made. We argue that due to the factorisation imposing collinearity of k_b and k_c , the loop momentum ℓ is almost null due to integration around the $\ell^2 \rightarrow 0$ limit. The region of integration is forcing the off-shell legs as close to null as possible, while retaining the information from NLO terms (i.e. integrals containing boxes, pentagons and so on). The nature of the on-shell recursion procedure provides this condition. This is combined with taking the limit of null momenta in the τ_n^{grav} currents, that makes the simplifications manifest similar to the Yang Mills currents in the previous chapter. Thus, the required orderings of products of gauge theory amplitudes via the KLT relations works for τ_n^{grav} with two legs *just* off shell.

The n -point KLT relations (4.25) are now rewritten under our labelling prescription, re-using $B + C = b + c$ for the off shell legs,

$$\begin{aligned} \tau_n^{\text{grav}}(B, C, \dots, n, a) &= i(-1)^{n+1} \left[\tau_n^{\text{YM}}(B, C, \dots, n, a) \times \right. \\ &\quad \sum_{\mathcal{P}_1, \mathcal{P}_2} f(i_1, \dots, i_k; B) \bar{f}(j_1, \dots, j_{k'}) \tau_n^{\text{YM}}(i_1, \dots, i_k, B, n, j_1, \dots, j_{k'}, a) \Big] \\ &\quad + \mathcal{P}_{\text{KLT}}(C, d, \dots, n-1), \end{aligned} \tag{7.7}$$

where \mathcal{P}_1 are the permutations of $(i_1, \dots, i_k) \in \mathcal{P}_1(C, \dots, n/2)$ and \mathcal{P}_2 are the permutations of $(j_1, \dots, j_{k'}) \in \mathcal{P}_2(n/2+1, \dots, n-1)$. $k = n/2 - 1$, $k' = n/2 - 2$, giving a total of $(n/2 - 1)! \times (n/2 - 2)!$ terms in the square brackets. The overall terms are permuted over in \mathcal{P}_{KLT} , for legs in both τ^{YM} currents with $(n - 3)!$ permutations. Therefore the

7.2 Tackling loop integration in pure gravity

entire KLT relation has $(n/2 - 1)! \times (n/2 - 2)! \times (n - 3)!$ terms. Here n is assumed to be even; the case of odd n is completely analogous.

The functions f and \bar{f} are given by

$$\begin{aligned} f(i_1, \dots, i_k; B) &= s(B, i_k) \prod_{m=1}^{k-1} \left(s(B, i_m) + \sum_{p=m+1}^k g(i_m, i_p) \right) \\ \bar{f}(j_1, \dots, j_{k'}) &= s(j_1, n) \prod_{m=2}^{k'} \left(s(j_m, n) + \sum_{p=1}^{m-1} g(j_p, j_m) \right) \end{aligned} \quad (7.8)$$

where we have made B an explicit argument of f , and

$$g(i, j) = \begin{cases} s(i, j) \equiv s_{ij}, & i > j, \\ 0, & \text{otherwise,} \end{cases} \quad (7.9)$$

This compact expression will be our guide for eventually providing all the terms necessary for the non-standard factorisation.

Firstly the type of integrals encountered for general cases where loop momentum occurs in both f and \bar{f} is considered in the following section. Then, we present the simplifications exhibited in the PUP contribution, by computing the required diagrams at 5-point explicitly. For $n > 5$ -point we require Yang-Mills off shell currents where the negative helicity gluon in the gauge theory amplitude is free to wander away from the off shell legs. This will be dealt with in its own section. It turns out, after some work, that these currents with a wandering negative helicity (wandering-minus), have a fairly simple extension to the analogue of the n -point Yang-Mills case. Finally, we present the n -point contribution to these complex factorisations (7.5), to complete a recursive ansatz for the n -point single-minus one-loop graviton amplitudes.

7.2 Tackling loop integration in pure gravity

The type of integrals where only MHV tree amplitudes appear will contain an arbitrary power of ℓ in the numerator, in general. For $n > 5$, the KLT relations increase the power of ℓ depending on the number of s_{Bx} or s_{Cy} in each term. We can construct the types of loop integrals to compute for any n -point contribution to C_{grav}^{n-sf} where the τ_n^{YM}

7.2 Tackling loop integration in pure gravity

are replaced by MHV amplitudes, using Feynman parametrisation (A.2), encountered in Appendix A,

$$\frac{1}{A_1 A_2 \cdots A_n} = \int_0^1 dx_1 \cdots dx_n \frac{\delta(\sum x_i - 1)(n-1)!}{[x_1 A_1 + \cdots + x_n A_n]^n}. \quad (7.10)$$

So, we shall consider integrals of the form,

$$\mathcal{I}_{\text{grav}}^{\text{MHV}} = 2 \int_0^1 dx_1 dx_2 dx_3 \frac{\int d^d \ell}{(2\pi)^4} \frac{\delta(x_1 + x_2 + x_3 - 1)}{[\ell^2 + 2\ell \cdot (x_2 b - x_3 c)]^3} \left(\frac{[b|\ell|a][c|\ell|a]}{\langle ba \rangle \langle ca \rangle} \right)^2 (s_{Bx})^p (s_{Cy})^q. \quad (7.11)$$

For generic integrals of high orders of loop momenta, we have seen there are tedious deconstruction techniques, such as Passarino Veltman. Fortunately we require only those terms that are singular as $s_{bc} \rightarrow 0$, and can make use of the following truncation of the formula [164],

$$\int \frac{d^4 \ell}{(2\pi)^4} \frac{\ell_{\mu_1} \ell_{\nu_2} \cdots \ell_{\sigma_n}}{(\ell^2 + M^2 + 2\ell \cdot p)^3} = \frac{i}{4\pi^2} \frac{(-1)^n}{2} \frac{p_{\mu_1} p_{\nu_2} \cdots p_{\sigma_n}}{(M^2 - p^2)} + \mathcal{O}\left(\frac{1}{(M^2 - p^2)^0}\right) \quad (7.12)$$

where sub-leading terms in p^2 up to ℓ^4 can also be found in Appendix B of [164]. This allows direct substitution of $\ell \rightarrow p = x_2 k_b - x_3 k_c$ upon integration, up to numerical factors. Thus we can identify terms of $1/p^2$ as $1/s_{bc}$ and safely ignore all terms of order $(p^2)^0$ as they vanish after the shift. So we can write down the result of the loop integration where only factors of $x_2 k_b$ and $x_3 k_c$ remain, akin to the case in Yang-Mills integrals seen in (A.5). See Appendix section A.2 for full details on evaluation of the remaining integral. There is not a compact expression for the integrals (7.11) for any generic p, q , due to the re-parametrisation of s_{Bx} and s_{Cy} ,

$$\begin{aligned} s_{Bx}^p &\rightarrow ((1 - x_2)s_{bx} + x_3 s_{cx})^p, \\ s_{Cy}^q &\rightarrow (x_2 s_{by} + (1 - x_3)s_{cy})^q. \end{aligned} \quad (7.13)$$

However the remaining integrals contain products of the form x_2^{r+1} and x_3^{s+1} , that yield

7.2 Tackling loop integration in pure gravity

Gamma functions,

$$\int_0^1 dx_2 \int_0^{1-x_2} dx_3 x_2^{r+1} x_3^{s+1} = \frac{\Gamma(r+2)\Gamma(s+2)}{\Gamma(5+r+s)} \quad (7.14)$$

that evaluate to simple factorials.

The rules for applying the substitutions in (7.13) require a re-definition of the functions f and \bar{f} from the KLT relations, given in (7.7),

$$\begin{aligned} f(i_1, \dots, i_k; B) &= s(B, i_k) \prod_{m=1}^{k-1} \left(s(B, i_m) + \sum_{p=m+1}^k g(i_m, i_p) \right), \\ \bar{f}(j_1, \dots, j_{k'}; n) &= s(j_1, n) \prod_{m=2}^{k'} \left(s(j_m, n) + \sum_{p=1}^{m-1} g(j_p, j_m) \right), \end{aligned} \quad (7.15)$$

where the lists i and j can admit any permutations from \mathcal{P}_1 or \mathcal{P}_2 respectively, as defined in (7.7). Both lists can admit C for some permutations. Therefore the function f can contain B and C while, C can only appear in \bar{f} .

Extracting the factors of x_2 and x_3 , we label the four possible functions that arise from the substitution of (7.13), in terms of a polynomial in g ,

$$\begin{aligned} f_{bb}(\dots, C, \dots; B) &= \sum_{p_b, q_b} g(x_2^{p_b}, x_3^{q_b}) f(\dots, b, \dots; b) \\ f_{bc}(\dots, C, \dots; B) &= \sum_{p_b, q_c} g(x_2^{p_b}, x_3^{q_c}) f(\dots, b, \dots; c) \\ f_{cb}(\dots, C, \dots; B) &= \sum_{p_c, q_b} g(x_2^{p_c}, x_3^{q_b}) f(\dots, c, \dots; b) \\ f_{cc}(\dots, C, \dots; B) &= \sum_{p_c, q_c} g(x_2^{p_c}, x_3^{q_c}) f(\dots, c, \dots; c) \end{aligned} \quad (7.16)$$

where the sums over coefficients p_i, q_i , for $i = b, c$ are given by the substitutions in (7.13). Doing the same with \bar{f} , the two possible functions as a result of the substitutions of

7.2 Tackling loop integration in pure gravity

(7.13) can be written,

$$\begin{aligned}\bar{f}_b(\dots, C, \dots) &= \sum_{p_b, q_b} g(x_2^{p_b}, x_3^{q_b}) \bar{f}(\dots, b, \dots) \\ \bar{f}_c(\dots, C, \dots) &= \sum_{p_c, q_c} g(x_2^{p_c}, x_3^{q_c}) \bar{f}(\dots, c, \dots)\end{aligned}\tag{7.17}$$

that we collect for f and \bar{f} into,

$$\begin{aligned}f(\dots, C, \dots; B) &= \sum_{i,j=b,c} \sum_{p_i, q_j} g(x_2^{p_i}, x_3^{q_j}) f(\dots, i, \dots; j) \\ \bar{f}(\dots, C, \dots) &= \sum_{k=b,c} \sum_{p_k, q_k} g(x_2^{p_k}, x_3^{q_k}) \bar{f}(\dots, k, \dots)\end{aligned}\tag{7.18}$$

Now the product of f and \bar{f} when (7.13) is applied can be put in terms of a product of the functions defined in (7.18), with an overall polynomial function in x_2 and x_3 to sum over,

$$f(\dots C \dots; B) \bar{f}(\dots C \dots) = \sum_{i,j,k=b,c} \sum_{p_i, k, q_j, k} g(x_2^{p_i+p_k}, x_3^{q_j+q_k}) f(\dots i \dots; j) \bar{f}(\dots k \dots)\tag{7.19}$$

where the coefficients p and q are determined by the substitution,

$$\begin{aligned}B &\rightarrow (1 - x_2)b + x_3c \\ C &\rightarrow x_2b + (1 - x_3)c\end{aligned}\tag{7.20}$$

We can handle the integrals over the factors of x_2 and x_3 using the result from (7.14), since an overall prefactor of x_2x_3 comes from the left hand side of the loop, to express the general integrated contribution from (7.11) as

$$\begin{aligned}\mathcal{J}_{\text{grav}}^{\text{MHV}} &= \int_0^1 dx_2 \int_0^{1-x_2} dx_3 x_2 x_3 f(\dots, C, \dots; B) \bar{f}(\dots, C, \dots) \\ &= \sum_{i,j,k=b,c} \sum_{p_i, k, q_j, k} \frac{\Gamma(2 + p_i + p_k) \Gamma(2 + q_j + q_k)}{\Gamma(5 + p_i + p_k + q_j + q_k)} f(\dots i \dots; j) \bar{f}(\dots k \dots).\end{aligned}\tag{7.21}$$

where the coefficients p and q are determined term by term in the expansion of f, \bar{f}

7.3 Complex factorisation for the 5-point case

(7.19) given by equations (7.16) and (7.17), due to the substitutions of (7.20).

See Appendix A.2 for a worked example, or proceed to the following section for the result at 5-point. This leads to increasingly cumbersome fractional contributions for $n > 5$ -point MHV contributions to C_{grav}^{n-sf} .

7.3 Complex factorisation for the 5-point case

The diagrams of interest are those that contribute to the following integral,

$$C_{\text{grav}}^{n-sf}|_5 = \int d^d \ell \left(\frac{[b|\ell|a][c|\ell|a]}{\langle ba \rangle \langle ca \rangle} \frac{\langle Ca \rangle^2}{\langle Ba \rangle^2} \right)^2 \frac{\tau_5^{\text{grav}}(a^-, B^-, C^+, d^+, e^+)}{\ell^2 B^2 C^2}. \quad (7.22)$$

We shall express τ_5^{grav} using the 5-point KLT relations (4.24) in terms of products of the known Yang-Mills off shell currents,

$$\begin{aligned} \tau_5^{\text{grav}}(a^-, B^-, C^+, d^+, e^+) &= s_{BC} s_{de} \tau_5^{\text{YM}}(a^-, B^-, C^+, d^+, e^+) \tau_5^{\text{YM}}(a^-, C^+, B^-, e^+, d^+) \\ &\quad + s_{Bd} s_{Ce} \tau_5^{\text{YM}}(a^-, B^-, d^+, C^+, e^+) \tau_5^{\text{YM}}(a^-, d^+, B^-, e^+, C^+) \end{aligned} \quad (7.23)$$

where only the first term contains a pole as $s_{BC} \rightarrow 0$, due to the appearance of a term with a $1/\langle BC \rangle$ factor in each τ_5^{YM} . The second term of (7.23) is finite in this limit, therefore we can replace instances of τ^{YM} by on shell MHV gauge theory amplitudes. We extract the loop momentum dependence from the second term using,

$$\frac{\langle CX \rangle}{\langle Ca \rangle} = \frac{\langle CX \rangle}{\langle Ca \rangle} \frac{\langle ca \rangle}{\langle ca \rangle} \rightarrow \frac{\langle cX \rangle}{\langle ca \rangle} + \mathcal{O}(\langle bc \rangle), \quad (7.24)$$

along with the corresponding simplification for B . The contribution from the second term of (7.23) that we label the b term of C_{grav}^{n-sf} , is then

$$\begin{aligned} C_{\text{grav}}^{n-sf}|_5^b &= \int d^d \ell \left(\frac{[b|\ell|a][c|\ell|a]}{\langle ba \rangle \langle ca \rangle} \right)^2 \frac{s_{Bd} s_{Ce}}{\ell^2 B^2 C^2} \frac{\langle ca \rangle^4}{\langle ba \rangle^4} \\ &\quad \times A_5^{\text{MHV}}(a^-, b^-, d^+, c^+, e^+) A_5^{\text{MHV}}(a^-, d^+, b^-, e^+, c^+) \end{aligned} \quad (7.25)$$

7.3 Complex factorisation for the 5-point case

We are now confronted with a momentum integral of order ℓ^6 in the numerator. This is one of the simplest cases of the type of integral encountered in the previous section. So applying the same process from Appendix A.2 to (7.25), outlined previously to give (7.21), we can perform the loop integrals to find,

$$C_{\text{grav}}^{\text{n-s f}}|_5^b = \frac{i}{16\pi^2} \frac{-1}{360} \frac{[bc]^3}{\langle bc \rangle} (2s_{be}s_{cd} + 3s_{ce}s_{cd} + 3s_{bd}s_{be} + 5s_{bd}s_{ce}) \times \frac{\langle ca \rangle^4}{\langle ba \rangle^4} A_5^{\text{MHV}}(a^-, b^-, d^+, c^+, e^+) A_5^{\text{MHV}}(a^-, d^+, b^-, e^+, c^+) \quad (7.26)$$

Evaluating at the pole of interest, $\langle \hat{b}c \rangle \rightarrow 0$, we can make the following substitutions,

$$\hat{\lambda}_b = \frac{\langle ba \rangle}{\langle ca \rangle} \lambda_c, \quad s_{\hat{b}x} = \frac{\langle cx \rangle}{\langle ca \rangle} [x|b|a], \quad s_{cx} = \frac{\langle cx \rangle}{\langle ca \rangle} [x|c|a], \quad (7.27)$$

such that the contribution of (7.25) to the final answer is,

$$C_{\text{grav}}^{\text{n-s f}}|_5^b = \frac{i}{16\pi^2} \frac{-1}{360} \frac{[bc]^3}{\langle bc \rangle} A_5^{\text{MHV}}(a^-, c^-, d^+, c^+, e^+) A_5^{\text{MHV}}(a^-, d^+, c^-, e^+, c^+) \times \frac{\langle cd \rangle \langle ce \rangle}{\langle ca \rangle^2} (2[d|c|a][e|b|a] + 3[e|c|a][d|c|a] + 3[d|b|a][e|b|a] + 5[d|b|a][e|c|a]) \quad (7.28)$$

7.3.1 Off shell contribution to $C_{\text{grav}}^{\text{n-s f}}|_5$

Turning to the first term in (7.23), that we shall label $C_{\text{grav}}^{\text{n-s f}}|_5^a$, we require the leading and sub-leading off shell terms from each Yang-Mills current. Making a suitable definition for $\tau^{\text{MHV}}(a^-, -K_i^-)$, we substitute in the Yang-Mills factors (6.37), according

7.3 Complex factorisation for the 5-point case

to the two orderings,

$$\begin{aligned}
& s_{BC}s_{de}\tau_5^{\text{YM}}(a^-, B^-, C^+, d^+, e^+)\tau_5^{\text{YM}}(a^-, C^+, B^-, e^+, d^+) = s_{bc}s_{de} \left(\frac{\langle Ba \rangle}{\langle Ca \rangle} \right)^4 \\
& \left[\frac{\langle a|B(b+c)|a\rangle}{s_{bc}} \frac{\tau^{\text{MHV}}(a^-, (b+c)^-, d^+, e^+)}{\langle P_{bca} \rangle^2} \right. \\
& + \sum_{i=d}^e \langle Ca \rangle^2 \langle a|BK_i|a\rangle \frac{\tau^{\text{sm}}(-\kappa_i^-, C^+, d^+, \dots, i^+)}{\langle \kappa_i a \rangle^2 \kappa_i^2} \frac{\tau^{\text{MHV}}(a^-, -K_i^-, (i+1)^+, \dots, e^+)}{\langle K_i a \rangle^2 K_i^2} \Big] \\
& \times \left[\frac{\langle a|C(b+c)|a\rangle}{s_{bc}} \frac{\tau^{\text{MHV}}(a^-, (b+c)^-, e^+, d^+)}{\langle P_{bca} \rangle^2} \right. \\
& + \sum_{i=e}^d \langle Ba \rangle^2 \langle a|CK_i|a\rangle \frac{\tau^{\text{sm}}(-\kappa_i^-, B^+, e^+, \dots, i^+)}{\langle \kappa_i a \rangle^2 \kappa_i^2} \frac{\tau^{\text{MHV}}(a^-, -K_i^-, (i+1)^+, \dots, d^+)}{\langle K_i a \rangle^2 K_i^2} \Big]
\end{aligned} \tag{7.29}$$

where each off shell current is split into a singular diagram plus a sum of finite diagrams as in figure 6.5. Using the explicit form for τ^{sm} given in (6.27), to order $1/\langle bc \rangle$, the first sum in (7.29) is independent of C , while the second sum is independent of B . The integrand is essentially the square of the Yang-Mills one, but we need only the leading double pole terms and cross terms and neglect order $\langle bc \rangle^0$ terms. Recall (6.24), such that we apply a similar method to compute the gravity loop integrals in the following special cases,

$$\int d^4\ell \frac{[b|\ell|a]^2 [c|\ell|a]^2 [X|B|a] \langle a|PC|a\rangle}{\ell^2 B^2 C^2 \langle ba \rangle^2 \langle ca \rangle^2} = \frac{1}{(4\pi)^2} \frac{[bc]^3}{\langle bc \rangle} \frac{\langle a|bc|a\rangle}{360} (2[X|b|a] + [X|c|a]), \tag{7.30}$$

$$\int d^4\ell \frac{[b|\ell|a]^2 [c|\ell|a]^2 [Y|C|a] \langle a|PB|a\rangle}{\ell^2 B^2 C^2 \langle ba \rangle^2 \langle ca \rangle^2} = \frac{1}{(4\pi)^2} \frac{[bc]^3}{\langle bc \rangle} \frac{\langle a|cb|a\rangle}{360} ([Y|b|a] + 2[Y|c|a]), \tag{7.31}$$

$$\int d^4\ell \frac{[b|\ell|a]^2 [c|\ell|a]^2 \langle a|PC|a\rangle \langle a|PB|a\rangle}{\ell^2 B^2 C^2 \langle ba \rangle^2 \langle ca \rangle^2} = \frac{1}{(4\pi)^2} \frac{[bc]^3}{\langle bc \rangle} \frac{\langle a|cb|a\rangle \langle a|bc|a\rangle}{360}, \tag{7.32}$$

7.3 Complex factorisation for the 5-point case

which are computed explicitly in Appendix A.2. The integrated contribution of (7.29), that we denote $C_{\text{grav}}^{\text{n-s f}}|_5^a$, is

$$\begin{aligned}
C_{\text{grav}}^{\text{n-s f}}|_5^a &= \frac{1}{(4\pi)^2} \frac{[bc]^3}{\langle bc \rangle} \frac{s_{bc}s_{de}}{360} \\
&\times \left[\frac{\langle a|cb|a \rangle}{s_{bc}} \frac{\tau^{\text{MHV}}(a^-, (b+c)^-, d^+, e^+)}{\langle P_{bc}a \rangle^2} \right. \\
&+ \sum_{i=d}^e \langle ca \rangle^2 \langle a|K_i(2b+c)|a \rangle \frac{\tau^{\text{sm}}(-\kappa_i^-, c^+, d^+, \dots, i^+)}{\langle \kappa_i a \rangle^2 \kappa_i^2} \frac{\tau^{\text{MHV}}(a^-, -K_i^-, (i+1)^+, \dots, e^+)}{\langle K_i a \rangle^2 K_i^2} \left. \right] \\
&\times \left[\frac{\langle a|bc|a \rangle}{s_{bc}} \frac{\tau^{\text{MHV}}(a^-, (b+c)^-, e^+, d^+)}{\langle P_{bc}a \rangle^2} \right. \\
&+ \sum_{i=e}^d \langle ba \rangle^2 \langle a|K_i(2c+b)|a \rangle \frac{\tau^{\text{sm}}(-\kappa_i^-, b^+, e^+, \dots, i^+)}{\langle \kappa_i a \rangle^2 \kappa_i^2} \frac{\tau^{\text{MHV}}(a^-, -K_i^-, (i+1)^+, \dots, d^+)}{\langle K_i a \rangle^2 K_i^2} \left. \right]
\end{aligned} \tag{7.33}$$

where κ_i and K_i are defined as they were in the Yang-Mills forms (6.37). Upon evaluation at the pole $\langle bc \rangle \rightarrow 0$, we only keep terms of order $1/\langle bc \rangle^2$ and $1/\langle bc \rangle$. The double pole contribution is contained in the product of two terms, each from the τ^{MHV} contribution,

$$\begin{aligned}
&\frac{1}{(4\pi)^2} \frac{[bc]^3}{\langle bc \rangle} \frac{s_{bc}s_{de}}{360} \\
&\times \frac{\langle a|cb|a \rangle}{s_{bc}} \frac{\tau^{\text{MHV}}(a^-, (b+c)^-, d^+, e^+)}{\langle P_{bc}a \rangle^2} \frac{\langle a|bc|a \rangle}{s_{bc}} \frac{\tau^{\text{MHV}}(a^-, (b+c)^-, e^+, d^+)}{\langle P_{bc}a \rangle^2}
\end{aligned} \tag{7.34}$$

where employing the explicit pole term from (6.28) in each τ^{MHV} factor provides the double pole (denoted DP),

$$C_{\text{grav}}^{\text{n-s f}}|_5^{\text{a, DP}} = \frac{1}{(4\pi)^2} \frac{[bc]^3}{\langle bc \rangle} \frac{s_{bc}s_{de}}{360} \frac{\langle a|cb|a \rangle}{s_{bc}} \frac{\langle a|(b+c)d|a \rangle}{t_{bcd}\langle ad \rangle \langle de \rangle \langle ea \rangle} \frac{\langle a|bc|a \rangle}{s_{bc}} \frac{\langle a|(b+c)e|a \rangle}{t_{bce}\langle ae \rangle \langle ed \rangle \langle da \rangle} \tag{7.35}$$

7.3 Complex factorisation for the 5-point case

We extract the residue of the double pole,

$$\text{Res} \left(\frac{1}{z} C_{\text{grav}}^{\text{n-s f}} \Big|_5^{\text{a,DP}} (\hat{a}^-, \hat{b}^+, c^+, d^+, e^+) \right) \Big|_{\langle \hat{b}c \rangle = 0} = \frac{1}{(4\pi)^2} [bc]^2 s_{de} \frac{\langle a|bc|a \rangle^2}{360} \frac{\langle a|(b+c)d|a \rangle}{\langle ad \rangle \langle de \rangle \langle ea \rangle} \frac{\langle a|(b+c)e|a \rangle}{\langle ae \rangle \langle ed \rangle \langle da \rangle} \left(\frac{1}{z} \frac{1}{\langle \hat{b}c \rangle^2 t_{\hat{b}cd} t_{\hat{b}ce}} \right) \Big|_{\langle \hat{b}c \rangle = 0} \quad (7.36)$$

which again, will yield pole under the pole contributions as sub-leading terms in order $\langle bc \rangle$. Analysing the shifted quantities, the residue without the prefactor is,

$$\text{Res} \left(\frac{1}{z} \frac{1}{\langle \hat{b}c \rangle^2 t_{\hat{b}cd} t_{\hat{b}ce}} \right) \Big|_{\langle \hat{b}c \rangle = 0} = \frac{\langle ac \rangle^2}{\langle bc \rangle^2 \langle a|(b+c)d|c \rangle \langle a|(b+c)e|c \rangle} \left(-1 + \frac{\langle a|(c+d)b|c \rangle}{\langle a|(b+c)d|c \rangle} + \frac{\langle a|(c+e)b|c \rangle}{\langle a|(b+c)e|c \rangle} \right). \quad (7.37)$$

Thus, the entire double pole contribution is contained in the first term of the residue,

$$\begin{aligned} C_{\text{grav}}^{\text{n-s f}} \Big|_5^{\text{a,DP}} &= \frac{-1}{(4\pi)^2} [bc]^2 s_{de} \frac{\langle a|bc|a \rangle^2}{360} \frac{\langle a|(b+c)d|a \rangle}{\langle ad \rangle \langle de \rangle \langle ea \rangle} \frac{\langle a|(b+c)e|a \rangle}{\langle ae \rangle \langle ed \rangle \langle da \rangle} \\ &\quad \times \frac{\langle ac \rangle^2}{\langle bc \rangle^2 \langle a|(b+c)d|c \rangle \langle a|(b+c)e|c \rangle} \\ &= -\frac{1}{(4\pi)^2} \frac{[bc]^2}{\langle bc \rangle^2} \frac{s_{de}}{360} \frac{\langle a|bc|a \rangle^2}{\langle ac \rangle^4} \frac{\langle ac \rangle^4}{\langle ac \rangle \langle cd \rangle \langle de \rangle \langle ea \rangle} \frac{\langle ac \rangle^4}{\langle ac \rangle \langle ce \rangle \langle ed \rangle \langle da \rangle} \\ &= -\frac{1}{(4\pi)^2} \frac{[bc]^2}{\langle bc \rangle^2} \frac{s_{de}}{360} \frac{\langle a|bc|a \rangle^2}{\langle ac \rangle^4} A_4^{\text{MHV}}(a^-, c^-, d^+, e^+) A_4^{\text{MHV}}(a^-, c^-, e^+, d^+) \end{aligned} \quad (7.38)$$

The sub-leading or PUP terms then come from the extra terms generated in (7.37) that are as yet unused, combined with the cross terms that survive at order $1/\langle bc \rangle$ from (7.33).

7.3 Complex factorisation for the 5-point case

7.3.2 Re-interpreting the sub-leading contribution in $C_{\text{grav}}^{\text{n-s f}}|_5^a$

The simplification first established for the Yang-Mills case [20], where the terms in the PUP contribution organised themselves into an interchanged MHV amplitude (6.46), is the goal for the pure gravity 5-point case. Here however, we must examine the cross terms between those with and without $1/s_{bc}$ factors from the unshifted contribution in (7.33). Expanding the instances of τ^{MHV} using (6.28), we rewrite the five-point result from (7.33),

$$\begin{aligned}
C_{\text{grav}}^{\text{n-s f}}|_5^a &= \frac{-1}{(4\pi)^2} [bc]^4 \frac{s_{de}}{360} \\
&\times \left[\frac{\langle a|cb|a\rangle}{\langle ad\rangle\langle de\rangle\langle ea\rangle} \left(\frac{\langle a|(b+c)d|a\rangle}{s_{ea}s_{bc}} + \frac{[qe]}{[aq][ae]} \right) \right. \\
&+ \sum_{i=d}^e \langle ca\rangle^2 \langle a|K_i(2b+c)|a\rangle \frac{\tau^{\text{sm}}(-\kappa_i^-, c^+, d^+, \dots, i^+)}{\langle \kappa_i a\rangle^2 \kappa_i^2} \frac{\tau^{\text{MHV}}(a^-, -K_i^-, (i+1)^+, \dots, e^+)}{\langle K_i a\rangle^2 K_i^2} \Big] \\
&\times \left[\frac{\langle a|bc|a\rangle}{\langle ae\rangle\langle ed\rangle\langle da\rangle} \left(\frac{\langle a|(b+c)e|a\rangle}{s_{da}s_{bc}} + \frac{[qd]}{[aq][ad]} \right) \right. \\
&+ \sum_{i=e}^d \langle ba\rangle^2 \langle a|K_i(2c+b)|a\rangle \frac{\tau^{\text{sm}}(-\kappa_i^-, b^+, e^+, \dots, i^+)}{\langle \kappa_i a\rangle^2 \kappa_i^2} \frac{\tau^{\text{MHV}}(a^-, -K_i^-, (i+1)^+, \dots, d^+)}{\langle K_i a\rangle^2 K_i^2} \Big]
\end{aligned} \tag{7.39}$$

where each quantity in the square brackets is just the square of the Yang-Mills current from (6.38). Into this, we can insert the two sub-leading factors that came from extracting the residue at the double pole in (7.37), one term for each square brackets. In this way we present a very similar form to the Yang-Mills case in (6.42). This will eventually allow each Yang-Mills current in the square brackets to be expressed in terms of the interchange MHV amplitudes.

The two sub-leading terms evaluated from the residue of the double pole in (7.37) contain the cross terms between the two Yang-Mills copies already, from the effects of the shifted s_{bcd} and s_{bce} . They are also the same under a $d \leftrightarrow e$ swap. Therefore in their final form they are unaffected by the shift and can be inserted into the $C_{\text{grav}}^{\text{n-s f}}|_5^a$

7.3 Complex factorisation for the 5-point case

contribution to leave,

$$\begin{aligned}
& C_{\text{grav}}^{\text{n-s f}} \Big|_5^a - \frac{s_{de}}{(4\pi)^2} \frac{[bc]^2}{360} \frac{\langle a|bc|a \rangle^2}{(\langle ad \rangle \langle de \rangle \langle ea \rangle)^2} \frac{\langle a|(b+c)d|a \rangle \langle a|(b+c)e|a \rangle \langle ac \rangle^2}{\langle a|(b+c)d|c \rangle \langle a|(b+c)e|c \rangle \langle bc \rangle^2} \\
& \times \left(\frac{\langle a|(c+d)b|c \rangle}{\langle a|(b+c)d|c \rangle} + \frac{\langle a|(c+e)b|c \rangle}{\langle a|(b+c)e|c \rangle} \right) = \frac{-1}{(4\pi)^2} [bc]^4 \frac{s_{de}}{360} \\
& \times \left[\frac{\langle a|cb|a \rangle}{\langle ad \rangle \langle de \rangle \langle ea \rangle} \left(\frac{\langle a|(b+c)d|a \rangle}{s_{ea} s_{bc}} + \frac{[qe]}{[aq][ae]} - \frac{\langle a|(b+c)d|a \rangle [b|c+d|a \rangle \langle ac \rangle}{[bc] \langle a|(b+c)d|c \rangle^2} \right) \right. \\
& + \sum_{i=d}^e \langle \gamma a \rangle^2 \langle a|K_i \beta|a \rangle \frac{\tau^{\text{sm}}(-\kappa_i^-, \gamma^+, d^+, \dots, i^+)}{\langle \kappa_i a \rangle^2 \kappa_i^2} \frac{\tau^{\text{MHV}}(a^-, -K_i^-, (i+1)^+, \dots, e^+)}{\langle K_i a \rangle^2 K_i^2} \Bigg] \\
& \times \left[\frac{\langle a|bc|a \rangle}{\langle ae \rangle \langle ed \rangle \langle da \rangle} \left(\frac{\langle a|(b+c)e|a \rangle}{s_{da} s_{bc}} + \frac{[qd]}{[aq][ad]} - \frac{\langle a|(b+c)e|a \rangle [b|c+e|a \rangle \langle ac \rangle}{[bc] \langle a|(b+c)e|c \rangle^2} \right) \right. \\
& + \sum_{i=e}^d \langle \rho a \rangle^2 \langle a|K_i \theta|a \rangle \frac{\tau^{\text{sm}}(-\kappa_i^-, \rho^+, e^+, \dots, i^+)}{\langle \kappa_i a \rangle^2 \kappa_i^2} \frac{\tau^{\text{MHV}}(a^-, -K_i^-, (i+1)^+, \dots, d^+)}{\langle K_i a \rangle^2 K_i^2} \Bigg]
\end{aligned} \tag{7.40}$$

where $\beta = 2b + c$, $\gamma = -b$ and $\theta = 2c + b$, $\rho = -c$. These identifications for the Greek letters come from the remnants of performing the loop integration. The off shell β comes from the integration over factors including $B = \ell + b$. Instances of β are counteracted by γ , that appear for the same reason they did in the original Yang-Mills case in (6.36). Those were to preserve momentum conservation, and write the Yang-Mills current as an interchange MHV amplitude in terms of β and γ as was obtained for (6.46). The reversed role applies for integration over $C = c - \ell$, which give rise to θ in the second Yang-Mills current in (7.40). For this Yang-Mills current, ρ preserves momentum conservation between combinations of $\rho + \theta$, which we will see can also be written as an interchange MHV amplitude with arguments ρ and θ .

Inside the first set of square brackets after the s_{bc} term, reproduces precisely the 5-point case of the C^{PUP} contribution we saw in Chapter 6 in equation (6.42). The sub-leading factors we have inserted from (7.37) into each Yang-Mills current is crucially, of the same form but with $d \leftrightarrow e$. Overall, however there is both a $b \leftrightarrow c$ and $d \leftrightarrow e$ symmetry between the rest of the Yang-Mills current inside each square brackets. The insertion of the sub-leading factors from (7.37) are not $b \leftrightarrow c$ symmetric due to the

7.3 Complex factorisation for the 5-point case

shift already applied when extracting the residue. This causes a subtle difference in the cancellations for the PUP contribution of the latter Yang-Mills current.

We shall now repeat the substitutions for each PUP contribution for an interchange MHV amplitude, identical to the five-point case of (6.43) in Chapter 6, for the Yang-Mills current in the first set of brackets. The second Yang-Mills current will have its PUP contribution substituted for the following interchange MHV amplitude,

$$\begin{aligned} \tau^{\text{MHV}}(a^-, \theta^-, e^+, \rho^+, d^+) &= \frac{[e|K_1|a]\langle\theta a\rangle^2}{\langle ea\rangle} \frac{\tau^{\text{MHV}}(a^-, -K_1^-, \rho^+, d^+)}{\langle K_1 a\rangle^2 K_1^2} \\ &+ \langle a|\theta\kappa_2|a\rangle\langle\theta a\rangle^2 \frac{\tau^{\text{sm}}(-\kappa_2^-, e^+, \rho^+)}{\langle\kappa_2 a\rangle^2 \kappa_2^2} \frac{\tau^{\text{MHV}}(a^-, -K_2^-, d)}{\langle K_2 a\rangle^2 K_2^2} \\ &+ \langle a|\theta\kappa_3|a\rangle\langle\theta a\rangle^2 \frac{\tau^{\text{sm}}(-\kappa_3^-, e^+, \rho^+, d^+)}{\langle\kappa_3 a\rangle^2 \kappa_3^2} \frac{\tau^{\text{MHV}}(a^-, -K_n^-)}{\langle K_n a\rangle^2 K_n^2} \end{aligned} \quad (7.41)$$

with a suitable definition for $\tau^{\text{MHV}}(a^-, -K_n^-)$. Thus we are following exactly the same substitutions as (6.44), albeit at the five-point case, which we shall neglect to write out in full. After the substitution for the terms using (6.43) and (7.41), we have two copies of Yang-Mills C^{PUP} contributions akin to (6.44) in Chapter 6. While the first set of cancellations that occur before the shift, where all coefficients of (6.45) and

$$\frac{[qd]}{[aq][ad]} - \sum_{l=d}^{n-1} \frac{\langle a|K_{a,l+1..d}l|a\rangle}{s_{a,l+1..d}s_{a,l..d}} \quad (7.42)$$

vanish apply here, the second round of cancellations is more subtle. Consider then substituting in the required interchange MHV amplitudes into (7.40) and removing all vanishing coefficients of (6.45) and (7.42) that occur before the shift. There is an $l = \gamma$ term from $\tau^{\text{MHV}}(a^-, -K_1^-, \gamma^+, e^+)$ (see (6.44)) and similarly for the $d \leftrightarrow e$ case, along with the pole and PUP factors that survive. We are just reorganising the terms from

7.3 Complex factorisation for the 5-point case

equation (7.40), that we now label $C_{\text{grav}}^{\text{n-s f}}|_5^{\text{a,PUP}}$, to leave us with,

$$\begin{aligned}
C_{\text{grav}}^{\text{n-s f}}|_5^{\text{a,PUP}} &= \frac{-1}{(4\pi)^2} [bc]^4 \frac{s_{de}}{360} \\
&\times \left[\frac{\langle a|cb|a\rangle}{\langle ad\rangle\langle de\rangle\langle ea\rangle} \frac{\langle a|(b+c)d|a\rangle}{s_{ea}s_{bc}} - \frac{\langle a|cb|a\rangle}{\langle ad\rangle\langle de\rangle\langle ea\rangle} \frac{\langle a|(b+c)d|a\rangle[b|c+d|a\rangle\langle ac\rangle}{[bc]\langle a|(b+c)d|c\rangle^2} \right. \\
&\quad \left. - \frac{[d|\beta|a\rangle}{\langle de\rangle\langle ea\rangle} \frac{\langle a|(\beta+d)\gamma|a\rangle}{s_{\beta d}t_{\beta\gamma d}} + \frac{\langle ad\rangle\langle\gamma e\rangle}{\langle a\gamma\rangle\langle de\rangle} \frac{\langle\gamma a\rangle^2}{\langle\beta a\rangle^2} \tau^{\text{MHV}}(a^-, \beta^-, d^+, \gamma^+, e^+) \right] \\
&\times \left[\frac{\langle a|bc|a\rangle}{\langle ae\rangle\langle ed\rangle\langle da\rangle} \frac{\langle a|(b+c)e|a\rangle}{s_{da}s_{bc}} - \frac{\langle a|bc|a\rangle}{\langle ae\rangle\langle ed\rangle\langle da\rangle} \frac{\langle a|(b+c)e|a\rangle[b|c+e|a\rangle\langle ac\rangle}{[bc]\langle a|(b+c)e|c\rangle^2} \right. \\
&\quad \left. - \frac{[e|\theta|a\rangle}{\langle ed\rangle\langle da\rangle} \frac{\langle a|(\theta+e)\rho|a\rangle}{s_{\theta e}t_{\theta\rho e}} + \frac{\langle ae\rangle\langle\rho d\rangle}{\langle a\rho\rangle\langle ed\rangle} \frac{\langle\rho a\rangle^2}{\langle\theta a\rangle^2} \tau^{\text{MHV}}(a^-, \theta^-, e^+, \rho^+, d^+) \right] \quad (7.43)
\end{aligned}$$

where we expect the final cancellations to occur between terms two and three in each set of parentheses for any scaling of β (or θ). We now show the second round of cancellations more carefully, to highlight where a factor of two appears in the final answer. It is related to the fact that the two sub-leading factors coming from extracting the residue at the double poles in (7.37) are not $b \leftrightarrow c$ symmetric. Furthermore, we shall attach an arbitrary scale to the off shell vectors β and ρ to show the final answer is independent of their scaling. We take β to scale as $x\beta = 2b + c$, and θ to scale as $y\theta = 2c + b$, where x and y are arbitrary and $x\beta + \gamma = y\theta + \rho = b + c$. On the pole,

$$\begin{aligned}
\hat{\lambda}_b &= \hat{\lambda}_c \frac{\langle ab\rangle}{\langle ac\rangle}, & t_{\hat{\beta}\gamma k} &= t_{\hat{\theta}\rho k} = \frac{\langle a|(b+c)k|c\rangle}{\langle ac\rangle}, \\
s_{\hat{\beta}d} &= \frac{1}{x} \frac{\langle a|(2b+c)d|c\rangle}{\langle ac\rangle}, & s_{\hat{\theta}e} &= \frac{1}{y} \frac{\langle a|(2c+b)e|c\rangle}{\langle ac\rangle}, \quad (7.44)
\end{aligned}$$

7.3 Complex factorisation for the 5-point case

such that the PUP terms that survive after the shift can be expressed as,

$$\begin{aligned}
C_{\text{grav}}^{\text{n-sf}}|_5^{\text{a,PUP}} = & \frac{1}{(4\pi)^2} \frac{[bc]^3}{\langle bc \rangle} \frac{s_{de}}{360} \left[\frac{\langle a|bc|a \rangle}{\langle ae \rangle \langle ed \rangle \langle da \rangle} \frac{\langle a|(b+c)e|a \rangle \langle ac \rangle}{\langle a|(b+c)e|c \rangle} \right. \\
& \times \left(\frac{\langle a|cb|a \rangle}{\langle de \rangle \langle ea \rangle} \frac{[b|c+d|a] \langle ac \rangle}{[bc] \langle dc \rangle \langle a|(b+c)d|c \rangle} \right. \\
& - x \frac{[d|2b+c|a]}{\langle de \rangle \langle ea \rangle} \frac{\langle a|(b+c+d)(b[1-\frac{2}{x}] + c[1-\frac{1}{x}])}{\langle a|(2b+c)d|c \rangle \langle a|(b+c)d|c \rangle} |a \rangle \langle ac \rangle^2 \\
& + x \frac{\langle ad \rangle \langle ce \rangle}{\langle ac \rangle \langle de \rangle} \tau^{\text{MHV}}(a^-, c^-, d^+, c^+, e^+) \Big) \\
& + \frac{\langle a|cb|a \rangle}{\langle ad \rangle \langle de \rangle \langle ea \rangle} \frac{\langle a|(b+c)d|a \rangle \langle ac \rangle}{\langle a|(b+c)d|c \rangle} \left(\frac{\langle a|bc|a \rangle}{\langle ed \rangle \langle da \rangle} \frac{[b|c+e|a] \langle ac \rangle}{[bc] \langle ec \rangle \langle a|(b+c)e|c \rangle} \right. \\
& - y \frac{[e|2c+b|a]}{\langle ed \rangle \langle da \rangle} \frac{\langle a|(b+c+e)(b[1-\frac{2}{y}] + c[1-\frac{1}{y}])}{\langle a|(2c+b)e|c \rangle \langle a|(b+c)e|c \rangle} |a \rangle \langle ac \rangle^2 \\
& \left. \left. + y \frac{\langle ae \rangle \langle cd \rangle}{\langle ac \rangle \langle ed \rangle} \tau^{\text{MHV}}(a^-, c^-, e^+, c^+, d^+) \right) \right]
\end{aligned} \tag{7.45}$$

where $\lambda_\beta, \lambda_\gamma, \lambda_\theta, \lambda_\rho \rightarrow \lambda_c$ after the shift, was also applied in the on shell MHV amplitudes. This simplifies to,

$$\begin{aligned}
C_{\text{grav}}^{\text{n-sf}}|_5^{\text{a,PUP}} = & \frac{1}{(4\pi)^2} \frac{[bc]^3}{\langle bc \rangle} \frac{s_{de}}{360} \left[\frac{\langle a|bc|a \rangle \langle ac \rangle}{\langle ce \rangle \langle ed \rangle \langle da \rangle} \left(x \frac{\langle ad \rangle \langle ce \rangle}{\langle ac \rangle \langle de \rangle} \tau^{\text{MHV}}(a^-, c^-, d^+, c^+, e^+) \right. \right. \\
& + \frac{\langle ac \rangle^2 \langle ab \rangle}{\langle dc \rangle \langle de \rangle \langle ea \rangle} \frac{[b|c+d|a]}{\langle a|(b+c)d|c \rangle} - \frac{\langle a|bc+db[x-2]+dc[x-1]|a \rangle \langle ac \rangle^2}{\langle de \rangle \langle ea \rangle \langle dc \rangle \langle a|(b+c)d|c \rangle} \Big) \\
& + \frac{\langle a|cb|a \rangle \langle ac \rangle}{\langle cd \rangle \langle de \rangle \langle ea \rangle} \left(y \frac{\langle ae \rangle \langle cd \rangle}{\langle ac \rangle \langle ed \rangle} \tau^{\text{MHV}}(a^-, c^-, e^+, c^+, d^+) \right. \\
& \left. \left. + \frac{\langle ab \rangle \langle ac \rangle^2}{\langle ce \rangle \langle ed \rangle \langle da \rangle} \frac{[b|c+e|a]}{\langle a|(b+c)e|c \rangle} - \frac{\langle a|bc+eb[y-1]+ec[y-2]|a \rangle \langle ac \rangle^2}{\langle ed \rangle \langle da \rangle \langle ec \rangle \langle a|(b+c)e|c \rangle} \right) \right]
\end{aligned} \tag{7.46}$$

where we can pull out the required $[b|d|a]$ factor to leave an overall $[1-x]\langle a|d(b+c)|a \rangle$ factor. The left over piece indeed cancels against the second term in the parentheses.

7.3 Complex factorisation for the 5-point case

Also, we can pull out the required $[b|e|a\rangle$ factor in the second half, to leave an overall $[2-y]\langle a|e(b+c)|a\rangle$ factor. Again, the rest cancels against the corresponding second term in the final parentheses, which leaves us with,

$$\begin{aligned}
C_{\text{grav}}^{\text{n-s f}}|_5^{\text{a,PUP}} &= \frac{s_{de}}{(4\pi)^2} \frac{[bc]^3}{\langle bc \rangle} \frac{\langle a|bc|a \rangle}{360} \left[\frac{A_4^{\text{MHV}}(a^-, c^-, e^+, d^+)}{\langle ac \rangle^2} \times \right. \\
&\quad \left(x \frac{\langle ad \rangle \langle ce \rangle}{\langle ac \rangle \langle de \rangle} \tau^{\text{MHV}}(a^-, c^-, d^+, c^+, e^+) + (1-x) \frac{\langle a|d(b+c)|a \rangle \langle ac \rangle^2}{\langle de \rangle \langle ea \rangle \langle dc \rangle \langle a|(b+c)d|c \rangle} \right) \\
&\quad - \frac{A_4^{\text{MHV}}(a^-, c^-, d^+, e^+)}{\langle ac \rangle^2} \times \\
&\quad \left. \left(y \frac{\langle ae \rangle \langle cd \rangle}{\langle ac \rangle \langle ed \rangle} \tau^{\text{MHV}}(a^-, c^-, e^+, c^+, d^+) + (2-y) \frac{\langle a|e(b+c)|a \rangle \langle ac \rangle^2}{\langle ed \rangle \langle da \rangle \langle ec \rangle \langle a|(b+c)e|c \rangle} \right) \right]
\end{aligned} \tag{7.47}$$

The coefficients attached to $(1-x)$ and $(2-y)$ match the MHV amplitudes already expressed as scaling according to x or y respectively, up to a minus sign. Therefore the coefficients are $1+x-x$ and $2+y-y$, and the terms are independent of the scaling in x and y . We are left with the desired cross terms of MHV amplitudes as the result of the entire PUP contribution from (7.29)

$$\begin{aligned}
C_{\text{grav}}^{\text{n-s f}}|_5^{\text{a,PUP}} &= \frac{s_{de}}{(4\pi)^2} \frac{[bc]^3}{\langle bc \rangle} \frac{\langle a|bc|a \rangle}{360} \left[\frac{A_4^{\text{MHV}}(a^-, c^-, e^+, d^+)}{\langle ac \rangle^2} \frac{\langle ad \rangle \langle ce \rangle}{\langle ac \rangle \langle de \rangle} A^{\text{MHV}}(a^-, c^-, d^+, c^+, e^+) \right. \\
&\quad \left. - 2 \frac{A_4^{\text{MHV}}(a^-, c^-, d^+, e^+)}{\langle ac \rangle^2} \frac{\langle ae \rangle \langle cd \rangle}{\langle ac \rangle \langle ed \rangle} A^{\text{MHV}}(a^-, c^-, e^+, c^+, d^+) \right]
\end{aligned} \tag{7.48}$$

The cancellation highlights where the factor of two is needed to draw out the cancellation for the opposing interchange amplitude. Our terms; $C_{\text{grav}}^{\text{n-s f}}|_5^{\text{a,PUP}}$ together with $C_{\text{grav}}^{\text{n-s f}}|_5^b$ given by (7.28), correctly reproduces the entire PUP contribution to the 5-point pure gravity amplitude, as first found in [158], albeit in a more elegant form.

Hence the final expressions for the contributions to the 5-point gravity $C_{\text{grav}}^{\text{n-s f}}$, contain simple products of MHV tree amplitudes in pure Yang-Mills gauge theory. The

7.3 Complex factorisation for the 5-point case

MHV factors appearing are reminiscent of the Yang-Mills interchange amplitudes in (6.47), with different orderings of their arguments governed by the KLT relation. Exploring further, the products of the MHV amplitudes and their orderings, governed by the KLT relations are enough to determine the entire C_{grav}^{n-sf} up to multiplicative factors. This can be seen by a simple rewriting of the interchange amplitude 5-point result $C_{\text{grav}}^{n-sf}|_5^{\text{a,PUP}}$ for (7.48) to include the double pole contribution $C_{\text{grav}}^{n-sf}|_5^{\text{a,DP}}$ from (7.38) into one equation,

$$C_{\text{grav}}^{n-sf}|_5^{\text{a,DP}} + C_{\text{grav}}^{n-sf}|_5^{\text{a,PUP}} = \frac{s_{de}}{(4\pi)^2} \frac{[bc]^3}{\langle bc \rangle} \frac{\langle a|bc|a \rangle}{360} \left[\frac{\langle ac \rangle \langle ab \rangle}{\langle cb \rangle} - 2 \frac{\langle ac \rangle \langle ae \rangle}{\langle ce \rangle} + \frac{\langle ac \rangle \langle ad \rangle}{\langle cd \rangle} \right] \\ \times \frac{A_4^{\text{MHV}}(a^-, c^-, e^+, d^+)}{\langle ac \rangle^2} \frac{A_4^{\text{MHV}}(a^-, c^-, d^+, e^+)}{\langle ac \rangle^2}. \quad (7.49)$$

Given that the MHV factors have $n-1$ arguments, they can still be thought of as a direct descendant of the KLT ordering of the first term in (7.23) with multiplicative factors. That is provided that post shift: $\tau_n^{\text{YM}}(\dots, B^-, C^+, \dots) \rightarrow A_{n-1}^{\text{MHV}}(\dots, c^-, \dots)$. The second term in (7.23) can be directly translated to the ordering of the result $C_{\text{grav}}^{n-sf}|_5^b$ given by (7.28), provided that post shift: $\tau_n^{\text{YM}}(\dots, B^-, \dots, C^+, \dots) \rightarrow A_n^{\text{MHV}}(\dots, c^-, \dots, c^+, \dots)$. Hence we have the entire result for the five-point C_{grav}^{n-sf} in terms of on shell MHV amplitudes with multiplicative factors (see (7.49) and (7.28)). The orderings of their arguments can be linked to the original five-point KLT relation for the τ^{YM} currents in (7.23). This will become very useful when we wish to build an n -point complex factorisation $C_{\text{grav}}^{n-sf}|_n$.

Although the route to the expression (7.49) is fairly cumbersome and complicated, the cancellations between the majority of the terms hints at a lot of structure between the overall combinations of gauge theory amplitudes. The simplification of the results even before the BCFW shift from vanishing coefficients of (6.45) and (7.42) occurs for calculations for any n -leg graviton calculation, as we saw in the Yang-Mills version in Chapter 6. The factor of two was highlighted through the corresponding interchange amplitude required to cancel the sub-leading factor in (7.37) that was not $b \leftrightarrow c$ symmetric post shift. This will be brought up again later in the n -point calculations. Thus the form of the terms presented in (7.49) suggests that to n -point calculations there will be similarly compact terms.

7.4 Off shell MHV current with wandering a^- leg

For $n > 5$ -point the KLT expressions will include τ^{YM} factors where the a^- leg is separated from the massive legs. This needs addressing, since more diagrams contribute to the complex factorisation when the negative helicity leg is allowed to wander. We depart now from graviton scattering, to take a section to define the sum of diagrams required for the τ^{YM} currents with wandering negative helicity.

We extend the contribution of C^{n-sf} to include off shell currents where the a^- leg is allowed to wander. By this we mean considering a generalisation of the τ^{YM} current to a picture more like that of figure 6.1, albeit still an MHV current, where the shifted a^- leg can occur anywhere between the two off shell momenta. Considering the two types of diagrams we need from figure 6.5, the τ^{MHV} currents must generalise to wandering a^- also. This requires a generalisation of the MHV off shell current (6.28) under the constraint that the a^- leg is non-adjacent to P . The off shell MHV current we are interested in is

$$\frac{\tau^{\text{MHV}}(a^-, b^+ \dots f^+, P^-, g^+ \dots n^+)}{P^2 \langle Pa \rangle^2} \quad (7.50)$$

where the two sets of null legs $b \dots f$ and $g \dots n$ can be of any length, and again we are specialising to $\lambda_q = \lambda_a$. Decomposing P into two arbitrary null momenta k_1 and k_2 , We shift k_a and k_1 via a CSW approach to building the current recursively. Basing the shift on $\lambda_q = \lambda_a$,

$$\begin{aligned} \bar{\lambda}_a &\rightarrow \bar{\lambda}_a - z \bar{\lambda}_{k_1} \\ \lambda_{k_1} &\rightarrow \lambda_{k_1} + z \lambda_a \end{aligned} \quad (7.51)$$

avoids some spurious poles, and helps to keep the large z behaviour under control. Recalling the scheme for promoting null spinors to four-vector momentum from (3.47),

$$\lambda_P = P[q], \quad \bar{\lambda}_P = \frac{P|a\rangle}{[q|P|a]}, \quad (7.52)$$

we see that $\langle Pa \rangle$ remains unshifted, and we choose to set $\bar{\lambda}_q = \bar{\lambda}_{k_1}$.

There are factorisations when $P_{b_r+1 \dots a \dots b_l}^2 = 0$, shown in figure 7.2 across two breaks in momenta, that we choose to label from $b_r + 1$ up to b_l . These labels are incorporated

7.4 Off shell MHV current with wandering a^- leg

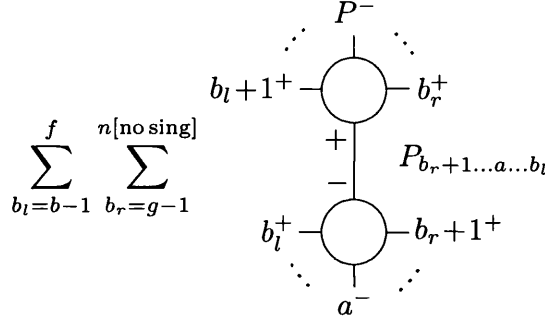


Figure 7.2: The set of diagrams for $\frac{\tau^{\text{MHV}}(a^-, b^+ \dots f^+, P^-, g^+ \dots n^+)}{P^2 \langle Pa \rangle^2}$

into a double sum over the possibilities for the left break b_l , and right break b_r . Thus the factorisations occur when,

$$\begin{aligned} P_{b_r+1\dots a\dots b_l}^2 &= z[k_1|P_{b_r+1\dots a\dots b_l}|a\rangle \\ \widehat{P_{b_r+1\dots a\dots b_l}} &= P_{b_r+1\dots a\dots b_l} - \frac{P_{b_r+1\dots a\dots b_l}^2}{[k_1|P_{b_r+1\dots a\dots b_l}|a\rangle} \end{aligned} \quad (7.53)$$

leading to an identical prescription for capping $P_{b_r+1\dots a\dots b_l}$ spinors using (7.52). The double sum over the possible break in momenta, includes the factorisation $\hat{P}^2 = 0$. The label [no sing] in the double sum denotes that both endpoints cannot allow for the a^- leg to be singled out as a lone factorisation, $\hat{k}_a^2 = 0$.

Applying the $[a, k_1]$ -shift and recursing on $\tau(a^-, b^+ \dots f^+, P^-, g^+ \dots n^+)/ (P^2 \langle Pa \rangle^2)$, we find

$$\begin{aligned} \frac{\tau(a^-, b^+ \dots f^+, P^-, g^+ \dots n^+)}{P^2 \langle Pa \rangle^2} &= \\ \sum_{b_l=b-1}^f \sum_{b_r=g-1}^{n[\text{no sing}]} &\frac{\tau^{\text{sm}}((b_l+1)^+ \dots f^+, P^-, g^+ \dots b_r^+, P_{b_r+1\dots a\dots b_l}^+)}{P^2 \langle Pa \rangle^2} \\ \times \frac{1}{P_{b_r+1\dots a\dots b_l}^2} &A^{\text{MHV}}(-P_{b_r+1\dots a\dots b_l}^-, (b_r+1)^+ \dots n^+, a^-, b^+ \dots b_l^+) \end{aligned} \quad (7.54)$$

7.4 Off shell MHV current with wandering a^- leg

which can be substituted for the explicit forms in terms of the null spinor for $P_{b_r+1\dots a\dots b_l}$,

$$\begin{aligned} \frac{\tau(a^-, b^+ \dots f^+, P^-, g^+ \dots n^+)}{P^2 \langle Pa \rangle^2} = & \sum_{b_l=b-1}^f \sum_{b_r=g-1}^{n[\text{no sing}]} \frac{1}{\langle ag \rangle \dots \langle b_r, P_{b_r+1\dots a\dots b_l} \rangle \langle P_{b_r+1\dots a\dots b_l}, b_l+1 \rangle \dots \langle fa \rangle} \\ & \times \frac{1}{P_{b_r+1\dots a\dots b_l}^2} \frac{\langle a, -P_{b_r+1\dots a\dots b_l} \rangle^4}{\langle ab \rangle \dots \langle b_l, -P_{b_r+1\dots a\dots b_l} \rangle \langle -P_{b_r+1\dots a\dots b_l}, b_r+1 \rangle \dots \langle na \rangle}. \end{aligned} \quad (7.55)$$

Now we can follow the capping procedure (7.52), to promote $P_{b_r+1\dots a\dots b_l}$ to a four-momentum,

$$\begin{aligned} \frac{\tau(a^-, b^+ \dots f^+, P^-, g^+ \dots n^+)}{P^2 \langle Pa \rangle^2} = & \sum_{b_l=b-1}^f \sum_{b_r=g-1}^{n[\text{no sing}]} \frac{1}{\langle ag \rangle \dots [k_1 | P_{b_r+1\dots a\dots b_l} | b_r] [k_1 | P_{b_r+1\dots a\dots b_l} | b_l+1] \dots \langle fa \rangle} \\ & \times \frac{1}{P_{b_r+1\dots a\dots b_l}^2} \frac{[k_1 | P_{b_r+1\dots a\dots b_l} | a]^4}{\langle ab \rangle \dots [k_1 | P_{b_r+1\dots a\dots b_l} | b_l] [k_1 | P_{b_r+1\dots a\dots b_l} | b_r+1] \dots \langle na \rangle}. \end{aligned} \quad (7.56)$$

Finally, the result organises itself over a common denominator where it must compensate in the numerator for the adjacent $\langle b_l, b_l+1 \rangle$ and similarly for the b_r terms. The wandering-minus current is now a compact expression for a double sum over the two breaks in momenta b_l and b_r ,

$$\begin{aligned} \frac{\tau^{\text{MHV}}(a^-, b^+ \dots f^+, P^-, g^+ \dots n^+)}{P^2 \langle Pa \rangle^2} = & \frac{1}{\langle ab \rangle \dots \langle fa \rangle \langle ag \rangle \dots \langle na \rangle} \sum_{b_l=b-1}^f \sum_{b_r=g-1}^{n[\text{no sing}]} \frac{1}{P_{b_r+1\dots a\dots b_l}^2} \\ & \times \frac{[k_1 | P_{b_r+1\dots a\dots b_l} | a]^4 \langle b_l, b_l+1 \rangle \langle b_r, b_r+1 \rangle}{[k_1 | P_{b_r+1\dots a\dots b_l} | b_r] [k_1 | P_{b_r+1\dots a\dots b_l} | b_l+1] [k_1 | P_{b_r+1\dots a\dots b_l} | b_l] [k_1 | P_{b_r+1\dots a\dots b_l} | b_r+1]}, \end{aligned} \quad (7.57)$$

that have special meaning for each end point. Specifically, when $b_l = b-1 \rightarrow a$ or $b_l = f+1 \rightarrow a$, by the prescriptions of employing $\lambda_g = \lambda_a$. Also, when $b_r = g-1 \rightarrow a$ or $b_r = n+1 \rightarrow a$ by the same arguments.

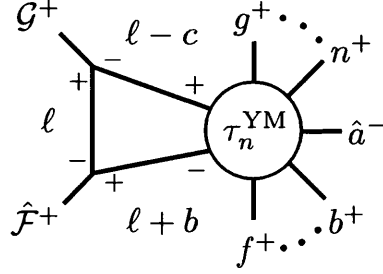


Figure 7.3: The set of diagrams required for the $C^{n-s\text{f}}$ where the negative helicity leg a^- is free to wander away from the off shell momenta B and C .

7.5 τ_n^{YM} with wandering-minus

Now that we have considered the a^- leg free to wander in the MHV current with P^- off shell (7.57), we can use it to build the contribution to the off shell diagrams τ_n^{YM} . The $C^{n-s\text{f}}$ that are interested in contains these off shell diagrams in the RHS of figure 7.3, which has the arguments,

$$\tau_n^{\text{YM}}(a^-, b^+ \dots f^+, B^-, C^+, g^+ \dots n^+) \quad (7.58)$$

where the two new null legs satisfy $\mathcal{F} + \mathcal{G} = B - C$. We have now denoted the two null legs on the LHS of the original loop as \mathcal{F}^+ and \mathcal{G}^+ rather than b^+ and c^+ to distinguish them from $(b^+ \dots f^+)$ and $(g^+ \dots n^+)$. Thus the off shell ℓ -dependent momenta in τ_n^{YM} are

$$\begin{aligned} B &= \ell + \mathcal{F}, \\ C &= \ell - \mathcal{G}, \end{aligned} \quad (7.59)$$

by momentum conservation. In general when we integrate, we use $B \rightarrow \frac{2}{3}\mathcal{F} + \frac{1}{3}\mathcal{G} \equiv \beta$ and $C \rightarrow \gamma$, where $B - C = \beta + \gamma$. Fortunately, after the $d^4\ell$ integral we can safely make these substitutions for B and C into β and γ .

Thus we need to compute the off shell current: $\tau_n(a^-, b^+ \dots f^+, \beta^-, \gamma^+, g^+ \dots n^+)$, which is the set of diagrams for the general off shell current to be fed in to the KLT relations (7.7). There are numerous cases for permutations of legs for wandering a^- where $n > 5$ -points is considered. Therefore we modify the set of diagrams from figure 6.5 to a set depending on the position of β . There are three distinct diagrammatic contributions for β off shell, that will require the sum of diagrams shown in figures 7.4,

7.5 and 7.6. The first includes β and γ linked in a three-vertex over a propagator in figure 7.4, and the latter two include the sets of diagrams with them separated in figures 7.5 and 7.6. These have directly incorporated the τ^{MHV} currents with wandering-minus leg from figure 7.2, that introduce a double sum over the breaks in momenta for all the required diagrams.

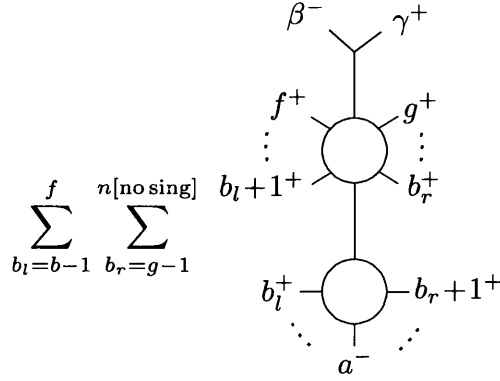


Figure 7.4: The first set of diagrams for $\tau(a^-, b^+ \dots f^+, \beta^-, \gamma^+, g^+ \dots n^+)$.

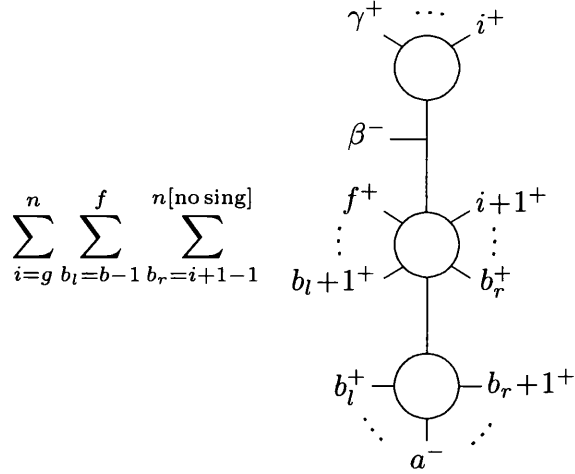


Figure 7.5: The second set of diagrams for $\tau(a^-, b^+ \dots f^+, \beta^-, \gamma^+, g^+ \dots n^+)$.

Going a step back from the three figures 7.4, 7.5 and 7.6, the contributions to $C^{n-s f}$

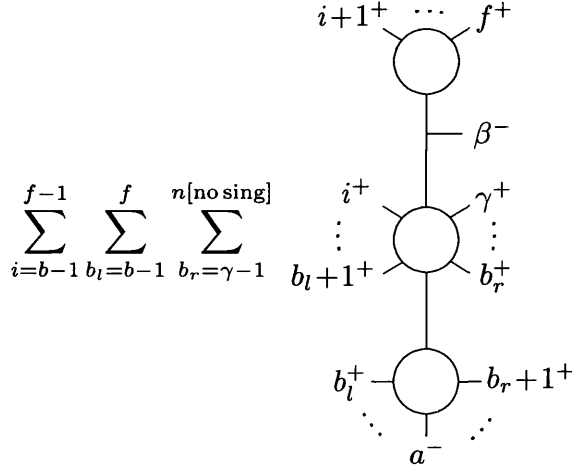


Figure 7.6: The third set of diagrams for $\tau(a^-, b^+ \dots f^+, \beta^-, \gamma^+, g^+ \dots n^+)$.

are the off shell MHV currents as written below,

$$\begin{aligned}
 C^{n-sf} = & -\frac{i}{32\pi^2} \frac{[\mathcal{FG}]}{\langle \mathcal{FG} \rangle} \left(\frac{\langle a|\beta P_{\mathcal{FG}}|a \rangle}{s_{\mathcal{FG}}} \frac{\tau^{\text{MHV}}(P_{\mathcal{FG}}^-, g^+ \dots n^+, a^-, b^+ \dots f^+)}{\langle P_{\mathcal{FG}} \rangle^2} \right. \\
 & + \sum_{i=g}^n \langle a|\beta P_{\gamma \dots i}|a \rangle \frac{\tau^{\text{sm}}(P_{\gamma \dots i}^-, \gamma^+, g^+ \dots i^+)}{P_{\gamma \dots i}^2 \langle P_{\gamma \dots i} a \rangle^2} \frac{\tau^{\text{MHV}}(P_{\beta \dots i}^-, (i+1)^+ \dots n^+, a^-, b^+ \dots f^+)}{P_{\beta \dots i}^2 \langle P_{\beta \dots i} a \rangle^2} \\
 & \left. + \sum_{i=b-1}^{f-1} \langle a|\beta P_{\gamma \dots i}|a \rangle \frac{\tau^{\text{sm}}(P_{\beta \dots i}^-, (i+1)^+, \dots f^+)}{P_{\beta \dots i}^2 \langle P_{\beta \dots i} a \rangle^2} \frac{\tau^{\text{MHV}}(P_{\gamma \dots i}^-, \gamma^+, g^+ \dots n^+, a^-, b^+ \dots i^+)}{P_{\gamma \dots i}^2 \langle P_{\gamma \dots i} a \rangle^2} \right) \quad (7.60)
 \end{aligned}$$

where we will use $[\mathcal{F}] \equiv [k_1]$ to nullify the massive momenta. This choice does not introduce bad pole behaviour since the recursion uses an $[a, \mathcal{F}]$ shift, where we are exposing the $\langle \hat{\mathcal{F}} \rangle$ double pole and sub-leading pole.

Using equation (7.57) we can write the form for the τ^{MHV} currents in equation (7.60) with the wandering-minus as the sum of the three figures 7.4, 7.5 and 7.6. Furthermore, once the τ^{sm} factors given by (6.27) are substituted in, an overall common denominator can still be pulled out, up to the $\langle i, i+1 \rangle / (\langle ia \rangle \langle a, i+1 \rangle)$ factors dependent on the sums over i in (7.60). The result is then in terms of double sums over the breaks in momenta,

to give us the full contribution to the non-standard factorisation,

$$\begin{aligned}
 C^{n-sf} = & -\frac{i}{32\pi^2} \frac{[\mathcal{F}\mathcal{G}]}{\langle \mathcal{F}\mathcal{G} \rangle} \frac{1}{\langle ab \rangle \cdots \langle fa \rangle \langle ag \rangle \cdots \langle na \rangle} \left(\langle a|\beta P_{\mathcal{F}\mathcal{G}}|a \rangle \sum_{b_l=b-1}^f \sum_{b_r=g-1}^{n[\text{no sing}]} \times \right. \\
 & \frac{1}{P_{b_r+1\dots a\dots b_l}^2} \frac{[\mathcal{F}|P_{b_r+1\dots a\dots b_l}|a\rangle^4 \langle b_l, b_l+1 \rangle \langle b_r, b_r+1 \rangle}{[\mathcal{F}|P_{b_r+1\dots a\dots b_l}|b_r\rangle [\mathcal{F}|P_{b_r+1\dots a\dots b_l}|b_l+1\rangle [\mathcal{F}|P_{b_r+1\dots a\dots b_l}|b_l\rangle [\mathcal{F}|P_{b_r+1\dots a\dots b_l}|b_r+1\rangle]} \\
 & - \sum_{i=g}^n \langle a|\beta P_{\gamma\dots i}|a \rangle \frac{\langle ag \rangle \langle a\gamma \rangle}{\langle \gamma g \rangle} \frac{\langle i, i+1 \rangle}{\langle ia \rangle \langle a, i+1 \rangle} \sum_{b_l=b-1}^f \sum_{b_r=i+1-1}^{n[\text{no sing}, *]} \times \\
 & \frac{1}{P_{b_r+1\dots a\dots b_l}^2} \frac{[\mathcal{F}|P_{b_r+1\dots a\dots b_l}|a\rangle^4 \langle b_l, b_l+1 \rangle \langle b_r, b_r+1 \rangle}{[\mathcal{F}|P_{b_r+1\dots a\dots b_l}|b_r\rangle [\mathcal{F}|P_{b_r+1\dots a\dots b_l}|b_l+1\rangle [\mathcal{F}|P_{b_r+1\dots a\dots b_l}|b_l\rangle [\mathcal{F}|P_{b_r+1\dots a\dots b_l}|b_r+1\rangle]} \\
 & - \sum_{i=b-1}^{f-1} \langle a|\beta P_{\gamma\dots i}|a \rangle \frac{\langle ag \rangle \langle a\gamma \rangle}{\langle \gamma g \rangle} \frac{\langle i, i+1 \rangle}{\langle ia \rangle \langle a, i+1 \rangle} \sum_{b_l=b-1}^i \sum_{b_r=\gamma-1}^{n[\text{no sing}, *]} \times \\
 & \left. \frac{1}{P_{b_r+1\dots a\dots b_l}^2} \frac{[\mathcal{F}|P_{b_r+1\dots a\dots b_l}|a\rangle^4 \langle b_l, b_l+1 \rangle \langle b_r, b_r+1 \rangle}{[\mathcal{F}|P_{b_r+1\dots a\dots b_l}|b_r\rangle [\mathcal{F}|P_{b_r+1\dots a\dots b_l}|b_l+1\rangle [\mathcal{F}|P_{b_r+1\dots a\dots b_l}|b_l\rangle [\mathcal{F}|P_{b_r+1\dots a\dots b_l}|b_r+1\rangle]} \right) \quad (7.61)
 \end{aligned}$$

This contains most of the terms that make up a diagrammatic consideration of the on shell MHV amplitude for the $\gamma \leftrightarrow g$ swap. Therefore (7.61) can be simplified by repeating a similar procedure to the specialised Yang-Mills case already considered by the substitutions (6.43) to organise the PUP contribution (6.44) in Chapter 6. We proceed by isolating all terms symmetric under the $\gamma \leftrightarrow g$ swap, that could be sucked into an interchange MHV amplitude, which reduces the remaining terms into three pieces. The first is the double pole term, from $b_l = f$, $b_r = g - 1$ in the first double sum, while the rest splits into two portions of which the first is symmetric, namely $Sym_{\gamma g}$, and lastly the non-symmetric portion that we identify as $\chi_{\gamma g}$.

The amplitude we are manipulating here is,

$$\begin{aligned}
 \frac{\langle \gamma a \rangle^2}{\langle \beta a \rangle^2} \tau^{\text{YM}}(a \dots, f, \beta, \gamma, g, h, \dots n) = & \frac{1}{\langle ab \rangle \cdots \langle fa \rangle \langle hi \rangle \cdots \langle na \rangle} \left(\right. \\
 & \frac{\langle a|\beta P_{\beta\gamma}|a\rangle [\mathcal{F}|P_{\beta\gamma}|a\rangle^2 \langle fa \rangle}{P_{\beta\gamma}^2 [\mathcal{F}|P_{\beta\gamma}|f\rangle [\mathcal{F}|P_{\beta\gamma}|g\rangle \langle gh \rangle]} + \chi_{\gamma g} + \frac{\langle a\gamma \rangle^2}{\langle a\gamma \rangle \langle \gamma g \rangle \langle gh \rangle} Sym_{\gamma g} \left. \right) \quad (7.62)
 \end{aligned}$$

where we would seek to replace $Sym_{\gamma g}$ with most of the terms of an interchange amplitude $\tau^{\text{YM}}(a \dots f, \beta, g, \gamma, h \dots n)$, up to a prefactor. However, after the rearrangement

into the form (7.62) and simplification of $\chi_{\gamma g}$, (which is presented in full in Appendix B) it was observed that $\text{Symm}_{\gamma g}$ vanishes. Therefore, a suitable rewriting of $\chi_{\gamma g}$ via the simplifications in Appendix B, provides all the PUP contribution to the complex factorisation with wandering a^- , as

$$\chi_{\gamma g} = \frac{\langle a\beta\rangle\langle a\gamma\rangle\langle ag\rangle\langle fa\rangle^2}{\langle f\beta\rangle\langle \gamma g\rangle\langle gf\rangle\langle gh\rangle} + \frac{\langle fa\rangle^3}{\langle gf\rangle\langle gh\rangle} \frac{[\mathcal{F}|\gamma|a]}{[\mathcal{F}|P_{\beta\gamma}|f]} \frac{\langle a\beta\rangle}{\langle \beta f\rangle} + \frac{\langle a\gamma\rangle\langle ag\rangle^2\langle fa\rangle}{\langle \gamma g\rangle\langle gf\rangle\langle gh\rangle} \frac{[\mathcal{F}|\beta|a]}{[\mathcal{F}|P_{\beta\gamma}|g]} \quad (7.63)$$

where some of the instances of momenta β and γ have been reduced to spinors in their nullified form, but we could still promote these back to their off shell momenta by capping with $[\mathcal{F}]$.

The form presented here for the entire contribution, repeated now for clarity is,

$$C^{\text{n-sf}} = -\frac{i}{32\pi^2} \frac{[\mathcal{F}\mathcal{G}]}{\langle \mathcal{F}\mathcal{G}\rangle} \frac{1}{\langle ab\rangle\cdots\langle ef\rangle} \frac{1}{\langle gh\rangle\cdots\langle na\rangle} \left(\frac{\langle a|\beta\gamma|a\rangle[\mathcal{F}|P_{\beta\gamma}|a]^2}{P_{\beta\gamma}^2[\mathcal{F}|P_{\beta\gamma}|f][\mathcal{F}|P_{\beta\gamma}|g]} \right. \\ \left. + \frac{\langle a\beta\rangle\langle a\gamma\rangle\langle ag\rangle\langle fa\rangle}{\langle f\beta\rangle\langle \gamma g\rangle\langle gf\rangle} + \frac{\langle fa\rangle^2}{\langle gf\rangle} \frac{[\mathcal{F}|\gamma|a]}{[\mathcal{F}|P_{\beta\gamma}|f]} \frac{\langle a\beta\rangle}{\langle \beta f\rangle} + \frac{\langle a\gamma\rangle\langle ag\rangle^2}{\langle \gamma g\rangle\langle gf\rangle} \frac{[\mathcal{F}|\beta|a]}{[\mathcal{F}|P_{\beta\gamma}|g]} \right) \quad (7.64)$$

Making the substitutions for β, γ in the double pole term, we can write the pure double pole contribution as,

$$C^{\text{n-sf}}|^{\text{DP}} = -\frac{i}{32\pi^2} \frac{[\mathcal{F}\mathcal{G}]}{\langle \mathcal{F}\mathcal{G}\rangle} \frac{1}{\langle ab\rangle\cdots\langle ef\rangle} \frac{1}{\langle gh\rangle\cdots\langle na\rangle} \frac{1}{3} \frac{\langle a|\mathcal{F}\mathcal{G}|a\rangle[\mathcal{F}|\mathcal{G}|a]^2}{s_{\mathcal{F}\mathcal{G}}[\mathcal{F}|\mathcal{G}|f][\mathcal{F}|\mathcal{G}|g]} \\ = -\frac{i}{32\pi^2} \frac{[\mathcal{F}\mathcal{G}]}{\langle \mathcal{F}\mathcal{G}\rangle} \frac{1}{\langle ab\rangle\cdots\langle ef\rangle} \frac{1}{\langle gh\rangle\cdots\langle na\rangle} \frac{1}{3} \frac{\langle a\mathcal{F}\rangle}{\langle \mathcal{G}\mathcal{F}\rangle} \frac{\langle \mathcal{G}a\rangle^3}{\langle \mathcal{G}f\rangle\langle \mathcal{G}g\rangle}. \quad (7.65)$$

We still want to express the single pole contribution in terms of the interchanged amplitudes when everything is evaluated on the pole. So when we apply the recursion machinery, the integrals from β contribute $\frac{2}{3}\mathcal{F} + \frac{1}{3}\mathcal{G}$. Recalling $\beta + \gamma = \mathcal{F} + \mathcal{G}$ then we have

$$\beta = \frac{2}{3}\mathcal{F} + \frac{1}{3}\mathcal{G}, \quad \gamma = \frac{1}{3}\mathcal{F} + \frac{2}{3}\mathcal{G}, \quad (7.66)$$

which can be traced back to the integrals over B and C respectively, that we saw first in Chapter 6. The results of the integrals there were all of the form $\frac{1}{3}[X|2\mathcal{F} + \mathcal{G}|a\rangle$. Now we have generalised to the wandering-minus case, there are now cases where an integration over C has yielded terms with $\frac{1}{3}[Y|\mathcal{F} + 2\mathcal{G}|a\rangle$ too. Therefore the BCFW-shift specific form for the single pole contribution,

$$C^{\text{n-s f}}|^{\text{SP}} = -\frac{i}{32\pi^2} \frac{[\mathcal{F}\mathcal{G}]}{\langle\mathcal{F}\mathcal{G}\rangle} \frac{1}{\langle ab\rangle \cdots \langle ef\rangle} \frac{1}{\langle gh\rangle \cdots \langle na\rangle} \left(\frac{\langle a\beta\rangle\langle a\gamma\rangle\langle ag\rangle\langle fa\rangle}{\langle f\beta\rangle\langle \gamma g\rangle\langle gf\rangle} + \frac{\langle fa\rangle^2}{\langle gf\rangle} \frac{[\mathcal{F}|\gamma|a\rangle}{[\mathcal{F}|P_{\beta\gamma}|f\rangle]} \frac{\langle a\beta\rangle}{\langle \beta f\rangle} + \frac{\langle a\gamma\rangle\langle ag\rangle^2}{\langle \gamma g\rangle\langle gf\rangle} \frac{[\mathcal{F}|\beta|a\rangle}{[\mathcal{F}|P_{\beta\gamma}|g\rangle]} \right) \quad (7.67)$$

becomes

$$C^{\text{n-s f}}|^{\text{SP}} = -\frac{i}{32\pi^2} \frac{[\mathcal{F}\mathcal{G}]}{\langle\mathcal{F}\mathcal{G}\rangle} \frac{1}{\langle ab\rangle \cdots \langle ef\rangle} \frac{1}{\langle gh\rangle \cdots \langle na\rangle} \left(\frac{\langle a\beta\rangle\langle a\gamma\rangle\langle ag\rangle\langle fa\rangle}{\langle f\beta\rangle\langle \gamma g\rangle\langle gf\rangle} + \frac{2}{3} \frac{\langle fa\rangle^2}{\langle gf\rangle} \frac{\langle \mathcal{G}a\rangle}{\langle \mathcal{G}f\rangle} \frac{\langle a\beta\rangle}{\langle \beta f\rangle} + \frac{1}{3} \frac{\langle a\gamma\rangle\langle ag\rangle^2}{\langle \gamma g\rangle\langle gf\rangle} \frac{\langle \mathcal{G}a\rangle}{\langle \mathcal{G}g\rangle} \right). \quad (7.68)$$

While on the pole, $\lambda_\beta, \lambda_\gamma \rightarrow \lambda_\mathcal{G}$, leading to

$$C^{\text{n-s f}}|^{\text{SP}} = -\frac{i}{32\pi^2} \frac{[\mathcal{F}\mathcal{G}]}{\langle\mathcal{F}\mathcal{G}\rangle} \frac{1}{\langle ab\rangle \cdots \langle ef\rangle} \frac{\langle a\mathcal{G}\rangle^2}{\langle gh\rangle \cdots \langle na\rangle} \times \left(\frac{\langle ag\rangle\langle fa\rangle}{\langle f\mathcal{G}\rangle\langle \mathcal{G}g\rangle\langle gf\rangle} - \frac{2}{3} \frac{\langle fa\rangle^2}{\langle \mathcal{G}f\rangle^2\langle gf\rangle} - \frac{1}{3} \frac{\langle ag\rangle^2}{\langle \mathcal{G}g\rangle^2\langle gf\rangle} \right), \quad (7.69)$$

with a clever Schouten identity between the remaining terms we are left with

$$C^{\text{n-s f}}|^{\text{SP}} = -\frac{i}{32\pi^2} \frac{[\mathcal{F}\mathcal{G}]}{\langle\mathcal{F}\mathcal{G}\rangle} \frac{1}{\langle ab\rangle \cdots \langle ef\rangle} \frac{\langle a\mathcal{G}\rangle^3}{\langle gh\rangle \cdots \langle na\rangle} \left(\frac{2}{3} \frac{\langle af\rangle}{\langle \mathcal{G}f\rangle^2\langle \mathcal{G}g\rangle} - \frac{1}{3} \frac{\langle ag\rangle}{\langle \mathcal{G}g\rangle^2\langle \mathcal{G}f\rangle} \right) \quad (7.70)$$

which in terms of interchange MHV amplitudes, can be written

$$C^{n-sf}|^{\text{SP}} = -\frac{i}{32\pi^2} \frac{[\mathcal{FG}]}{\langle \mathcal{FG} \rangle} \left(\frac{2}{3} \frac{\langle \mathcal{G}e \rangle \langle af \rangle}{\langle ef \rangle \langle a\mathcal{G} \rangle} A(\dots, e, \mathcal{G}, f, \mathcal{G}, g, \dots) \right. \\ \left. - \frac{1}{3} \frac{\langle \mathcal{G}h \rangle \langle ag \rangle}{\langle gh \rangle \langle a\mathcal{G} \rangle} A(\dots, f, \mathcal{G}, g, \mathcal{G}, h, \dots) \right). \quad (7.71)$$

Furthermore, along with the result for the double pole contribution (7.65), the entire contribution of the non-standard factorisation with a wandering a^- can be expressed in terms of one MHV amplitude,

$$C^{n-sf} = -\frac{i}{96\pi^2} \frac{[\mathcal{FG}]}{\langle \mathcal{FG} \rangle} \frac{A^{\text{MHV}}(a^- \dots e^+, f^+, \mathcal{G}^-, g^+, h^+ \dots n^+)}{\langle a\mathcal{G} \rangle} \left(\frac{\langle a\mathcal{F} \rangle}{\langle \mathcal{G}\mathcal{F} \rangle} + 2 \frac{\langle af \rangle}{\langle \mathcal{G}f \rangle} - \frac{\langle ag \rangle}{\langle \mathcal{G}g \rangle} \right) \quad (7.72)$$

where the contribution is evaluated on the residue $\langle \hat{\mathcal{F}}\mathcal{G} \rangle \rightarrow 0$. The only shifted variables affected are the two instances of \mathcal{F} 's in the denominator of (7.72), leaving us the n -point wandering-minus solution for Yang-Mills,

$$\text{Res} \left(\frac{1}{z} C^{n-sf}(\hat{a}^-, b^+, \dots, f^+, \hat{\mathcal{F}}^+, \mathcal{G}^+, g^+, \dots, n^+) \right) \Big|_{\langle \hat{\mathcal{F}}\mathcal{G} \rangle=0} \\ = -\frac{i}{96\pi^2} \frac{[\mathcal{FG}]}{\langle \mathcal{FG} \rangle} \frac{A^{\text{MHV}}(a^- \dots e^+, f^+, \mathcal{G}^-, g^+, h^+ \dots n^+)}{\langle a\mathcal{G} \rangle} \left(\frac{\langle a\mathcal{F} \rangle}{\langle \mathcal{F}\mathcal{G} \rangle} - 2 \frac{\langle af \rangle}{\langle \mathcal{G}f \rangle} + \frac{\langle ag \rangle}{\langle \mathcal{G}g \rangle} \right) \quad (7.73)$$

in terms of one MHV amplitude. For the set of legs $b^+ \dots f^+$ missing, $-2 \frac{\langle af \rangle}{\langle \mathcal{G}f \rangle}$ vanishes and (7.73) agrees with the Bern et al result [102]. Notice that the factor of 2 that surfaced from the cancellations in the 5-point gravity amplitude (7.48) can be traced back to an insertion of the more generalised Yang-Mills off shell current derived above. The form of the current (7.72) lends itself to direct insertion into the KLT expressions, albeit with different numerical factors from integration. Indeed, if you substitute in the products of Yang-Mills currents from (7.72) according to the first term of the KLT form for $C_{\text{grav}}^{n-sf}|_5^a$ in (7.23), the form expressed in (7.49) readily drops out, up to factors that come from integration. The full analytic derivation of the tedious simplification of $\chi_{\gamma g}$

along with the terms contained in $Symm_{\gamma g}$ (that is a complicated way of expressing zero), is an extreme example of finding underlying structure for the wandering-minus current with off shell β . Hence the relegation to the Appendix B of the details, while the final answer yields a simple structure. Hence we have a powerful tool to utilise the KLT relations to build the contributions to $C_{\text{grav}}^{n-s f}$ to complete the modified recursion relation for the one-loop single-minus graviton amplitudes.

7.6 The n -point complex factorisation: $C_{\text{grav}}^{n-s f}$

Now we consider the contributions to the complex factorisations in graviton scattering, according to the n -point $C_{\text{grav}}^{n-s f}$ from (7.5), that we recall now,

$$C_{\text{grav}}^{n-s f} = \int d^d \ell \left(\frac{[b|\ell|a][c|\ell|a] \langle Ca \rangle^2}{\langle ba \rangle \langle ca \rangle \langle Ba \rangle^2} \right)^2 \frac{\tau_n^{\text{grav}}(a^-, B^-, C^+, d^+, \dots, n^+)}{\ell^2 B^2 C^2} \quad (7.74)$$

to complete the calculation via the usual shift and extraction of the residue on the pole $\langle \hat{b}c \rangle \rightarrow 0$.

Substituting τ^{grav} (using the KLT relations), for products of gauge theory off shell currents, now armed with the wandering-minus Yang-Mills current (7.72) makes the process much simpler than ever before.

7.6.1 Employing the KLT relation

The n -point KLT relations (4.25) are reexpressed as in (7.7), re-using $B + C = b + c$ for the off shell legs,

$$\begin{aligned} \tau_n^{\text{grav}}(B, C, \dots, n, a) &= i(-1)^{n+1} \left[\tau_n^{\text{YM}}(B, C, \dots, n, a) \sum_{\mathcal{P}_1, \mathcal{P}_2} f(i_1, \dots, i_k) \bar{f}(j_1, \dots, j_{k'}) \right. \\ &\quad \left. \times \tau_n^{\text{YM}}(i_1, \dots, i_k, B, n, j_1, \dots, j_{k'}, a) \right] \\ &\quad + \mathcal{P}_{\text{KLT}}(C, d, \dots, n-1), \end{aligned} \quad (7.75)$$

where the permutations $\mathcal{P}_1, \mathcal{P}_2$ over lists i and j respectively, along with the permutation \mathcal{P}_{KLT} obey the same rules as defined by (7.7). The functions f and \bar{f} are given

by

$$\begin{aligned} f(i_1, \dots, i_k; B) &= s(B, i_k) \prod_{m=1}^{k-1} \left(s(B, i_m) + \sum_{p=m+1}^k g(i_m, i_p) \right) \\ \bar{f}(j_1, \dots, j_{k'}) &= s(j_1, n) \prod_{m=2}^{k'} \left(s(j_m, n) + \sum_{p=1}^{m-1} g(l_p, l_m) \right) \end{aligned} \quad (7.76)$$

where we have made B an explicit argument of f , and

$$g(i, j) = \begin{cases} s(i, j) \equiv s_{ij}, & i > j, \\ 0, & \text{otherwise,} \end{cases} \quad (7.77)$$

where we marked out B as the special leg to appear as the first argument in the super-gravity amplitude. This ensures that one of the gauge theory amplitudes $A(\dots, i_k, B, \dots)$ comes with a s_{Bi_k} factor, such that when $i_k = C$, the pole in the amplitude is cancelled by the corresponding momentum invariant. Therefore, there is only a true pole in the τ^{grav} expression for the terms where there is an explicit pole in the other gauge theory amplitude. This will provide the necessary singular structure for the off shell currents split across three cases.

7.6.2 Terms including a double pole

Firstly, there are terms that will appear of the form,

$$\tau_n^{\text{YM}}(\dots d^+, C^+, B^-, e^+ \dots) \tau_n^{\text{YM}}(\dots, f^+, B^-, C^+, g^+, \dots) s_{BC} s_{xy} (s_{Bw} + s_{Cw}) \quad (7.78)$$

where each τ_n^{YM} factor contains an s_{bc} pole in one of its terms, and null legs w, x, y are arbitrary. When combined with the pole from the loop integration, this leading term would yield a triple pole, but that is counteracted by the explicit s_{BC} above. Thus we shall redefine the leading f function to remove the explicit s_{BC} pole in the following

way,

$$f^{\text{lead}}(i_1, \dots, i_k; B) = \prod_{m=1}^{k-1} \left(s(B, i_m) + \sum_{p=m+1}^j g(i_m, i_p) \right) \quad (7.79)$$

Furthermore, in the limit of $\ell^2 \rightarrow 0$, all instances of the latter factor inside the parentheses in (7.78) reduce to $[w|b + c|w]$. The ℓ -dependence only appears in the leading τ^{YM} factors as in (7.29), therefore the loop integral result for these terms is always the special case (7.32). Factors of B and C can immediately be replaced with β and γ respectively, such that we can utilise the Yang-Mills result with wandering-minus current (7.72). We can then immediately write down the contribution to $C_{\text{grav}}^{n-s f}$ from cases such as (7.78), that we denote with a ,

$$\begin{aligned} C_{\text{grav}}^{n-s f} |^a &= \frac{(-1)^{n_i} [bc]^3}{(4\pi)^2 \langle bc \rangle} s_{bc} \frac{A_{n-1}^{\text{MHV}}(a^-, \dots, d^+, c^-, e^+, \dots)}{\langle ca \rangle} \left(\frac{\langle ab \rangle}{\langle cb \rangle} + 2 \frac{\langle ae \rangle}{\langle ce \rangle} - \frac{\langle ad \rangle}{\langle cd \rangle} \right) \\ &\times \frac{A_{n-1}^{\text{MHV}}(a^-, \dots, f^+, c^-, g^+, \dots)}{\langle ca \rangle} \left(\frac{\langle ab \rangle}{\langle cb \rangle} + 2 \frac{\langle af \rangle}{\langle cf \rangle} - \frac{\langle ag \rangle}{\langle cg \rangle} \right) \\ &\times \frac{f^{\text{lead}}(c, \dots, n/2; b) \bar{f}(n/2 + 1, \dots, n-1)}{360} \end{aligned} \quad (7.80)$$

where we have used the wandering-minus solution (7.72), and f^{lead} highlights the inclusion of null legs b and c . From this position it becomes much easier to see the mixture of leading and sub-leading poles coming from each Yang-Mills current, that was studied at five-point extensively already (7.29)-(7.49). Thus from terms of type $C_{\text{grav}}^{n-s f} |^a$, we can expand the two leading $1/\langle bc \rangle$ terms to create the double pole term that we shall denote $C_{\text{grav}}^{n-s f} |^{DP}$. The cross terms between the leading $1/\langle bc \rangle$ term from one current and the two terms from the other in (7.80) yields a total of four possible combinations for the sub-leading terms. These shall be labelled of the type $C_{\text{grav}}^{n-s f} |^{PUP, a}$ that shall be dealt with later. Hence, we can consider *all* the double pole terms directly from the KLT relation (7.75) for the choice of leg $i_k = C$, and restricting all currents (7.72) to

the leading $1/\langle bc \rangle$ terms from (7.80) only,

$$\begin{aligned}
 C_{\text{grav}}^{\text{n-s f}} \Big|^{DP} &= \frac{i(-1)^{n+1} - 1}{(4\pi)^2} \frac{[bc]^4 \langle ab \rangle^2}{360 \langle bc \rangle^2 \langle ac \rangle^2} \times \\
 &\quad \left[A_{n-1}(c^-, d^+, \dots, n^+, a^-) \sum_{\mathcal{P}_3, \mathcal{P}_2} f^{\text{lead}}(i_1, \dots, i_k, c; b) \bar{f}(j_1, \dots, j_{k'}) \right. \\
 &\quad \left. \times A_{n-1}(i_1, \dots, i_k, c^-, n, j_1, \dots, j_{k'}, a^-) \right] + \mathcal{P}_{\text{KLT}}(d, e, \dots, n-1), \tag{7.81}
 \end{aligned}$$

and all amplitudes are on shell. Now, \mathcal{P}_3 are $(i_1, \dots, i_k) \in \mathcal{P}_3(d, e, \dots, n/2)$, with $k = n/2 - 2$, highlighting the permutations are over a list one element shorter to distinguish it from \mathcal{P}_1 in (7.7). $(j_1, \dots, j_{k'}) \in \mathcal{P}_2(n/2 + 1, \dots, n-1)$, with $j' = n/2 - 2$, as before, giving a total of $(n/2 - 2)! \times (n/2 - 2)!$ terms in the square brackets.

For example, taking $n = 5$, the list (i_1, \dots, i_k) is empty, while $(j_1, \dots, j_{k'})$ admits just d^+ . Thus $f^{\text{lead}} = 1$ and $\bar{f} = s_{de}$, to give us the single term in the square brackets, that is the entire double pole contribution from (7.38),

$$C_{\text{grav}}^{\text{n-s f}} \Big|_5^{DP} = \frac{i}{(4\pi)^2} \frac{-1}{360} \frac{[bc]^4 \langle ab \rangle^2}{\langle bc \rangle^2 \langle ac \rangle^2} s_{de} A_4(c^-, d^+, e^+, a^-) A_4(c^-, e^+, d^+, a^-) \tag{7.82}$$

7.6.3 Applying BCFW shift to double pole terms

In this setup, there are no longer sub-leading terms generated on evaluation of the residue on double pole terms (7.81). Schematically, the only terms affected by the shift other than the double pole, are those appearing in f or \bar{f} ,

$$\text{Res} \left(\frac{1}{z} C_{\text{grav}}^{\text{n-s f}} \Big|^{DP} \left(\frac{s_{bx} + s_{cx}}{\langle \hat{bc} \rangle^2} \right) \right)_{\langle \hat{bc} \rangle \rightarrow 0} = C_{\text{grav}}^{\text{n-s f}} \Big|^{DP} \left(- \frac{s_{bx} + s_{cx}}{\langle bc \rangle^2} \right) \tag{7.83}$$

Therefore the double pole contribution to the n -point non-standard factorisation, after

the shift is

$$\begin{aligned} \widehat{C_{\text{grav}}^{n-s f}} \Big|^{DP} &= \frac{i(-1)^{n+1}}{(4\pi)^2} \frac{1}{360} \frac{[bc]^4}{\langle bc \rangle^2} \frac{\langle ab \rangle^2}{\langle ac \rangle^2} \times \\ &\quad \left[A_{n-1}(c^-, d^+, \dots, n^+, a^-) \sum_{\mathcal{P}_3, \mathcal{P}_2} f^{\text{lead}}(i_1, \dots, i_k, c; b) \bar{f}(j_1, \dots, j_{k'}) \right. \\ &\quad \left. \times A_{n-1}(i_1, \dots, i_k, c^-, n, j_1, \dots, j_{k'}, a^-) \right] + \mathcal{P}_{\text{KLT}}(d, e, \dots, n-1), \end{aligned} \quad (7.84)$$

where f^{lead} is defined in (7.79), and the permutations $\mathcal{P}_3, \mathcal{P}_2$ were defined for the lists i and j in (7.81). Recall this is only the ordering for one particular factorisation, namely the diagram presented in figure 7.1. Therefore all double pole terms must include a final sum over the factorisation diagrams, that from the figure are permutations of $\mathcal{P}_D(c \in c, \dots, n)$.

7.6.4 PUP contributions: class a

The PUP contributions that we labelled $C_{\text{grav}}^{n-s f} \Big|^{PUP, a}$ from (7.80) only appear from cross terms, as we showed in the 5-point case, see (7.29)-(7.49). Notice that there is no preference of the position of the a^- leg in the MHV amplitudes, and for any instance that legs B or C are adjacent to a^- , the corresponding factors that give $\langle aa \rangle$ in the wandering-minus factors from (7.80) vanish. Therefore, for the form of the KLT relation presented (7.7), one of the four possible combinations of sub-leading factors vanishes from $C_{\text{grav}}^{n-s f} \Big|^{PUP, a}$ due to B adjacent to a at all times. Thus the entire PUP contribution from the case where legs B and C are adjacent in both Yang-Mills currents

from (7.80) is,

$$\begin{aligned}
 C_{\text{grav}}^{n-s f} \Big|^{PUP,a} &= \frac{i(-1)^n - 1}{(4\pi)^2} \frac{[bc]^4}{360} \frac{\langle ab \rangle}{\langle bc \rangle} \frac{\langle ab \rangle}{\langle ac \rangle} \times \\
 &\quad \left[A_{n-1}(c_1^-, d^+, \dots, n^+, a^-) \sum_{\mathcal{P}_3, \mathcal{P}_2} \left(f^{\text{lead}}(i_1, \dots, i_k, c; b) \bar{f}(j_1, \dots, j_{k'}) \right. \right. \\
 &\quad \times A_{n-1}(i_1, \dots, i_k, c_2^-, n, j_1, \dots, j_{k'}, a^-) \\
 &\quad \times \left. \left(2 \frac{\langle a, i_k \rangle}{\langle c_2, i_k \rangle} - \frac{\langle a, c_1 + 1 \rangle}{\langle c_1, c_1 + 1 \rangle} - \frac{\langle an \rangle}{\langle c_2 n \rangle} \right) \right) + \mathcal{P}_{\text{KLT}}(d, e, \dots, n-1), \Big]
 \end{aligned} \tag{7.85}$$

where we have stripped out the leading s_{bc} pole from f and written f^{lead} from (7.79). Again, $\mathcal{P}_3, \mathcal{P}_2$ permutations are one element shorter than normal, with $k = n/2 - 2$, $k' = n/2 - 2$, to reflect the MHV amplitudes contain $(n-1)$ arguments. Numerical labels for legs c_1^- and c_2^- are to distinguish which MHV amplitude has the factors such as $\langle c_2, i_k \rangle$ to be included in the permutation \mathcal{P}_3 , for example.

7.6.5 PUP contributions: class b

The second case of the type of term that contributes to $C_{\text{grav}}^{n-s f} \Big|^{PUP}$ occurs when one of the gauge theory amplitudes permits a permutation of legs where B and C are separated, but preserves B adjacent to C in the other gauge theory amplitude,

$$\tau_n^{\text{YM}}(\dots, f^+, B^-, g^+, \dots, h^+, C^+, i^+, \dots) \tau_n^{\text{YM}}(\dots d^+, B^-, C^+, e^+ \dots) s_{BC} s_{xy} s_{Bw} s_{Cz}. \tag{7.86}$$

Where a factor of s_{BC} comes from f again, and legs w, x, y, z are arbitrary. In this case, the currents are all part of the sub-leading PUP contributions, due to the explicit s_{BC} . Thus we only require the leading pole term from the wandering-minus solution (7.72) for the second gauge theory amplitude. However we need to include the Feynman parametrisation of the loop momenta to complete integrals of the type seen in (7.14). The other gauge theory amplitude can be replaced by an on shell MHV, once the

ℓ -dependence has been removed, recalling

$$\frac{\langle CX \rangle}{\langle Ca \rangle} = \frac{\langle CX \rangle}{\langle Ca \rangle} \frac{\langle ca \rangle}{\langle ca \rangle} \rightarrow \frac{\langle cX \rangle}{\langle ca \rangle} + \mathcal{O}(\langle bc \rangle), \quad (7.87)$$

and its corresponding result for B . Thus to order $1/\langle bc \rangle$, the currents can be written independently of the loop momenta, providing we supplement the integrals with $(x_2 x_3)$ from the LHS of the loop, multiplied by a $(1 - x_2 - x_3)$ factor from the wandering-minus current where B and C are adjacent, (see Appendix A.2.2 for full details on this type of integral). The remaining integration comes from the s_{Bw} and s_{Cz} factors once expanded in terms of the new parameters. Remembering from the 5-point case that on the pole, we can substitute $\hat{\lambda}_b = \frac{\langle ba \rangle}{\langle ca \rangle} \lambda_c$ inside the MHV amplitudes to leave

$$\begin{aligned} C_{\text{grav}}^{n-sf} \Big|^{PUP,b} &= \frac{-i}{(4\pi)^2} \frac{[bc]^3}{\langle bc \rangle} \frac{s_{bc}}{\langle ca \rangle} A_n^{\text{MHV}}(a^-, \dots, c^-, \dots, c^+, \dots) A_{n-1}^{\text{MHV}}(a^- \dots d^+, c^-, e^+ \dots) \\ &\times \frac{\langle ab \rangle}{\langle cb \rangle} \int_0^1 dx_2 \int_0^{1-x_2} dx_3 x_2 x_3 (1 - x_2 - x_3) \left((1 - x_2) s_{bw} + x_3 s_{cw} \right) \left(x_2 s_{bz} + (1 - x_3) s_{cz} \right) \end{aligned} \quad (7.88)$$

where the remaining integral is not so different from (7.14).

So for any term of the KLT expression of the form (7.86) that we have highlighted one example of, the integrals over the new parameters in f, \bar{f} become important. We have already dealt with these kinds of integrals by defining the expansion of f, \bar{f} according to (7.18) and (7.19) for the substitutions of B and C in (7.20). We present the KLT terms in terms of either MHV amplitudes with n legs where B and C were separated in τ^{YM} , or MHV amplitudes with $(n - 1)$ legs where B and C were adjacent, giving a pole term, $1/\langle bc \rangle$. The two cases also include sums of Gamma functions involved from the functions f, \bar{f} , which are modified by one integer in the Gamma function in the denominator due to the extra $(1 - x_2 - x_3)$ factor.

Terms of the form (7.88), then fall into two categories when trying to present them in the form of the KLT relations (7.7). Firstly, the Yang-Mills current with B non-adjacent to C can occur for some permutation of the KLT relation \mathcal{P}_{KLT} for the first τ^{YM} term, that we shall group into $C_{\text{grav}}^{n-sf} \Big|^{PUP,b_1}$ contributions. Secondly, The Yang-Mills current with B non-adjacent to C can occur for some permutation of the inner sum over \mathcal{P}_1 for the second τ^{YM} term, that we shall group into $C_{\text{grav}}^{n-sf} \Big|^{PUP,b_2}$ contributions. The first case in the KLT relations can be isolated by choosing $i_k = C$, to shorten

the permutation list from $\mathcal{P}_1 \rightarrow \mathcal{P}_3$ as we have seen before in the double pole case. Here however, we still need to include all permutations over the positive helicity legs in \mathcal{P}_{KLT} ,

$$\begin{aligned}
 C_{\text{grav}}^{n-s f} \big|^{PUP, b_1} &= \frac{i(-1)^{n+1}}{(4\pi)^2} \frac{[bc]^3}{\langle bc \rangle} \frac{\langle a|bc|a \rangle}{\langle ca \rangle^2} \left[A_n(c^-; c^+, d^+ \dots, (n-1)^+; n^+, a^-) \right. \\
 &\sum_{\mathcal{P}_3, \mathcal{P}_2} \left(\sum_{i, j, k=b, c} \sum_{p_i, k, q_j, k} \frac{\Gamma(2+p_i+p_k)\Gamma(2+q_j+q_k)}{\Gamma(6+p_i+p_k+q_j+q_k)} f^{\text{lead}}(\dots i; j) \bar{f}(\dots k \dots) \right. \\
 &\quad \left. \times A_{n-1}(i_1, \dots, i_k, c^-, n^+, j_1, \dots, j_{k'}, a^-) \right) + \mathcal{P}_{\text{KLT}}(c^+, d^+, \dots, (n-1)^+) \Big],
 \end{aligned} \tag{7.89}$$

where $f^{\text{lead}}(\dots, i; j)$ appears in (7.79), and $\mathcal{P}_3, \mathcal{P}_2$ are the same as they were defined for (7.81). The sums over the coefficients p_i, q_i for the Gamma functions come from the definitions of (7.19) from the substitution of (7.20). Any permutation over $\mathcal{P}_{\text{KLT}}(c^+, d^+, \dots, (n-1)^+)$ that puts c^-, c^+ adjacent in the first MHV amplitude we set to zero, as it was dealt with in the double pole cases.

The second case in the KLT relations for B and C adjacent in the first τ^{YM} current we can take from the first overall KLT permutation, thus there is no \mathcal{P}_{KLT} required. The sum over $\mathcal{P}_1, \mathcal{P}_2$ continues as normal, but again we send any terms where $A_n(\dots, c^-, c^+, \dots) \rightarrow 0$ as they are dealt with in the double pole terms. So we have for the second case of type b_2 ,

$$\begin{aligned}
 C_{\text{grav}}^{n-s f} \big|^{PUP, b_2} &= \frac{i(-1)^{n+1}}{(4\pi)^2} \frac{[bc]^3}{\langle bc \rangle} \frac{\langle a|bc|a \rangle}{\langle ca \rangle^2} A_{n-1}(c^-, d^+ \dots, n^+, a^-) \\
 &\sum_{\mathcal{P}_1, \mathcal{P}_2} \left(\sum_{i, j, k=b, c} \sum_{p_i, k, q_j, k} \frac{\Gamma(2+p_i+p_k)\Gamma(2+q_j+q_k)}{\Gamma(6+p_i+p_k+q_j+q_k)} f^{\text{lead}}(\dots i \dots; j) \bar{f}(\dots k \dots) \right. \\
 &\quad \left. \times A_n(i_1, \dots, i_k, c^-, n^+, j_1, \dots, j_{k'}, a^-) \right),
 \end{aligned} \tag{7.90}$$

where $f^{\text{lead}}(\dots, i \dots; j)$ is identical to the definition for $f^{\text{lead}}(\dots, i \dots; j)$ in $C_{\text{grav}}^{n-s f} \big|^{PUP, b_1}$. The sums over the coefficients p_i, q_i for the Gamma functions come from the definitions

of (7.19) from the substitution of (7.20). $\mathcal{P}_1, \mathcal{P}_2$ are $(i_1, \dots, i_j) \in \mathcal{P}_1(c, d, \dots, n/2)$, $(l_1, \dots, l_{j'}) \in \mathcal{P}_2(n/2 + 1, \dots, n - 1)$, $j = n/2 - 1$, $j' = n/2 - 2$, to highlight this is the full length set of permutations again.

7.6.6 PUP contributions: class c

The third set of terms that contribute to the complex factorisation are those where the off shell legs B and C are non-adjacent in both of the gauge theory amplitudes,

$$\tau_n^{\text{YM}}(\dots, B^-, \dots, C^+, \dots) \tau_n^{\text{YM}}(\dots, B^-, \dots, C^+, \dots) (s_{BC} + s_{Bv}) s_{xy} s_{Bw} s_{Cz} \quad (7.91)$$

and hence contribute no direct poles. Then the only pole comes from the integration around the loop, and instances of s_{BC} from f or \bar{f} vanish entirely after the shift. Since both gauge theory amplitudes can be replaced by on shell amplitudes, we recall (7.87) to remove the ℓ -dependence, at order $1/\langle bc \rangle$. Again, we substitute $\hat{\lambda}_b = \frac{\langle ba \rangle}{\langle ca \rangle} \lambda_c$ inside the MHV amplitudes. Thus, the only ℓ -dependent terms occur from the LHS of the loop and the functions f, \bar{f} . These we have dealt with before in section 7.2.1 where we defined the general sum for $\mathcal{J}_{\text{grav}}^{\text{MHV}}$ in (7.21). Hence the final contribution to $C_{\text{grav}}^{n-s f}$ is,

$$\begin{aligned} C_{\text{grav}}^{n-s f} |^{PUP, c} &= \frac{i(-1)^{n+1} [bc]^3}{(4\pi)^2 \langle bc \rangle} \left[A_n(c^-, c^+, \dots, n^+, a^-) \right. \\ &\sum_{\mathcal{P}_1, \mathcal{P}_2} \left(\sum_{i, j, k=b, c} \sum_{p_i, k, q_j, k} \frac{\Gamma(2+p_i+p_k)\Gamma(2+q_j+q_k)}{\Gamma(5+p_i+p_k+q_j+q_k)} f(\dots i \dots; j) \bar{f}(\dots k \dots) \right. \\ &\left. \left. \times A_n(i_1, \dots, i_k, c^-, n^+, j_1, \dots, j_{k'}, a^-) \right) + \mathcal{P}_{\text{KLT}}(c^+, d^+, \dots, (n-1)^+) \right] \quad (7.92) \end{aligned}$$

where the sums over the coefficients p_i, q_i for the Gamma functions come from the definitions of (7.19) from the substitution of (7.20). $\mathcal{P}_1, \mathcal{P}_2$ are over the full length permutations for lists i and j as we saw in (7.90). Any cases where either MHV amplitude has a permutation where c^+, c^- are adjacent, the term is set to zero, as these were dealt with in the double pole terms or earlier cases.

7.6.7 Putting it all together

The three PUP cases a, b, c we have outlined can be combined into a total contribution where we have identified parts of the n -point KLT relations as transforming into A_n and A_{n-1} partial gauge theory amplitudes. This depends on whether B and C were adjacent or not in the original τ^{YM} current. We define the total contribution to the complex factorisation as,

$$C_{\text{grav}}^{n-s f} = C_{\text{grav}}^{n-s f} \Big|^{DP} + C_{\text{grav}}^{n-s f} \Big|^{PUP,a} + C_{\text{grav}}^{n-s f} \Big|^{PUP,b_1} + C_{\text{grav}}^{n-s f} \Big|^{PUP,b_2} + C_{\text{grav}}^{n-s f} \Big|^{PUP,c} \quad (7.93)$$

where the individual pieces are given in equations (7.81), (7.85), (7.89), (7.90) and (7.92).

The BCFW shifted $\widehat{C_{\text{grav}}^{n-s f}} \Big|^{DP}$ we have already discussed in (7.84), as it is a “pure” double pole that only introduces a minus sign to the contribution. To shift the PUP contribution, a minus sign is also introduced, but we also must shift instances of \hat{b} in the numerator that occur in the f, \bar{f} functions. Thus the entire shifted PUP contribution

to $C_{\text{grav}}^{\text{n-s f}}$ is given by,

$$\begin{aligned}
 \widehat{C_{\text{grav}}^{\text{n-s f}}} \Big|^{PUP} = & \frac{(-1)^{n_i} [bc]^3}{(4\pi)^2 \langle bc \rangle} \left\{ \frac{1}{360} \frac{\langle a|bc|a \rangle}{\langle ac \rangle^3} \left[A_{n-1}(c_1^-, d^+, \dots, n^+, a^-) \right. \right. \\
 & \times \sum_{\mathcal{P}_3, \mathcal{P}_2} f^{\text{lead}}(i_1, \dots, i_k, c; \lambda_c \bar{\lambda}_b \frac{\langle ba \rangle}{\langle ca \rangle}) \bar{f}(j_1, \dots, j_{k'}) A_{n-1}(i_1, \dots, i_k, c_2^-, n, j_1, \dots, j_{k'}, a^-) \\
 & \times \left(2 \frac{\langle a, i_k \rangle}{\langle c_2, i_k \rangle} - \frac{\langle a, c_1 + 1 \rangle}{\langle c_1, c_1 + 1 \rangle} - \frac{\langle an \rangle}{\langle c_2 n \rangle} \right) + \mathcal{P}_{\text{KLT}}(d, e, \dots, n-1) \Big] \\
 & + \frac{\langle a|bc|a \rangle}{\langle ac \rangle^2} \left[A_n(c^-; c^+, d^+ \dots, (n-1)^+; n^+, a^-) \right. \\
 & \times \sum_{\mathcal{P}_3, \mathcal{P}_2} \left(\sum_{i,j,k=\lambda_c \bar{\lambda}_b \frac{\langle ba \rangle}{\langle ca \rangle}, c} \sum_{p_i, k, q_j, k} \frac{\Gamma(2+p_i+p_k)\Gamma(2+q_j+q_k)}{\Gamma(6+p_i+p_k+q_j+q_k)} f^{\text{lead}}(\dots i; j) \bar{f}(\dots k \dots) \right. \\
 & \quad \times A_{n-1}(i_1, \dots, i_k, c^-, n^+, j_1, \dots, j_{k'}, a^-) \Big) + \mathcal{P}_{\text{KLT}}(c^+, d^+, \dots, (n-1)^+) \Big] \\
 & + \frac{\langle a|bc|a \rangle}{\langle ac \rangle^2} A_{n-1}(c^-, d^+ \dots, n^+, a^-) \\
 & \times \sum_{\mathcal{P}_1, \mathcal{P}_2} \left(\sum_{i,j,k=\lambda_c \bar{\lambda}_b \frac{\langle ba \rangle}{\langle ca \rangle}, c} \sum_{p_i, k, q_j, k} \frac{\Gamma(2+p_i+p_k)\Gamma(2+q_j+q_k)}{\Gamma(6+p_i+p_k+q_j+q_k)} f^{\text{lead}}(\dots i \dots; j) \bar{f}(\dots k \dots) \right. \\
 & \quad \times A_n(i_1, \dots, i_k, c^-, n^+, j_1, \dots, j_{k'}, a^-) \Big) \\
 & + \left[A_n(c^-, c^+, \dots, n^+, a^-) \right. \\
 & \times \sum_{\mathcal{P}_1, \mathcal{P}_2} \left(\sum_{i,j,k=\lambda_c \bar{\lambda}_b \frac{\langle ba \rangle}{\langle ca \rangle}, c} \sum_{p_i, k, q_j, k} \frac{\Gamma(2+p_i+p_k)\Gamma(2+q_j+q_k)}{\Gamma(5+p_i+p_k+q_j+q_k)} f(\dots i \dots; j) \bar{f}(\dots k \dots) \right. \\
 & \quad \times A_n(i_1, \dots, i_k, c^-, n^+, j_1, \dots, j_{k'}, a^-) \Big) + \mathcal{P}_{\text{KLT}}(c^+, d^+, \dots, (n-1)^+) \Big] \Big\}
 \end{aligned} \tag{7.94}$$

where the permutations are; \mathcal{P}_1 is $(i_1, \dots, i_k) \in \mathcal{P}(c, d, \dots, n/2)$, $k = n/2 - 1$. \mathcal{P}_2 is $(j_1, \dots, j_{k'}) \in \mathcal{P}_2(n/2+1, \dots, n-1)$, $k' = n/2 - 2$. \mathcal{P}_3 is $(i_1, \dots, i_k) \in \mathcal{P}_3(d, e, \dots, n/2)$, $k = n/2 - 2$. Any instances of $A_n(\dots, c^-, c^+, \dots)$ occurring under a permutation allowed by $\mathcal{P}_1(c, d, \dots, n/2)$ vanish in our definition, as they have been dealt with in

7.7 Ansatz for n -point recursion relation

other double pole cases. The sums over the coefficients p_i, q_i for the Gamma functions come from the definitions of (7.19) from the substitution of (7.20).

We have provided a non-trivial prescription that requires summation over combinations of momentum invariants in terms of simple Gamma functions. The result of the non-standard factorisation is entirely in terms of MHV amplitudes, plus f, \bar{f} does not contain leg \hat{a}^- for any permutation, so only \hat{b}^+ is affected on the BCFW shift. Hence, the only occurrence of shifted variables occur in the functions f, \bar{f} that shift according to $\hat{b} = \frac{\langle ba \rangle}{\langle ca \rangle} \lambda_c \bar{\lambda}_b$.

The permutations over \mathcal{P}_{KLT} occur for all positive helicity legs of their arguments. Altogether, the different double pole and sub-leading cases make up modifications of a single n -point KLT relation. The MHV amplitudes all have factors of $\langle ac \rangle^4$, as we have not yet accounted for the summation over other non-standard factorisations occurring in figure 7.1. Therefore the permutation of $\mathcal{P}_D(c \in c, \dots, n)$ must come outside the $\{ \}$ brackets in (7.94).

Implementation of this complex factorisation $\widehat{C_{\text{grav}}^{n-s} f} |^{DP} + \widehat{C_{\text{grav}}^{n-s} f} |^{PUP}$ is most easily realised via computer coded models. The n -point KLT relation computer coded to single out the double pole and three pole under the pole cases with substitutions for MHV amplitudes can generate the required n -point $\widehat{C_{\text{grav}}^{n-s} f}$ solution. An implementation in Mathematica code for the solution is available, but can be readily generated using the rules described throughout this section, and the n -point KLT relations (7.7).

7.7 Ansatz for n -point recursion relation

The definitions for $C_{\text{grav}}^{n-s} f$ in the previous section, along with the standard factorisations described in (7.1) and (7.2) can therefore be combined into an ansatz for the n -point

7.7 Ansatz for n -point recursion relation

single-minus one-loop gravity amplitude,

$$\begin{aligned}
M_n^{1\text{-loop}}(a^-, b^+, c^+ d^+, \dots, n^+) &= \sum_{i=4}^{n-1} \left[M_{n-i+2}^{\text{tree}}((i+1)^+, \dots, n^+, \hat{a}^-, \hat{K}_{b\dots i}^-) \right. \\
&\quad \times \frac{i}{K_{b\dots i}^2} M_i^{1\text{-loop}}(\hat{b}^+, \dots, i^+, -\hat{K}_{b\dots i}^+) + \mathcal{P}_D(c, \dots, i \in c, \dots, n) \Big] \\
&+ \left[M_{n-1}^{1\text{-loop}}(d^+, \dots, n^+, \hat{a}^-, \hat{K}_{bc}^+) \frac{i}{K_{bc}^2} M_3^{\text{tree}}(\hat{b}^+, c^+, -\hat{K}_{bc}^-) \right. \\
&\quad + \frac{i(-1)^{n+1}}{(4\pi)^2} \frac{1}{360} \frac{[bc]^4}{\langle bc \rangle^2} \frac{\langle ab \rangle^2}{\langle ac \rangle^2} \\
&\quad \times \left[A_{n-1}(c^-, d^+, \dots, n^+, a^-) \sum_{\mathcal{P}_3, \mathcal{P}_2} f^{\text{lead}}(i_1, \dots, i_{j-1}, c; b) \bar{f}(l_1, \dots, l_{j'}) \right. \\
&\quad \times A_{n-1}(i_1, \dots, i_{j-1}, c^-, n, l_1, \dots, l_{j'}, a^-) \Big] + \mathcal{P}_{\text{KLT}}(d, e, \dots, n-1) \\
&\quad + \frac{(-1)^n i}{(4\pi)^2} \frac{[bc]^3}{\langle bc \rangle} \left\{ \frac{1}{360} \frac{\langle a|bc|a \rangle}{\langle ac \rangle^3} \left[A_{n-1}(c_1^-, d^+, \dots, n^+, a^-) \right. \right. \\
&\quad \times \sum_{\mathcal{P}_3, \mathcal{P}_2} f^{\text{lead}}(i_1, \dots, i_k, c; \lambda_c \bar{\lambda}_b \frac{\langle ba \rangle}{\langle ca \rangle}) \bar{f}(j_1, \dots, j_{k'}) A_{n-1}(i_1, \dots, i_k, c_2^-, n, j_1, \dots, j_{k'}, a^-) \\
&\quad \times \left(2 \frac{\langle a, i_k \rangle}{\langle c_2, i_k \rangle} - \frac{\langle a, c_1 + 1 \rangle}{\langle c_1, c_1 + 1 \rangle} - \frac{\langle an \rangle}{\langle c_2 n \rangle} \right) + \mathcal{P}_{\text{KLT}}(d, e, \dots, n-1) \Big] \\
&\quad + \frac{\langle a|bc|a \rangle}{\langle ac \rangle^2} \left[A_n(c^-; c^+, d^+ \dots, (n-1)^+; n^+, a^-) \right. \\
&\quad \times \sum_{\mathcal{P}_3, \mathcal{P}_2} \left(\sum_{i,j,k=\lambda_c \bar{\lambda}_b \frac{\langle ba \rangle}{\langle ca \rangle}, c} \sum_{p_i, k, q_j, k} \frac{\Gamma(2+p_i+p_k)\Gamma(2+q_j+q_k)}{\Gamma(6+p_i+p_k+q_j+q_k)} f^{\text{lead}}(\dots i; j) \bar{f}(\dots k \dots) \right. \\
&\quad \times A_{n-1}(i_1, \dots, i_k, c^-, n^+, j_1, \dots, j_{k'}, a^-) \Big) + \mathcal{P}_{\text{KLT}}(c^+, d^+, \dots, (n-1)^+) \Big] \\
&\quad + \frac{\langle a|bc|a \rangle}{\langle ac \rangle^2} A_{n-1}(c^-, d^+ \dots, n^+, a^-) \\
&\quad \times \sum_{\mathcal{P}_1, \mathcal{P}_2} \left(\sum_{i,j,k=\lambda_c \bar{\lambda}_b \frac{\langle ba \rangle}{\langle ca \rangle}, c} \sum_{p_i, k, q_j, k} \frac{\Gamma(2+p_i+p_k)\Gamma(2+q_j+q_k)}{\Gamma(6+p_i+p_k+q_j+q_k)} f^{\text{lead}}(\dots i \dots; j) \bar{f}(\dots k \dots) \right. \\
&\quad \times A_n(i_1, \dots, i_k, c^-, n^+, j_1, \dots, j_{k'}, a^-) \Big) + \left[A_n(c^-, c^+, \dots, n^+, a^-) \right. \\
&\quad \times \sum_{\mathcal{P}_1, \mathcal{P}_2} \left(\sum_{i,j,k=\lambda_c \bar{\lambda}_b \frac{\langle ba \rangle}{\langle ca \rangle}, c} \sum_{p_i, k, q_j, k} \frac{\Gamma(2+p_i+p_k)\Gamma(2+q_j+q_k)}{\Gamma(5+p_i+p_k+q_j+q_k)} f(\dots i \dots; j) \bar{f}(\dots k \dots) \right. \\
&\quad \times A_n(i_1, \dots, i_k, c^-, n^+, j_1, \dots, j_{k'}, a^-) \Big) + \mathcal{P}_{\text{KLT}}(c, d, \dots, n-1) \Big] \Big\} + \mathcal{P}_D(c \in c, \dots, n) \Big] \\
\end{aligned} \tag{7.95}$$

7.7 Ansatz for n -point recursion relation

where the permutation sums for \mathcal{P}_1 , \mathcal{P}_2 , \mathcal{P}_3 , \mathcal{P}_{KLT} and \mathcal{P}_D are explained after equations (7.94), (7.7) and in figure 7.1. The three former permutation sums all come from the certain cases of the form of the KLT relations presented in (7.7). Any instances of $A_n(\dots, c^-, c^+, \dots)$ occurring under a permutation allowed by $\mathcal{P}(c, d, \dots, n/2)$ vanish in our definition, as they have been dealt with in other double pole cases. The sums over the coefficients p_i, q_i for the Gamma functions come from the definitions of (7.19) from the substitution of (7.20). We have provided a non-trivial prescription that requires summation over combinations of momentum invariants in terms of simple Gamma functions. The result of the non-standard factorisation is entirely in terms of MHV amplitudes, plus f, \bar{f} does not contain leg \hat{a}^- for any permutation, so only \hat{b}^+ is affected on the BCFW shift. Hence, the only occurrence of shifted variables occur in the functions f, \bar{f} that shift according to $\hat{b} = \frac{\langle ba \rangle}{\langle ca \rangle} \lambda_c \bar{\lambda}_b$.

The final ansatz for the recursion relation has a non-standard factorisation in terms of combinations of gauge theory amplitudes. The result for $\widehat{C_{\text{grav}}^{n-s} f}$ as presented in (7.95) contains no shifted variables and requires only the definitions for f, \bar{f} given in (7.19) from the substitution of (7.20), and the MHV amplitudes (3.51). However, the results presented for the standard factorisations from figure 7.1 contain functions with hatted variables from the recursion procedure that are evaluated at each pole where $\hat{K}_{b\dots i}^2 = 0$. The entire recursion relation as presented will inherently grow in complexity very quickly due to all the permutation sums and factorisations including lower-point amplitudes. The total number of factorisations that can occur as n grows is under control though, and the ansatz can be coded up to generate any n -point single-minus one-loop amplitude from 5-point onwards.

This ansatz has been shown to numerically match the previous results of the five- and six-graviton single-minus one-loop amplitudes, calculated in [158]. It was used to generate the seven-graviton single-minus one-loop amplitude that obeys the correct symmetries and collinear factorisations to lower point results to suggest that it is correct. There are further non-trivial checks that could be performed. For example, generating new results in some color-kinematic dual form that obey the BCJ relations should agree with our results. Furthermore, there may be simplifications possible in other ways of expressing the KLT relation that have yet to be investigated.

Chapter 8

Conclusions

The desire to understand gauge theories by categorising the amplitudes of the \mathcal{S} -matrix is driving particle physics forward in many new directions. Much of the developments have been driven in recent years by the need to understand NLO multi-parton processes at the LHC. Such as determining improved measurements of the QCD “background” against which new physics is distinguished such as the new scalar boson found last summer. For nearly thirty years, the considerable advancement in technology and theoretical techniques has led theorists to strive for results presented at their most simple or elegant; a tough task since the simplicity of the n -point MHV amplitudes were discerned by Parke and Taylor [59]. Considering how many Feynman diagrams would need to be computed at for example 20-points, the reduction to the Parke Taylor form (3.51) indicates gauge theories overall are far simpler than first thought.

Techniques for handling the NLO one-loop amplitudes have seen major developments that have not been so straightforward, dealing with a number of issues not encountered at tree level. Those include incorporating dimensional regularisation to deal with infrared and ultraviolet singularities and handling branch cuts in momenta. These have been dealt with by unitarity [44]; reusing on-shell tree amplitudes as its ingredients. In general there is now a well defined prescription for the cut-containing terms using generalised unitarity [110–121], certainly at one-loop level and even beyond in supersymmetric field theories [122–132]. The power of reusing technology from tree level has inspired many other approaches. The CSW rules have also been utilised at one-loop, which have been successfully applied in supersymmetric theories [165–167]

and the cut-constructible parts of Yang-Mills amplitudes [168].

Rational terms that appear at one-loop, in both pure QCD and graviton scattering, have proven the hardest to discern. Furthermore, the original tree-level BCFW recursion relations [133] have been developed to deal with the rational terms R_n at one-loop [102–106], albeit determined up to boundary terms for non-vanishing parts of an amplitude as $z \rightarrow \infty$. This is one possible method for determining R_n when using generalised unitarity in four dimensions for the cut containing terms. This also allows for the simplest application of the unitarity method. However, BCFW on-shell recursion can determine entire one-loop amplitudes that *lack* branch cuts, negating the need to cancel spurious poles in the cut-containing parts. Other methods of attack for rational terms in QCD include resorting to integration in $4 - 2\epsilon$ dimensions included in the cut-containing parts [116–118], or other recursive methods [102–106]. Developments in graviton scattering for rational terms include augmented recursion procedures [158] and now complex factorisations [20].

In this thesis we have developed techniques for analysing the single-minus one-loop S-matrix elements in pure Yang-Mills and pure Einstein gravity. The focus has been introducing a constructive approach to dealing with non-standard factorisations in one-loop recursion relations where complex momenta induce higher order singularities. Recently, the issue of inducing double poles in complex momenta in one-loop recursion has been understood by modifying the factorisation of all-plus loop splitting amplitudes in section 6.1 to a new description of non-standard or complex factorisations in section 6.2. This was realised by using axial gauge techniques, that preserve the structure of on-shell amplitudes, by nullifying any off-shell momenta with judicious reference momenta choices.

It is worth highlighting that the particular gauge choice in these calculations benefited us in many ways. Firstly, the gauge choice of $\lambda_q = \lambda_a$ which forced all four-vertices in the theory to vanish by virtue of $\langle aq \rangle$ prefactors. Secondly, identifying q with the required nullifying momenta for the recursion procedure allows us to easily switch between null and off-shell four-vectors when considering factorisations where $\hat{K}^2 = 0$. The second choice of making $\bar{\lambda}_q = \bar{\lambda}_b$ then forces the number of possible diagrams down dramatically by insisting leg \hat{b}^+ can only enter on a $\overline{\text{MHV}}$ vertex while the first choice

permits \hat{a}^- to only enter diagrams via an MHV vertex. Lastly, any spurious poles such as $\langle \hat{a}q \rangle$ were avoided with our choice of reference momentum.

The new non-standard factorisation was detailed for a particular rational one-loop amplitude; firstly the five-point single-minus Yang-Mills amplitude in section 6.3, recalculated from the example in Chapter 5. This highlighted that in the limit $\ell^2 \rightarrow 0$, the diagrams reduce to a very simple set of integrals. Taking the calculation to n -points, required summing contributions to an n -point off-shell amplitude τ_n , which split naturally into two sub-currents, (see figure 6.5). The first being those that were the leading pole contribution, that due to further BCFW affected factors in the denominator, produced pole under the pole (PUP) terms when the residue at the double pole was extracted (6.40). The second case were all sub-leading in the pole structure, that as $\ell^2 \rightarrow 0$ allowed a fairly concise reinterpretation for those contributions (6.37).

After integration and extraction of the poles from the residue, the double pole and PUP terms were reorganised with some work into a form matching the original Bern et al result (6.47). Through the constructive derivation in this section, we have shown how the double pole and PUP terms come from combinations of loop diagrams that make up a leading MHV amplitude plus another sub-leading MHV amplitude with legs interchanged (6.47) [20]. The interchange MHV amplitude, contains factors that are affected by the BCFW shift, coming from the loop integration. Thus we have proven the conjectured sub-leading pole for the single-minus one-loop amplitudes in Yang-Mills, using axial gauge techniques. Like usual Feynman diagram techniques, the method can prove rather cumbersome. However, the technique was successfully applied to acquire the rational terms of the five-point graviton MHV amplitude analytically [20].

Furthermore, the same technique was applied in Chapter 7 to determine a recursion relation for the pure graviton one-loop n -point amplitudes; $M^{1\text{-loop}}(a^-, b^+, c^+, \dots, n^+)$. Building a better understanding of the \mathcal{S} -matrix for a perturbative description of gravity is providing data on the current conjecture of the finiteness of $\mathcal{N} = 8$ supergravity debate, see Chapter 4. The developments in perturbative graviton scattering took their lead from the efficient techniques developed in Yang-Mills theories, utilising the KLT relations [21]. We argued that the KLT relations hold for two legs marginally off-shell, allowing direct substitution of the Yang-Mills currents τ_n , from Chapter 6 into the explicit five-point calculation of the non-standard factorisation. A concise form was achieved by the same methods of reorganisation into interchanged MHV amplitudes for

the five-point result. These were shown to be directly linked to the KLT orderings used originally (7.49).

The KLT relations required a new off-shell MHV amplitude τ_n where the negative helicity leg was allowed to wander between the other positive helicity legs. The final form for the wandering-minus current included just three terms which significantly simplified all terms that would be applied in the n -point KLT relation. The full reorganisation of this current was relegated from section 7.4 to Appendix B, which contains the full details of pulling out the simpler underlying structure from the complicated sums over diagrams and breaks in momenta. This allowed all possible orderings in the n -point KLT relation to be dealt with, and the process of dealing with the different double pole and PUP terms was described through section 7.6. By benefit of the simple loop integrals inherited from Yang-Mills, all the instances of loop dependence in the τ_n currents were substituted for wandering-minus currents (7.72) in terms of off-shell momentum β . The loop integration coming from the momenta invariants in the KLT relations was also dealt with, introduced as sums over Gamma functions in section 7.2.

The full n -point complex factorisation was categorised, after extraction of its poles. It correctly reproduces the five- and six-point results [158] when substituted into the n -point single-minus one-loop graviton recursion relation. The final ansatz for the relation presents the standard factorisations of lower point one-loop gravity amplitudes plus the complex factorisation, which was used to generate the seven-point single-minus one-loop gravity amplitude. It obeys the symmetry requirements and collinear factorisations to suggest that it is correct. Thus we have derived a new ansatz for the pure gravity n -point single-minus one-loop amplitudes using our construction. In actually computing the lower point amplitudes and in building the recursion relation, there were astounding simplifications at many steps along the way, not least the Yang-Mills wandering minus current that reduced to three terms. Further checks on results gained from this relation need to be addressed, such as the possibility highlighted previously of generating an amplitude via BCJ relations to check against. There may well also be other versions of the KLT relation that require investigation on simplifying the final result. Also, in its current form the ansatz preserves the remnants of the choice of hatted legs a and b in the recursion, which for the KLT relation in the non-standard factorisation may now be simplified as there are no hatted variables remaining.

Thus we have shown how the use of axial gauge techniques preserve the structure of on-shell amplitudes when constructing one-loop amplitudes. There is no need to restrict ourselves to purely rational one-loop amplitudes or just gluons in the loop, to apply the complex factorisation when complex momenta go collinear. For the future, work on rational terms in the MHV one-loop amplitudes for supergravity theories that contain double poles must be addressed. Here the rational terms contain many more spurious singularities that must cancel against those in the cut-containing terms, and the integrals to combat are more tedious. This technique has already been applied in the limit where the off-shell current does not diverge at all in the case of the MHV scalar five-point graviton amplitude [20]. However, the six-point and higher MHV one-loop amplitudes will induce double poles where the pole structure of the tree amplitude is more complicated. For example, the six-point MHV amplitude $(- - + + + +)$ allows factorisations for complex momenta on an $[a, x]$ -shift, with a divergence in the $\langle xy \rangle \rightarrow 0$ limit. However, the complex factorisation will contain terms proportional to $1/\langle xy \rangle$ and $1/[xy]$ in the off-shell amplitude $\tau_6(- - - + + +)$. Thus double poles and sub-leading PUP contributions as both holomorphic and anti-holomorphic spinor contributions vanish need to be accounted for.

Further extensions of complex factorisations along the same lines include any one-loop amplitude with number of positive helicities $n_+ \geq 4$ and number of negative helicities $n_- \geq 2$. This opens up the study of rational terms in one-loop amplitudes for the seven-point NMHV and eight point NMHV and NNMHV amplitudes to name a few. Therefore, both the study of off-shell currents and the behaviour of loop splitting amplitudes in the region of vanishing complex momenta requires much further work. For gravity amplitudes, the process reuses the KLT relations in an unusual off-shell setting, but in the limit of loop momenta going on-shell. This could lead to many developments in determining new one-loop amplitudes in gravity theories.

Appendix A

Loop integration

A.1 Yang Mills integrals

We consider the evaluation of the loop dependent integrals that occur in Chapter 6. These calculations yield simple results that will feed back into the off shell currents. From (6.23) we have reduced the problem to set of triangle integrals of the form,

$$\mathcal{J} = \int \frac{d^4\ell}{(2\pi)^4} \frac{[b|\ell|a][c|\ell|a][X|B|a]}{\ell^2 B^2 C^2}. \quad (\text{A.1})$$

Using Feynman parametrisation, we redefine the products of propagators $A_1 A_2 \dots A_n$ using,

$$\frac{1}{A_1 A_2 \dots A_n} = \int_0^1 dx_1 \dots dx_n \frac{\delta(\sum x_i - 1)(n-1)!}{[x_1 A_1 + \dots + x_n A_n]^n} \quad (\text{A.2})$$

to rewrite our triangle integrals (A.1) as follows,

$$\mathcal{J} = 2 \int_0^1 dx_1 dx_2 dx_3 \frac{d^4\ell}{(2\pi)^4} \delta(x_1 + x_2 + x_3 - 1) \frac{[b|\ell|a][c|\ell|a][X|B|a]}{[x_1 \ell^2 + x_2 B^2 + x_3 C^2]^3} \quad (\text{A.3})$$

Performing some algebra on the new denominator, making use of the delta function on

the x_i ,

$$[x_1 \ell^2 + x_2 B^2 + x_3 C^2]^3 = [\ell^2 + 2\ell \cdot (x_2 k_b - x_3 k_c)]^3 = [(\ell + x_2 k_b - x_3 k_c)^2 + x_2 x_3 s_{bc}]^3. \quad (\text{A.4})$$

With a particular change of variable in mind, $\ell = p - x_2 k_b + x_3 k_c$, the integrals can be written,

$$\mathcal{J} = 2 \int_0^1 dx_1 dx_2 dx_3 \frac{d^4 p}{(2\pi)^4} \delta(x_1 + x_2 + x_3 - 1) \frac{[b|p + x_3 c|a][c|p - x_2 b|a][X|p - (x_2 - 1)b + x_3 c|a]}{[p^2 + x_2 x_3 s_{bc}]^3}. \quad (\text{A.5})$$

When analysing (A.5), expanding in powers of p ; the odd terms vanish by parity, the quadratic terms vanish as the integral with $p^\mu p^\nu$ in the numerator contributes an $\eta^{\mu\nu}$ which in our case gives $\langle aa \rangle$ factors. Thus only the constant piece survives,

$$\mathcal{J} = 2 \int_0^1 dx_1 dx_2 dx_3 \frac{d^4 p}{(2\pi)^4} \delta(x_1 + x_2 + x_3 - 1) \frac{-x_2 x_3 [b|c|a][c|b|a][X|(1 - x_2)b + x_3 c|a]}{[p^2 + x_2 x_3 s_{bc}]^3}. \quad (\text{A.6})$$

leaving us an integral that we can readily compute. Specifically, we make use of the known dimensional regularisation integrals, taken from Appendix B of [164]. The results are given in terms of Gamma functions,

$$\int \frac{d^{2\omega} \ell}{(2\pi)^{2\omega}} \frac{1}{(\ell^2 + M^2 + 2\ell \cdot p)^A} = \frac{\Gamma(A - \omega)}{(4\pi)^\omega \Gamma(A)} \frac{1}{(M^2 - p^2)^{A - \omega}} \quad (\text{A.7})$$

such that for $M^2 = 0$ and $m > 2$, we can apply it to (A.6),

$$\int \frac{d^4 p}{(2\pi)^4} \frac{1}{[p^2 - \Delta]^m} = i \frac{(-1)^m}{(4\pi)^2} \frac{1}{(m - 1)(m - 2)} \frac{1}{\Delta^{m-2}}. \quad (\text{A.8})$$

Thus we can evaluate the integral over p ;

$$\mathcal{J} = i \frac{1}{(4\pi)^2} \int_0^1 dx_1 dx_2 dx_3 \delta(x_1 + x_2 + x_3 - 1) \frac{x_2 x_3 [b|c|a][c|b|a][X|(1 - x_2)b + x_3 c|a]}{-x_2 x_3 s_{bc}}. \quad (\text{A.9})$$

A.2 Gravity Integrals

The remaining x_i integrals are handled as follows. Suppose we have some extra momenta Y inside the final spinor string, then in general these triangle integrals will always be of the following form:

$$\mathcal{J} = i \frac{1}{(4\pi)^2} \int_0^1 dx_1 dx_2 dx_3 \delta(x_1 + x_2 + x_3 - 1) \frac{x_2 x_3 [b|c|a][c|b|a][X|(1-x_2)b + x_3c + Y|a]}{-x_2 x_3 s_{bc}}. \quad (\text{A.10})$$

The x_1 integration can be performed using the δ -function;

$$\mathcal{J} = -\frac{i}{(4\pi)^2} \frac{[b|c|a][c|b|a]}{s_{bc}} \int_0^1 dx_2 \int_0^{1-x_2} dx_3 [X|(1-x_2)b + x_3c + Y|a]. \quad (\text{A.11})$$

secondly the x_3 integration;

$$\begin{aligned} \mathcal{J} &= -\frac{i}{(4\pi)^2} \frac{[b|c|a][c|b|a]}{s_{bc}} \int_0^1 dx_2 [X|x_3(1-x_2)b + \frac{x_3^2}{2}c + x_3Y|a] \Big|_0^{1-x_2} \\ &= -\frac{i}{(4\pi)^2} \frac{[b|c|a][c|b|a]}{s_{bc}} \int_0^1 dx_2 [X|(1-x_2)^2b + \frac{(1-x_2)^2}{2}c + (1-x_2)Y|a], \end{aligned} \quad (\text{A.12})$$

and finally the x_2 integration;

$$\begin{aligned} \mathcal{J} &= -\frac{i}{(4\pi)^2} \frac{[b|c|a][c|b|a]}{s_{bc}} [X|\frac{(1-x_2)^3}{3}b + \frac{(1-x_2)^3}{6}c + \frac{(1-x_2)^2}{2}Y|a] \Big|_0^1 \\ &= \frac{i}{96\pi^2} \frac{\langle a|bc|a \rangle}{\langle bc \rangle} [X|2b + c + 3Y|a]. \end{aligned} \quad (\text{A.13})$$

A.2 Gravity Integrals

A.2.1 Dealing with higher rank in ℓ

For $n > 5$ -point, the KLT relations increase the power of ℓ depending on the number of s_{Bx} or s_{Cy} in each term. Therefore, the simplification afforded by (A.7) is not guaranteed for powers of ℓ in the numerator. We can construct the types of loop integrals to compute for any n -point contribution to $C_{\text{grav}}^{n-\text{s f}}$ in (7.93), where the τ_n^{YM} are replaced by MHV amplitudes.

A.2 Gravity Integrals

Again, our first step is to replace the propagators using Feynman parametrisation (A.2),

$$\frac{1}{A_1 A_2 \cdots A_n} = \int_0^1 dx_1 \cdots dx_n \frac{\delta(\sum x_i - 1)(n-1)!}{[x_1 A_1 + \cdots + x_n A_n]^n} \quad (\text{A.14})$$

We are taking the KLT relations off shell such that two momenta are ℓ -dependent that require integration over, including in s_{Bx} and s_{Cy} invariants, in general. In singling out terms in the KLT relations that yield MHV tree amplitudes for us, such as (7.25), we require integration over loop momentum of high order as n -points grows. So, we shall consider integrals of the form,

$$\mathcal{J}_{\text{grav}}^{\text{MHV}} = 2 \int_0^1 dx_1 dx_2 dx_3 \frac{\int d^d \ell}{(2\pi)^4} \frac{\delta(x_1 + x_2 + x_3 - 1)}{[\ell^2 + 2\ell \cdot (x_2 b - x_3 c)]^3} \left(\frac{[b|\ell|a][c|\ell|a]}{\langle ba \rangle \langle ca \rangle} \right)^2 (s_{Bx})^p (s_{Cy})^q. \quad (\text{A.15})$$

where the ℓ -dependent propagators were rewritten using (A.4). For generic integrals of high orders of loop momenta, we have seen there are tedious deconstruction techniques, such as Passarino Veltman. However, taking as a reference the dimensional regularisation formulae from Appendix B of [164], we have,

$$\int \frac{d^{2\omega} \ell}{(2\pi)^{2\omega}} \frac{\ell_\mu}{(\ell^2 + M^2 + 2\ell \cdot p)^A} = -\frac{\Gamma(A - \omega)}{(4\pi)^\omega \Gamma(A)} \frac{p_\mu}{(M^2 - p^2)^{A-\omega}} \quad (\text{A.16})$$

for rank 1 loop momentum. From the same source we find that for rank 2 loop polynomial, we have,

$$\frac{d^{2\omega} \ell}{(2\pi)^{2\omega}} \frac{\ell_\mu \ell_\nu}{(\ell^2 + M^2 + 2\ell \cdot p)^A} = \frac{1}{(4\pi)^\omega \Gamma(A)} \left[p_\mu p_\nu \frac{\Gamma(A - \omega)}{(M^2 - p^2)^{A-\omega}} + \frac{1}{2} \delta_{\mu\nu} \frac{\Gamma(A - 1 - \omega)}{(M^2 - p^2)^{A-1-\omega}} \right] \quad (\text{A.17})$$

Fortunately we require only those terms that are singular as $s_{bc} \rightarrow 0$, and can make use of the following truncation of the formulae,

$$\int \frac{d^4 \ell}{(2\pi)^4} \frac{\ell_{\mu_1} \ell_{\nu_2} \cdots \ell_{\sigma_n}}{(\ell^2 + M^2 + 2\ell \cdot p)^3} = \frac{i}{(4\pi)^2} \frac{(-1)^n}{2} \frac{p_{\mu_1} p_{\nu_2} \cdots p_{\sigma_n}}{(M^2 - p^2)} + \mathcal{O}\left(\frac{1}{(M^2 - p^2)^0}\right) \quad (\text{A.18})$$

A.2 Gravity Integrals

which holds for any rank of loop momentum. Subleading terms in p^2 up to ℓ^4 can also be found in Appendix B of [164]. This truncation allows direct substitution of $\ell \rightarrow p - x_2 k_b + x_3 k_c$ into the spinor products and the s_{Bx} , s_{Cy} invariants. Thus we can identify terms of $1/p^2$ in (A.18) as $1/s_{bc}$ and safely ignore all terms of order $(p^2)^0$ as they vanish after the shift. So we can write down the result of the loop integration where only factors of $x_2 k_b$ and $x_3 k_c$ remain, akin to the case in Yang Mills integrals seen in (A.5). The integral then becomes,

$$\begin{aligned} \mathcal{I}_{\text{grav}}^{\text{MHV}} = & \frac{1}{(4\pi)^2} \int_0^1 dx_1 dx_2 dx_3 \frac{\delta(x_1 + x_2 + x_3 - 1)}{x_2 x_3 s_{bc}} \left(x_2 x_3 \frac{[b|c|a][c|b|a]}{\langle ba \rangle \langle ca \rangle} \right)^2 \\ & \times \left((1 - x_2) s_{bx} + x_3 s_{cx} \right)^p \left(x_2 s_{by} + (1 - x_3) s_{cy} \right)^q \end{aligned} \quad (\text{A.19})$$

where the integral over x_1 can be done using the delta function as before (A.11),

$$\mathcal{I}_{\text{grav}}^{\text{MHV}} = \frac{-1}{(4\pi)^2} \frac{[bc]^3}{\langle bc \rangle} \int_0^1 dx_2 \int_0^{1-x_2} dx_3 x_2 x_3 \left((1 - x_2) s_{bx} + x_3 s_{cx} \right)^p \left(x_2 s_{by} + (1 - x_3) s_{cy} \right)^q. \quad (\text{A.20})$$

We are left a much simpler two dimensional integral than we could have been left with if not for vanishing terms thanks to the BCFW shift. There is not a compact expression for the integrals (A.15) for any generic p, q , due to the reparametrisation of s_{Bx} and s_{Cy} ,

$$\begin{aligned} s_{Bx}^p & \rightarrow ((1 - x_2) s_{bx} + x_3 s_{cx})^p \\ s_{Cy}^q & \rightarrow (x_2 s_{by} + (1 - x_3) s_{cy})^q \end{aligned} \quad (\text{A.21})$$

However the remaining integrals contain products of the form x_2^{r+1} and x_3^{s+1} , that yield Gamma functions,

$$\int_0^1 dx_2 \int_0^{1-x_2} dx_3 x_2^{r+1} x_3^{s+1} = \frac{\Gamma(r+2)\Gamma(s+2)}{\Gamma(5+r+s)} \quad (\text{A.22})$$

A.2 Gravity Integrals

that evaluate to simple factorials. Thus we can express the general integrated contribution with

$$\mathcal{J}_{\text{grav}}^{\text{MHV}} = \frac{i}{4\pi^2} \frac{[bc]^3}{\langle bc \rangle} \sum_{i,j,k=b,c} \sum_{p_{i,j,k}, q_{i,j,k}} \frac{\Gamma(2+p_i+p_k)\Gamma(2+q_j+q_k)}{\Gamma(5+p_i+p_k+q_j+q_k)} f(\dots i \dots; j) \bar{f}(\dots k \dots). \quad (\text{A.23})$$

where the coefficients p and q are determined term by term in the expansion of f, \bar{f} (7.19) given by equations (7.16) and (7.17), due to the substitutions of (7.20).

This leads to increasingly cumbersome fractional contributions for $n > 5$ -point MHV contributions to C_{grav}^{n-sf} . We shall evaluate the example of (7.25), albeit the loop dependent part only,

$$\mathcal{J}_{\text{ex}} = \int d^4\ell \left(\frac{[b|\ell|a][c|\ell|a]}{\langle ba \rangle \langle ca \rangle} \right)^2 \frac{s_{Bd}s_{Ce}}{\ell^2 B^2 C^2} \quad (\text{A.24})$$

that appears in Chapter 7, for which the result is presented in equation (7.26).

Once the Feynman parametrisation (A.2) has been applied, along with the rewriting of the denominator using (A.4), we have the following integral,

$$\mathcal{J}_{\text{ex}} = 2 \int_0^1 dx_1 dx_2 dx_3 \frac{\int d^4\ell}{(2\pi)^4} \frac{\delta(x_1+x_2+x_3-1)}{[\ell^2+2\ell \cdot (x_2b-x_3c)]^3} \left(\frac{[b|\ell|a][c|\ell|a]}{\langle ba \rangle \langle ca \rangle} \right)^2 s_{Bd}s_{Ce}. \quad (\text{A.25})$$

Using (A.18), we compute the p -integration, after identifying $\ell \rightarrow p - x_2b + x_3c$ using (A.8), we have

$$\begin{aligned} \mathcal{J}_{\text{ex}} = & \frac{1}{(4\pi)^2} \int_0^1 dx_1 dx_2 dx_3 \frac{\delta(x_1+x_2+x_3-1)}{x_2 x_3 s_{bc}} \left(x_2 x_3 \frac{[b|c|a][c|b|a]}{\langle ba \rangle \langle ca \rangle} \right)^2 \\ & \times \left((1-x_2)s_{bd} + x_3 s_{cd} \right) \left(x_2 s_{be} + (1-x_3)s_{ce} \right). \end{aligned} \quad (\text{A.26})$$

Cleaning up some of the factors and doing the x_1 integration using the delta function,

A.2 Gravity Integrals

we are left with,

$$\mathcal{J}_{\text{ex}} = \frac{1}{(4\pi)^2} \frac{[bc]^3}{\langle bc \rangle} \int_0^1 dx_2 \int_0^{1-x_2} dx_3 x_2 x_3 \left((1-x_2)s_{bd} + x_3 s_{cd} \right) \left(x_2 s_{be} + (1-x_3)s_{ce} \right). \quad (\text{A.27})$$

So, expanding out the four momentum invariants we first apply the integration over x_3 ,

$$\begin{aligned} \mathcal{J}_{\text{ex}} = \frac{1}{(4\pi)^2} \frac{[bc]^3}{\langle bc \rangle} \int_0^1 dx_2 \frac{x_2 x_3^2}{12} & \left(-2(1-x_2)s_{bd}(3x_2 s_{be} + (3-2x_3)s_{ce}) \right. \\ & \left. - x_3 s_{cd}(4x_2 s_{be} + (4-3x_3)s_{ce}) \right) \Big|_0^{1-x_2}, \end{aligned} \quad (\text{A.28})$$

evaluating the limits we are left with,

$$\begin{aligned} \mathcal{J}_{\text{ex}} = \frac{-1}{(4\pi)^2} \frac{[bc]^3}{\langle bc \rangle} \int_0^1 dx_2 \frac{(1-x_2)^3 x_2}{12} & \left(2s_{bd}(3x_2 s_{be} + (1+2x_2)s_{ce}) \right. \\ & \left. + s_{cd}(4x_2 s_{be} + (1+3x_2)s_{ce}) \right). \end{aligned} \quad (\text{A.29})$$

The last integral we evaluate in one line to save expanding to many factors,

$$\mathcal{J}_{\text{ex}} = \frac{1}{(4\pi)^2} \frac{[bc]^3}{\langle bc \rangle} \frac{-1}{360} \left(3s_{bd}s_{be} + 2s_{be}s_{cd} + 5s_{bd}s_{ce} + 3s_{cd}s_{ce} \right), \quad (\text{A.30})$$

which is used in part of the calculation of $C_{\text{grav}}^{\text{n-sf}}|_5^b$ in (7.26) from Chapter 7. In terms of sums of Gamma functions, the integral (A.23) would expand out in the following way,

$$\begin{aligned} \mathcal{J}_{\text{ex}} = \frac{1}{(4\pi)^2} \frac{[bc]^3}{\langle bc \rangle} \int_0^1 dx_2 \int_0^{1-x_2} dx_3 & \left((x_2^3 x_3 - x_2^2 x_3)s_{bd}s_{be} - x_2^2 x_3^2 s_{be}s_{cd} \right. \\ & \left. + (x_2^2 x_3 + x_2 x_3^2 - x_2 x_3 - x_2^2 x_3^2)s_{bd}s_{ce} + (x_2 x_3^3 - x_2 x_3^2)s_{cd}s_{ce} \right). \end{aligned} \quad (\text{A.31})$$

A.2 Gravity Integrals

such that we can use the set of integrals from (A.22) to give,

$$\begin{aligned} \mathcal{J}_{\text{ex}} = & \frac{1}{(4\pi)^2} \frac{[bc]^3}{\langle bc \rangle} \left(\left(\frac{\Gamma(4)\Gamma(2)}{\Gamma(7)} - \frac{\Gamma(3)\Gamma(2)}{\Gamma(6)} \right) s_{bd}s_{be} - \frac{\Gamma(3)\Gamma(3)}{\Gamma(7)} s_{be}s_{cd} \right. \\ & \left. + \left(2\frac{\Gamma(3)\Gamma(2)}{\Gamma(6)} - \frac{\Gamma(2)\Gamma(2)}{\Gamma(5)} - \frac{\Gamma(3)\Gamma(3)}{\Gamma(7)} \right) s_{bd}s_{ce} + \left(\frac{\Gamma(2)\Gamma(4)}{\Gamma(7)} - \frac{\Gamma(2)\Gamma(3)}{\Gamma(6)} \right) s_{cd}s_{ce} \right). \end{aligned} \quad (\text{A.32})$$

which is identical to the result given in (A.30).

A.2.2 More examples

We consider three more cases, all of which are explicit results that are used in Chapter 7 to deal with the leading pole terms and cross terms in (7.29), from one of the KLT terms from the five-point single-minus one-loop amplitude. We repeat it now,

$$\begin{aligned} s_{BC}s_{de}\tau_5^{\text{YM}}(a^-, B^-, C^+, d^+, e^+)\tau_5^{\text{YM}}(a^-, C^+, B^-, e^+, d^+) = & s_{bc}s_{de} \left(\frac{\langle Ba \rangle}{\langle Ca \rangle} \right)^4 \\ & \left[\frac{\langle a|B(b+c)|a\rangle}{s_{bc}} \frac{\tau^{\text{MHV}}(a^-, (b+c)^-, d^+, e^+)}{\langle P_{bc}a \rangle^2} \right. \\ & + \sum_{i=d}^e \langle Ca \rangle^2 \langle a|BK_i|a\rangle \frac{\tau^{\text{sm}}(-\kappa_i^-, C^+, d^+, \dots, i^+)}{\langle \kappa_i a \rangle^2 \kappa_i^2} \frac{\tau^{\text{MHV}}(a^-, -K_i^-, (i+1)^+, \dots, e^+)}{\langle K_i a \rangle^2 K_i^2} \left. \right] \\ \times & \left[\frac{\langle a|C(b+c)|a\rangle}{s_{bc}} \frac{\tau^{\text{MHV}}(a^-, (b+c)^-, e^+, d^+)}{\langle P_{bc}a \rangle^2} \right. \\ & + \sum_{i=e}^d \langle Ba \rangle^2 \langle a|CK_i|a\rangle \frac{\tau^{\text{sm}}(-\kappa_i^-, B^+, e^+, \dots, i^+)}{\langle \kappa_i a \rangle^2 \kappa_i^2} \frac{\tau^{\text{MHV}}(a^-, -K_i^-, (i+1)^+, \dots, d^+)}{\langle K_i a \rangle^2 K_i^2} \left. \right] \end{aligned} \quad (\text{A.33})$$

to highlight where the loop dependence arises.

Firstly, we shall deal with two very similar integrals, that arise from cross terms between leading and subleading pole terms in (A.33). The loop momentum dependence is restricted to the leading B and C dependent factors in both parts, such that we are

A.2 Gravity Integrals

left with the following types of integral to evaluate,

$$\mathcal{I}_1 = \int d^4\ell \frac{[b|\ell|a]^2 [c|\ell|a]^2 [X|B|a] \langle a|PC|a \rangle}{\ell^2 B^2 C^2 \langle ba \rangle^2 \langle ca \rangle^2}, \quad (\text{A.34})$$

and

$$\mathcal{I}_2 = \int d^4\ell \frac{[b|\ell|a]^2 [c|\ell|a]^2 [Y|C|a] \langle a|PB|a \rangle}{\ell^2 B^2 C^2 \langle ba \rangle^2 \langle ca \rangle^2}. \quad (\text{A.35})$$

We apply the same tricks using (A.14) and (A.4), as before, to rewrite the integrals over new variables x_i and $p = \ell + x_2 k_b - x_3 k_c$,

$$\begin{aligned} \mathcal{I}_1 = 2 \int_0^1 dx_1 dx_2 dx_3 \frac{d^4 p}{(2\pi)^4} \delta(x_1 + x_2 + x_3 - 1) \times \\ \frac{[b|p + x_3 c|a]^2 [c|p - x_2 b|a]^2 [X|p - (x_2 - 1)b + x_3 c|a] (1 - x_2 - x_3) \langle a|bc|a \rangle}{[p^2 + x_2 x_3 s_{bc}]^3 \langle ba \rangle^2 \langle ca \rangle^2}, \end{aligned} \quad (\text{A.36})$$

and

$$\begin{aligned} \mathcal{I}_2 = 2 \int_0^1 dx_1 dx_2 dx_3 \frac{d^4 p}{(2\pi)^4} \delta(x_1 + x_2 + x_3 - 1) \times \\ \frac{[b|p + x_3 c|a]^2 [c|p - x_2 b|a]^2 [Y|p - x_2 b + (1 - x_3)c|a] (1 - x_2 - x_3) \langle a|cb|a \rangle}{[p^2 + x_2 x_3 s_{bc}]^3 \langle ba \rangle^2 \langle ca \rangle^2}. \end{aligned} \quad (\text{A.37})$$

where the $(1 - x_2 - x_3)$ factor came from expanding the leading loop dependent factor from τ^{MHV} . The integration over p is considered as before, using truncation on (A.18) to directly leave us with the x_2, x_3 integrals, after x_1 integration is done using the delta function,

$$\mathcal{I}_1 = -\frac{\langle a|bc|a \rangle [bc]^3}{(4\pi)^2 \langle bc \rangle} \int_0^1 dx_2 \int_0^{1-x_2} dx_3 x_2 x_3 (1 - x_2 - x_3) [X|(1 - x_2)b + x_3 c|a], \quad (\text{A.38})$$

A.2 Gravity Integrals

and

$$\mathcal{J}_2 = -\frac{\langle a|cb|a\rangle}{(4\pi)^2} \frac{[bc]^3}{\langle bc\rangle} \int_0^1 dx_2 \int_0^{1-x_2} dx_3 x_2 x_3 (1-x_2-x_3) [Y|x_2 b + (1-x_3)c|a]. \quad (\text{A.39})$$

Applying the integral over x_3 and then x_2 to both integrals, and evaluating the limits,

$$\begin{aligned} \mathcal{J}_1 &= -\frac{1}{(4\pi)^2} \frac{[bc]^3}{\langle bc\rangle} \frac{\langle a|bc|a\rangle}{12} \int_0^1 dx_2 x_2 (1-x_2)^4 [X|2b+c|a] \\ &= \frac{1}{(4\pi)^2} \frac{[bc]^3}{\langle bc\rangle} \frac{\langle a|bc|a\rangle}{360} [X|2b+c|a], \end{aligned} \quad (\text{A.40})$$

and

$$\begin{aligned} \mathcal{J}_2 &= -\frac{1}{(4\pi)^2} \frac{[bc]^3}{\langle bc\rangle} \frac{\langle a|cb|a\rangle}{12} \int_0^1 x_2 (1-x_2)^3 [Y|x_2 b + (1-x_2)c|a] \\ &= \frac{1}{(4\pi)^2} \frac{[bc]^3}{\langle bc\rangle} \frac{\langle a|cb|a\rangle}{360} [Y|b+2c|a]. \end{aligned} \quad (\text{A.41})$$

These integrals can also be completed for a general power of x_2 or x_3 coming from an expansion in f, \bar{f} over loop dependent factors. For $n > 5$ -point integrals, sums over the expansions in f, \bar{f} according to (7.18) using (7.20) for *cross* terms of the sort that appear in (A.33) are required. These match the formula of (A.23), up to an extra integer in the Gamma function of the denominator, due to the extra overall $(1-x_2-x_3)$ factor,

$$\mathcal{J}_{\text{grav}}^{\text{cross}} = \frac{i}{4\pi^2} \frac{[bc]^3}{\langle bc\rangle} \sum_{i,j,k=b,c} \sum_{p_{i,j,k}, q_{i,j,k}} \frac{\Gamma(2+p_i+p_k)\Gamma(2+q_j+q_k)}{\Gamma(6+p_i+p_k+q_j+q_k)} f(\dots i \dots; j) \bar{f}(\dots k \dots). \quad (\text{A.42})$$

Lastly, the integral from the leading pole term combines the loop dependence from the leading τ^{MHV} factors, where we apply the same tricks using (A.14) and (A.4). Then rewrite the integrals over new variables x_i and $p = \ell + x_2 k_b - x_3 k_c$,

$$\begin{aligned} \mathcal{J}_3 &= 2 \int_0^1 dx_1 dx_2 dx_3 \frac{d^4 p}{(2\pi)^4} \delta(x_1 + x_2 + x_3 - 1) \times \\ &\quad \frac{[b|p+x_3 c|a]^2 [c|p-x_2 b|a]^2 (1-x_2-x_3)^2 \langle a|bc|a\rangle \langle a|cb|a\rangle}{[p^2 + x_2 x_3 s_{bc}]^3 \langle ba\rangle^2 \langle ca\rangle^2}, \end{aligned} \quad (\text{A.43})$$

A.2 Gravity Integrals

Again, the integration over p is considered as before, using truncation on (A.18) to directly leave us with the x_2, x_3 integrals, after x_1 integration is done using the delta function, so that pieces proportional to p drop out,

$$\begin{aligned} \mathcal{J}_3 &= -\frac{1}{(4\pi)^2} \frac{[bc]^3}{\langle bc \rangle} \langle a|bc|a \rangle \langle a|cb|a \rangle \int_0^1 dx_2 \int_0^{1-x_2} dx_3 x_2 x_3 (1-x_2-x_3)^2 \\ &= \frac{1}{(4\pi)^2} \frac{[bc]^3}{\langle bc \rangle} \frac{\langle a|bc|a \rangle \langle a|cb|a \rangle}{360}, \end{aligned} \tag{A.44}$$

where we have computed the final two integrals in one step. This type of integral with the factor $1/360$ appears for every n -point calculation that involves the double pole, due to the simple dependence on the loop momenta highlighted in the leading terms from the τ^{YM} factors in (A.33).

Appendix B

Reorganisation of the wandering minus current

Using equation (7.57) we can write the form for the τ^{MHV} currents in from Chapter 7, equation (7.60) with the wandering minus as the sum of the three figures 7.4, 7.5 and 7.6, to give us the full contribution to the non-standard factorisation,

$$\begin{aligned}
\mathcal{C}^{n-\text{sf}} = & -\frac{i}{32\pi^2} \frac{[\mathcal{FG}]}{\langle \mathcal{FG} \rangle} \frac{1}{\langle ab \rangle \cdots \langle fa \rangle} \frac{1}{\langle ag \rangle \cdots \langle na \rangle} \left(\langle a | \beta P_{\mathcal{FG}} | a \rangle \sum_{b_l=b-1}^f \sum_{b_r=g-1}^{n[\text{no sing}]} \times \right. \\
& \frac{1}{P_{b_r+1 \dots a \dots b_l}^2} \frac{[\mathcal{F} | P_{b_r+1 \dots a \dots b_l} | a \rangle^4 \langle b_l, b_l+1 \rangle \langle b_r, b_r+1 \rangle}{[\mathcal{F} | P_{b_r+1 \dots a \dots b_l} | b_r \rangle [\mathcal{F} | P_{b_r+1 \dots a \dots b_l} | b_l+1 \rangle [\mathcal{F} | P_{b_r+1 \dots a \dots b_l} | b_l \rangle [\mathcal{F} | P_{b_r+1 \dots a \dots b_l} | b_r+1 \rangle]} \\
& - \sum_{i=g}^n \langle a | \beta P_{\gamma \dots i} | a \rangle \frac{\langle ag \rangle \langle a\gamma \rangle}{\langle \gamma g \rangle} \frac{\langle i, i+1 \rangle}{\langle ia \rangle \langle a, i+1 \rangle} \sum_{b_l=b-1}^f \sum_{b_r=i+1-1}^{n[\text{no sing}, *]} \times \\
& \frac{1}{P_{b_r+1 \dots a \dots b_l}^2} \frac{[\mathcal{F} | P_{b_r+1 \dots a \dots b_l} | a \rangle^4 \langle b_l, b_l+1 \rangle \langle b_r, b_r+1 \rangle}{[\mathcal{F} | P_{b_r+1 \dots a \dots b_l} | b_r \rangle [\mathcal{F} | P_{b_r+1 \dots a \dots b_l} | b_l+1 \rangle [\mathcal{F} | P_{b_r+1 \dots a \dots b_l} | b_l \rangle [\mathcal{F} | P_{b_r+1 \dots a \dots b_l} | b_r+1 \rangle]} \\
& - \sum_{i=b-1}^{f-1} \langle a | \beta P_{\gamma \dots i} | a \rangle \frac{\langle ag \rangle \langle a\gamma \rangle}{\langle \gamma g \rangle} \frac{\langle i, i+1 \rangle}{\langle ia \rangle \langle a, i+1 \rangle} \sum_{b_l=b-1}^i \sum_{b_r=\gamma-1}^{n[\text{no sing}, *]} \times \\
& \left. \frac{1}{P_{b_r+1 \dots a \dots b_l}^2} \frac{[\mathcal{F} | P_{b_r+1 \dots a \dots b_l} | a \rangle^4 \langle b_l, b_l+1 \rangle \langle b_r, b_r+1 \rangle}{[\mathcal{F} | P_{b_r+1 \dots a \dots b_l} | b_r \rangle [\mathcal{F} | P_{b_r+1 \dots a \dots b_l} | b_l+1 \rangle [\mathcal{F} | P_{b_r+1 \dots a \dots b_l} | b_l \rangle [\mathcal{F} | P_{b_r+1 \dots a \dots b_l} | b_r+1 \rangle]} \right) \quad (\text{B.1})
\end{aligned}$$

We bring out symmetrical terms in γ and g , i.e. those sums without γ or g at the

end points. We will put away symmetrical terms into a function called $Symm_{\gamma g}$. The first double sum is left alone for now, however the first triple sum is symmetrical for $i \geq h$, whilst the final triple sum is symmetrical for $b_r \geq h$. Thus we have,

$$\begin{aligned}
\mathcal{C}^{\text{n-sf}} = & -\frac{i}{32\pi^2} \frac{[\mathcal{FG}]}{\langle \mathcal{FG} \rangle} \frac{1}{\langle ab \rangle \cdots \langle fa \rangle} \frac{1}{\langle ag \rangle \cdots \langle na \rangle} \left(\langle a | \beta P_{\mathcal{FG}} | a \rangle \sum_{b_l=b-1}^f \sum_{b_r=g-1}^{n[\text{no sing}]} \times \right. \\
& \frac{1}{P_{b_r+1 \dots a \dots b_l}^2} \frac{[\mathcal{F}|P_{b_r+1 \dots a \dots b_l}|a\rangle^4 \langle b_l, b_l+1 \rangle \langle b_r, b_r+1 \rangle}{[\mathcal{F}|P_{b_r+1 \dots a \dots b_l}|b_r\rangle [\mathcal{F}|P_{b_r+1 \dots a \dots b_l}|b_l+1\rangle [\mathcal{F}|P_{b_r+1 \dots a \dots b_l}|b_l\rangle [\mathcal{F}|P_{b_r+1 \dots a \dots b_l}|b_r+1\rangle]} \\
& - \langle a | \beta P_{\gamma g} | a \rangle \frac{\langle ag \rangle \langle a\gamma \rangle}{\langle \gamma g \rangle} \frac{\langle gh \rangle}{\langle ga \rangle \langle ah \rangle} \sum_{b_l=b-1}^f \sum_{b_r=h-1}^{n[\text{no sing}, *]} \times \\
& \frac{1}{P_{b_r+1 \dots a \dots b_l}^2} \frac{[\mathcal{F}|P_{b_r+1 \dots a \dots b_l}|a\rangle^4 \langle b_l, b_l+1 \rangle \langle b_r, b_r+1 \rangle}{[\mathcal{F}|P_{b_r+1 \dots a \dots b_l}|b_r\rangle [\mathcal{F}|P_{b_r+1 \dots a \dots b_l}|b_l+1\rangle [\mathcal{F}|P_{b_r+1 \dots a \dots b_l}|b_l\rangle [\mathcal{F}|P_{b_r+1 \dots a \dots b_l}|b_r+1\rangle]} \\
& - \sum_{i=b-1}^{f-1} \langle a | \beta P_{\gamma \dots i} | a \rangle \frac{\langle ag \rangle \langle a\gamma \rangle}{\langle \gamma g \rangle} \frac{\langle i, i+1 \rangle}{\langle ia \rangle \langle a, i+1 \rangle} \sum_{b_l=b-1}^i \sum_{b_r=\gamma-1}^g \times \\
& \left. \frac{1}{P_{b_r+1 \dots a \dots b_l}^2} \frac{[\mathcal{F}|P_{b_r+1 \dots a \dots b_l}|a\rangle^4 \langle b_l, b_l+1 \rangle \langle b_r, b_r+1 \rangle}{[\mathcal{F}|P_{b_r+1 \dots a \dots b_l}|b_r\rangle [\mathcal{F}|P_{b_r+1 \dots a \dots b_l}|b_l+1\rangle [\mathcal{F}|P_{b_r+1 \dots a \dots b_l}|b_l\rangle [\mathcal{F}|P_{b_r+1 \dots a \dots b_l}|b_r+1\rangle]} \right) \\
& + Symm_{\gamma g}
\end{aligned} \tag{B.2}$$

where

$$\begin{aligned}
Symm_{\gamma g} = & -\frac{i}{32\pi^2} \frac{[\mathcal{FG}]}{\langle \mathcal{FG} \rangle} \frac{1}{\langle ab \rangle \cdots \langle fa \rangle} \frac{1}{\langle ag \rangle \cdots \langle na \rangle} \left(\right. \\
& - \sum_{i=h}^n \langle a | \beta P_{\gamma \dots i} | a \rangle \frac{\langle ag \rangle \langle a\gamma \rangle}{\langle \gamma g \rangle} \frac{\langle i, i+1 \rangle}{\langle ia \rangle \langle a, i+1 \rangle} \sum_{b_l=b-1}^f \sum_{b_r=i+1-1}^{n[\text{no sing}, *]} \times \\
& \frac{1}{P_{b_r+1 \dots a \dots b_l}^2} \frac{[\mathcal{F}|P_{b_r+1 \dots a \dots b_l}|a\rangle^4 \langle b_l, b_l+1 \rangle \langle b_r, b_r+1 \rangle}{[\mathcal{F}|P_{b_r+1 \dots a \dots b_l}|b_r\rangle [\mathcal{F}|P_{b_r+1 \dots a \dots b_l}|b_l+1\rangle [\mathcal{F}|P_{b_r+1 \dots a \dots b_l}|b_l\rangle [\mathcal{F}|P_{b_r+1 \dots a \dots b_l}|b_r+1\rangle]} \\
& - \sum_{i=b-1}^{f-1} \langle a | \beta P_{\gamma \dots i} | a \rangle \frac{\langle ag \rangle \langle a\gamma \rangle}{\langle \gamma g \rangle} \frac{\langle i, i+1 \rangle}{\langle ia \rangle \langle a, i+1 \rangle} \sum_{b_l=b-1}^i \sum_{b_r=h}^{n[\text{no sing}, *]} \times \\
& \left. \frac{1}{P_{b_r+1 \dots a \dots b_l}^2} \frac{[\mathcal{F}|P_{b_r+1 \dots a \dots b_l}|a\rangle^4 \langle b_l, b_l+1 \rangle \langle b_r, b_r+1 \rangle}{[\mathcal{F}|P_{b_r+1 \dots a \dots b_l}|b_r\rangle [\mathcal{F}|P_{b_r+1 \dots a \dots b_l}|b_l+1\rangle [\mathcal{F}|P_{b_r+1 \dots a \dots b_l}|b_l\rangle [\mathcal{F}|P_{b_r+1 \dots a \dots b_l}|b_r+1\rangle]} \right)
\end{aligned} \tag{B.3}$$

Now the first two double sums are very similar except for the endpoint at $b_r = g - 1$, up to spinor factors. Thus for $b_r \geq h$, we can use the following simplification between the prefactors,

$$\begin{aligned}
\langle a|\beta P_{\mathcal{FG}}|a\rangle - \langle a|\beta P_{\gamma g}|a\rangle \frac{\langle ag\rangle\langle a\gamma\rangle}{\langle \gamma g\rangle} \frac{\langle gh\rangle}{\langle ga\rangle\langle ah\rangle} &= \langle a|\beta P_{\gamma}|a\rangle + \langle a|\beta P_{\gamma g}|a\rangle \frac{\langle a\gamma\rangle}{\langle \gamma g\rangle} \frac{\langle gh\rangle}{\langle ah\rangle} \\
&= \frac{\langle a\gamma\rangle}{\langle \gamma g\rangle\langle ah\rangle} \left(\langle a|\beta P_{\gamma g}|a\rangle\langle gh\rangle - \langle a|\beta|\gamma\rangle\langle \gamma g\rangle\langle ah\rangle \right) \\
&= \frac{\langle a\gamma\rangle}{\langle \gamma g\rangle\langle ah\rangle} \left(\langle a|\beta P_{\gamma g}|a\rangle\langle gh\rangle - \langle a|\beta P_{\gamma g}|g\rangle\langle ah\rangle \right) \\
&= \frac{\langle a\gamma\rangle\langle ga\rangle}{\langle \gamma g\rangle\langle ah\rangle} \langle a|\beta P_{\gamma g}|h\rangle
\end{aligned} \tag{B.4}$$

to put those terms for $b_r \geq h$ into $Symm_{\gamma g}$ also. We keep the $b_r = g - 1, g$ terms from the first double sum and the $b_r = h - 1$ term from the second double sum. We are left with,

$$\begin{aligned}
\mathcal{C}^{\text{n-sf}} &= -\frac{i}{32\pi^2} \frac{[\mathcal{FG}]}{[\mathcal{FG}]} \frac{1}{\langle ab\rangle \dots \langle fa\rangle} \frac{1}{\langle ag\rangle \dots \langle na\rangle} \left(\langle a|\beta P_{\beta\gamma}|a\rangle \sum_{b_l=b-1}^f \sum_{b_r=g-1}^{g[\text{no sing}]} \times \right. \\
&\quad \frac{1}{P_{b_r+1\dots a\dots b_l}^2} \frac{[\mathcal{F}|P_{b_r+1\dots a\dots b_l}|a\rangle^4 \langle b_l, b_l+1\rangle \langle b_r, b_r+1\rangle}{[\mathcal{F}|P_{b_r+1\dots a\dots b_l}|b_r\rangle [\mathcal{F}|P_{b_r+1\dots a\dots b_l}|b_l+1\rangle [\mathcal{F}|P_{b_r+1\dots a\dots b_l}|b_l\rangle [\mathcal{F}|P_{b_r+1\dots a\dots b_l}|b_r+1\rangle]} \\
&\quad - \langle a|\beta P_{\gamma g}|a\rangle \frac{\langle ag\rangle\langle a\gamma\rangle}{\langle \gamma g\rangle} \frac{\langle gh\rangle}{\langle ga\rangle\langle ah\rangle} \sum_{b_l=b-1}^{f[\text{no sing},*]} \frac{1}{P_{b_l+1\dots a\dots b_l}^2} \frac{[\mathcal{F}|P_{b_l+1\dots a\dots b_l}|a\rangle^3 \langle b_l, b_l+1\rangle \langle ah\rangle}{[\mathcal{F}|P_{b_l+1\dots a\dots b_l}|b_l+1\rangle [\mathcal{F}|P_{b_l+1\dots a\dots b_l}|b_l\rangle [\mathcal{F}|P_{b_l+1\dots a\dots b_l}|h\rangle]} \\
&\quad - \sum_{i=b-1}^{f-1} \langle a|\beta P_{\gamma\dots i}|a\rangle \frac{\langle ag\rangle\langle a\gamma\rangle}{\langle \gamma g\rangle} \frac{\langle i, i+1\rangle}{\langle ia\rangle\langle a, i+1\rangle} \sum_{b_l=b-1}^i \sum_{b_r=\gamma-1}^g \times \\
&\quad \left. \frac{1}{P_{b_r+1\dots a\dots b_l}^2} \frac{[\mathcal{F}|P_{b_r+1\dots a\dots b_l}|a\rangle^4 \langle b_l, b_l+1\rangle \langle b_r, b_r+1\rangle}{[\mathcal{F}|P_{b_r+1\dots a\dots b_l}|b_r\rangle [\mathcal{F}|P_{b_r+1\dots a\dots b_l}|b_l+1\rangle [\mathcal{F}|P_{b_r+1\dots a\dots b_l}|b_l\rangle [\mathcal{F}|P_{b_r+1\dots a\dots b_l}|b_r+1\rangle]} \right) \\
&\quad + Symm_{\gamma g}
\end{aligned} \tag{B.5}$$

where

$$\begin{aligned}
Symm_{\gamma g} = & -\frac{i}{32\pi^2} \frac{[\mathcal{FG}]}{[\mathcal{FG}]} \frac{1}{\langle ab \rangle \cdots \langle fa \rangle} \frac{1}{\langle ag \rangle \cdots \langle na \rangle} \left(\right. \\
& + \frac{\langle a\gamma \rangle \langle ga \rangle}{\langle \gamma g \rangle \langle ah \rangle} \langle a | \beta P_{\gamma g} | h \rangle \sum_{b_l=b-1}^f \sum_{b_r=h}^{n[\text{no sing},*]} \times \\
& \frac{1}{P_{b_r+1\dots a\dots b_l}^2} \frac{[\mathcal{F}|P_{b_r+1\dots a\dots b_l}|a\rangle^4 \langle b_l, b_l+1 \rangle \langle b_r, b_r+1 \rangle}{[\mathcal{F}|P_{b_r+1\dots a\dots b_l}|b_r\rangle [\mathcal{F}|P_{b_r+1\dots a\dots b_l}|b_l+1\rangle [\mathcal{F}|P_{b_r+1\dots a\dots b_l}|b_l\rangle [\mathcal{F}|P_{b_r+1\dots a\dots b_l}|b_r+1\rangle]} \\
& - \sum_{i=h}^n \langle a | \beta P_{\gamma\dots i} | a \rangle \frac{\langle ag \rangle \langle a\gamma \rangle}{\langle \gamma g \rangle} \frac{\langle i, i+1 \rangle}{\langle ia \rangle \langle a, i+1 \rangle} \sum_{b_l=b-1}^f \sum_{b_r=i+1-1}^{n[\text{no sing},*]} \times \\
& \frac{1}{P_{b_r+1\dots a\dots b_l}^2} \frac{[\mathcal{F}|P_{b_r+1\dots a\dots b_l}|a\rangle^4 \langle b_l, b_l+1 \rangle \langle b_r, b_r+1 \rangle}{[\mathcal{F}|P_{b_r+1\dots a\dots b_l}|b_r\rangle [\mathcal{F}|P_{b_r+1\dots a\dots b_l}|b_l+1\rangle [\mathcal{F}|P_{b_r+1\dots a\dots b_l}|b_l\rangle [\mathcal{F}|P_{b_r+1\dots a\dots b_l}|b_r+1\rangle]} \\
& - \sum_{i=b-1}^{f-1} \langle a | \beta P_{\gamma\dots i} | a \rangle \frac{\langle ag \rangle \langle a\gamma \rangle}{\langle \gamma g \rangle} \frac{\langle i, i+1 \rangle}{\langle ia \rangle \langle a, i+1 \rangle} \sum_{b_l=b-1}^i \sum_{b_r=h}^{n[\text{no sing},*]} \times \\
& \left. \frac{1}{P_{b_r+1\dots a\dots b_l}^2} \frac{[\mathcal{F}|P_{b_r+1\dots a\dots b_l}|a\rangle^4 \langle b_l, b_l+1 \rangle \langle b_r, b_r+1 \rangle}{[\mathcal{F}|P_{b_r+1\dots a\dots b_l}|b_r\rangle [\mathcal{F}|P_{b_r+1\dots a\dots b_l}|b_l+1\rangle [\mathcal{F}|P_{b_r+1\dots a\dots b_l}|b_l\rangle [\mathcal{F}|P_{b_r+1\dots a\dots b_l}|b_r+1\rangle]} \right) \\
& \quad \quad \quad (B.6)
\end{aligned}$$

The two contributions to b_r in the first term will need further manipulating so we explicitly write these, along with the $i = b - 1$ and subsequently $b_l = i$ terms from the triple sum to leave,

$$\begin{aligned}
\mathbb{C}^{\text{sp}} = & -\frac{i}{32\pi^2} \frac{[\mathcal{F}\mathcal{G}]}{\langle \mathcal{F}\mathcal{G} \rangle} \frac{1}{\langle ab \rangle \cdots \langle fa \rangle} \frac{1}{\langle ag \rangle \cdots \langle na \rangle} \left(\right. \\
& \langle a|\beta P_{\beta\gamma}|a \rangle \sum_{b_l=b-1}^{f-1} \frac{1}{P_{g\dots a\dots b_l}^2} \frac{[\mathcal{F}|P_{g\dots a\dots b_l}|a]^3 \langle b_l, b_l+1 \rangle \langle ag \rangle}{[\mathcal{F}|P_{g\dots a\dots b_l}|b_l+1][\mathcal{F}|P_{g\dots a\dots b_l}|b_l][\mathcal{F}|P_{g\dots a\dots b_l}|g]} \\
& + \langle a|\beta P_{\beta\gamma}|a \rangle \sum_{b_l=b-1}^f \frac{1}{P_{h\dots a\dots b_l}^2} \frac{[\mathcal{F}|P_{h\dots a\dots b_l}|a]^4 \langle b_l, b_l+1 \rangle \langle gh \rangle}{[\mathcal{F}|P_{h\dots a\dots b_l}|g][\mathcal{F}|P_{h\dots a\dots b_l}|b_l+1][\mathcal{F}|P_{h\dots a\dots b_l}|b_l][\mathcal{F}|P_{h\dots a\dots b_l}|h]} \\
& + \langle a|\beta P_{\gamma g}|a \rangle \frac{\langle a\gamma \rangle \langle gh \rangle}{\langle \gamma g \rangle \langle ah \rangle} \sum_{b_l=b-1}^{f[\text{no sing},*]} \frac{1}{P_{h\dots a\dots b_l}^2} \frac{[\mathcal{F}|P_{h\dots a\dots b_l}|a]^3 \langle b_l, b_l+1 \rangle \langle ah \rangle}{[\mathcal{F}|P_{h\dots a\dots b_l}|b_l+1][\mathcal{F}|P_{h\dots a\dots b_l}|b_l][\mathcal{F}|P_{h\dots a\dots b_l}|h]} \\
& - \langle a|\beta P_{\gamma\dots a}|a \rangle \frac{\langle ag \rangle \langle a\gamma \rangle}{\langle \gamma g \rangle} \sum_{b_r=\gamma-1}^g \frac{1}{P_{b_r+1\dots a}^2} \frac{[\mathcal{F}|P_{b_r+1\dots a}|a]^2 \langle b_r, b_r+1 \rangle}{[\mathcal{F}|P_{b_r+1\dots a}|b_r][\mathcal{F}|P_{b_r+1\dots a}|b_r+1]} \\
& - \sum_{i=b}^{f-1} \langle a|\beta P_{\gamma\dots i}|a \rangle \frac{\langle ag \rangle \langle a\gamma \rangle}{\langle \gamma g \rangle} \frac{\langle i, i+1 \rangle}{\langle ia \rangle \langle a, i+1 \rangle} \sum_{b_r=\gamma-1}^g \times \\
& \quad \frac{1}{P_{i+1\dots a\dots b_r}^2} \frac{[\mathcal{F}|P_{i+1\dots a\dots b_r}|a]^3 \langle ia \rangle \langle b_r, b_r+1 \rangle}{[\mathcal{F}|P_{i+1\dots a\dots b_r}|b_r][\mathcal{F}|P_{i+1\dots a\dots b_r}|i][\mathcal{F}|P_{i+1\dots a\dots b_r}|b_r+1]} \\
& - \sum_{i=b}^{f-1} \langle a|\beta P_{\gamma\dots i}|a \rangle \frac{\langle ag \rangle \langle a\gamma \rangle}{\langle \gamma g \rangle} \frac{\langle i, i+1 \rangle}{\langle ia \rangle \langle a, i+1 \rangle} \sum_{b_l=b-1}^{i-1} \sum_{b_r=\gamma-1}^g \times \\
& \quad \frac{1}{P_{b_r+1\dots a\dots b_l}^2} \frac{[\mathcal{F}|P_{b_r+1\dots a\dots b_l}|a]^4 \langle b_l, b_l+1 \rangle \langle b_r, b_r+1 \rangle}{[\mathcal{F}|P_{b_r+1\dots a\dots b_l}|b_r][\mathcal{F}|P_{b_r+1\dots a\dots b_l}|b_l+1][\mathcal{F}|P_{b_r+1\dots a\dots b_l}|b_l][\mathcal{F}|P_{b_r+1\dots a\dots b_l}|b_r+1]} \Big) \\
& + \text{Symm}_{\gamma g}
\end{aligned} \tag{B.7}$$

where we have dropped the $b_l = f$ term from the first sum since this is the double pole contribution.

Now some mileage is gained by reordering the final double sum involving i , we reorganise them to run up to $(f - 1)$ and $(f - 2)$ rather than from $(b - 1)$ and b , such

that the following are equivalent,

$$\sum_{i=b}^{f-1} \sum_{b_l=b-1}^{i-1} \equiv \sum_{b_l=b-1}^{f-2} \sum_{i=b_l+1}^{f-1} \quad (\text{B.8})$$

and we can make the following simplification,

$$\begin{aligned} \sum_{b_l=b-1}^{f-2} \sum_{i=b_l+1}^{f-1} \langle a | \beta P_{\gamma \dots i} | a \rangle \frac{\langle i, i+1 \rangle}{\langle ia \rangle \langle a, i+1 \rangle} &= \sum_{b_l=b-1}^{f-2} \sum_{i=b_l+1}^{f-1} \frac{\langle a | \beta P_{\gamma \dots i} | i+1 \rangle \langle ia \rangle + \langle a | \beta P_{\gamma \dots i} | i \rangle \langle a, i+1 \rangle}{\langle ia \rangle \langle a, i+1 \rangle} \\ &= \sum_{b_l=b-1}^{f-2} \sum_{i=b_l+1}^{f-1} \frac{\langle a | \beta P_{\gamma \dots i} | i \rangle}{\langle ia \rangle} - \frac{\langle a | \beta P_{\gamma \dots i} | i+1 \rangle}{\langle i+1, a \rangle} \\ &= \sum_{b_l=b-1}^{f-2} \frac{\langle a | \beta P_{\gamma \dots b_l} | b_l+1 \rangle}{\langle b_l+1, a \rangle} - \frac{\langle a | \beta P_{\gamma \dots f} | f \rangle}{\langle fa \rangle} \end{aligned} \quad (\text{B.9})$$

where the final term is equal to β^2 that we are insensitive to in the calculation.

Thus the contribution becomes,

$$\begin{aligned}
\mathcal{C}^{\text{sp}} = & -\frac{i}{32\pi^2} \frac{[\mathcal{F}\mathcal{G}]}{\langle \mathcal{F}\mathcal{G} \rangle} \frac{1}{\langle ab \rangle \cdots \langle fa \rangle} \frac{1}{\langle ag \rangle \cdots \langle na \rangle} \left(\right. \\
& \langle a | \beta P_{\beta\gamma} | a \rangle \sum_{b_l=b-1}^{f-1} \frac{1}{P_{g\dots a\dots b_l}^2} \frac{[\mathcal{F}|P_{g\dots a\dots b_l}|a\rangle^3 \langle b_l, b_l+1 \rangle \langle ag \rangle}{[\mathcal{F}|P_{g\dots a\dots b_l}|b_l+1\rangle [\mathcal{F}|P_{g\dots a\dots b_l}|b_l\rangle [\mathcal{F}|P_{g\dots a\dots b_l}|g\rangle} \\
& + \langle a | \beta P_{\beta\gamma} | a \rangle \sum_{b_l=b-1}^f \frac{1}{P_{h\dots a\dots b_l}^2} \frac{[\mathcal{F}|P_{h\dots a\dots b_l}|a\rangle^4 \langle b_l, b_l+1 \rangle \langle gh \rangle}{[\mathcal{F}|P_{h\dots a\dots b_l}|g\rangle [\mathcal{F}|P_{h\dots a\dots b_l}|b_l+1\rangle [\mathcal{F}|P_{h\dots a\dots b_l}|b_l\rangle [\mathcal{F}|P_{h\dots a\dots b_l}|h\rangle} \\
& + \langle a | \beta P_{\gamma g} | a \rangle \frac{\langle a\gamma \rangle \langle gh \rangle}{\langle \gamma g \rangle \langle ah \rangle} \sum_{b_l=b-1}^{f[\text{no sing},*]} \frac{1}{P_{h\dots a\dots b_l}^2} \frac{[\mathcal{F}|P_{h\dots a\dots b_l}|a\rangle^3 \langle b_l, b_l+1 \rangle \langle ah \rangle}{[\mathcal{F}|P_{h\dots a\dots b_l}|b_l+1\rangle [\mathcal{F}|P_{h\dots a\dots b_l}|b_l\rangle [\mathcal{F}|P_{h\dots a\dots b_l}|h\rangle} \\
& - \langle a | \beta P_{\gamma\dots a} | a \rangle \frac{\langle ag \rangle \langle a\gamma \rangle}{\langle \gamma g \rangle} \sum_{b_r=\gamma-1}^g \frac{1}{P_{b_r+1\dots a}^2} \frac{[\mathcal{F}|P_{b_r+1\dots a}|a\rangle^2 \langle b_r, b_r+1 \rangle}{[\mathcal{F}|P_{b_r+1\dots a}|b_r\rangle [\mathcal{F}|P_{b_r+1\dots a}|b_r+1\rangle} \\
& - \sum_{i=b}^{f-1} \langle a | \beta P_{\gamma\dots i} | a \rangle \frac{\langle ag \rangle \langle a\gamma \rangle}{\langle \gamma g \rangle} \frac{\langle i, i+1 \rangle}{\langle ia \rangle \langle a, i+1 \rangle} \sum_{b_r=\gamma-1}^g \times \\
& \quad \frac{1}{P_{i+1\dots a\dots b_l}^2} \frac{[\mathcal{F}|P_{i+1\dots a\dots b_l}|a\rangle^3 \langle ia \rangle \langle b_r, b_r+1 \rangle}{[\mathcal{F}|P_{i+1\dots a\dots b_l}|b_r\rangle [\mathcal{F}|P_{i+1\dots a\dots b_l}|i\rangle [\mathcal{F}|P_{i+1\dots a\dots b_l}|b_r+1\rangle} \\
& - \sum_{b_r=\gamma-1}^g \sum_{b_l=b-1}^{f-2} \frac{\langle a | \beta P_{\gamma\dots b_l} | b_l+1 \rangle}{\langle b_l+1, a \rangle} \frac{\langle ag \rangle \langle a\gamma \rangle}{\langle \gamma g \rangle} \times \\
& \quad \frac{1}{P_{b_r+1\dots a\dots b_l}^2} \frac{[\mathcal{F}|P_{b_r+1\dots a\dots b_l}|a\rangle^4 \langle b_l, b_l+1 \rangle \langle b_r, b_r+1 \rangle}{[\mathcal{F}|P_{b_r+1\dots a\dots b_l}|b_r\rangle [\mathcal{F}|P_{b_r+1\dots a\dots b_l}|b_l+1\rangle [\mathcal{F}|P_{b_r+1\dots a\dots b_l}|b_l\rangle [\mathcal{F}|P_{b_r+1\dots a\dots b_l}|b_r+1\rangle} \Big) \\
& + \text{Symm}_{\gamma g}
\end{aligned} \tag{B.10}$$

where we can suck the single sum over b_r proportional to $-\langle a | \beta P_{\gamma\dots a} | a \rangle$ as the $i = b-1$ term into the double sum below it. Thus we can combine the common pieces of the double sum by identifying i 's summations as equivalent to that of b_l 's up to a spare term from the original $i = f-1$ term,

$$\begin{aligned}
\mathcal{C}^{\text{sp}} = & -\frac{i}{32\pi^2} \frac{[\mathcal{F}\mathcal{G}]}{\langle \mathcal{F}\mathcal{G} \rangle} \frac{1}{\langle ab \rangle \cdots \langle fa \rangle} \frac{1}{\langle ag \rangle \cdots \langle na \rangle} \left(\right. \\
& \langle a | \beta P_{\beta\gamma} | a \rangle \sum_{b_l=b-1}^{f-1} \frac{1}{P_{g\dots a\dots b_l}^2} \frac{[\mathcal{F}|P_{g\dots a\dots b_l}|a\rangle^3 \langle b_l, b_l+1 \rangle \langle ag \rangle}{[\mathcal{F}|P_{g\dots a\dots b_l}|b_l+1\rangle [\mathcal{F}|P_{g\dots a\dots b_l}|b_l\rangle [\mathcal{F}|P_{g\dots a\dots b_l}|g\rangle]} \\
& + \langle a | \beta P_{\beta\gamma} | a \rangle \sum_{b_l=b-1}^f \frac{1}{P_{h\dots a\dots b_l}^2} \frac{[\mathcal{F}|P_{h\dots a\dots b_l}|a\rangle^4 \langle b_l, b_l+1 \rangle \langle gh \rangle}{[\mathcal{F}|P_{h\dots a\dots b_l}|g\rangle [\mathcal{F}|P_{h\dots a\dots b_l}|b_l+1\rangle [\mathcal{F}|P_{h\dots a\dots b_l}|b_l\rangle [\mathcal{F}|P_{h\dots a\dots b_l}|h\rangle]} \\
& + \langle a | \beta P_{\gamma g} | a \rangle \frac{\langle a\gamma \rangle \langle gh \rangle}{\langle \gamma g \rangle \langle ah \rangle} \sum_{b_l=b-1}^{f[\text{no sing},*]} \frac{1}{P_{h\dots a\dots b_l}^2} \frac{[\mathcal{F}|P_{h\dots a\dots b_l}|a\rangle^3 \langle b_l, b_l+1 \rangle \langle ah \rangle}{[\mathcal{F}|P_{h\dots a\dots b_l}|b_l+1\rangle [\mathcal{F}|P_{h\dots a\dots b_l}|b_l\rangle [\mathcal{F}|P_{h\dots a\dots b_l}|h\rangle]} \\
& - \langle a | \beta P_{\gamma\dots f-1} | a \rangle \frac{\langle ag \rangle \langle a\gamma \rangle}{\langle \gamma g \rangle} \frac{\langle f-1, f \rangle}{\langle af \rangle} \sum_{b_r=\gamma-1}^g \times \\
& \frac{1}{P_{b_r+1\dots a\dots f-1}^2} \frac{[\mathcal{F}|P_{b_r+1\dots a\dots f-1}|a\rangle^3 \langle b_r, b_r+1 \rangle}{[\mathcal{F}|P_{b_r+1\dots a\dots f-1}|b_r\rangle [\mathcal{F}|P_{b_r+1\dots a\dots f-1}|f-1\rangle [\mathcal{F}|P_{b_r+1\dots a\dots f-1}|b_r+1\rangle]} \\
& - \frac{\langle ag \rangle \langle a\gamma \rangle}{\langle \gamma g \rangle} \sum_{b_r=\gamma-1}^g \sum_{b_l=b-1}^{f-2} \frac{\langle a | \beta P_{\gamma\dots b_l} | b_l+1 \rangle [\mathcal{F}|P_{b_r+1\dots a\dots b_l}|a\rangle - \langle a | \beta P_{\gamma\dots b_l} | a \rangle [\mathcal{F}|P_{b_r+1\dots a\dots b_l}|b_l+1\rangle}{\langle b_l+1, a \rangle} \\
& \times \frac{1}{P_{b_r+1\dots a\dots b_l}^2} \frac{[\mathcal{F}|P_{b_r+1\dots a\dots b_l}|a\rangle^3 \langle b_l, b_l+1 \rangle \langle b_r, b_r+1 \rangle}{[\mathcal{F}|P_{b_r+1\dots a\dots b_l}|b_r\rangle [\mathcal{F}|P_{b_r+1\dots a\dots b_l}|b_l+1\rangle [\mathcal{F}|P_{b_r+1\dots a\dots b_l}|b_l\rangle [\mathcal{F}|P_{b_r+1\dots a\dots b_l}|b_r+1\rangle]} \Big) \\
& + \text{Symm}_{\gamma g}
\end{aligned} \tag{B.11}$$

where the terms left in the double sum can be simplified using the Schouten identity, and also all terms with $P_{h\dots a\dots b_l}$ combine to use the Schouten identity in a similar way.

Once used twice, we are left with,

$$\begin{aligned}
\mathcal{C}^{\text{sp}} = & -\frac{i}{32\pi^2} \frac{[\mathcal{FG}]}{[\mathcal{FG}]} \frac{1}{\langle ab \rangle \cdots \langle fa \rangle} \frac{1}{\langle ag \rangle \cdots \langle na \rangle} \left(\right. \\
& \langle a | \beta P_{\beta\gamma} | a \rangle \sum_{b_l=b-1}^{f-1} \frac{1}{P_{g\dots a\dots b_l}^2} \frac{[\mathcal{F}|P_{g\dots a\dots b_l}|a\rangle^3 \langle b_l, b_l+1 \rangle \langle ag \rangle}{[\mathcal{F}|P_{g\dots a\dots b_l}|b_l+1\rangle [\mathcal{F}|P_{g\dots a\dots b_l}|b_l\rangle [\mathcal{F}|P_{g\dots a\dots b_l}|g\rangle} \\
& + \frac{\langle gh \rangle \langle a\gamma \rangle \langle ag \rangle}{\langle \gamma g \rangle} \sum_{b_l=b-1}^f \frac{1}{P_{h\dots a\dots b_l}^2} \frac{\langle a | \beta P_{\gamma g} P_{h\dots a\dots b_l} | \mathcal{F} \rangle [\mathcal{F}|P_{h\dots a\dots b_l}|a\rangle^3 \langle b_l, b_l+1 \rangle}{[\mathcal{F}|P_{h\dots a\dots b_l}|b_l+1\rangle [\mathcal{F}|P_{h\dots a\dots b_l}|b_l\rangle [\mathcal{F}|P_{h\dots a\dots b_l}|h\rangle [\mathcal{F}|P_{h\dots a\dots b_l}|g\rangle} \\
& - \langle a | \beta P_{\gamma\dots f-1} | a \rangle \frac{\langle ag \rangle \langle a\gamma \rangle}{\langle \gamma g \rangle} \frac{\langle f-1, f \rangle}{\langle af \rangle} \sum_{b_r=\gamma-1}^g \times \\
& \frac{1}{P_{b_r+1\dots a\dots f-1}^2} \frac{[\mathcal{F}|P_{b_r+1\dots a\dots f-1}|a\rangle^3 \langle b_r, b_r+1 \rangle}{[\mathcal{F}|P_{b_r+1\dots a\dots f-1}|b_r\rangle [\mathcal{F}|P_{b_r+1\dots a\dots f-1}|f-1\rangle [\mathcal{F}|P_{b_r+1\dots a\dots f-1}|b_r+1\rangle} \\
& - \frac{\langle ag \rangle \langle a\gamma \rangle}{\langle \gamma g \rangle} \sum_{b_r=\gamma-1}^g \sum_{b_l=b-1}^{f-2} \langle a | \beta P_{\gamma\dots b_l} P_{b_r+1\dots a\dots b_l} | \mathcal{F} \rangle \\
& \times \frac{1}{P_{b_r+1\dots a\dots b_l}^2} \frac{[\mathcal{F}|P_{b_r+1\dots a\dots b_l}|a\rangle^3 \langle b_l, b_l+1 \rangle \langle b_r, b_r+1 \rangle}{[\mathcal{F}|P_{b_r+1\dots a\dots b_l}|b_r\rangle [\mathcal{F}|P_{b_r+1\dots a\dots b_l}|b_l+1\rangle [\mathcal{F}|P_{b_r+1\dots a\dots b_l}|b_l\rangle [\mathcal{F}|P_{b_r+1\dots a\dots b_l}|b_r+1\rangle} \Big) \\
& + \text{Symm}_{\gamma g}
\end{aligned} \tag{B.12}$$

where we see some tantalising glimpses of $P_{\beta\gamma g}^2$ that will hopefully cancel with propagators later on.

Expanding out the sums in b_r we are left with,

$$\begin{aligned}
\mathbb{C}^{\text{sp}} = & -\frac{i}{32\pi^2} \frac{[\mathcal{FG}]}{\langle \mathcal{FG} \rangle} \frac{1}{\langle ab \rangle \cdots \langle fa \rangle} \frac{1}{\langle ag \rangle \cdots \langle na \rangle} \left(\right. \\
& \langle a|\beta P_{\beta\gamma}|a \rangle \sum_{b_l=b-1}^{f-1} \frac{1}{P_{g\dots a\dots b_l}^2} \frac{[\mathcal{F}|P_{g\dots a\dots b_l}|a \rangle^3 \langle b_l, b_l+1 \rangle \langle ag \rangle}{[\mathcal{F}|P_{g\dots a\dots b_l}|b_l+1 \rangle [\mathcal{F}|P_{g\dots a\dots b_l}|b_l \rangle [\mathcal{F}|P_{g\dots a\dots b_l}|g \rangle} \\
& + \frac{\langle gh \rangle \langle a\gamma \rangle \langle ag \rangle}{\langle \gamma g \rangle} \sum_{b_l=b-1}^f \frac{1}{P_{h\dots a\dots b_l}^2} \frac{\langle a|\beta P_{\gamma g} P_{h\dots a\dots b_l} |\mathcal{F}| [\mathcal{F}|P_{h\dots a\dots b_l}|a \rangle^3 \langle b_l, b_l+1 \rangle}{[\mathcal{F}|P_{h\dots a\dots b_l}|b_l+1 \rangle [\mathcal{F}|P_{h\dots a\dots b_l}|b_l \rangle [\mathcal{F}|P_{h\dots a\dots b_l}|h \rangle [\mathcal{F}|P_{h\dots a\dots b_l}|g \rangle} \\
& - \langle a|\beta P_{\gamma\dots f-1}|a \rangle \frac{\langle ag \rangle \langle a\gamma \rangle \langle f-1, f \rangle}{\langle \gamma g \rangle \langle af \rangle} \frac{1}{P_{\gamma\dots a\dots f-1}^2} \frac{[\mathcal{F}|P_{\gamma\dots a\dots f-1}|a \rangle^2 \langle a\gamma \rangle}{[\mathcal{F}|P_{\gamma\dots a\dots f-1}|f-1 \rangle [\mathcal{F}|P_{\gamma\dots a\dots f-1}|\gamma \rangle} \\
& - \langle a|\beta P_{\gamma\dots f-1}|a \rangle \frac{\langle ag \rangle \langle a\gamma \rangle \langle f-1, f \rangle}{\langle \gamma g \rangle \langle af \rangle} \frac{1}{P_{g\dots a\dots f-1}^2} \frac{[\mathcal{F}|P_{g\dots a\dots f-1}|a \rangle^3 \langle \gamma g \rangle}{[\mathcal{F}|P_{g\dots a\dots f-1}|\gamma \rangle [\mathcal{F}|P_{g\dots a\dots f-1}|f-1 \rangle [\mathcal{F}|P_{g\dots a\dots f-1}|g \rangle} \\
& - \langle a|\beta P_{\gamma\dots f-1}|a \rangle \frac{\langle ag \rangle \langle a\gamma \rangle \langle f-1, f \rangle}{\langle \gamma g \rangle \langle af \rangle} \frac{1}{P_{h\dots a\dots f-1}^2} \frac{[\mathcal{F}|P_{h\dots a\dots f-1}|a \rangle^3 \langle gh \rangle}{[\mathcal{F}|P_{h\dots a\dots f-1}|g \rangle [\mathcal{F}|P_{h\dots a\dots f-1}|f-1 \rangle [\mathcal{F}|P_{h\dots a\dots f-1}|h \rangle} \\
& - \frac{\langle ag \rangle \langle a\gamma \rangle}{\langle \gamma g \rangle} \sum_{b_l=b-1}^{f-2} \frac{\langle a|\beta P_{\gamma\dots b_l} P_{\gamma\dots a\dots b_l} |\mathcal{F}|}{P_{\gamma\dots a\dots b_l}^2} \frac{[\mathcal{F}|P_{\gamma\dots a\dots b_l}|a \rangle^2 \langle b_l, b_l+1 \rangle \langle a\gamma \rangle}{[\mathcal{F}|P_{\gamma\dots a\dots b_l}|b_l+1 \rangle [\mathcal{F}|P_{\gamma\dots a\dots b_l}|b_l \rangle [\mathcal{F}|P_{\gamma\dots a\dots b_l}|\gamma \rangle} \\
& - \frac{\langle ag \rangle \langle a\gamma \rangle}{\langle \gamma g \rangle} \sum_{b_l=b-1}^{f-2} \frac{1}{P_{g\dots a\dots b_l}^2} \frac{\langle a|\beta P_{\gamma\dots b_l} P_{g\dots a\dots b_l} |\mathcal{F}| [\mathcal{F}|P_{g\dots a\dots b_l}|a \rangle^3 \langle b_l, b_l+1 \rangle \langle \gamma g \rangle}{[\mathcal{F}|P_{g\dots a\dots b_l}|\gamma \rangle [\mathcal{F}|P_{g\dots a\dots b_l}|b_l+1 \rangle [\mathcal{F}|P_{g\dots a\dots b_l}|b_l \rangle [\mathcal{F}|P_{g\dots a\dots b_l}|g \rangle} \\
& - \frac{\langle ag \rangle \langle a\gamma \rangle}{\langle \gamma g \rangle} \sum_{b_l=b-1}^{f-2} \frac{1}{P_{h\dots a\dots b_l}^2} \frac{\langle a|\beta P_{\gamma\dots b_l} P_{h\dots a\dots b_l} |\mathcal{F}| [\mathcal{F}|P_{h\dots a\dots b_l}|a \rangle^3 \langle b_l, b_l+1 \rangle \langle gh \rangle}{[\mathcal{F}|P_{h\dots a\dots b_l}|g \rangle [\mathcal{F}|P_{h\dots a\dots b_l}|b_l+1 \rangle [\mathcal{F}|P_{h\dots a\dots b_l}|b_l \rangle [\mathcal{F}|P_{h\dots a\dots b_l}|h \rangle} \left. \right) \\
& + \text{Symm}_{\gamma g}
\end{aligned} \tag{B.13}$$

Now all the $P_{h\dots a\dots b_l}$ terms have a common $\langle gh \rangle$ factor that can be used to cancel against factors in the denominator as follows,

$$[\mathcal{F}|P_{h\dots a\dots b_l}|a \rangle \langle gh \rangle = [\mathcal{F}|P_{h\dots a\dots b_l}|g \rangle \langle ah \rangle + [\mathcal{F}|P_{h\dots a\dots b_l}|h \rangle \langle ga \rangle \tag{B.14}$$

while the first term reveals some new $g \leftrightarrow \gamma$ interchangeable terms which can be put into $\text{Symm}_{\gamma g}$, while the second terms clean up some of the denominators. Moving the

like terms into similar groupings, we are then left with,

$$\begin{aligned}
\mathbb{C}^{\text{sp}} = & -\frac{i}{32\pi^2} \frac{[\mathcal{FG}]}{[\mathcal{FG}]} \frac{1}{\langle ab \rangle \cdots \langle fa \rangle} \frac{1}{\langle ag \rangle \cdots \langle na \rangle} \left(\right. \\
& - \frac{\langle ag \rangle \langle a\gamma \rangle}{\langle \gamma g \rangle} \sum_{b_l=b-1}^{f-2} \frac{\langle a|\beta P_{\gamma\dots b_l} P_{\gamma\dots a\dots b_l}|\mathcal{F}\rangle}{P_{\gamma\dots a\dots b_l}^2} \frac{[\mathcal{F}|P_{\gamma\dots a\dots b_l}|a\rangle^2 \langle b_l, b_l+1 \rangle \langle a\gamma \rangle}{[\mathcal{F}|P_{\gamma\dots a\dots b_l}|b_l+1\rangle [\mathcal{F}|P_{\gamma\dots a\dots b_l}|b_l\rangle [\mathcal{F}|P_{\gamma\dots a\dots b_l}|\gamma\rangle} \\
& - \langle a|\beta P_{\gamma\dots f-1}|a\rangle \frac{\langle ag \rangle \langle a\gamma \rangle}{\langle \gamma g \rangle} \frac{\langle f-1, f \rangle}{\langle af \rangle} \frac{1}{P_{\gamma\dots a\dots f-1}^2} \frac{[\mathcal{F}|P_{\gamma\dots a\dots f-1}|a\rangle^2 \langle a\gamma \rangle}{[\mathcal{F}|P_{\gamma\dots a\dots f-1}|f-1\rangle [\mathcal{F}|P_{\gamma\dots a\dots f-1}|\gamma\rangle} \\
& + \langle a|\beta P_{\beta\gamma}|a\rangle \sum_{b_l=b-1}^{f-1} \frac{1}{P_{g\dots a\dots b_l}^2} \frac{[\mathcal{F}|P_{g\dots a\dots b_l}|a\rangle^3 \langle b_l, b_l+1 \rangle \langle ag \rangle}{[\mathcal{F}|P_{g\dots a\dots b_l}|b_l+1\rangle [\mathcal{F}|P_{g\dots a\dots b_l}|b_l\rangle [\mathcal{F}|P_{g\dots a\dots b_l}|g\rangle} \\
& - \langle a|\beta P_{\gamma\dots f-1}|a\rangle \frac{\langle ag \rangle \langle a\gamma \rangle}{\langle \gamma g \rangle} \frac{\langle f-1, f \rangle}{\langle af \rangle} \frac{1}{P_{g\dots a\dots f-1}^2} \frac{[\mathcal{F}|P_{g\dots a\dots f-1}|a\rangle^3 \langle \gamma g \rangle}{[\mathcal{F}|P_{g\dots a\dots f-1}|\gamma\rangle [\mathcal{F}|P_{g\dots a\dots f-1}|f-1\rangle [\mathcal{F}|P_{g\dots a\dots f-1}|g\rangle} \\
& - \frac{\langle ag \rangle \langle a\gamma \rangle}{\langle \gamma g \rangle} \sum_{b_l=b-1}^{f-2} \frac{1}{P_{g\dots a\dots b_l}^2} \frac{\langle a|\beta P_{\gamma\dots b_l} P_{g\dots a\dots b_l}|\mathcal{F}\rangle [\mathcal{F}|P_{g\dots a\dots b_l}|a\rangle^3 \langle b_l, b_l+1 \rangle \langle \gamma g \rangle}{[\mathcal{F}|P_{g\dots a\dots b_l}|\gamma\rangle [\mathcal{F}|P_{g\dots a\dots b_l}|b_l+1\rangle [\mathcal{F}|P_{g\dots a\dots b_l}|b_l\rangle [\mathcal{F}|P_{g\dots a\dots b_l}|g\rangle} \\
& - \langle a|\beta P_{\gamma\dots f-1}|a\rangle \frac{\langle ag \rangle \langle a\gamma \rangle}{\langle \gamma g \rangle} \frac{\langle f-1, f \rangle}{\langle af \rangle} \frac{1}{P_{h\dots a\dots f-1}^2} \frac{[\mathcal{F}|P_{h\dots a\dots f-1}|a\rangle^3 \langle gh \rangle}{[\mathcal{F}|P_{h\dots a\dots f-1}|g\rangle [\mathcal{F}|P_{h\dots a\dots f-1}|f-1\rangle [\mathcal{F}|P_{h\dots a\dots f-1}|h\rangle} \\
& + \frac{\langle ga \rangle \langle a\gamma \rangle \langle ag \rangle}{\langle \gamma g \rangle} \sum_{b_l=b-1}^f \frac{1}{P_{h\dots a\dots b_l}^2} \frac{\langle a|\beta P_{\gamma g} P_{h\dots a\dots b_l}|\mathcal{F}\rangle [\mathcal{F}|P_{h\dots a\dots b_l}|a\rangle^2 \langle b_l, b_l+1 \rangle}{[\mathcal{F}|P_{h\dots a\dots b_l}|b_l+1\rangle [\mathcal{F}|P_{h\dots a\dots b_l}|b_l\rangle [\mathcal{F}|P_{h\dots a\dots b_l}|g\rangle} \\
& - \frac{\langle ag \rangle \langle a\gamma \rangle}{\langle \gamma g \rangle} \sum_{b_l=b-1}^{f-2} \frac{1}{P_{h\dots a\dots b_l}^2} \frac{\langle a|\beta P_{\gamma\dots b_l} P_{h\dots a\dots b_l}|\mathcal{F}\rangle [\mathcal{F}|P_{h\dots a\dots b_l}|a\rangle^2 \langle b_l, b_l+1 \rangle \langle ga \rangle}{[\mathcal{F}|P_{h\dots a\dots b_l}|g\rangle [\mathcal{F}|P_{b_l+1\dots a\dots b_l}|b_l+1\rangle [\mathcal{F}|P_{h\dots a\dots b_l}|b_l\rangle} \Big) \\
& + \text{Symm}_{\gamma g}
\end{aligned} \tag{B.15}$$

where

$$\begin{aligned}
Symm_{\gamma g} = & -\frac{i}{32\pi^2} \frac{[\mathcal{F}\mathcal{G}]}{\langle \mathcal{F}\mathcal{G} \rangle} \frac{1}{\langle ab \rangle \cdots \langle fa \rangle} \frac{1}{\langle ag \rangle \cdots \langle na \rangle} \left(\right. \\
& - \frac{\langle ag \rangle \langle a\gamma \rangle}{\langle \gamma g \rangle} \sum_{b_l=b-1}^{f-2} \frac{1}{P^2_{b-1 \dots a \dots b_l}} \frac{\langle a|\beta P_{\gamma \dots b_l} P_{h \dots a \dots b_l} |\mathcal{F}\rangle [\mathcal{F}|P_{h \dots a \dots b_l} |a\rangle^2 \langle b_l, b_l+1 \rangle \langle ah \rangle}{[\mathcal{F}|P_{b_r+1 \dots a \dots b_l} |b_l+1\rangle [\mathcal{F}|P_{h \dots a \dots b_l} |b_l\rangle [\mathcal{F}|P_{h \dots a \dots b_l} |h\rangle]} \\
& + \frac{\langle a\gamma \rangle \langle ga \rangle}{\langle \gamma g \rangle} \sum_{b_l=b-1}^f \frac{1}{P^2_{b-1 \dots a \dots b_l}} \langle ha \rangle \frac{\langle a|\beta P_{\gamma g} P_{h \dots a \dots b_l} |\mathcal{F}\rangle [\mathcal{F}|P_{h \dots a \dots b_l} |a\rangle^2 \langle b_l, b_l+1 \rangle}{[\mathcal{F}|P_{h \dots a \dots b_l} |b_l+1\rangle [\mathcal{F}|P_{h \dots a \dots b_l} |b_l\rangle [\mathcal{F}|P_{h \dots a \dots b_l} |h\rangle]} \\
& + \frac{\langle a\gamma \rangle \langle ga \rangle}{\langle \gamma g \rangle \langle ah \rangle} \langle a|\beta P_{\gamma g} |h\rangle \sum_{b_l=b-1}^f \sum_{b_r=h}^{n[\text{no sing},*]} \times \\
& \frac{1}{P^2_{b_r+1 \dots a \dots b_l}} \frac{[\mathcal{F}|P_{b_r+1 \dots a \dots b_l} |a\rangle^4 \langle b_l, b_l+1 \rangle \langle b_r, b_r+1 \rangle}{[\mathcal{F}|P_{b_r+1 \dots a \dots b_l} |b_r\rangle [\mathcal{F}|P_{b_r+1 \dots a \dots b_l} |b_l+1\rangle [\mathcal{F}|P_{b_r+1 \dots a \dots b_l} |b_l\rangle [\mathcal{F}|P_{b_r+1 \dots a \dots b_l} |b_r+1\rangle]} \\
& - \sum_{i=h}^n \langle a|\beta P_{\gamma \dots i} |a\rangle \frac{\langle ag \rangle \langle a\gamma \rangle}{\langle \gamma g \rangle} \frac{\langle i, i+1 \rangle}{\langle ia \rangle \langle a, i+1 \rangle} \sum_{b_l=b-1}^f \sum_{b_r=i+1-1}^{n[\text{no sing},*]} \times \\
& \frac{1}{P^2_{b_r+1 \dots a \dots b_l}} \frac{[\mathcal{F}|P_{b_r+1 \dots a \dots b_l} |a\rangle^4 \langle b_l, b_l+1 \rangle \langle b_r, b_r+1 \rangle}{[\mathcal{F}|P_{b_r+1 \dots a \dots b_l} |b_r\rangle [\mathcal{F}|P_{b_r+1 \dots a \dots b_l} |b_l+1\rangle [\mathcal{F}|P_{b_r+1 \dots a \dots b_l} |b_l\rangle [\mathcal{F}|P_{b_r+1 \dots a \dots b_l} |b_r+1\rangle]} \\
& - \sum_{i=b-1}^{f-1} \langle a|\beta P_{\gamma \dots i} |a\rangle \frac{\langle ag \rangle \langle a\gamma \rangle}{\langle \gamma g \rangle} \frac{\langle i, i+1 \rangle}{\langle ia \rangle \langle a, i+1 \rangle} \sum_{b_l=b-1}^i \sum_{b_r=h}^{n[\text{no sing},*]} \times \\
& \frac{1}{P^2_{b_r+1 \dots a \dots b_l}} \frac{[\mathcal{F}|P_{b_r+1 \dots a \dots b_l} |a\rangle^4 \langle b_l, b_l+1 \rangle \langle b_r, b_r+1 \rangle}{[\mathcal{F}|P_{b_r+1 \dots a \dots b_l} |b_r\rangle [\mathcal{F}|P_{b_r+1 \dots a \dots b_l} |b_l+1\rangle [\mathcal{F}|P_{b_r+1 \dots a \dots b_l} |b_l\rangle [\mathcal{F}|P_{b_r+1 \dots a \dots b_l} |b_r+1\rangle]} \left. \right) \\
\end{aligned} \tag{B.16}$$

Now this simplifies further upon noticing that $P_{\gamma \dots f-1} = -\beta - f$. The free terms can be identified with the $b_l = f - 1$ cases and so the terms fit into the sums, leaving us with,

$$\begin{aligned}
\mathcal{C}^{\text{sp}} = & -\frac{i}{32\pi^2} \frac{[\mathcal{FG}]}{[\mathcal{FG}]} \frac{1}{\langle ab \rangle \cdots \langle fa \rangle} \frac{1}{\langle ag \rangle \cdots \langle na \rangle} \left(\right. \\
& + \frac{\langle ag \rangle \langle a\gamma \rangle}{\langle \gamma g \rangle} \sum_{b_l=b-1}^{f-1} \frac{\langle a|\beta P_{\gamma\dots b_l} P_{\gamma\dots a\dots b_l}|\mathcal{F}\rangle}{P_{\gamma\dots a\dots b_l}^2} \frac{[\mathcal{F}|P_{\gamma\dots a\dots b_l}|a]^2 \langle b_l, b_l+1 \rangle \langle a\gamma \rangle}{[\mathcal{F}|P_{\gamma\dots a\dots b_l}|b_l+1][\mathcal{F}|P_{\gamma\dots a\dots b_l}|b_l][\mathcal{F}|P_{\gamma\dots a\dots b_l}|\gamma]} \\
& + \langle a|\beta P_{\beta\gamma}|a \rangle \sum_{b_l=b-1}^{f-1} \frac{1}{P_{g\dots a\dots b_l}^2} \frac{[\mathcal{F}|P_{g\dots a\dots b_l}|a]^3 \langle b_l, b_l+1 \rangle \langle ag \rangle}{[\mathcal{F}|P_{g\dots a\dots b_l}|b_l+1][\mathcal{F}|P_{g\dots a\dots b_l}|b_l][\mathcal{F}|P_{g\dots a\dots b_l}|g]} \\
& + \frac{\langle ag \rangle \langle a\gamma \rangle}{\langle \gamma g \rangle} \sum_{b_l=b-1}^{f-1} \frac{1}{P_{g\dots a\dots b_l}^2} \frac{\langle a|\beta P_{\gamma\dots b_l} P_{g\dots a\dots b_l}|\mathcal{F}\rangle [\mathcal{F}|P_{g\dots a\dots b_l}|a]^3 \langle b_l, b_l+1 \rangle \langle \gamma g \rangle}{[\mathcal{F}|P_{g\dots a\dots b_l}|\gamma][\mathcal{F}|P_{g\dots a\dots b_l}|b_l+1][\mathcal{F}|P_{g\dots a\dots b_l}|b_l][\mathcal{F}|P_{g\dots a\dots b_l}|g]} \\
& + \frac{\langle ga \rangle \langle a\gamma \rangle \langle ag \rangle}{\langle \gamma g \rangle} \sum_{b_l=b-1}^f \frac{1}{P_{h\dots a\dots b_l}^2} \frac{\langle a|\beta P_{\gamma g} P_{h\dots a\dots b_l}|\mathcal{F}\rangle [\mathcal{F}|P_{h\dots a\dots b_l}|a]^2 \langle b_l, b_l+1 \rangle}{[\mathcal{F}|P_{h\dots a\dots b_l}|b_l+1][\mathcal{F}|P_{h\dots a\dots b_l}|b_l][\mathcal{F}|P_{h\dots a\dots b_l}|g]} \\
& + \frac{\langle ga \rangle \langle ag \rangle \langle a\gamma \rangle}{\langle \gamma g \rangle} \sum_{b_l=b-1}^{f-1} \frac{1}{P_{h\dots a\dots b_l}^2} \frac{\langle a|\beta P_{\gamma\dots b_l} P_{h\dots a\dots b_l}|\mathcal{F}\rangle [\mathcal{F}|P_{h\dots a\dots b_l}|a]^2 \langle b_l, b_l+1 \rangle}{[\mathcal{F}|P_{h\dots a\dots b_l}|g][\mathcal{F}|P_{b_r+1\dots a\dots b_l}|b_l+1][\mathcal{F}|P_{h\dots a\dots b_l}|b_l]} \left. \right) \\
& + \text{Symm}_{\gamma g}
\end{aligned} \tag{B.17}$$

where the overlapping sums can be combined to cancel off the P^2 factors to leave,

$$\begin{aligned}
\mathcal{C}^{\text{sp}} = & -\frac{i}{32\pi^2} \frac{[\mathcal{FG}]}{[\mathcal{FG}]} \frac{1}{\langle ab \rangle \cdots \langle fa \rangle} \frac{1}{\langle ag \rangle \cdots \langle na \rangle} \left(\right. \\
& + \frac{\langle ag \rangle \langle a\gamma \rangle}{\langle \gamma g \rangle} \sum_{b_l=b-1}^{f-1} \frac{\langle a|\beta|\mathcal{F}\rangle [\mathcal{F}|P_{\gamma\dots a\dots b_l}|a]^2 \langle b_l, b_l+1 \rangle \langle a\gamma \rangle}{[\mathcal{F}|P_{\gamma\dots a\dots b_l}|b_l+1][\mathcal{F}|P_{\gamma\dots a\dots b_l}|b_l][\mathcal{F}|P_{\gamma\dots a\dots b_l}|\gamma]} \\
& + \frac{\langle ag \rangle \langle a\gamma \rangle}{\langle \gamma g \rangle} \sum_{b_l=b-1}^{f-1} \frac{\langle a|\beta|\mathcal{F}\rangle [\mathcal{F}|P_{g\dots a\dots b_l}|a]^3 \langle b_l, b_l+1 \rangle \langle \gamma g \rangle}{[\mathcal{F}|P_{g\dots a\dots b_l}|\gamma][\mathcal{F}|P_{g\dots a\dots b_l}|b_l+1][\mathcal{F}|P_{g\dots a\dots b_l}|b_l][\mathcal{F}|P_{g\dots a\dots b_l}|g]} \\
& + \frac{\langle ag \rangle \langle a\gamma \rangle}{\langle \gamma g \rangle} \sum_{b_l=b-1}^{f-1} \frac{\langle a|\beta|\mathcal{F}\rangle [\mathcal{F}|P_{h\dots a\dots b_l}|a]^2 \langle b_l, b_l+1 \rangle \langle ga \rangle}{[\mathcal{F}|P_{h\dots a\dots b_l}|g][\mathcal{F}|P_{b_r+1\dots a\dots b_l}|b_l+1][\mathcal{F}|P_{h\dots a\dots b_l}|b_l]} \\
& + \frac{\langle ga \rangle \langle a\gamma \rangle \langle ag \rangle}{\langle \gamma g \rangle} \frac{\langle a|\beta|\mathcal{F}\rangle [\mathcal{F}|P_{\beta\gamma g}|a] \langle fa \rangle}{[\mathcal{F}|P_{\beta\gamma g}|f][\mathcal{F}|P_{\beta\gamma g}|g]} \left. \right) + \text{Symm}_{\gamma g}
\end{aligned} \tag{B.18}$$

Now we use the Schouten identity to expand the middle sum using the $\langle \gamma g \rangle$ factor,

$$\begin{aligned}
\mathcal{C}^{\text{sp}} = & -\frac{i}{32\pi^2} \frac{[\mathcal{F}\mathcal{G}]}{\langle \mathcal{F}\mathcal{G} \rangle} \frac{1}{\langle ab \rangle \cdots \langle fa \rangle} \frac{1}{\langle ag \rangle \cdots \langle na \rangle} \left(\right. \\
& + \frac{\langle ag \rangle \langle a\gamma \rangle}{\langle \gamma g \rangle} \sum_{b_l=b-1}^{f-1} \frac{\langle a|\beta|\mathcal{F}][\mathcal{F}|P_{\gamma\dots a\dots b_l}|a\rangle^2 \langle b_l, b_l+1 \rangle \langle a\gamma \rangle}{[\mathcal{F}|P_{\gamma\dots a\dots b_l}|b_l+1\rangle [\mathcal{F}|P_{\gamma\dots a\dots b_l}|b_l\rangle [\mathcal{F}|P_{\gamma\dots a\dots b_l}|\gamma\rangle} \\
& + \frac{\langle ag \rangle \langle a\gamma \rangle}{\langle \gamma g \rangle} \sum_{b_l=b-1}^{f-1} \frac{\langle a|\beta|\mathcal{F}][\mathcal{F}|P_{g\dots a\dots b_l}|a\rangle^2 \langle b_l, b_l+1 \rangle \langle \gamma a \rangle}{[\mathcal{F}|P_{g\dots a\dots b_l}|\gamma\rangle [\mathcal{F}|P_{g\dots a\dots b_l}|b_l+1\rangle [\mathcal{F}|P_{g\dots a\dots b_l}|b_l\rangle} \\
& + \frac{\langle ag \rangle \langle a\gamma \rangle}{\langle \gamma g \rangle} \sum_{b_l=b-1}^{f-1} \frac{\langle a|\beta|\mathcal{F}][\mathcal{F}|P_{g\dots a\dots b_l}|a\rangle^2 \langle b_l, b_l+1 \rangle \langle ag \rangle}{[\mathcal{F}|P_{g\dots a\dots b_l}|b_l+1\rangle [\mathcal{F}|P_{g\dots a\dots b_l}|b_l\rangle [\mathcal{F}|P_{g\dots a\dots b_l}|g\rangle} \\
& + \frac{\langle ag \rangle \langle a\gamma \rangle}{\langle \gamma g \rangle} \sum_{b_l=b-1}^{f-1} \frac{\langle a|\beta|\mathcal{F}][\mathcal{F}|P_{h\dots a\dots b_l}|a\rangle^2 \langle b_l, b_l+1 \rangle \langle ga \rangle}{[\mathcal{F}|P_{h\dots a\dots b_l}|g\rangle [\mathcal{F}|P_{b_r+1\dots a\dots b_l}|b_l+1\rangle [\mathcal{F}|P_{h\dots a\dots b_l}|b_l\rangle} \\
& + \left. \frac{\langle ga \rangle \langle a\gamma \rangle \langle ag \rangle}{\langle \gamma g \rangle} \frac{\langle a|\beta|\mathcal{F}][\mathcal{F}|P_{\beta\gamma g}|a\rangle \langle fa \rangle}{[\mathcal{F}|P_{\beta\gamma g}|f\rangle [\mathcal{F}|P_{\beta\gamma g}|g\rangle} \right) + \text{Symm}_{\gamma g}
\end{aligned} \tag{B.19}$$

and further expand by Schoutening all the $\langle b_l, b_l+1 \rangle$ terms, and grouping by b_l or b_l+1 terms,

$$\begin{aligned}
\mathcal{C}^{\text{sp}} = & -\frac{i}{32\pi^2} \frac{[\mathcal{F}\mathcal{G}]}{\langle \mathcal{F}\mathcal{G} \rangle} \frac{1}{\langle ab \rangle \cdots \langle fa \rangle} \frac{1}{\langle ag \rangle \cdots \langle na \rangle} \left(\frac{\langle ag \rangle \langle a\gamma \rangle}{\langle \gamma g \rangle} \langle a|\beta|\mathcal{F} \sum_{b_l=b-1}^{f-1} \left(\right. \right. \\
& \frac{[\mathcal{F}|P_{\gamma\dots a\dots b_l}|a\rangle \langle a, b_l+1 \rangle \langle a\gamma \rangle}{[\mathcal{F}|P_{\gamma\dots a\dots b_l}|b_l+1\rangle [\mathcal{F}|P_{\gamma\dots a\dots b_l}|\gamma\rangle} + \frac{[\mathcal{F}|P_{g\dots a\dots b_l}|a\rangle \langle a, b_l+1 \rangle \langle \gamma a \rangle}{[\mathcal{F}|P_{g\dots a\dots b_l}|\gamma\rangle [\mathcal{F}|P_{g\dots a\dots b_l}|b_l+1\rangle} \\
& + \frac{[\mathcal{F}|P_{\gamma\dots a\dots b_l}|a\rangle \langle b_l a \rangle \langle a\gamma \rangle}{[\mathcal{F}|P_{\gamma\dots a\dots b_l}|b_l\rangle [\mathcal{F}|P_{\gamma\dots a\dots b_l}|\gamma\rangle} + \frac{[\mathcal{F}|P_{g\dots a\dots b_l}|a\rangle \langle b_l a \rangle \langle \gamma a \rangle}{[\mathcal{F}|P_{g\dots a\dots b_l}|\gamma\rangle [\mathcal{F}|P_{g\dots a\dots b_l}|b_l\rangle} \\
& + \frac{[\mathcal{F}|P_{g\dots a\dots b_l}|a\rangle \langle a, b_l+1 \rangle \langle ag \rangle}{[\mathcal{F}|P_{g\dots a\dots b_l}|b_l+1\rangle [\mathcal{F}|P_{g\dots a\dots b_l}|g\rangle} + \frac{[\mathcal{F}|P_{h\dots a\dots b_l}|a\rangle \langle a, b_l+1 \rangle \langle ga \rangle}{[\mathcal{F}|P_{h\dots a\dots b_l}|g\rangle [\mathcal{F}|P_{b_r+1\dots a\dots b_l}|b_l+1\rangle} \\
& + \left. \frac{[\mathcal{F}|P_{g\dots a\dots b_l}|a\rangle \langle b_l a \rangle \langle ag \rangle}{[\mathcal{F}|P_{g\dots a\dots b_l}|b_l\rangle [\mathcal{F}|P_{g\dots a\dots b_l}|g\rangle} + \frac{[\mathcal{F}|P_{h\dots a\dots b_l}|a\rangle \langle b_l a \rangle \langle ga \rangle}{[\mathcal{F}|P_{h\dots a\dots b_l}|g\rangle [\mathcal{F}|P_{h\dots a\dots b_l}|b_l\rangle} \right) \\
& + \frac{\langle ga \rangle \langle a\gamma \rangle \langle ag \rangle}{\langle \gamma g \rangle} \frac{\langle a|\beta|\mathcal{F}][\mathcal{F}|P_{\beta\gamma g}|a\rangle \langle fa \rangle}{[\mathcal{F}|P_{\beta\gamma g}|f\rangle [\mathcal{F}|P_{\beta\gamma g}|g\rangle} \left. \right) + \text{Symm}_{\gamma g}
\end{aligned} \tag{B.20}$$

We can now reapply the Schouten identity again to combine the terms on each line via

the following substitution,

$$\begin{aligned}
& \frac{[\mathcal{F}|P_{\gamma\dots a\dots b_l}|a\rangle}{[\mathcal{F}|P_{\gamma\dots a\dots b_l}|b_l+1\rangle][\mathcal{F}|P_{\gamma\dots a\dots b_l}|\gamma\rangle]} - \frac{[\mathcal{F}|P_{g\dots a\dots b_l}|a\rangle}{[\mathcal{F}|P_{g\dots a\dots b_l}|\gamma\rangle][\mathcal{F}|P_{g\dots a\dots b_l}|b_l+1\rangle]} \\
&= \frac{1}{[\mathcal{F}|P_{g\dots a\dots b_l}|\gamma\rangle]} \left(\frac{[\mathcal{F}|P_{\gamma\dots a\dots b_l}|a\rangle}{[\mathcal{F}|P_{\gamma\dots a\dots b_l}|b_l+1\rangle]} - \frac{[\mathcal{F}|P_{g\dots a\dots b_l}|a\rangle}{[\mathcal{F}|P_{g\dots a\dots b_l}|b_l+1\rangle]} \right) \\
&= \frac{[\mathcal{F}|P_{\gamma\dots a\dots b_l}|a\rangle][\mathcal{F}|P_{g\dots a\dots b_l}|b_l+1\rangle] - [\mathcal{F}|P_{g\dots a\dots b_l}|a\rangle][\mathcal{F}|P_{\gamma\dots a\dots b_l}|b_l+1\rangle]}{[\mathcal{F}|P_{g\dots a\dots b_l}|\gamma\rangle][\mathcal{F}|P_{\gamma\dots a\dots b_l}|b_l+1\rangle][\mathcal{F}|P_{g\dots a\dots b_l}|b_l+1\rangle]} \\
&= \frac{[\mathcal{F}|P_{\gamma\dots a\dots b_l}P_{g\dots a\dots b_l}|\mathcal{F}]\langle b_l+1, a\rangle}{[\mathcal{F}|P_{g\dots a\dots b_l}|\gamma\rangle][\mathcal{F}|P_{\gamma\dots a\dots b_l}|b_l+1\rangle][\mathcal{F}|P_{g\dots a\dots b_l}|b_l+1\rangle]} \\
&= \frac{[\mathcal{F}|\gamma P_{g\dots a\dots b_l}|\mathcal{F}]\langle b_l+1, a\rangle}{[\mathcal{F}|P_{g\dots a\dots b_l}|\gamma\rangle][\mathcal{F}|P_{\gamma\dots a\dots b_l}|b_l+1\rangle][\mathcal{F}|P_{g\dots a\dots b_l}|b_l+1\rangle]} \\
&= \frac{[\mathcal{F}\gamma]\langle b_l+1, a\rangle}{[\mathcal{F}|P_{\gamma\dots a\dots b_l}|b_l+1\rangle][\mathcal{F}|P_{g\dots a\dots b_l}|b_l+1\rangle]}
\end{aligned} \tag{B.21}$$

and we are left with,

$$\begin{aligned}
\mathcal{C}^{\text{sp}} &= -\frac{i}{32\pi^2} \frac{[\mathcal{F}\mathcal{G}]}{\langle \mathcal{F}\mathcal{G} \rangle} \frac{1}{\langle ab \rangle \dots \langle fa \rangle} \frac{1}{\langle ag \rangle \dots \langle na \rangle} \left(\frac{\langle ag \rangle \langle a\gamma \rangle}{\langle \gamma g \rangle} \langle a|\beta|\mathcal{F} \right) \sum_{b_l=b-1}^{f-1} \left(\right. \\
& \quad \frac{[\mathcal{F}\gamma]\langle b_l+1, a \rangle^2 \langle \gamma a \rangle}{[\mathcal{F}|P_{\gamma\dots a\dots b_l}|b_l+1\rangle[\mathcal{F}|P_{g\dots a\dots b_l}|b_l+1\rangle]} - \frac{[\mathcal{F}\gamma]\langle b_l a \rangle^2 \langle \gamma a \rangle}{[\mathcal{F}|P_{\gamma\dots a\dots b_l}|b_l\rangle[\mathcal{F}|P_{g\dots a\dots b_l}|b_l\rangle]} \\
& \quad + \frac{[\mathcal{F}g]\langle b_l+1, a \rangle^2 \langle ga \rangle}{[\mathcal{F}|P_{g\dots a\dots b_l}|b_l+1\rangle[\mathcal{F}|P_{h\dots a\dots b_l}|b_l+1\rangle]} - \frac{[\mathcal{F}g]\langle b_l a \rangle^2 \langle ga \rangle}{[\mathcal{F}|P_{g\dots a\dots b_l}|b_l\rangle[\mathcal{F}|P_{h\dots a\dots b_l}|b_l\rangle]} \Bigg) \\
& \quad + \frac{\langle ga \rangle \langle a\gamma \rangle \langle ag \rangle}{\langle \gamma g \rangle} \frac{\langle a|\beta|\mathcal{F}[\mathcal{F}|P_{\beta\gamma g}|a\rangle\langle fa \rangle}{[\mathcal{F}|P_{\beta\gamma g}|f\rangle[\mathcal{F}|P_{\beta\gamma g}|g\rangle]} \Bigg) + \text{Symm}_{\gamma g}
\end{aligned} \tag{B.22}$$

We can see that the terms in the sum cancel term by term leaving the end points, while

the $b_l = b - 1$ term vanishes due to the $\langle b_l a \rangle$ factors leaving just the $b_l = f - 1$ term,

$$\begin{aligned} \mathcal{C}^{\text{sp}} = & -\frac{i}{32\pi^2} \frac{[\mathcal{FG}]}{\langle \mathcal{FG} \rangle} \frac{1}{\langle ab \rangle \cdots \langle fa \rangle} \frac{1}{\langle ag \rangle \cdots \langle na \rangle} \left(\right. \\ & - \frac{\langle ag \rangle \langle a\gamma \rangle^2}{\langle \gamma g \rangle} \langle a|\beta|\mathcal{F} \rangle \frac{[\mathcal{F}\gamma] \langle fa \rangle^2}{[\mathcal{F}|P_{\gamma\dots a\dots f}|f] [\mathcal{F}|P_{g\dots a\dots f}|f]} \\ & - \frac{\langle ag \rangle^2 \langle a\gamma \rangle}{\langle \gamma g \rangle} \langle a|\beta|\mathcal{F} \rangle \frac{[\mathcal{F}g] \langle fa \rangle^2}{[\mathcal{F}|P_{g\dots a\dots f}|f] [\mathcal{F}|P_{h\dots a\dots f}|f]} \\ & \left. + \frac{\langle a\gamma \rangle \langle ag \rangle^2}{\langle \gamma g \rangle} \frac{\langle a|\beta|\mathcal{F} \rangle [\mathcal{F}|P_{\beta\gamma g}|a] \langle fa \rangle}{[\mathcal{F}|P_{\beta\gamma g}|f] [\mathcal{F}|P_{\beta\gamma g}|g]} \right) + \text{Symm}_{\gamma g} \end{aligned} \quad (\text{B.23})$$

Performing some algebraic manipulations on the denominators,

$$\begin{aligned} \mathcal{C}^{\text{sp}} = & -\frac{i}{32\pi^2} \frac{[\mathcal{FG}]}{\langle \mathcal{FG} \rangle} \frac{1}{\langle ab \rangle \cdots \langle fa \rangle} \frac{1}{\langle ag \rangle \cdots \langle na \rangle} \left(\right. \\ & - \frac{\langle ag \rangle \langle a\gamma \rangle^2}{\langle \gamma g \rangle \langle \gamma f \rangle} \langle a|\beta|\mathcal{F} \rangle \langle fa \rangle^2 \left(\frac{1}{[\mathcal{F}|\beta|f]} - \frac{1}{[\mathcal{F}|P_{\beta\gamma}|f]} \right) \\ & - \frac{\langle ag \rangle^2 \langle a\gamma \rangle}{\langle \gamma g \rangle \langle gf \rangle} \langle a|\beta|\mathcal{F} \rangle \langle fa \rangle^2 \left(\frac{1}{[\mathcal{F}|P_{\beta\gamma}|f]} - \frac{1}{[\mathcal{F}|P_{\beta\gamma g}|f]} \right) \\ & \left. + \frac{\langle a\gamma \rangle \langle ag \rangle^2}{\langle \gamma g \rangle} \frac{\langle a|\beta|\mathcal{F} \rangle [\mathcal{F}|P_{\beta\gamma g}|a] \langle fa \rangle}{[\mathcal{F}|P_{\beta\gamma g}|f] [\mathcal{F}|P_{\beta\gamma g}|g]} \right) + \text{Symm}_{\gamma g} \end{aligned} \quad (\text{B.24})$$

If we reinstate the double pole term that contains the $P_{\beta\gamma}^2$ term, we can then write the entire contribution we have been modifying: $\frac{\langle \gamma a \rangle^2}{\langle \beta a \rangle^2} \tau(\dots, \beta, \gamma, g, h, \dots)$ in terms of the $P_{\beta\gamma}^2$ term, those terms not invariant under $\gamma \leftrightarrow g$ swap above as $\chi_{\gamma g}$, plus Symm with the common $\frac{\langle a\gamma \rangle \langle ag \rangle}{\langle \gamma g \rangle}$ factor removed,

$$\begin{aligned} \frac{\langle \gamma a \rangle^2}{\langle \beta a \rangle^2} \tau(\dots, \beta, \gamma, g, h, \dots) = & \frac{1}{\langle ab \rangle \cdots \langle fa \rangle \langle hi \rangle \cdots \langle na \rangle} \left(\right. \\ & \frac{\langle a|\beta P_{\beta\gamma}|a \rangle [\mathcal{F}|P_{\beta\gamma}|a]^2 \langle fa \rangle}{P_{\beta\gamma}^2 [\mathcal{F}|P_{\beta\gamma}|f] [\mathcal{F}|P_{\beta\gamma}|g] \langle gh \rangle} + \chi_{\gamma g} + \frac{\langle a\gamma \rangle^2}{\langle a\gamma \rangle \langle \gamma g \rangle \langle gh \rangle} \text{Symm}_{\gamma g} \left. \right) \end{aligned} \quad (\text{B.25})$$

where

$$\begin{aligned}
\chi_{\gamma g} = & -\frac{\langle a\gamma \rangle^2}{\langle \gamma g \rangle \langle \gamma f \rangle \langle gh \rangle} \langle a|\beta|\mathcal{F}\rangle \langle fa \rangle^2 \left(\frac{1}{[\mathcal{F}|\beta|f]} - \frac{1}{[\mathcal{F}|P_{\beta\gamma}|f]} \right) \\
& - \frac{\langle ag \rangle \langle a\gamma \rangle}{\langle \gamma g \rangle \langle gf \rangle \langle gh \rangle} \langle a|\beta|\mathcal{F}\rangle \langle fa \rangle^2 \left(\frac{1}{[\mathcal{F}|P_{\beta\gamma}|f]} - \frac{1}{[\mathcal{F}|P_{\beta\gamma g}|f]} \right) \\
& + \frac{\langle a\gamma \rangle \langle ag \rangle}{\langle \gamma g \rangle \langle gh \rangle} \frac{\langle a|\beta|\mathcal{F}\rangle [\mathcal{F}|P_{\beta\gamma g}|a] \langle fa \rangle}{[\mathcal{F}|P_{\beta\gamma g}|f] [\mathcal{F}|P_{\beta\gamma g}|g]} \quad (B.26)
\end{aligned}$$

It has been verified numerically that $Symm$ vanishes, so we are left with a compact expression for expressing $\mathcal{C}^{n\text{-sf}}$ with a wandering minus, in terms of the double pole and terms dependent on the $\gamma \leftrightarrow g$ swap.

For null momenta, we can see that τ reduces to the MHV contribution, such that

$$\begin{aligned}
\frac{\langle \gamma a \rangle^2 \langle \beta a \rangle^2}{\langle f \beta \rangle \langle \beta \gamma \rangle \langle \gamma g \rangle} &= + \frac{\langle a \gamma \rangle^2}{\langle \gamma g \rangle \langle \gamma f \rangle} \langle a | \beta | \mathcal{F} \rangle \langle f a \rangle \left(\frac{1}{[\mathcal{F} | \beta | f]} + \frac{1}{[\mathcal{F} | P_{\beta \gamma} | f]} \right) \\
&+ \frac{\langle a g \rangle \langle a \gamma \rangle}{\langle \gamma g \rangle \langle g f \rangle} \langle a | \beta | \mathcal{F} \rangle \langle f a \rangle \left(\frac{1}{[\mathcal{F} | P_{\beta \gamma} | f]} + \frac{1}{[\mathcal{F} | P_{\beta \gamma g} | f]} \right) \\
&+ \frac{\langle a \gamma \rangle \langle a g \rangle}{\langle \gamma g \rangle} \frac{\langle a | \beta | \mathcal{F} \rangle [\mathcal{F} | P_{\beta \gamma g} | a]}{[\mathcal{F} | P_{\beta \gamma g} | f] [\mathcal{F} | P_{\beta \gamma g} | g]} + \frac{\langle a | \beta P_{\beta \gamma} | a \rangle [\mathcal{F} | P_{\beta \gamma} | a]^2}{P_{\beta \gamma}^2 [\mathcal{F} | P_{\beta \gamma} | f] [\mathcal{F} | P_{\beta \gamma} | g]} \\
&= \frac{\langle a \gamma \rangle^2}{\langle \gamma g \rangle \langle \gamma f \rangle} \langle a | \beta | \mathcal{F} \rangle \langle f a \rangle \left(\frac{1}{[\mathcal{F} | \beta | f]} - \frac{1}{[\mathcal{F} | P_{\beta \gamma} | f]} \right) + \frac{\langle a g \rangle \langle a \gamma \rangle}{\langle \gamma g \rangle \langle g f \rangle} \frac{\langle a | \beta | \mathcal{F} \rangle \langle f a \rangle}{[\mathcal{F} | P_{\beta \gamma} | f]} \\
&+ \frac{\langle a g \rangle \langle a \gamma \rangle}{\langle \gamma g \rangle \langle g f \rangle} \langle a | \beta | \mathcal{F} \rangle \frac{\langle a g \rangle}{[\mathcal{F} | P_{\beta \gamma g} | g]} - \frac{\langle a \beta \rangle \langle a \gamma \rangle [\mathcal{F} | P_{\beta \gamma} | a]^2}{\langle \beta \gamma \rangle [\mathcal{F} | P_{\beta \gamma} | f] [\mathcal{F} | P_{\beta \gamma} | g]} \\
&= \frac{\langle a \gamma \rangle^2}{\langle \gamma g \rangle \langle \gamma f \rangle} \frac{\langle a | \beta | \mathcal{F} \rangle \langle f a \rangle}{[\mathcal{F} | \beta | f]} - \frac{\langle a \gamma \rangle^2}{\langle \gamma g \rangle \langle \gamma f \rangle} \frac{\langle a | \beta | \mathcal{F} \rangle \langle f a \rangle}{[\mathcal{F} | P_{\beta \gamma} | f]} + \frac{\langle a g \rangle \langle a \gamma \rangle}{\langle \gamma g \rangle \langle g f \rangle} \frac{\langle a | \beta | \mathcal{F} \rangle \langle f a \rangle}{[\mathcal{F} | P_{\beta \gamma} | f]} \\
&+ \frac{\langle a g \rangle \langle a \gamma \rangle}{\langle \gamma g \rangle \langle g f \rangle} \langle a | \beta | \mathcal{F} \rangle \frac{\langle a g \rangle}{[\mathcal{F} | P_{\beta \gamma} | g]} - \frac{\langle a \beta \rangle \langle a \gamma \rangle [\mathcal{F} | P_{\beta \gamma} | a]^2}{\langle \beta \gamma \rangle [\mathcal{F} | P_{\beta \gamma} | f] [\mathcal{F} | P_{\beta \gamma} | g]} \\
&= \frac{\langle \gamma a \rangle}{\langle \gamma g \rangle} \langle f a \rangle \frac{[\mathcal{F} | \gamma | a]}{[\mathcal{F} | P_{\beta \gamma} | f]} \frac{\langle \beta a \rangle}{\langle \beta f \rangle} + \frac{\langle a \gamma \rangle \langle a g \rangle \langle f a \rangle}{\langle \gamma g \rangle \langle g f \rangle} \frac{\langle a \beta \rangle}{\langle f \beta \rangle} \left(1 - \frac{\langle a | \gamma | \mathcal{F} \rangle \langle f \gamma \rangle}{[\mathcal{F} | P_{\beta \gamma} | f] \langle a \gamma \rangle} \right) \\
&+ \frac{\langle a \gamma \rangle \langle a g \rangle}{\langle \gamma g \rangle \langle g f \rangle} \langle a | \beta | \mathcal{F} \rangle \frac{\langle a g \rangle}{[\mathcal{F} | P_{\beta \gamma} | g]} - \frac{\langle a \beta \rangle \langle a \gamma \rangle [\mathcal{F} | P_{\beta \gamma} | a]^2}{\langle \beta \gamma \rangle [\mathcal{F} | P_{\beta \gamma} | f] [\mathcal{F} | P_{\beta \gamma} | g]} \\
&= \frac{\langle a \beta \rangle \langle a \gamma \rangle \langle a g \rangle \langle f a \rangle}{\langle f \beta \rangle \langle \gamma g \rangle \langle g f \rangle} + \frac{\langle \gamma a \rangle}{\langle \gamma g \rangle} \langle f a \rangle \frac{[\mathcal{F} | \gamma | a]}{[\mathcal{F} | P_{\beta \gamma} | f]} \frac{\langle \beta a \rangle}{\langle \beta f \rangle} \left(1 + \frac{\langle a g \rangle \langle f \gamma \rangle}{\langle g f \rangle \langle a \gamma \rangle} \right) \\
&+ \frac{\langle a \gamma \rangle \langle a g \rangle^2}{\langle \gamma g \rangle \langle g f \rangle} \frac{\langle a | \beta | \mathcal{F} \rangle}{[\mathcal{F} | P_{\beta \gamma} | g]} - \frac{\langle a \beta \rangle \langle a \gamma \rangle [\mathcal{F} | P_{\beta \gamma} | a]^2}{\langle \beta \gamma \rangle [\mathcal{F} | P_{\beta \gamma} | f] [\mathcal{F} | P_{\beta \gamma} | g]} \\
&= \frac{\langle a \beta \rangle \langle a \gamma \rangle \langle a g \rangle \langle f a \rangle}{\langle f \beta \rangle \langle \gamma g \rangle \langle g f \rangle} + \frac{\langle f a \rangle^2}{\langle g f \rangle} \frac{[\mathcal{F} | \gamma | a]}{[\mathcal{F} | P_{\beta \gamma} | f]} \frac{\langle a \beta \rangle}{\langle \beta f \rangle} + \frac{\langle a \gamma \rangle \langle a g \rangle^2}{\langle \gamma g \rangle \langle g f \rangle} \frac{[\mathcal{F} | \beta | a]}{[\mathcal{F} | P_{\beta \gamma} | g]} \\
&- \frac{\langle a \beta \rangle \langle a \gamma \rangle [\mathcal{F} | P_{\beta \gamma} | a]^2}{\langle \beta \gamma \rangle [\mathcal{F} | P_{\beta \gamma} | f] [\mathcal{F} | P_{\beta \gamma} | g]}
\end{aligned} \tag{B.27}$$

This has been verified for null momenta, but we could easily promote β and γ back to their full momenta by capping with \mathcal{F} . The last term highlights the pure $\langle \beta \gamma \rangle^{-1}$ pole from the Parke Taylor form, and as such the single pole contribution is the remaining pieces without the last term.

The form presented here for the entire contribution, repeated now for clarity,

$$\mathfrak{C}^{\text{n-sf}} = -\frac{i}{32\pi^2} \frac{[\mathcal{FG}]}{[\mathcal{FG}]} \frac{1}{\langle ab \rangle \cdots \langle ef \rangle} \frac{1}{\langle gh \rangle \cdots \langle na \rangle} \left(\frac{\langle a|\beta\gamma|a \rangle [\mathcal{F}|P_{\beta\gamma}|a]^2}{P_{\beta\gamma}^2 [\mathcal{F}|P_{\beta\gamma}|f] [\mathcal{F}|P_{\beta\gamma}|g]} \right. \\ \left. \frac{\langle a\beta \rangle \langle a\gamma \rangle \langle ag \rangle \langle fa \rangle}{\langle f\beta \rangle \langle \gamma g \rangle \langle gf \rangle} + \frac{\langle fa \rangle^2}{\langle gf \rangle} \frac{[\mathcal{F}|\gamma|a]}{[\mathcal{F}|P_{\beta\gamma}|f]} \frac{\langle a\beta \rangle}{\langle \beta f \rangle} + \frac{\langle a\gamma \rangle \langle ag \rangle^2}{\langle \gamma g \rangle \langle gf \rangle} \frac{[\mathcal{F}|\beta|a]}{[\mathcal{F}|P_{\beta\gamma}|g]} \right) \quad (\text{B.28})$$

References

- [1] P. A. Dirac, “The Quantum theory of electron,” *Proc.Roy.Soc.Lond.* **A117** (1928) 610–624. 1
- [2] C.-N. Yang and R. L. Mills, “Conservation of Isotopic Spin and Isotopic Gauge Invariance,” *Phys.Rev.* **96** (1954) 191–195. 2, 8, 12, 13
- [3] P. W. Higgs, “Broken Symmetries and the Masses of Gauge Bosons,” *Phys.Rev.Lett.* **13** (1964) 508–509. 3
- [4] P. W. Higgs, “Broken symmetries, massless particles and gauge fields,” *Phys.Lett.* **12** (1964) 132–133. 3
- [5] **ATLAS** Collaboration, G. Aad *et al.*, “Observation of a new particle in the search for the Standard Model Higgs boson with the ATLAS detector at the LHC,” *Phys.Lett.* **B716** (2012) 1–29, [arXiv:1207.7214 \[hep-ex\]](#). 3, 7
- [6] **CMS** Collaboration, S. Chatrchyan *et al.*, “Observation of a new boson at a mass of 125 GeV with the CMS experiment at the LHC,” *Phys.Lett.* **B716** (2012) 30–61, [arXiv:1207.7235 \[hep-ex\]](#). 3, 7
- [7] **CMS** Collaboration, S. Chatrchyan *et al.*, “On the mass and spin-parity of the Higgs boson candidate via its decays to Z boson pairs,” *Phys. Rev. Lett.* **110** (2013) 081803, [arXiv:1212.6639 \[hep-ex\]](#). 3
- [8] C. Berger, Z. Bern, L. J. Dixon, F. Febres Cordero, D. Forde, *et al.*, “Precise Predictions for W + 4 Jet Production at the Large Hadron Collider,” *Phys.Rev.Lett.* **106** (2011) 092001, [arXiv:1009.2338 \[hep-ph\]](#). 4, 7
- [9] H. Ita and K. Ozeren, “Colour Decompositions of Multi-quark One-loop QCD Amplitudes,” *JHEP* **1202** (2012) 118, [arXiv:1111.4193 \[hep-ph\]](#). 4
- [10] H. Ita, Z. Bern, L. Dixon, F. Febres Cordero, D. Kosower, *et al.*, “Precise Predictions for Z + 4 Jets at Hadron Colliders,” *Phys.Rev.* **D85** (2012) 031501, [arXiv:1108.2229 \[hep-ph\]](#). 4
- [11] K. G. Wilson, “Confinement of Quarks,” *Phys.Rev.* **D10** (1974) 2445–2459. 5
- [12] S. Durr, Z. Fodor, J. Frison, C. Hoelbling, R. Hoffmann, *et al.*, “Ab-Initio Determination of Light Hadron Masses,” *Science* **322** (2008) 1224–1227, [arXiv:0906.3599 \[hep-lat\]](#). 5
- [13] J. M. Maldacena, “The Large N limit of superconformal field theories and supergravity,” *Adv.Theor.Math.Phys.* **2** (1998) 231–252, [arXiv:hep-th/9711200 \[hep-th\]](#). 5, 51

REFERENCES

- [14] E. Witten, “Anti-de Sitter space and holography,” *Adv.Theor.Math.Phys.* **2** (1998) 253–291, [arXiv:hep-th/9802150](#) [hep-th]. 5
- [15] M. E. Peskin and D. V. Schroeder, “An Introduction to quantum field theory,” . 6, 12, 16, 18, 62, 63
- [16] G. ’t Hooft and M. Veltman, “Regularization and Renormalization of Gauge Fields,” *Nucl.Phys.* **B44** (1972) 189–213. 8, 21
- [17] J. D. Lykken, “Introduction to supersymmetry,” [arXiv:hep-th/9612114](#) [hep-th]. 8, 42
- [18] S. R. Coleman and J. Mandula, “All possible symmetries of the S matrix,” *Phys.Rev.* **159** (1967) 1251–1256. 8
- [19] R. Haag, J. T. Lopuszanski, and M. Sohnius, “All Possible Generators of Supersymmetries of the s Matrix,” *Nucl.Phys.* **B88** (1975) 257. 8
- [20] S. D. Alston, D. C. Dunbar, and W. B. Perkins, “Complex Factorisation and Recursion for One-Loop Amplitudes,” *Phys.Rev.* **D86** (2012) 085022, [arXiv:1208.0190](#) [hep-th]. 10, 84, 92, 111, 112, 115, 125, 157, 158, 160
- [21] H. Kawai, D. Lewellen, and S. Tye, “A Relation Between Tree Amplitudes of Closed and Open Strings,” *Nucl.Phys.* **B269** (1986) 1. 11, 41, 51, 111, 158
- [22] G. M. Shore, “Quantum Field Theory.” Lecture notes given in: Course 1178 at Champs et Particules, Université de Genève, 1999-2000. 12
- [23] I. Aitchison and A. Hey, “Gauge theories in particle physics: A practical introduction. Vol. 2: Non-Abelian gauge theories: QCD and the electroweak theory,”. 16
- [24] M. L. Mangano and S. J. Parke, “Multiparton amplitudes in gauge theories,” *Phys.Rept.* **200** (1991) 301–367, [arXiv:hep-th/0509223](#) [hep-th]. 17, 26, 58
- [25] D. Gross and F. Wilczek, “Ultraviolet Behavior of Nonabelian Gauge Theories,” *Phys.Rev.Lett.* **30** (1973) 1343–1346. 18, 19
- [26] H. D. Politzer, “Reliable Perturbative Results for Strong Interactions?,” *Phys.Rev.Lett.* **30** (1973) 1346–1349. 18
- [27] G. Prospero, M. Raciti, and C. Simolo, “On the running coupling constant in QCD,” *Prog.Part.Nucl.Phys.* **58** (2007) 387–438, [arXiv:hep-ph/0607209](#) [hep-ph]. 19
- [28] Y. L. Dokshitzer, “Calculation of the Structure Functions for Deep Inelastic Scattering and $e^+ e^-$ Annihilation by Perturbation Theory in Quantum Chromodynamics,” *Sov.Phys.JETP* **46** (1977) 641–653. 20
- [29] V. Gribov and L. Lipatov, “Deep inelastic $e p$ scattering in perturbation theory,” *Sov.J.Nucl.Phys.* **15** (1972) 438–450. 20
- [30] L. Lipatov, “The parton model and perturbation theory,” *Sov.J.Nucl.Phys.* **20** (1975) 94–102. 20
- [31] G. Altarelli and G. Parisi, “Asymptotic Freedom in Parton Language,” *Nucl.Phys.* **B126** (1977) 298. 20
- [32] G. Passarino and M. Veltman, “One Loop Corrections for $e^+ e^-$ Annihilation Into $\mu^+ \mu^-$ in the Weinberg Model,” *Nucl.Phys.* **B160** (1979) 151. 20

REFERENCES

- [33] G. 't Hooft and M. Veltman, “Scalar One Loop Integrals,” *Nucl.Phys.* **B153** (1979) 365–401. 20
- [34] A. Denner, “Techniques for calculation of electroweak radiative corrections at the one loop level and results for W physics at LEP-200,” *Fortsch.Phys.* **41** (1993) 307–420, [arXiv:0709.1075 \[hep-ph\]](#). 20, 23
- [35] R. K. Ellis, Z. Kunszt, K. Melnikov, and G. Zanderighi, “One-loop calculations in quantum field theory: from Feynman diagrams to unitarity cuts,” *Phys.Rept.* **518** (2012) 141–250, [arXiv:1105.4319 \[hep-ph\]](#). 20, 22
- [36] T. Kinoshita, “Mass singularities of Feynman amplitudes,” *J.Math.Phys.* **3** (1962) 650–677. 21
- [37] W. Marciano, “Dimensional Regularization and Mass Singularities,” *Phys.Rev.* **D12** (1975) 3861. 21
- [38] Z. Bern, L. J. Dixon, D. C. Dunbar, and D. A. Kosower, “Fusing gauge theory tree amplitudes into loop amplitudes,” *Nucl.Phys.* **B435** (1995) 59–101, [arXiv:hep-ph/9409265 \[hep-ph\]](#). 24, 66, 67
- [39] F. A. Berends and W. Giele, “The Six Gluon Process as an Example of Weyl-Van Der Waerden Spinor Calculus,” *Nucl.Phys.* **B294** (1987) 700. 26, 28
- [40] M. L. Mangano, S. J. Parke, and Z. Xu, “Duality and Multi - Gluon Scattering,” *Nucl.Phys.* **B298** (1988) 653. 26, 28
- [41] M. L. Mangano, “The Color Structure of Gluon Emission,” *Nucl.Phys.* **B309** (1988) 461. 26, 28
- [42] L. J. Dixon, “Calculating scattering amplitudes efficiently,” [arXiv:hep-ph/9601359 \[hep-ph\]](#). 26, 27, 28, 33, 47, 48, 57, 58
- [43] Z. Bern and D. A. Kosower, “Color decomposition of one loop amplitudes in gauge theories,” *Nucl.Phys.* **B362** (1991) 389–448. 26, 27, 29
- [44] Z. Bern, L. J. Dixon, D. C. Dunbar, and D. A. Kosower, “One loop n point gauge theory amplitudes, unitarity and collinear limits,” *Nucl.Phys.* **B425** (1994) 217–260, [arXiv:hep-ph/9403226 \[hep-ph\]](#). 26, 29, 41, 59, 66, 67, 156
- [45] E. Witten, “Perturbative gauge theory as a string theory in twistor space,” *Commun.Math.Phys.* **252** (2004) 189–258, [arXiv:hep-th/0312171 \[hep-th\]](#). 29, 34, 44
- [46] B. Feng and M. Luo, “An Introduction to On-shell Recursion Relations,” [arXiv:1111.5759 \[hep-th\]](#). 29
- [47] F. A. Berends, R. Kleiss, P. De Causmaecker, R. Gastmans, and T. T. Wu, “Single Bremsstrahlung Processes in Gauge Theories,” *Phys.Lett.* **B103** (1981) 124. 29
- [48] F. A. Berends, R. Kleiss, P. De Causmaecker, R. Gastmans, W. Troost, *et al.*, “Multiple Bremsstrahlung in Gauge Theories at High-Energies. 2. Single Bremsstrahlung,” *Nucl.Phys.* **B206** (1982) 61. 29
- [49] Z. Xu, D.-H. Zhang, and L. Chang, “Helicity amplitudes for multiple Bremsstrahlung in massless non-Abelian gauge theory. 1. New Defintion of polarization vector and formulation of amplitudes in Grassmann algebra,”. 29

REFERENCES

- [50] R. Kleiss and W. J. Stirling, “Spinor Techniques for Calculating p anti- p to W^{+-} / Z^0 + Jets,” *Nucl.Phys.* **B262** (1985) 235–262. 29
- [51] J. Gunion and Z. Kunszt, “Improved Analytic Techniques for Tree Graph Calculations and the $G g q$ anti- q Lepton anti-Lepton Subprocess,” *Phys.Lett.* **B161** (1985) 333. 29
- [52] Z. Xu, D.-H. Zhang, and L. Chang, “Helicity Amplitudes for Multiple Bremsstrahlung in Massless Nonabelian Gauge Theories,” *Nucl.Phys.* **B291** (1987) 392. 29
- [53] R. Penrose, “Twistor algebra,” *J.Math.Phys.* **8** (1967) 345. 30
- [54] L. J. Dixon, “Twistor string theory and QCD,” *PoS HEP2005* (2006) 405, [arXiv:hep-ph/0512111 \[hep-ph\]](#). 30, 31
- [55] Z. Bern, L. J. Dixon, and D. A. Kosower, “On-Shell Methods in Perturbative QCD,” *Annals Phys.* **322** (2007) 1587–1634, [arXiv:0704.2798 \[hep-ph\]](#). 33, 34, 72, 74, 75, 78
- [56] C. Schwinn and S. Weinzierl, “Scalar diagrammatic rules for Born amplitudes in QCD,” *JHEP* **0505** (2005) 006, [arXiv:hep-th/0503015 \[hep-th\]](#). 35, 36
- [57] D. A. Kosower, “Next-to-maximal helicity violating amplitudes in gauge theory,” *Phys.Rev.* **D71** (2005) 045007, [arXiv:hep-th/0406175 \[hep-th\]](#). 35
- [58] F. Cachazo, P. Svrcek, and E. Witten, “MHV vertices and tree amplitudes in gauge theory,” *JHEP* **0409** (2004) 006, [arXiv:hep-th/0403047 \[hep-th\]](#). 37
- [59] S. J. Parke and T. Taylor, “An Amplitude for n Gluon Scattering,” *Phys.Rev.Lett.* **56** (1986) 2459. 38, 40, 58, 156
- [60] F. A. Berends and W. Giele, “Recursive Calculations for Processes with n Gluons,” *Nucl.Phys.* **B306** (1988) 759. 40, 58, 92
- [61] M. Sohnius, “Introducing Supersymmetry,” *Phys.Rept.* **128** (1985) 39–204. 42
- [62] I. Buchbinder and S. Kuzenko, “Ideas and methods of supersymmetry and supergravity: A Walk through superspace,” . 43
- [63] J. Drummond, J. Henn, G. Korchemsky, and E. Sokatchev, “Dual superconformal symmetry of scattering amplitudes in $N=4$ super-Yang-Mills theory,” *Nucl.Phys.* **B828** (2010) 317–374, [arXiv:0807.1095 \[hep-th\]](#). 43
- [64] J. Drummond, “Hidden Simplicity of Gauge Theory Amplitudes,” *Class.Quant.Grav.* **27** (2010) 214001, [arXiv:1010.2418 \[hep-th\]](#). 43, 45, 46, 80, 81
- [65] N. Beisert, C. Ahn, L. F. Alday, Z. Bajnok, J. M. Drummond, *et al.*, “Review of AdS/CFT Integrability: An Overview,” *Lett.Math.Phys.* **99** (2012) 3–32, [arXiv:1012.3982 \[hep-th\]](#). 44
- [66] L. F. Alday and J. M. Maldacena, “Gluon scattering amplitudes at strong coupling,” *JHEP* **0706** (2007) 064, [arXiv:0705.0303 \[hep-th\]](#). 45
- [67] L. F. Alday and J. Maldacena, “Null polygonal Wilson loops and minimal surfaces in Anti-de-Sitter space,” *JHEP* **0911** (2009) 082, [arXiv:0904.0663 \[hep-th\]](#). 45
- [68] L. F. Alday, D. Gaiotto, and J. Maldacena, “Thermodynamic Bubble Ansatz,” *JHEP* **1109** (2011) 032, [arXiv:0911.4708 \[hep-th\]](#). 45
- [69] L. F. Alday, J. Maldacena, A. Sever, and P. Vieira, “Y-system for Scattering Amplitudes,” *J.Phys.* **A43** (2010) 485401, [arXiv:1002.2459 \[hep-th\]](#). 45

REFERENCES

-
- [70] V. Nair, “A current algebra for some gauge theory amplitudes,” *Phys.Lett.* **B214** (1988) 215–46
 - [71] Z. Bern and D. A. Kosower, “The Computation of loop amplitudes in gauge theories,” *Nucl.Phys.* **B379** (1992) 451–561. 47
 - [72] Z. Bern, “A Compact representation of the one loop N gluon amplitude,” *Phys.Lett.* **B296** (1992) 85–94. 47
 - [73] Z. Bern, “String based perturbative methods for gauge theories,” [arXiv:hep-ph/9304249](#) [[hep-ph](#)]. 47
 - [74] H. Nicolai, K. Peeters, and M. Zamaklar, “Loop quantum gravity: An Outside view,” *Class.Quant.Grav.* **22** (2005) R193, [arXiv:hep-th/0501114](#) [[hep-th](#)]. 49
 - [75] M. Bojowald, “Loop quantum cosmology,” *Living Rev.Rel.* **8** (2005) 11, [arXiv:gr-qc/0601085](#) [[gr-qc](#)]. 49
 - [76] P. Nicolini, “Noncommutative Black Holes, The Final Appeal To Quantum Gravity: A Review,” *Int.J.Mod.Phys.* **A24** (2009) 1229–1308, [arXiv:0807.1939](#) [[hep-th](#)]. 49
 - [77] J. Ambjorn, J. Jurkiewicz, and R. Loll, “Dynamically triangulating Lorentzian quantum gravity,” *Nucl.Phys.* **B610** (2001) 347–382, [arXiv:hep-th/0105267](#) [[hep-th](#)]. 49
 - [78] J. Ambjorn, J. Gizbert-Studnicki, A. Goerlich, J. Jurkiewicz, and R. Loll, “The transfer matrix method in four-dimensional causal dynamical triangulations,” *AIP Conf.Proc.* **1514** (2012) 67–72, [arXiv:1302.2210](#) [[hep-th](#)]. 49
 - [79] J. Ambjorn, L. Glaser, Y. Sato, and Y. Watabiki, “2d CDT is 2d Horava-Lifshitz quantum gravity,” *Phys.Lett.* **B722** (2013) 172–175, [arXiv:1302.6359](#) [[hep-th](#)]. 49
 - [80] S. Capozziello and M. De Laurentis, “Extended Theories of Gravity,” *Phys.Rept.* **509** (2011) 167–321, [arXiv:1108.6266](#) [[gr-qc](#)]. 50
 - [81] M. R. Douglas and S. Kachru, “Flux compactification,” *Rev.Mod.Phys.* **79** (2007) 733–796, [arXiv:hep-th/0610102](#) [[hep-th](#)]. 50
 - [82] R. Maartens, “Brane world gravity,” *Living Rev.Rel.* **7** (2004) 7, [arXiv:gr-qc/0312059](#) [[gr-qc](#)]. 50
 - [83] Z. Bern, J. J. Carrasco, L. J. Dixon, H. Johansson, and R. Roiban, “Amplitudes and Ultraviolet Behavior of $N = 8$ Supergravity,” *Fortsch.Phys.* **59** (2011) 561–578, [arXiv:1103.1848](#) [[hep-th](#)]. 50, 51
 - [84] Z. Bern, J. Carrasco, L. J. Dixon, H. Johansson, and R. Roiban, “The Ultraviolet Behavior of $N=8$ Supergravity at Four Loops,” *Phys.Rev.Lett.* **103** (2009) 081301, [arXiv:0905.2326](#) [[hep-th](#)]. 50
 - [85] Z. Bern, J. Carrasco, L. J. Dixon, H. Johansson, D. Kosower, *et al.*, “Three-Loop Superfiniteness of $N=8$ Supergravity,” *Phys.Rev.Lett.* **98** (2007) 161303, [arXiv:hep-th/0702112](#) [[hep-th](#)]. 50
 - [86] Z. Bern, J. Carrasco, L. J. Dixon, H. Johansson, and R. Roiban, “Manifest Ultraviolet Behavior for the Three-Loop Four-Point Amplitude of $N=8$ Supergravity,” *Phys.Rev.* **D78** (2008) 105019, [arXiv:0808.4112](#) [[hep-th](#)]. 50
 - [87] N. Beisert, H. Elvang, D. Z. Freedman, M. Kiermaier, A. Morales, *et al.*, “E7(7) constraints on counterterms in $N=8$ supergravity,” *Phys.Lett.* **B694** (2010) 265–271, [arXiv:1009.1643](#) [[hep-th](#)]. 51

REFERENCES

-
- [88] G. Bossard, P. Howe, and K. Stelle, “On duality symmetries of supergravity invariants,” *JHEP* **1101** (2011) 020, [arXiv:1009.0743 \[hep-th\]](#). 51
 - [89] D. Singleton, “General relativistic analog solutions for Yang-Mills theory,” *Theor.Math.Phys.* **117** (1998) 1351–1363, [arXiv:hep-th/9904125 \[hep-th\]](#). 51
 - [90] L. J. Dixon, “Ultraviolet Behavior of $N = 8$ Supergravity,” [arXiv:1005.2703 \[hep-th\]](#). 52, 53
 - [91] Z. Bern, L. J. Dixon, M. Perelstein, and J. Rozowsky, “Multileg one loop gravity amplitudes from gauge theory,” *Nucl.Phys.* **B546** (1999) 423–479, [arXiv:hep-th/9811140 \[hep-th\]](#). 53, 111
 - [92] Z. Bern, J. Carrasco, and H. Johansson, “New Relations for Gauge-Theory Amplitudes,” *Phys.Rev.* **D78** (2008) 085011, [arXiv:0805.3993 \[hep-ph\]](#). 54
 - [93] Z. Bern, S. Davies, T. Dennen, Y.-t. Huang, and J. Nohle, “Color-Kinematics Duality for Pure Yang-Mills and Gravity at One and Two Loops,” [arXiv:1303.6605 \[hep-th\]](#). 54
 - [94] D. C. Dunbar and P. S. Norridge, “Calculation of graviton scattering amplitudes using string based methods,” *Nucl.Phys.* **B433** (1995) 181–208, [arXiv:hep-th/9408014 \[hep-th\]](#). 55, 111
 - [95] M. L. Mangano and S. J. Parke, “Quark - Gluon Amplitudes in the Dual Expansion,” *Nucl.Phys.* **B299** (1988) 673. 58
 - [96] Z. Bern, G. Chalmers, L. J. Dixon, and D. A. Kosower, “One loop N gluon amplitudes with maximal helicity violation via collinear limits,” *Phys.Rev.Lett.* **72** (1994) 2134–2137, [arXiv:hep-ph/9312333 \[hep-ph\]](#). 59
 - [97] Z. Bern and G. Chalmers, “Factorization in one loop gauge theory,” *Nucl.Phys.* **B447** (1995) 465–518, [arXiv:hep-ph/9503236 \[hep-ph\]](#). 59, 60, 61, 74
 - [98] R. Cutkosky, “Singularities and discontinuities of Feynman amplitudes,” *J.Math.Phys.* **1** (1960) 429–433. 64, 66
 - [99] W. van Neerven, “Dimensional regularization of mass and infrared singularities in two loop on-shell vertex functions,” *Nucl.Phys.* **B268** (1986) 453. 67, 82
 - [100] Z. Bern and A. Morgan, “Massive loop amplitudes from unitarity,” *Nucl.Phys.* **B467** (1996) 479–509, [arXiv:hep-ph/9511336 \[hep-ph\]](#). 67, 82
 - [101] C. Anastasiou, R. Britto, B. Feng, Z. Kunszt, and P. Mastrolia, “Unitarity cuts and Reduction to master integrals in d dimensions for one-loop amplitudes,” *JHEP* **0703** (2007) 111, [arXiv:hep-ph/0612277 \[hep-ph\]](#). 67, 82
 - [102] Z. Bern, L. J. Dixon, and D. A. Kosower, “On-shell recurrence relations for one-loop QCD amplitudes,” *Phys.Rev.* **D71** (2005) 105013, [arXiv:hep-th/0501240 \[hep-th\]](#). 67, 81, 82, 85, 87, 88, 89, 91, 94, 95, 107, 110, 111, 141, 157
 - [103] Z. Bern, L. J. Dixon, and D. A. Kosower, “The last of the finite loop amplitudes in QCD,” *Phys.Rev.* **D72** (2005) 125003, [arXiv:hep-ph/0505055 \[hep-ph\]](#). 67, 82, 157
 - [104] Z. Bern, L. J. Dixon, and D. A. Kosower, “Bootstrapping multi-parton loop amplitudes in QCD,” *Phys.Rev.* **D73** (2006) 065013, [arXiv:hep-ph/0507005 \[hep-ph\]](#). 67, 82, 157

REFERENCES

- [105] C. F. Berger, Z. Bern, L. J. Dixon, D. Forde, and D. A. Kosower, “Bootstrapping One-Loop QCD Amplitudes with General Helicities,” *Phys.Rev.* **D74** (2006) 036009, [arXiv:hep-ph/0604195 \[hep-ph\]](#). 67, 82, 111, 157
- [106] C. F. Berger, Z. Bern, L. J. Dixon, D. Forde, and D. A. Kosower, “All One-loop Maximally Helicity Violating Gluonic Amplitudes in QCD,” *Phys.Rev.* **D75** (2007) 016006, [arXiv:hep-ph/0607014 \[hep-ph\]](#). 67, 82, 157
- [107] Z. Xiao, G. Yang, and C.-J. Zhu, “The Rational Part of QCD Amplitude. III. The Six-Gluon,” *Nucl.Phys.* **B758** (2006) 53–89, [arXiv:hep-ph/0607017 \[hep-ph\]](#). 67
- [108] T. Binoth, J. P. Guillet, and G. Heinrich, “Algebraic evaluation of rational polynomials in one-loop amplitudes,” *JHEP* **0702** (2007) 013, [arXiv:hep-ph/0609054 \[hep-ph\]](#).
- [109] Eden, R.J. and Landshoff, P.V. and Olive, D.I. and Polkinghorne, J.C., *The Analytic S-Matrix*. 70
- [110] R. Britto, F. Cachazo, and B. Feng, “Generalized unitarity and one-loop amplitudes in N=4 super-Yang-Mills,” *Nucl.Phys.* **B725** (2005) 275–305, [arXiv:hep-th/0412103 \[hep-th\]](#). 70, 156
- [111] Z. Bern, L. J. Dixon, and D. A. Kosower, “One loop amplitudes for e+ e- to four partons,” *Nucl.Phys.* **B513** (1998) 3–86, [arXiv:hep-ph/9708239 \[hep-ph\]](#). 71, 156
- [112] G. Ossola, C. G. Papadopoulos, and R. Pittau, “Reducing full one-loop amplitudes to scalar integrals at the integrand level,” *Nucl.Phys.* **B763** (2007) 147–169, [arXiv:hep-ph/0609007 \[hep-ph\]](#). 71, 156
- [113] D. Forde, “Direct extraction of one-loop integral coefficients,” *Phys.Rev.* **D75** (2007) 125019, [arXiv:0704.1835 \[hep-ph\]](#). 71, 156
- [114] R. Britto and B. Feng, “Unitarity cuts with massive propagators and algebraic expressions for coefficients,” *Phys.Rev.* **D75** (2007) 105006, [arXiv:hep-ph/0612089 \[hep-ph\]](#). 71, 156
- [115] R. K. Ellis, W. T. Giele, Z. Kunszt, and K. Melnikov, “Masses, fermions and generalized D-dimensional unitarity,” *Nucl.Phys.* **B822** (2009) 270–282, [arXiv:0806.3467 \[hep-ph\]](#). 71, 156
- [116] A. Brandhuber, S. McNamara, B. J. Spence, and G. Travaglini, “Loop amplitudes in pure Yang-Mills from generalised unitarity,” *JHEP* **0510** (2005) 011, [arXiv:hep-th/0506068 \[hep-th\]](#). 71, 156, 157
- [117] S. Badger, “Direct Extraction Of One Loop Rational Terms,” *JHEP* **0901** (2009) 049, [arXiv:0806.4600 \[hep-ph\]](#). 71, 156, 157
- [118] W. T. Giele, Z. Kunszt, and K. Melnikov, “Full one-loop amplitudes from tree amplitudes,” *JHEP* **0804** (2008) 049, [arXiv:0801.2237 \[hep-ph\]](#). 71, 156, 157
- [119] R. Britto, E. Buchbinder, F. Cachazo, and B. Feng, “One-loop amplitudes of gluons in SQCD,” *Phys.Rev.* **D72** (2005) 065012, [arXiv:hep-ph/0503132 \[hep-ph\]](#). 72, 156
- [120] R. Britto, B. Feng, and P. Mastrolia, “The Cut-constructible part of QCD amplitudes,” *Phys.Rev.* **D73** (2006) 105004, [arXiv:hep-ph/0602178 \[hep-ph\]](#). 72, 156
- [121] C. Anastasiou, R. Britto, B. Feng, Z. Kunszt, and P. Mastrolia, “D-dimensional unitarity cut method,” *Phys.Lett.* **B645** (2007) 213–216, [arXiv:hep-ph/0609191 \[hep-ph\]](#). 72, 156

REFERENCES

- [122] S. Badger, H. Frellesvig, and Y. Zhang, “Hepta-Cuts of Two-Loop Scattering Amplitudes,” *JHEP* **1204** (2012) 055, [arXiv:1202.2019 \[hep-ph\]](#). 72, 156
- [123] Z. Bern, L. J. Dixon, and V. A. Smirnov, “Iteration of planar amplitudes in maximally supersymmetric Yang-Mills theory at three loops and beyond,” *Phys.Rev.* **D72** (2005) 085001, [arXiv:hep-th/0505205 \[hep-th\]](#). 72, 156
- [124] Z. Bern, M. Czakon, L. J. Dixon, D. A. Kosower, and V. A. Smirnov, “The Four-Loop Planar Amplitude and Cusp Anomalous Dimension in Maximally Supersymmetric Yang-Mills Theory,” *Phys.Rev.* **D75** (2007) 085010, [arXiv:hep-th/0610248 \[hep-th\]](#). 72, 156
- [125] Z. Bern, J. Carrasco, H. Johansson, and D. Kosower, “Maximally supersymmetric planar Yang-Mills amplitudes at five loops,” *Phys.Rev.* **D76** (2007) 125020, [arXiv:0705.1864 \[hep-th\]](#). 72, 156
- [126] Z. Bern, J. Rozowsky, and B. Yan, “Two loop four gluon amplitudes in N=4 superYang-Mills,” *Phys.Lett.* **B401** (1997) 273–282, [arXiv:hep-ph/9702424 \[hep-ph\]](#). 72, 156
- [127] Z. Bern, L. Dixon, D. Kosower, R. Roiban, M. Spradlin, *et al.*, “The Two-Loop Six-Gluon MHV Amplitude in Maximally Supersymmetric Yang-Mills Theory,” *Phys.Rev.* **D78** (2008) 045007, [arXiv:0803.1465 \[hep-th\]](#). 72, 156
- [128] D. Kosower, R. Roiban, and C. Vergu, “The Six-Point NMHV amplitude in Maximally Supersymmetric Yang-Mills Theory,” *Phys.Rev.* **D83** (2011) 065018, [arXiv:1009.1376 \[hep-th\]](#). 72, 156
- [129] L. J. Dixon, J. M. Drummond, and J. M. Henn, “Analytic result for the two-loop six-point NMHV amplitude in N=4 super Yang-Mills theory,” *JHEP* **1201** (2012) 024, [arXiv:1111.1704 \[hep-th\]](#). 72, 156
- [130] E. I. Buchbinder and F. Cachazo, “Two-loop amplitudes of gluons and octa-cuts in N=4 super Yang-Mills,” *JHEP* **0511** (2005) 036, [arXiv:hep-th/0506126 \[hep-th\]](#). 72, 156
- [131] F. Cachazo, “Sharpening The Leading Singularity,” [arXiv:0803.1988 \[hep-th\]](#). 72, 156
- [132] F. Cachazo, M. Spradlin, and A. Volovich, “Leading Singularities of the Two-Loop Six-Particle MHV Amplitude,” *Phys.Rev.* **D78** (2008) 105022, [arXiv:0805.4832 \[hep-th\]](#). 72, 156
- [133] R. Britto, F. Cachazo, B. Feng, and E. Witten, “Direct proof of tree-level recursion relation in Yang-Mills theory,” *Phys.Rev.Lett.* **94** (2005) 181602, [arXiv:hep-th/0501052 \[hep-th\]](#). 75, 76, 157
- [134] J. Drummond and J. Henn, “All tree-level amplitudes in N=4 SYM,” *JHEP* **0904** (2009) 018, [arXiv:0808.2475 \[hep-th\]](#). 80, 81
- [135] N. Arkani-Hamed and J. Kaplan, “On Tree Amplitudes in Gauge Theory and Gravity,” *JHEP* **0804** (2008) 076, [arXiv:0801.2385 \[hep-th\]](#). 80
- [136] L. J. Dixon, J. M. Henn, J. Plefka, and T. Schuster, “All tree-level amplitudes in massless QCD,” *JHEP* **1101** (2011) 035, [arXiv:1010.3991 \[hep-ph\]](#). 81
- [137] F. Cachazo and P. Svrcek, “Tree level recursion relations in general relativity,” [arXiv:hep-th/0502160 \[hep-th\]](#). 81

REFERENCES

- [138] N. Arkani-Hamed, F. Cachazo, and J. Kaplan, “What is the Simplest Quantum Field Theory?,” *JHEP* **1009** (2010) 016, [arXiv:0808.1446 \[hep-th\]](#). 81
- [139] J. Drummond, M. Spradlin, A. Volovich, and C. Wen, “Tree-Level Amplitudes in N=8 Supergravity,” *Phys.Rev.* **D79** (2009) 105018, [arXiv:0901.2363 \[hep-th\]](#). 81
- [140] J. Bedford, A. Brandhuber, B. J. Spence, and G. Travaglini, “A Recursion relation for gravity amplitudes,” *Nucl.Phys.* **B721** (2005) 98–110, [arXiv:hep-th/0502146 \[hep-th\]](#). 81, 112
- [141] A. Hall, “On-shell recursion relations for gravity,” *Phys.Rev.* **D77** (2008) 124004, [arXiv:0803.0215 \[hep-th\]](#). 81
- [142] K. Risager, “A Direct proof of the CSW rules,” *JHEP* **0512** (2005) 003, [arXiv:hep-th/0508206 \[hep-th\]](#). 81
- [143] M.-x. Luo and C.-k. Wen, “Recursion relations for tree amplitudes in super gauge theories,” *JHEP* **0503** (2005) 004, [arXiv:hep-th/0501121 \[hep-th\]](#). 81
- [144] M.-x. Luo and C.-k. Wen, “Compact formulas for all tree amplitudes of six partons,” *Phys.Rev.* **D71** (2005) 091501, [arXiv:hep-th/0502009 \[hep-th\]](#). 81
- [145] D. de Florian and J. Zurita, “The Last of the seven-parton tree amplitudes,” *JHEP* **0611** (2006) 080, [arXiv:hep-ph/0609099 \[hep-ph\]](#). 81
- [146] D. de Florian and J. Zurita, “Seven parton amplitudes from recursion relations,” *JHEP* **0605** (2006) 073, [arXiv:hep-ph/0605291 \[hep-ph\]](#). 81
- [147] S. Badger, E. N. Glover, V. Khoze, and P. Srvcck, “Recursion relations for gauge theory amplitudes with massive particles,” *JHEP* **0507** (2005) 025, [arXiv:hep-th/0504159 \[hep-th\]](#). 81
- [148] S. Badger, E. N. Glover, and V. V. Khoze, “Recursion relations for gauge theory amplitudes with massive vector bosons and fermions,” *JHEP* **0601** (2006) 066, [arXiv:hep-th/0507161 \[hep-th\]](#). 81
- [149] D. Forde and D. A. Kosower, “All-multiplicity amplitudes with massive scalars,” *Phys.Rev.* **D73** (2006) 065007, [arXiv:hep-th/0507292 \[hep-th\]](#). 81
- [150] K. Ozeren and W. Stirling, “Scattering amplitudes with massive fermions using BCFW recursion,” *Eur.Phys.J.* **C48** (2006) 159–168, [arXiv:hep-ph/0603071 \[hep-ph\]](#). 81
- [151] C. F. Berger, V. Del Duca, and L. J. Dixon, “Recursive Construction of Higgs-Plus-Multiparton Loop Amplitudes: The Last of the Phi-nite Loop Amplitudes,” *Phys.Rev.* **D74** (2006) 094021, [arXiv:hep-ph/0608180 \[hep-ph\]](#). 81
- [152] K. Ozeren and W. Stirling, “MHV techniques for QED processes,” *JHEP* **0511** (2005) 016, [arXiv:hep-th/0509063 \[hep-th\]](#). 81
- [153] D. Vaman and Y.-P. Yao, “The Space-Cone Gauge, Lorentz Invariance and On-Shell Recursion for One-Loop Yang-Mills amplitudes,” [arXiv:0805.2645 \[hep-th\]](#). 91
- [154] G. Mahlon, “Multi - gluon helicity amplitudes involving a quark loop,” *Phys.Rev.* **D49** (1994) 4438–4453, [arXiv:hep-ph/9312276 \[hep-ph\]](#). 91, 104
- [155] D. A. Kosower, “Light Cone Recurrence Relations for QCD Amplitudes,” *Nucl.Phys.* **B335** (1990) 23. 104

REFERENCES

- [156] Z. Bern, D. C. Dunbar, and T. Shimada, “String based methods in perturbative gravity,” *Phys.Lett.* **B312** (1993) 277–284, [arXiv:hep-th/9307001](#) [[hep-th](#)]. 111
- [157] M. T. Grisaru and J. Zak, “One loop scalar field contributions to graviton-graviton scattering and helicity nonconservation in quantum gravity,” *Phys.Lett.* **B90** (1980) 237. 111
- [158] D. C. Dunbar, J. H. Eittle, and W. B. Perkins, “Augmented Recursion For One-loop Gravity Amplitudes,” *JHEP* **1006** (2010) 027, [arXiv:1003.3398](#) [[hep-th](#)]. 111, 112, 130, 155, 157, 159
- [159] D. C. Dunbar, J. H. Eittle, and W. B. Perkins, “Perturbative expansion of $N < 8$ Supergravity,” *Phys.Rev.* **D83** (2011) 065015, [arXiv:1011.5378](#) [[hep-th](#)]. 111
- [160] D. C. Dunbar, J. H. Eittle, and W. B. Perkins, “Obtaining One-loop Gravity Amplitudes Using Spurious Singularities,” *Phys.Rev.* **D84** (2011) 125029, [arXiv:1109.4827](#) [[hep-th](#)]. 111
- [161] D. C. Dunbar, J. H. Eittle, and W. B. Perkins, “The n-point MHV one-loop Amplitude in $N=4$ Supergravity,” *Phys.Rev.Lett.* **108** (2012) 061603, [arXiv:1111.1153](#) [[hep-th](#)]. 111
- [162] D. C. Dunbar, J. H. Eittle, and W. B. Perkins, “Constructing Gravity Amplitudes from Real Soft and Collinear Factorisation,” *Phys.Rev.* **D86** (2012) 026009, [arXiv:1203.0198](#) [[hep-th](#)]. 111
- [163] A. Brandhuber, S. McNamara, B. Spence, and G. Travaglini, “Recursion relations for one-loop gravity amplitudes,” *JHEP* **0703** (2007) 029, [arXiv:hep-th/0701187](#) [[hep-th](#)]. 112
- [164] P. Ramond, “Field Theory: A Modern Primer,” *Front.Phys.* **51** (1981) 1–397. 117, 162, 164, 165
- [165] A. Brandhuber, B. J. Spence, and G. Travaglini, “One-loop gauge theory amplitudes in $N=4$ super Yang-Mills from MHV vertices,” *Nucl.Phys.* **B706** (2005) 150–180, [arXiv:hep-th/0407214](#) [[hep-th](#)]. 156
- [166] C. Quigley and M. Rozali, “One-loop MHV amplitudes in supersymmetric gauge theories,” *JHEP* **0501** (2005) 053, [arXiv:hep-th/0410278](#) [[hep-th](#)]. 156
- [167] J. Bedford, A. Brandhuber, B. J. Spence, and G. Travaglini, “A Twistor approach to one-loop amplitudes in $N=1$ supersymmetric Yang-Mills theory,” *Nucl.Phys.* **B706** (2005) 100–126, [arXiv:hep-th/0410280](#) [[hep-th](#)]. 156
- [168] J. Bedford, A. Brandhuber, B. J. Spence, and G. Travaglini, “Non-supersymmetric loop amplitudes and MHV vertices,” *Nucl.Phys.* **B712** (2005) 59–85, [arXiv:hep-th/0412108](#) [[hep-th](#)]. 157